UNIVERSITÀ DEGLI STUDI DI MESSINA

Dipartimento di Ingegneria

Corso di Dottorato di Ricerca in
"Ingegneria e Chimica
dei Materiali e delle Costruzioni"
XXIX Ciclo

Methods for the analysis of structural systems subjected to seismic acceleration modelled as stochastic processes

Coordinatore:

Prof. **Signorino GALVAGNO**

Tesi di Dottorato di:

Tiziana ALDERUCCI

Tutor:

Chiar.mo Prof. Ing.
Giuseppe MUSCOLINO

TRIENNIO 2014-2016

To my little daughter

Carlotta

Acknowledgments

It is very difficult for me to write these few words, since it means that my Ph.D. is coming to the end.

First of all my sincere thank goes to Professor Muscolino, who followed, supported (and tolerate!) me during these three years. It was a beautiful experience to work with him, since he continuously gave me ideas and suggestions for my study. Professor Muscolino contributed to my professional growth, making me “fall in love” with research.

An important thank goes to my family, major presence in my life; my parents always encouraged me, and they have spurred me to never give up.

Last, but not least, a special thank goes to my husband Sebastiano, who patiently waited for me every time that commitments made me come back home late.

And to my little Carlotta… Thanks!

Index

Summary **1**

Chapter 1 - Preliminary definitions **5**

1.1 Introduction 5

1.2 Random variables and random process 5

1.3 Stationary Gaussian random processes 9

1.4 Stationary spectral moments 12

1.5 Distribution of extreme values for stationary random process 16

Chapter 2 - Models of the ground motion acceleration process **21**

2.1 Introduction 21

2.2 Real earthquakes 26

2.3 The evolutionary process model 36

2.3.1 Definition of the non-stationary stochastic input 36

2.3.2 Models of the non-stationary random process 38

2.4 Wavelet analysis 42

2.5 Adaptive chirplet decomposition 45

2.6 Fully non-stationary spectrum compatible seismic waves 48

2.6.1 Simulation of the random process samples 48

2.6.2 Stationary spectrum-compatible accelerograms 50

2.6.3 Non-stationary spectrum-compatible accelerograms 52

2.7 Multi-correlated seismic input 56

2.7.1 Introduction 56

2.7.2 The evolutionary process model for multi-correlated input 57

2.7.3 The sigma-oscillatory process model for multi-correlated input 62

2.7.4 Simulation of non-stationary stochastic multi-correlated sigma-oscillatory vector processes 68

2.8 Numerical Applications 73

2.8.1 Fully non-stationary spectrum-compatible artificial earthquakes 73

2.8.2 Multi-correlated seismic input 80

2.9 Summary and conclusions 87

Chapter 3 - Spectral characteristics of the response 91

3.1 Introduction 91

3.2 Classically damped structures subjected to mono-correlated input 93

3.2.1 Equations of motion 93

3.2.2 Evaluation of *NGSMs* 96

3.2.2 Stationary *SMs*……..…96

3.3 Classically damped structures subjected to multi-correlated input 102

3.3.1 Equations of motion 102

3.2.2 Evaluation of the *NGSMs* 104

3.4 Non-Classically damped structures subjected to mono-correlated input 109

3.4.1 Equations of motion 109

3.4.2 Evaluation of the *NGSMs* 111

3.5 Monte Carlo simulation for the evaluation of *NGSMs* 114

3.5.1 Classically damped structures subjected to mono-correlated input 115

3.5.2 Classically damped structures subjected to multi-correlated input 117

3.5.3 Non-Classically damped structures subjected to mono-correlated input 119

3.6 The Role of *NGSMs* in reliability analysis of structures 120

3.7 Summary and conclusions 122

Chapter 4 - Closed form solutions of the *EPSD* function matrix of the response 125

4.1 Introduction 125

4.2 Closed form solution of the *EPSD* matrix 127

4.2.1 Closed form solutions for classically damped structures subjected to mono-correlated input 127

4.2.2 Closed form solutions for classically damped structures subjected to multi-correlated input.....132

4.2.3 Closed form solutions for non-classically damped structures subjected to mono-correlated input 139

4.3 Numerical applications.....143

4.3.1 Classically damped systems subjected to mono correlated input.....143

4.3.2 Classically damped systems subjected to multi-correlated input.....162

4.3.3 Non-classically damped system subjected to mono-correlated input.....168

4.4 Summary and conclusions.....186

Chapter 5 - First passage probability problem 189

5.1 Introduction.....189

5.2 First passage probability problem: preliminary concepts.....193

5.2.1 Methods requiring the mean up-crossing rate of given thresholds.....193

5.2.2 Methods requiring censored closures 198

5.3 Reliability assessment 203

5.4 Numerical Applications.....205

5.4.1 Single-Degree of Freedom systems.....205

5.4.2 Multi-Degrees of Freedom systems.....211

5.5 Summary and conclusions.....226

Conclusions 229

Appendix A - *TFR* vector functions 233

A.1 Evolutionary process model..... 233

A.1.1 General solution 233

A.1.2 Normalized exponential type I modulating function.... 234

A.1.3 Normalized exponential type II modulating function .. 236

A.1.4 Normalized Jennings et al type modulating function.. 238

A.1.5 Spanos and Solomos model of the fully non-stationary process..... 241

A.2. Sigma-oscillatory process model..... 242

A.3 Adaptive chirplet decomposition..... 244

References 249

"Earthquakes systematically bring out the mistakes made in design and construction – even the most minute mistake;

it is this aspect of earthquake engineering that makes it challenging and fascinating, and gives it an educational value far beyond its immediate objectives"

Newland N.M. and Rosenblueth E. *Fundamentals of earthquake engineering*, (1971), Prentice-Hall Inc., Englewood Cliffs, N. J..

Summary

In the framework of the design and of the reliability assessment of fixed structures, among the static and dynamic loads that have to be considered, certainly the most important one is the seismic load, due to its terrible and disastrous consequences, not only in terms of the breakdown of the structure but also for the preservation of life. In fact during the past decades Italy has been the scene of terrible earthquakes, that destroyed whole cities and with a lot of human victims. First of all, in terms of magnitude and, unfortunately, a large number of deaths, Messina earthquake, in 1908, caused about 120000 victims, between Messina and Reggio Calabria, with an estimated magnitude of 7.1 (Richter scale). Then Irpinia earthquake, in 1980 (2914 victims, 6.5 Ricther), L'Aquila earthquake, in 2009 (309 victims, 5.9 Ricther) and the last events in 2016 in the centre of Italy, see Amatrice (299 victims, 6 Richter), Ussita (5.9 Richter), and Norcia (2 victims, 6.1 Ricther).

Due to the difficulty in the prevision of the seismic event, one of the most important and hard problem in seismic engineering is the correct characterization of the ground motion acceleration; in fact it has been demonstrated that it is possible to increase the reliability level of the structures defining in a suitable way the seismic input and shaping realistically the structure.

Nowadays, from the analysis of the large amount of data of recorded events, it is possible to study the main characteristics of real earthquakes and reproduce them with analytical models. In particular, because of the randomness of the seismic event, in terms of energy distribution and intensity, propagation path of the seismic waves through any specified location from the earthquake focus to the epicenter, etc…, it has been shown that it should be modelled as a stochastic process.

On the other hand, once the input has been defined, the second problem in the seismic engineering is the reliability assessment of the structures subjected to the ground motion acceleration. It is obvious that, if the excitations are modelled as random processes, the dynamic responses are random processes too, and the structural safety needs to be evaluated in a probabilistic sense. Among the models of failure, the simplest one, which is also the most widely used in practical analyses, is based on the assumption that a structure fails as soon as the response at a critical location exits a prescribed safe domain for the first time. In random vibration theory, the problem of probabilistically predicting this event is termed *first passage problem*. Unfortunately, this is one of the most complicated problem in computational stochastic mechanics. Therefore, several approximate procedures have been proposed. These procedures lead to the probabilistic assessment of structural failure as a function of barrier crossing rates, distribution of peaks and extreme values. The latter quantities can be evaluated, for non-stationary input process, as a function of the well-known *Non-Geometric Spectral Moments* (*NGSMs*).

Aim of this thesis is to propose a novel procedure to obtain closed form solutions of the spectral characteristics of the response of linear structural systems subjected to seismic acceleration modelled as

stochastic processes. The proposed method is a powerful tool in the analysis of both classically and non-classically damped systems, in reliability assessment problems and takes into account also the case of multi-correlated forcing input.

In Chapter 1 the preliminary definitions of probability theory are outlined, starting from the concept of random variable and stochastic process, analysing the stationary Gaussian random process with its statistics, with a short discussion on the probability distribution for maxima.

Chapter 2 focuses on the characterization of the ground motion acceleration, thanks' to a statistical analysis of a set of real earthquakes; the different strategies to model the ground motion acceleration stochastic process will be investigated. Furthermore, in order to follow the prescriptions of the building codes, a procedure to generate artificial fully non-stationary spectrum-compatible accelerograms will be proposed.

The spectral characteristics of the response of linear structural systems, subjected to non-stationary excitation, will be obtained in Chapter 3 and, in Chapter 4, closed form solutions of the *Time-Frequency varying Response* (*TFR*) *vector function* will be proposed. In particular the main steps of the proposed approach are: i) the use of modal analysis, or the complex modal analysis, to decouple the equation of motion; ii) the introduction of the modal state variable in order to evaluate the *NGSMs*, in the time domain, as element of the *Pre-Envelope Covariance* (*PEC*) matrix; iii) the determination, in state variable, by very handy explicit closed-form solutions, of the *TFR vector functions* and of the *Evolutionary Power Spectral Density* (*EPSD*) matrix function of the structural response for the most common adopted models of the seismic input in the framework of stochastic analysis; iv) the evaluation of the

spectral characteristics of the stochastic response by adopting the closed-form expression of the *EPSD* matrix function.

Finally, in Chapter 5 the reliability assessment of structural systems will be performed; in particular two different approaches for the first passage probability problem will be used: the method requiring the evaluation of the mean up-crossing rate of given thresholds, considered independent or occurring in clumps, and the method requiring censored closures of the non-stationary extreme value random response process.

Several numerical applications will be done in order to test the effectiveness of the proposed procedure; in particular the presented results will be compared with the Monte Carlo simulation method, that will confirm the validity and the generality of the proposed method.

Chapter 1

Preliminary definitions

1.1 Introduction

The main aim of this Chapter is to give general, preliminary definitions that may be useful in reading this thesis.

The concept of random variable and random process will be firstly introduced, in order to probabilistically describe a random event. Then the class of stationary Gaussian random process and their statistics will be discussed, together with their characterization both in the time domain and in the frequency domain.

The last part of this Chapter is dedicated to a short discussion on the distribution of the extreme value of a random process, that will be further discussed in the last Chapter in the framework of reliability assessment.

1.2 Random variables and random process

A variable X is called *random variable* (or *stochastic variable*) when it mathematically describes the results of a random event whose domain is a numeric ensemble.

With the concept of a random variable, we can adopt numerical values to describe the results of any random experiment. For

instance, an elementary event is expressed in the form that a random variable X is equal to one deterministic number (i.e. $X = x$), while any arbitrary event can be expressed in a way that X takes values over an interval $x_1 \le X \le x_2$ and its probability of occurring is denoted by $\Pr\langle x_1 \le X \le x_2 \rangle$. There are two basic types of random variable: *discrete* random variable, when it assumes values in a finite set, and *continuous* random variable, if it can take any value in one or several intervals (Li and Chen 2009).

The *Cumulative Distribution Function* (*CDF*) and the *Probability Density Function* (*PDF*) of the random variable X are defined, respectively, as:

$$L_X(x) = \Pr\langle X \le x \rangle; \quad p_X(x) = \frac{\mathrm{d}}{\mathrm{d}x} L_X(x). \tag{1.1}$$

Then a *random process* $X(t)$ is a family of *n* random variables related to a similar phenomenon which may be functions of one or more independent variables.

The stochastic process can be viewed in terms of its possible time-histories; for example, considering the ground motion acceleration as a stochastic process, any earthquake ground acceleration record might be thought as one of the many time histories that could have occurred for an earthquake with the same intensity at that site (Lutes and Sarkani 1997).

As shown in Figure 1.1 the samples of the stochastic process are indicated with $X^{(r)}(t)$ $(r = 1, 2, \ldots, \infty)$.

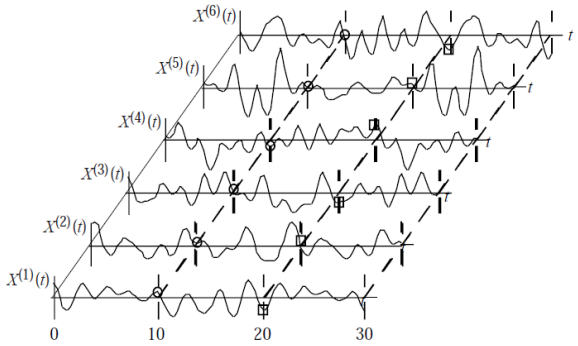

Figure 1. 1 Ensemble of time histories of $X(t)$ (Lutes and Sarkani 1997).

The ensemble of the coordinates for a given instant $X^{(r)}(t_1)$ $(r=1,2,\ldots,\infty)$ gives the realizations of the random variable $X(t_1)$. In this way, the basic idea is that for every possible t_1 value there is a random variable $X(t_1)\equiv X_1$, whose *CDF* and *PDF* are defined, respectively, as:

$$L_{X_1}(x_1)=\Pr\langle X_1\le x_1\rangle\equiv\Pr\langle X(t_1)\le x_1\rangle;\quad p_{X_1}(x_1)=\frac{\mathrm{d}}{\mathrm{d}x_1}L_{X_1}(x_1). \quad (1.2)$$

It is obvious that in order to have a complete probabilistic description of a stochastic process $X(t)$, one must know the probability distribution for every set of random variables belonging to that process.

Alternatively, the stochastic process $X(t)$ can also be defined from the knowledge of the moment functions of various orders, which are defined as:

$$\mathrm{E}\left[X\left(t_1\right)\right]=\int_{-\infty}^{+\infty} x_1\, p_{X(t_1)}\left(x_1\right)\mathrm{d}x_1$$

$$\mathrm{E}\left[X\left(t_1\right)X\left(t_2\right)\right]=\int_{-\infty}^{+\infty}\int_{-\infty}^{+\infty} x_1 x_2\, p_{X(t_1)}\left(x_1\right)p_{X(t_2)}\left(x_2\right)\mathrm{d}x_1\mathrm{d}x_2 \qquad (1.3)$$

……

Specifically, the *mean value*, or expected value, $\mu_X\left(t\right)$, of the random process $X\left(t\right)$ coincides with the first order moment:

$$\mu_X\left(t\right)=\mathrm{E}\left[X\left(t\right)\right]=\int_{-\infty}^{+\infty} x\, p_{X(t)}\left(x\right)\mathrm{d}x. \qquad (1.4)$$

The *variance* at time t, $\sigma_X^2\left(t\right)$, of the random process $X\left(t\right)$ is calculated as a function of the mean value $\mu_X\left(t\right)$ and of the *mean square value*, $\varphi_X^2\left(t\right)$:

$$\sigma_X^2\left(t\right)=\varphi_X^2\left(t\right)-\mu_X^2\left(t\right)=\int_{-\infty}^{+\infty} x^2\, p_{X(t)}\left(x\right)\mathrm{d}x-\mu_X^2\left(t\right). \qquad (1.5)$$

Furthermore the most important joint measure in a random process is the correlation of the process with itself at two different times, $X\left(t_1\right)$ and $X\left(t_2\right)$. This measure of correlation is called autocorrelation function and it is defined as:

$$R_X\left(t_1,t_2\right)=\mathrm{E}\left[X\left(t_1\right)X\left(t_2\right)\right]=\int_{-\infty}^{+\infty}\int_{-\infty}^{+\infty} x_1 x_2\, p_{X(t_1)}\left(x_1\right)p_{X(t_2)}\left(x_2\right)\mathrm{d}x_1\mathrm{d}x_2. \qquad (1.6)$$

1.3 Stationary Gaussian random processes

For many situations in random vibrations, the probability distribution do not appear to evolve over the time intervals of interest to the engineer. In these situations important simplifications in the mathematical analysis may be made (Wirsching et al. 1995).

A process is called *strictly stationary* if the joint probability distribution of $\{X(t_1), X(t_2), X(t_3), \ldots, X(t_n)\}$ is identical to the joint distribution of the same variables displaced an arbitrary amount of time, τ, that is $\{X(t_1+\tau), X(t_2+\tau), X(t_3+\tau), \ldots, X(t_n+\tau)\}$.

The process is called *weakly stationary* (or *stationary in wide sense*) if the mean and the variance of the process are constants, independent of *t*, and the autocorrelation function depends only upon the difference between t_1 and t_2:

$$\begin{aligned} &\mu_X(t) = \mu_X, \\ &\sigma_X^2(t) = \sigma_X^2, \\ &R_X(t_1,t_2) = R_X(t,t+\tau) \equiv R_X(\tau) = \mathrm{E}\left[X(t)X(t+\tau)\right]. \end{aligned} \tag{1.7}$$

In the framework of stochastic dynamics one of the most important random process is the *Gaussian random process*; for this random process the joint distribution of $\{X(t_1), X(t_2), X(t_3), \ldots, X(t_n)\}$ is a normal distribution. Since a normal random variable is completely defined by its mean and variance, all higher moments of the density function are dependent on the variance. Particularly important for application to vibration analysis is the fact that any linear combination of jointly Gaussian random variables is itself Gaussian, and jointly Gaussian with other such linear combinations.

The probability density function of the Gaussian random process is:

$$p_{X_k X_l}\left(x_k, x_l\right) = p_{X_k X_l}\left(x_k, x_l; t_k, t_l\right) = \\ = \frac{1}{2\pi\left(\mathrm{Det}\left[\mathbf{R}_X\left(t_k, t_l\right)\right]\right)^{\frac{1}{2}}} \exp\left[-\frac{1}{2}\boldsymbol{\xi}^T \mathbf{R}_X^{-1}\left(t_k, t_l\right)\boldsymbol{\xi}\right] \tag{1.8}$$

where

$$\boldsymbol{\xi} = \begin{bmatrix} x_k \\ x_l \end{bmatrix} - \mathrm{E}\begin{bmatrix} X_k \\ X_l \end{bmatrix} = \begin{bmatrix} x_k - \mathrm{E}\left[X_k\right] \\ x_l - \mathrm{E}\left[X_l\right] \end{bmatrix}. \tag{1.9}$$

In Eq. (1.8) $\mathbf{R}_X\left(t_k, t_l\right)$ is the correlation matrix, defined as:

$$\mathbf{R}_X\left(t_k, t_l\right) = \begin{bmatrix} R_X\left(t_k, t_k\right) & R_X\left(t_k, t_l\right) \\ R_X\left(t_l, t_k\right) & R_X\left(t_l, t_l\right) \end{bmatrix} = \\ = \begin{bmatrix} \mathrm{E}\left[X_k^2\right] & \mathrm{E}\left[X_k X_l\right] \\ \mathrm{E}\left[X_l X_k\right] & \mathrm{E}\left[X_l^2\right] \end{bmatrix} - \begin{bmatrix} \left(\mathrm{E}\left[X_k\right]\right)^2 & \mathrm{E}\left[X_k\right]\mathrm{E}\left[X_l\right] \\ \mathrm{E}\left[X_l\right]\mathrm{E}\left[X_k\right] & \left(\mathrm{E}\left[X_l\right]\right)^2 \end{bmatrix} \tag{1.10}$$

and it is a simmetrix function, since the relation $R_X\left(t_k, t_l\right) = R_X\left(t_l, t_k\right)$ is satisfied.

In the class of Gaussian random process, a particular attention goes to the *stationary* Gaussian random process (notice that if a Gaussian process is weakly stationary it is also strictly stationary).

A stationary Gaussian process is completely defined from the knowledge of its mean μ_X and its autocorrelation function $R_X\left(\tau\right)$,

in the time domain; however stationary random vibration are more usefully studied in the frequency domain. In this case the stationary Gaussian random process is defined by its mean μ_X and its Power Spectral Density (*PSD*) function $S_X(\omega)$. The *PSD* function of the stationary Gaussian random process is given by the following relation:

$$S_X(\omega) = \frac{1}{2\pi} \int_{-\infty}^{+\infty} R_X(\tau) \exp(-i\omega\tau) \, \mathrm{d}\tau \tag{1.11}$$

that is, except for the coefficient $1/2\pi$, the Fourier transform of the autocorrelation function. The inverse Fourier transform of the *PSD* gives the autocorrelation function:

$$R_X(\tau) = \int_{-\infty}^{+\infty} S_X(\omega) \exp(i\omega\tau) \, \mathrm{d}\omega. \tag{1.12}$$

The Eqs. (1.11) and (1.12) are the celebrated *Wiener-Khinchine relations*, that play a fundamental role in the random vibration analysis.

The variance of the process $X(t)$ represents the area of the *PSD* function; in fact, by substituting $\tau = 0$ in Eq. (1.12):

$$\sigma_X^2 = R_X(0) = \int_{-\infty}^{+\infty} S_X(\omega) \, \mathrm{d}\omega. \tag{1.13}$$

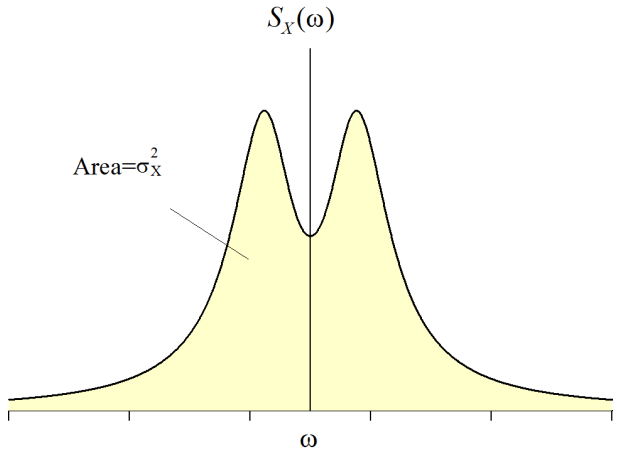

Figure 1. 2 Area between *PSD* function and ω-axis.

Figure 1.2 shows the area between the PSD function and the ω-axis.

1.4 Stationary spectral moments

For a given stationary process, $X(t)$, defined by its mean μ_X, its variance σ_X^2, its autocorrelation function $R_X(\tau)$ and *PSD* function $S_X(\omega)$, the function $G_X(\omega)$

$$G_X(\omega) = \begin{cases} 2S_X(\omega) & 0 \le \omega < +\infty \\ 0 & \omega < 0 \end{cases} \tag{1.14}$$

is called *one-sided PSD function.* This function is a real and positive function in the domain $[0,+\infty)$ ad its area is equal to the area of the *PSD* function, defined in the domain $(-\infty,+\infty)$.

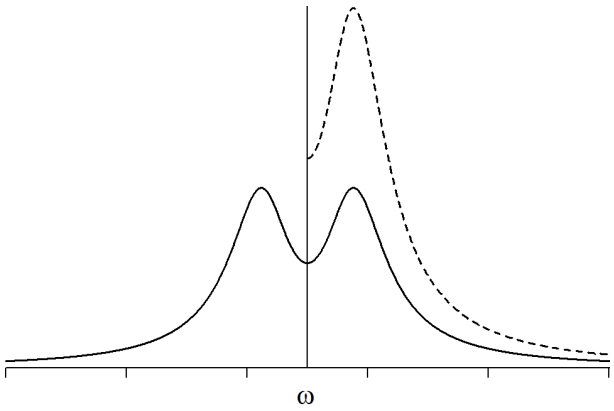

Figure 1. 3 *PSD* function $S_X(\omega)$ (continuous line) and one-sided *PSD* function $G_X(\omega)$ (dashed line) of a stationary random process.

The *Spectral Moments* (*SMs*) $\lambda_{i,X}$, introduced by Vanmarcke (1972), are the moments of the one-sided *PSD* function with respect to the $\omega = 0$ axis:

$$\lambda_{i,X} = \int_0^{+\infty} \omega^i G_X(\omega) \mathrm{d}\omega \qquad i = 0,1,... \tag{1.15}$$

In particular $\lambda_{0,X}$, that represents the area of the function $G_X(\omega)$, is equal to the variance of the process $X(t)$, since the *PSD* function $S_X(\omega)$ is a symmetric function with respect of the axis $\omega = 0$:

$$\lambda_{0,X} = \int_0^{+\infty} G_X(\omega) \mathrm{d}\omega = \int_0^{+\infty} 2S_X(\omega) \mathrm{d}\omega \equiv \int_{-\infty}^{+\infty} S_X(\omega) \mathrm{d}\omega = \sigma_X^2 . \tag{1.16}$$

Then, other useful spectral parameters can be defined:

$$\omega_{1,\mathrm{X}} = \frac{\int_0^{+\infty} \omega G_X(\omega)\,\mathrm{d}\omega}{\int_0^{+\infty} G_X(\omega)\,\mathrm{d}\omega} = \frac{\lambda_{1,X}}{\lambda_{0,X}}, \tag{1.17}$$

$$\omega_{2,\mathrm{X}} = \left(\frac{\int_0^{+\infty} \omega^2 G_X(\omega)\,\mathrm{d}\omega}{\int_0^{+\infty} G_X(\omega)\,\mathrm{d}\omega} \right)^{1/2} = \sqrt{\frac{\lambda_{2,X}}{\lambda_{0,X}}} \tag{1.18}$$

where $\omega_{1,X}$ is the frequency at the area centric of $G_X(\omega)$, that indicates where the spectral density concentrates, and $\omega_{2,X}$ is the is the gyration radius of the area under the function $G_X(\omega)$.

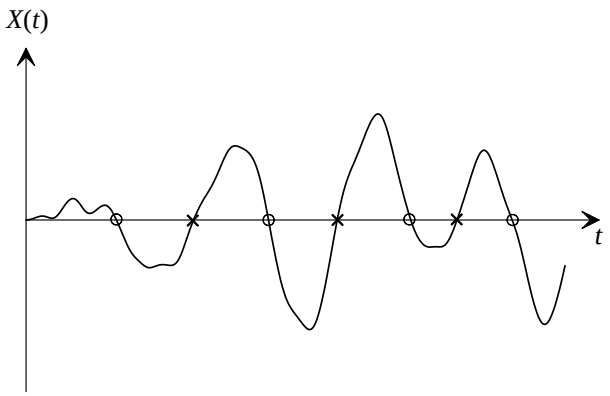

Figure 1. 4 Up-crossing (×) and down-crossing (○) rate of the time axis of the random process $X(t)$.

Another important parameter is the mean frequency, ν_X^+, which evaluates the variation in time of the mean up-crossing rate of the time axis (see Figure 1.4):

$$\nu_X^+ = \frac{\omega_{2,X}}{2\pi}. \tag{1.19}$$

The barycenter gyration radius $\varpi_{2,X}$, or the measure of the dispersion around the frequency at the area centric of $G_X(\omega)$, is:

$$\varpi_{2,X} = \sqrt{\frac{1}{\lambda_{0,X}}\left(\lambda_{2,X} - \frac{\lambda_{1,X}^2}{\lambda_{0,X}}\right)} = \delta_X \omega_{2,X} \tag{1.20}$$

where

$$\delta_X = \sqrt{1 - \frac{\lambda_{1,X}^2}{\lambda_{0,X}\lambda_{2,X}}} \qquad 0 \le \delta_X \le 1 \tag{1.21}$$

is a non-dimensional parameter and it is called *bandwidth parameter*, directly corresponding to coefficient of variation, that measures the variation in the time of the narrowness of the stochastic process $X(t)$.

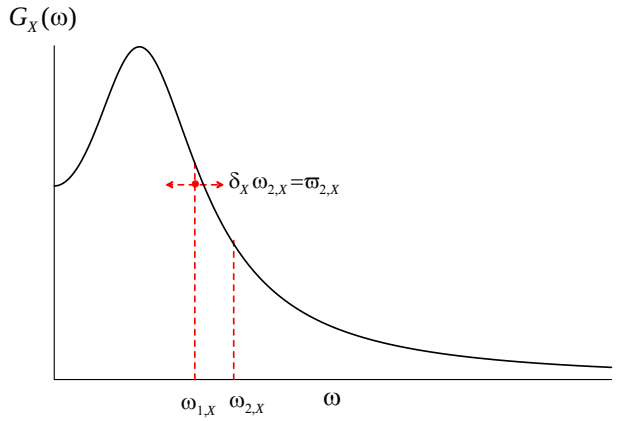

Figure 1. 5 Geometric representation of the *SMs* of the one-sided *PSD* function $G_X(\omega)$.

From the analysis of Figure 1.5 it is possible to have an immediate geometric representation of the *SMs* of the one-sided *PSD* function $G_X(\omega)$.

1.5 Distribution of extreme values for stationary random process

The probability distribution of extrema of a random process is of particular interest in engineering design problems. In general, the extreme value of a stochastic process is a random variable.

Consider a zero-mean stationary Gaussian process $X(t)$ having an arbitrary *PSD* function $S_X(\omega)$. A sample of this process shows positive and negative maxima and positive and negative minima. For simplicity it is possible to define a new random process $X_{\max}(t)$ that represents the extreme value of $X(t)$:

$$X_{\max}(t)=\max_{0\le s\le t}\left|X(s)\right| \tag{1.22}$$

where the symbol $|\bullet|$ denotes absolute value.

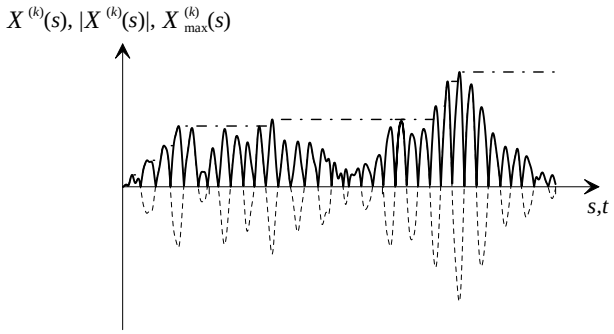

Figure 1. 6 Samples of the random process $X(t)$ (dashed line), of the corresponding absolute value $|X(t)|$ (continuous line) and of the extreme value random process $X_{\max}(t)$ (dash dot line).

In this way, the extreme value distribution for $X(t)$ is simply the distribution of the $X_{\max}(t)$ random variable. The *CDF* of the $X_{\max}(t)$ random variable can be expressed as:

$$L_{X_{\max}(t)}(u,t) \equiv \Pr\left\langle X_{\max}(t) \le u \right\rangle \equiv \Pr\left\langle X(s) \le u : 0 \le s \le t \right\rangle \tag{1.23}$$

in which the notation on the final term means that the $X(s) \le u$ inequality holds for all the given *s* values. The *PDF* for the extreme value, of course, is simply the derivative

$$p_{X_{\max}(t)}(u) = \frac{\mathrm{d}}{\mathrm{d}u} L_{X_{\max}(t)}(u,t) \tag{1.24}$$

and from this information one can also calculate the mean, variance, and so forth.

Once the *PDF* of the random process $X_{\max}(t)$ is defined, it is possible to derive another important parameter, very useful in engineering design problems, that is the lower fractile $X_{t,\mathrm{p}}$; $X_{t,\mathrm{p}}$ represents the probability p that the maximum of the process $|X(t)|$ is inferior or equal to $X_{t,\mathrm{p}}$ in the time interval $[0,t]$:

$$F_{X_{\max}}\left(X_{t,\mathrm{p}};t\right) \equiv \Pr\langle X_{\max}(t) \le X_{t,\mathrm{p}}\rangle = \mathrm{p}. \tag{1.25}$$

The previous equation is a non-linear differential equation that can be alternatively solved introducing the dimensionless quantity $\eta_X(t,\mathrm{p})$:

$$\eta_X(t,\mathrm{p}) = X_{t,\mathrm{p}} / \sigma_X . \tag{1.26}$$

$\eta_X(t,\mathrm{p})$ is called *peak factor* and represents the lower fractile of probability p of the dimensionless random process $Y(t) = X_{\max}(t)/\sigma_X$. The peak factor can be obtained from the solution of the differential equation:

$$F_{X_{\max}}\left(\eta_X(t,\mathrm{p})\sigma_X;t\right) \equiv \Pr\langle X_{\max}(t)/\sigma_X \le \eta_X(t,\mathrm{p})\rangle = \mathrm{p}. \tag{1.27}$$

A lot of hypothesis for the evaluation of the peak factor have been done in the literature; in particular for narrow band process the peak factor is given as (Vanmarcke 1975):

$$\eta_X(t,\mathrm{p}) = \left\{ 2\ln\left\{ \frac{t}{\pi}\sqrt{\frac{\lambda_{2,X}}{\lambda_{0,X}}}\left(-\ln \mathrm{p}\right)^{-1} \right.\right. \\ \left.\left. \times\left[1-\exp\left[-\delta_X^{1.2}\sqrt{\pi\ln\left(\frac{t}{\pi}\sqrt{\frac{\lambda_{2,X}}{\lambda_{0,X}}}\left(-\ln \mathrm{p}\right)^{-1} \right)} \right] \right] \right\}^{1/2} . \tag{1.28}$$

Once the peak factor $\eta_X(t,\mathrm{p})$ and the lower fractile $X_{t,\mathrm{p}}$ have been defined it is possible to deal with the reliability assessment of linear structures subjected to zero-mean stationary Gaussian random process. This problem will be further discussed in Chapter 5.

Chapter 2

Models of the ground motion acceleration process

2.1 Introduction

The first step in structural engineering deals with a proper definition of the structural model and loads. For earthquake-resistant design of structures, the earthquake-induced ground motion is generally represented in the form of a response spectrum of pseudo-acceleration or displacement. The spectrum used as input is usually obtained by scaling an elastic spectrum by factors that account for, amongst other phenomena, the influence of inelastic structural response (Chopra 1995). There are, however, situations in which the scaled response spectrum is not considered appropriate, and a fully dynamic analysis is required. These situations may include structures with configuration in plan or elevation that is highly irregular; structures for which higher modes are likely to be excited; structures with special devices to reduce the dynamic response; buildings designed for a high degree of ductility and so on. Faced with these special situations, the engineer will generally have to employ time-history analysis, for which the requirements are

appropriate linear or non-linear models for the structure and a suitable suite of accelerograms to represent the seismic excitation (Bommer and Acevedo 2004).

There are three basic options available to the engineer in terms of obtaining suitable accelerograms. The first approach requires the generation of synthetic accelerograms from seismological source models and accounting for path and site effects (Lam et al. 2000, Rezaeian and Der Kiureghian 2010). In general, there are actual difficulties in defining appropriate input parameters such as the source, path, and site characteristics. Moreover, to generate synthetic accelerograms there is a need for a definition of a specific earthquake scenario in terms of magnitude, rupture mechanism in addition to geological conditions and location of the site. Generally, most of these parameters are not often available, particularly when using seismic design codes. It follows that the main limit of this approach is that practitioners cannot always accurately characterize the seismological threat to generate appropriate synthetic signals.

The second approach adopts real accelerograms recorded during earthquakes (Iervolino et al. 2010, Katsanos et al. 2010). Real accelerograms contain a wealth of information about the nature of the ground shaking, carry all the ground-motion characteristics (amplitude, frequency, and energy content, duration and phase characteristics), and reflect all the factors that influence accelerograms (characteristics of the source, path, and site). Due to the increase of available strong ground motion acceleration records, using and scaling real recorded accelerograms becomes one of most referenced contemporary research issues in this field. Despite the continued growth of the global strong motion database, there are many combinations of earthquake parameters such as magnitude, rupture mechanism, source-to-site distance and site classification

that are not well represented. It follows that their manipulation is relatively simple but often confusing and it is difficult to obtain suitable records in some circumstances.

The third approach uses artificial spectrum-compatible accelerograms. Artificial accelerograms are generated to match a target elastic response spectrum by obtaining a *Power Spectral Density* (*PSD*) function from the smoothed response spectrum, and then to derive harmonic signals having random phase angles (Vanmarcke and Gaparini 1977, Kaul 1978, Pfaffinger 1983, Preumont 1984, Cacciola et al. 2004). The attraction of these approaches is obvious because it is possible to obtain acceleration time-series that are almost completely compatible with the elastic design spectrum, which in some cases will be the only information available to the design engineer regarding the nature of the ground motions to be considered.

The simulation of artificial accelerograms is usually based upon a stationary stochastic zero-mean Gaussian process assumption; the stationary non-white models were suggested first by Kanai (1957), Tajimi (1960), Housner and Jennings (1964). These models, which account for site properties and for the dominant frequency in ground motion, fail to reproduce the typical characteristics of the real earthquakes: stationary artificial accelerograms generally have an excessive number of cycles of strong motion and consequently they possess unreasonably high energy content (Wang et al. 2005). Furthermore, the stationary model suffers the major drawback of neglecting the changes in amplitude and frequency content.

In order to overcome this drawback the so-called *quasi-stationary* (or *uniformly modulated non-stationary*) random processes have been introduced (see Shinozuka and Sato 1967, Aming and Ang 1968, Iyengar and Iyengar 1969, Jennings et al.

1969, Hsu and Bernard 1978, Iwan and Hou 1989). These processes are constructed as the product of a stationary zero-mean Gaussian random process by a deterministic function of time; for this reason they are also called *separable non-stationary stochastic processes*.

Furthermore, a time-varying frequency content is observed in actual accelerogram records. This non-stationary frequency is prevalently due to different arrival times of the primary, secondary and surface waves that propagate at different velocities through the earth crust. Moreover, it has been shown that the non-stationarity in frequency content can have significant effects on the response of structures (see e.g. Saragoni and Hart 1973, Yeh and Wen 1990). The stochastic processes involving both the amplitude and the frequency changes are referred in literature as *fully non-stationary* random processes. The spectral characterization of the fully non-stationary processes is usually performed by introducing the *Evolutionary Power Spectral Density* (*EPSD*) function (Priestley 1965). On the contrary of the stationary case, the *EPSD* function cannot be defined univocally. Then, several models have been proposed in literature. In particular Preumont (1985) derived the *EPSD* function by imposing to the non-stationary model the equality of the average energy for each frequency with respect the stationary case. Saragoni and Hart (1973) proposed a fully non-stationary model by juxtaposing time segments of gamma-functions modulated filtered zero-mean Gaussian white noises; Spanos and Solomos (1983) proposed a *non-separable* model introducing a particular *EPSD* function; Yeh and Wen (1990) and Fan and Ahmadi (1990) proposed a generalization of the Kanai-Tajimi model; Conte and Peng (1997) defined the ground motion acceleration as the sum of a finite number of pairwise independent uniformly modulated zero-

mean Gaussian stochastic process, the so-called sigma-oscillatory processes.

Another powerful strategy to analyse the evolutionary frequency content is based on the wavelet analysis (Spanos and Failla 2004, Spanos et al. 2005, Mallat 2009). Wavelet analysis is well suited to identify and preserve non-stationarity because the wavelet basis consist of compact functions of varying lengths. Each wavelet function corresponds to a finite portion of the time domain and has a different bandwidth in the frequency domain. The multiscale nature of wavelet analysis facilitates the simultaneous evaluation of non-stationarity in the time and frequency domains. Wavelet analysis has been performed by Suàrez and Montejo (2005) to simulate non-stationary ground motions. Moreover, several studies have been carried out to obtain fully non-stationary spectrum-compatible artificial accelerograms (Mukherjee and Gupta 2002, Giaralis and Spanos 2009 and Cecini and Palmeri 2015).

Alternatively, adaptive signal processing techniques can be adopted, such as the decomposition of the signal on a Gaussian chirplet set of functions and the empirical mode decomposition (see Yin et al. 2002, Politis et al. 2006, Spanos et al. 2007).

After a deep analysis of real earthquakes, in order to understand their main characteristics, the principal purpose of this Chapter is to examine the different models of the ground motion acceleration process that have been proposed in literature, for both the mono-correlated and the multi-correlated input process.

Furthermore, a procedure to generate artificial spectrum-compatible fully non-stationary accelerograms is proposed; the generation of fully non-stationary accelerograms is performed in three steps. In the first step the spectrum-compatible *PSD* function in the hypothesis of stationary excitations is derived. In the second step

the spectrum-compatible *EPSD* function is obtained by an iterative procedure to improve the match with the target response spectrum starting from the stationary *PSD* function, once a time-frequency modulating function is chosen. In the third step the accelerograms are generated by the Shinozuka and Jan (1972) formula and deterministic analyses can be performed to evaluate the structural response.

2.2 Real earthquakes

Earthquakes are vibrations of the earth surface caused by sudden movements of the earth crust which consists of rock plates that float on the earth mantle. The ground motion is due to the rupture of the rock when the shear stress exceeds the strength of the rock and the energy is released in the form of seismic waves. Two of the most common parameters related to a seismic event are the earthquake *magnitude* (M) and *distance* (R) (in km) of the rupture zone from the site of interest.

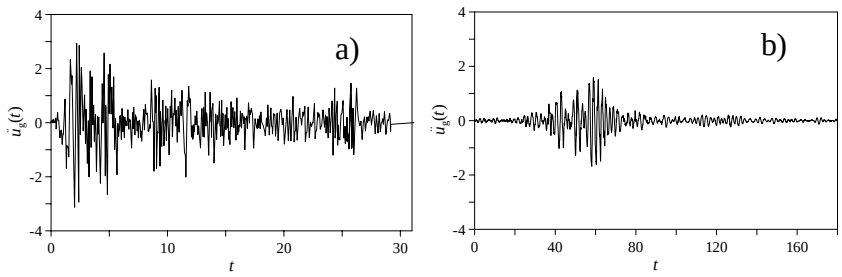

Figure 2. 1 a) El Centro NS recorded earthquake, 1940; b) Mexico City N90W recorded earthquake, 1985.

It is obvious that every accelerogram is sensitively different from the others, as shown in Figure 2.1, mainly due to the characteristics of the specific location of the propagation path of the seismic waves.

For engineering purposes, the ground motion caused by seismic waves is measured by accelerometers or accelerographs which record three components of the ground acceleration, two horizontal and one vertical. The earthquake accelerograms by themselves provide general information among which the *Peak Ground Acceleration* (*PGA*) and the *total seismic duration* t_d. The *PGA* is the most simple and widely used intensity index for seismic structural analysis purposes. It is also adopted in many structural design codes or provisions worldwide. Although *PGA* is an important intensity index, its scope of application is limited because a single measure is unable to fully describe the complex earthquake characteristics. For further information an elaboration of the accelerograms is necessary. The results of this elaboration are characteristic parameters, either in the time or in the frequency domain. Some parameters in the time domain are the *ARIAS intensity*, the *HUSID diagram*, *the Strong Motion Duration* (*SMD*). On the other hand, some parameters in the frequency domain are the s*pectral intensities* and the *Fourier spectra*. The ARIAS intensity is a measure of the strength of a ground motion and it is usually defined by the following relationship:

$$I_{\mathrm{A}} = \frac{\pi}{2\mathrm{g}} \int_0^{t_d} \ddot{u}_{\mathrm{g}}^2(t)\,\mathrm{d}t\,, \tag{2.1}$$

where g is the acceleration due to gravity and $\ddot{u}_{\mathrm{g}}(t)$ is the recorded accelerogram. The HUSID diagram, $H(t)$, is the time history of the seismic energy content scaled to the total energy content and it is defined by the following relation:

$$H(t)=\frac{\int_0^t \ddot{u}_g^2(\tau)\,\mathrm{d}\tau}{\int_0^{t_d} \ddot{u}_g^2(t)\,\mathrm{d}t}. \tag{2.2}$$

By means of the HUSID diagram it is possible to define the *SMD*, T_s, as the time elapsed between the 5% and 95% of the HUSID diagram defined by the following relation:

$$T_s = t_{0.95} - t_{0.05} \tag{2.3}$$

where $t_{0.95}$ is the time elapsed at the 95% of the HUSID diagram and $t_{0.05}$ the time elapsed at the 5% of the HUSID diagram.

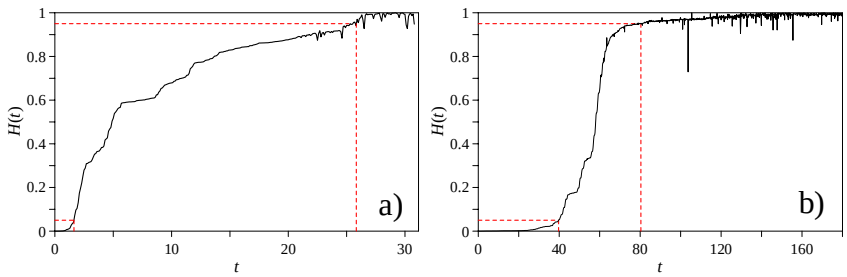

Figure 2. 2 Husid Function and definition of the *SMD*: a) El Centro NS, 1940; b) Mexico city N90W, 1985.

Table 2. I Characteristics of real earthquakes.

Site	Year	*PGA* a_{max} [m/s^2]	Arias Intensity I_A [m/s]	Duration t_d [s]	*SMD* T_s [s]	$t_{0.05}$ [s]	$t_{0.95}$ [s]
El Centro NS	1940	3.13	1.78	31.16	24.20	1.63	25.83
Mexico City	1985	1.68	2.45	180.08	40.71	39.68	80.38

In order to understand the main characteristics of real earthquakes, a statistical study has been performed, by selecting a

set of recorded accelerograms and analysing the time-frequency behaviour.

The chosen database is the "PEER: Pacific Earthquake Engineering Research Center: NGA Database"; 30 recorded accelerograms have been selected to perform the statistical analysis. In particular, all of them are time histories of seismic events that happened in the Imperial Valley (California) (see Figures 2.3, 2.4).

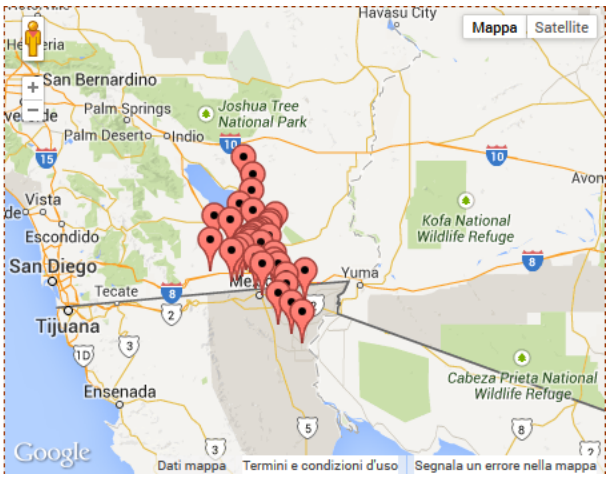

Figure 2. 3 Some of the seismic events in Imperial Valley.

In the following Figures all the ground motion time history are shown.

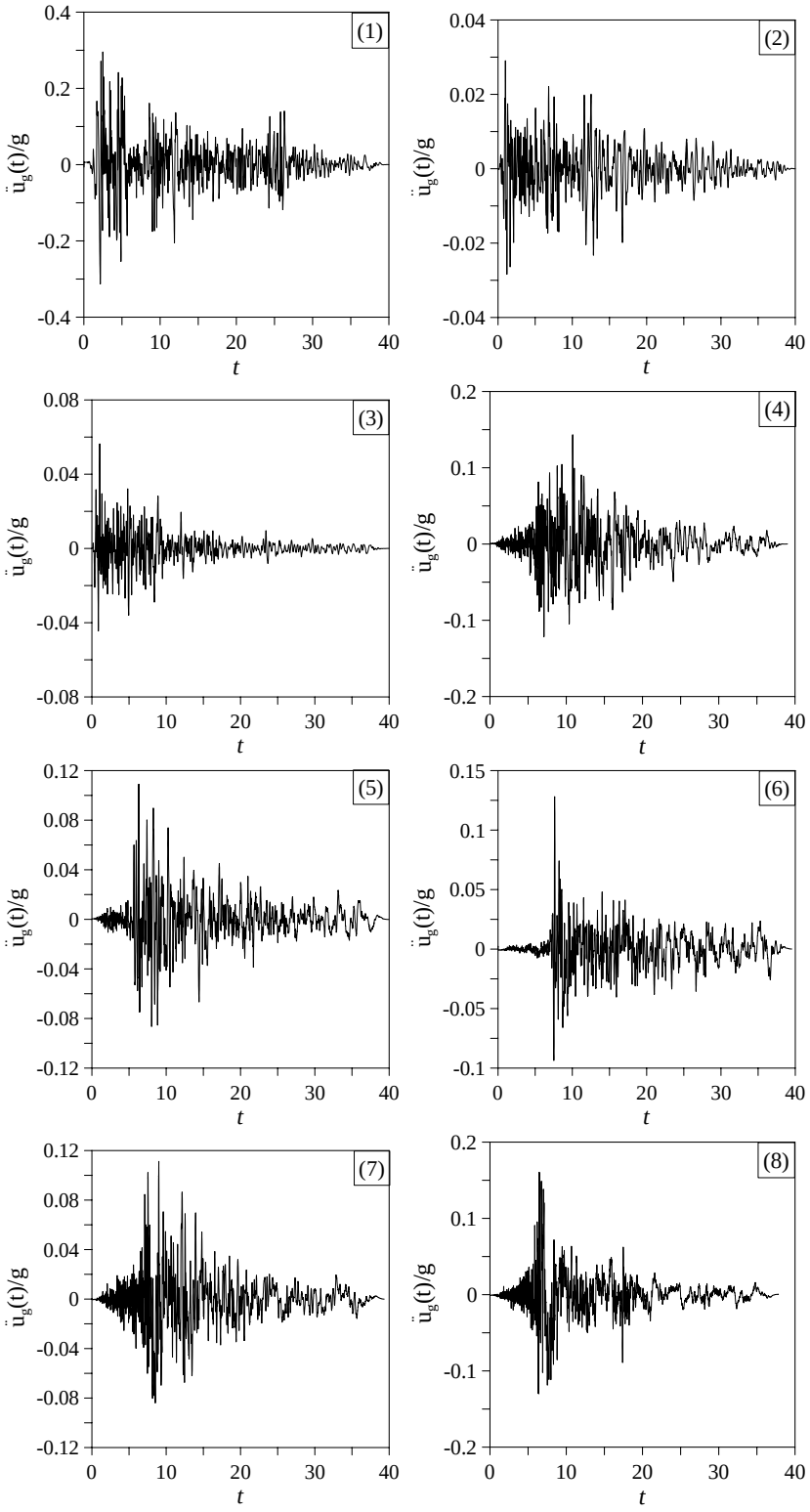

Figure 2.4 a) Registration of earthquakes in the Imperial Valley, California.

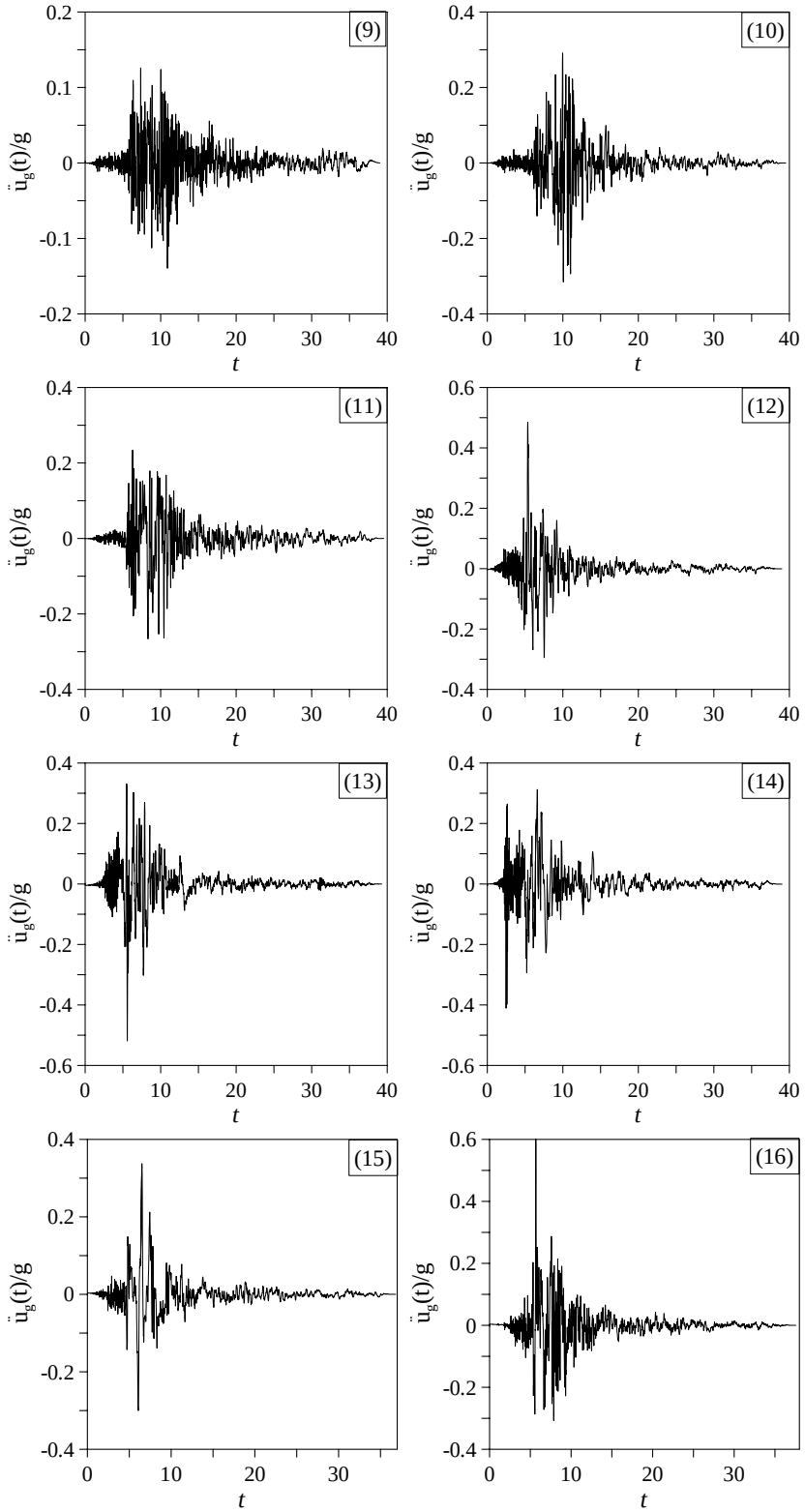

Figure 2.4 b) Registration of earthquakes in the Imperial Valley, California.

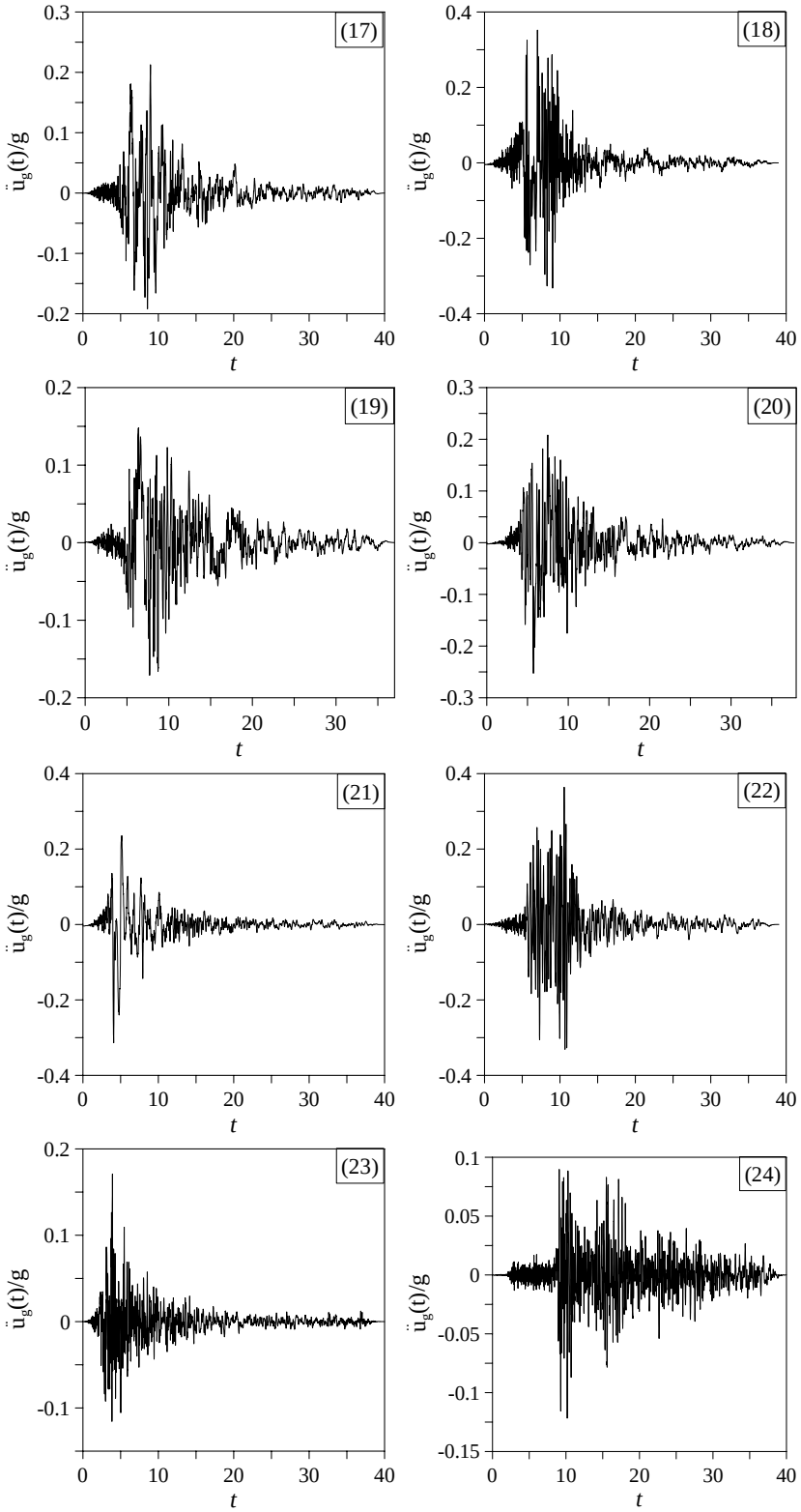

Figure 2.4 c) Registration of earthquakes in the Imperial Valley, California.

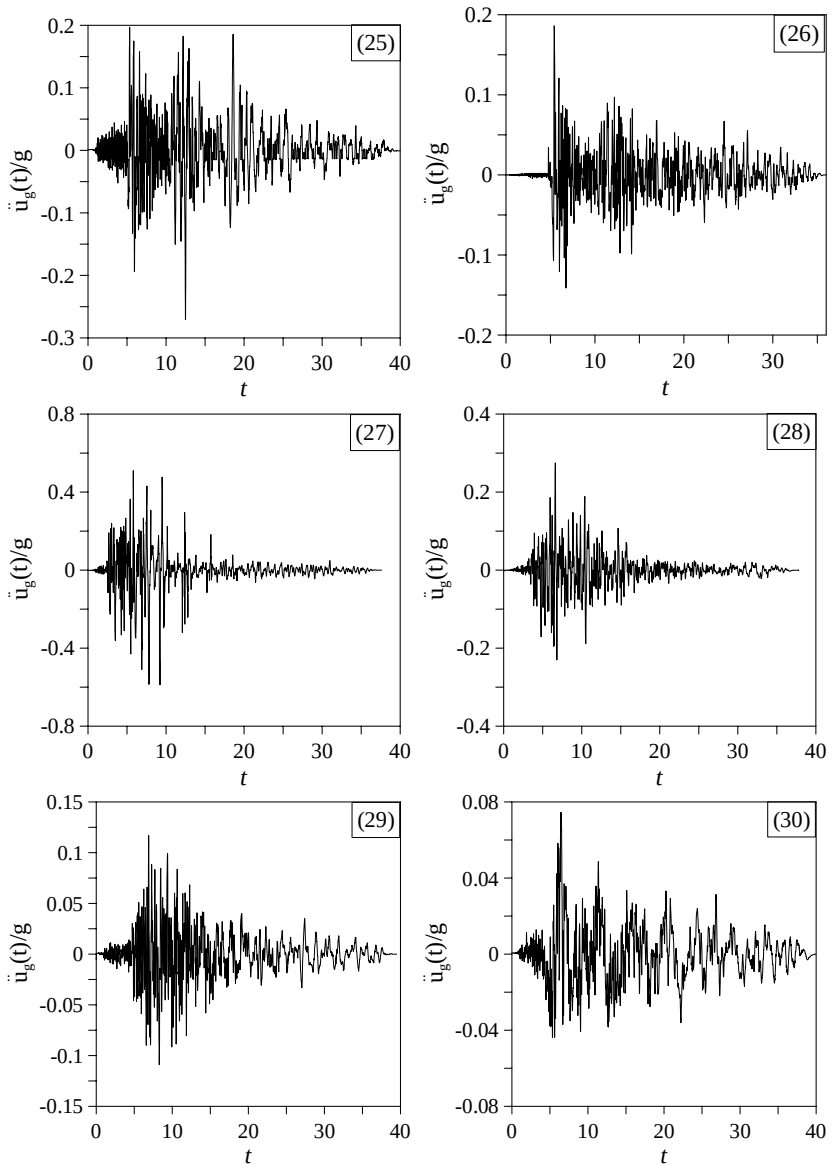

Figure 2. 4 d) Registration of earthquakes in the Imperial Valley, California.

For each of the recorded accelerograms the mean frequency has been evaluated, as shown in Figure 2.5.

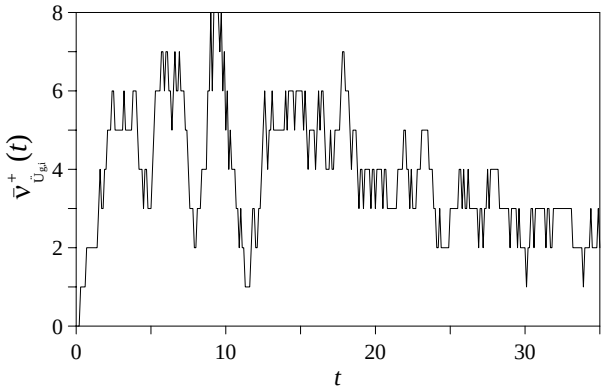

Figure 2. 5 Mean frequency of the *i*-th accelerogram.

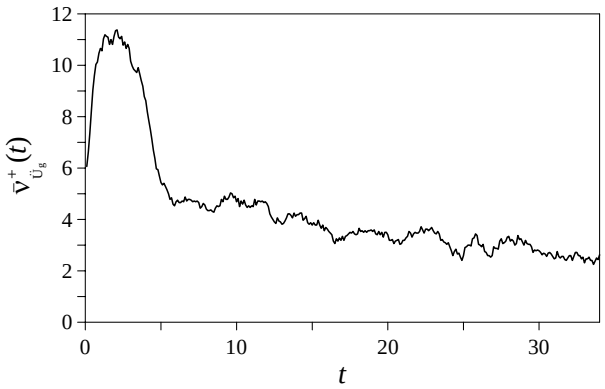

Figure 2. 6 Arithmetic average of the up-crossing time axis rate, $\bar{\nu}^{+}_{\ddot{U}_g}(t)$ [s^{-1}], of the 30 accelerograms recorded in the Imperial Valley (California-USA).

Then, in order to perform a statistical analysis the average of the mean frequency $\bar{\nu}^{+}_{\ddot{U}_g}(t)$ (see Figure 2.6) has been determined. This figure shows both the time-varying amplitude and frequency content of recorded accelerogram.

In Table 2.II the main characteristics of these 30 accelerograms are reported. Namely: the *station name*, the *date* of the recorded event, the *magnitude*, the *PGA*, the *energy*, the *strong motion duration* as well as $t_{0.05}$ and $t_{0.95}$. From the analysis of these accelerograms the following average parameters are obtained: $\bar{T}_s = 14.40\,[\mathrm{s}]$, $\bar{t}_{0.05} = 5.04\,[\mathrm{s}]$ and $\bar{t}_{0.95} = 19.44\,[\mathrm{s}]$.

Table 2. II Main characteristics of the accelerograms recorded in the Imperial Valley (California-USA)

n	Station	Date	Magn.	*PGA* a_{max} [m/s^2]	Energy $\frac{2g}{\pi} I_A$ [m^2/s^3]	Duration t_d [s]	*SMD* T_s [s]	$t_{0.05}$ [s]	$t_{0.95}$ [s]
1	El Centro Array #9	19/05/1940	6.53	3.07	10.30	40.00	23.50	1.96	25.47
2	El Centro Array #9	24/01/1951	6.53	0.28	0.12	40.00	25.44	0.99	26.44
3	El Centro Array #9	17/12/1955	6.53	0.55	0.18	40.00	16.82	0.77	17.59
4	El Centro Array #12	15/10/1979	6.53	1.40	2.38	39.01	19.16	6.41	25.58
5	Niland Fire Station	15/10/1979	6.53	1.07	1.14	39.98	22.20	5.83	28.03
6	Calipatria Fire Station	15/10/1979	6.53	1.26	0.89	39.52	22.35	7.52	29.87
7	Parachute Test Site	15/10/1979	6.53	1.09	1.25	39.33	17.52	6.91	24.44
8	Brawley Airport	15/10/1979	6.53	1.57	1.81	37.82	11.89	6.12	18.01
9	El Centro Array #1	15/10/1979	6.53	1.37	1.68	39.03	12.84	6.25	19.09
10	El Centro Array #2	15/10/1979	5.01	3.09	7.82	39.52	8.59	7.12	15.71
11	El Centro Array #3	15/10/1979	6.53	2.61	7.11	39.54	12.48	6.13	18.61
12	El Centro Array #4	15/10/1979	6.53	4.76	8.33	39.00	6.72	4.80	11.52
13	El Centro Array #5	15/10/1979	6.53	5.09	10.08	39.28	6.07	4.36	10.43
14	El Centro Array #6	15/10/1979	6.53	4.02	9.07	39.03	10.65	2.51	13.16
15	El Centro Array #7	15/10/1979	6.53	3.31	5.33	36.82	6.50	4.78	11.28
16	El Centro Array #8	15/10/1979	6.53	5.90	9.90	37.56	6.68	5.39	12.08
17	EC Country Center FF	15/10/1979	6.53	2.09	4.70	39.98	11.01	6.04	17.06
18	El Centro Diff. Array	15/10/1979	6.53	3.45	10.66	38.96	6.92	5.31	12.24
19	El Centro Array #10	15/10/1979	6.53	1.68	3.52	36.97	12.36	5.42	17.78
20	Holtville Post Office	15/10/1979	5.62	2.48	5.40	37.74	11.59	4.72	16.31
21	El Centro-Mel. Geot. Array	15/10/1979	6.53	3.08	5.34	39.98	8.16	3.87	12.03
22	El Centro Array #11	15/10/1979	6.53	3.57	12.19	39.03	8.48	6.17	14.65
23	Westmorland Fire Station	16/10/1979	5.62	1.68	1.05	40.00	8.82	2.81	11.64
24	Victoria	15/10/1979	6.53	1.19	1.21	40.00	20.85	9.12	29.97
25	Chihuahua	15/10/1979	6.53	2.65	7.17	40.00	19.17	5.36	24.54
26	Compuertas	15/10/1979	6.53	1.83	2.71	36.00	28.29	5.40	33.70
27	Bonds Corner	15/10/1979	6.53	5.77	24.20	37.60	9.36	3.09	12.46
28	Calexico Fire Station	15/10/1979	6.53	2.69	5.34	37.80	11.77	4.71	16.49
29	El Centro Array #13	15/10/1979	6.53	1.15	1.66	39.50	21.96	5.89	27.86
30	Westmorland Fire Station	15/10/1979	6.53	0.73	0.76	39.98	23.76	5.22	28.98

2.3 The evolutionary process model

In this section the characterization of the non-stationary model of the ground motion acceleration process will be done following the Priestley (1965, 1967) evolutionary process model. Firstly the spectral description of the non-stationary stochastic process is done; then four models of modulating functions, for both the quasi-stationary and fully non-stationary process, amongst the most common present in literature, will be presented.

2.3.1 Definition of the non-stationary stochastic input

In order to define the *fully non-stationary stochastic input*, the evolutionary spectral representation of non-stationary processes is often adopted (Priestley 1965). According to this representation, the non-stationary stochastic process is defined by the following *Fourier-Stieltjes integral* (Priestley 1965, Priestley 1967):

$$F(t) = \int_{-\infty}^{+\infty} \exp(\mathrm{i}\omega t)\, a(\omega, t)\, \mathrm{d}N(\omega) \tag{2.4}$$

where $\mathrm{i} = \sqrt{-1}$ is the imaginary unit, $a(\omega, t)$ is a slowly varying complex deterministic time-frequency modulating function, which has to satisfy the condition: $a(\omega, t) \equiv a^*(-\omega, t)$, where the asterisk denotes the complex conjugate; $N(\omega)$ is a process with orthogonal increments, so that its increments $\mathrm{d}N(\omega_1)$ and $\mathrm{d}N(\omega_2)$ at any two distinct points ω_1 and ω_2 are uncorrelated random variables, satisfying the conditions:

$$\mathrm{E}\left\langle \mathrm{d}N(\omega_1)\, \mathrm{d}N^*(\omega_2) \right\rangle = \delta(\omega_1 - \omega_2)\, S_0(\omega_1)\, \mathrm{d}\omega_1 \mathrm{d}\omega_2 \ . \tag{2.5}$$

In Eq. (2.5) the symbol $\mathrm{E}\langle\bullet\rangle$ means stochastic average and $\delta(\bullet)$ is the Dirac delta defined as:

$$\delta(t-t_0)=\begin{cases}0, & t\le t_0;\\ +\infty, & t>t_0;\end{cases} \tag{2.6}$$

$S_0(\omega)$ is the *PSD* function of the so-called "embedded" stationary counterpart process (Michaelov et al. 1999a). It is a real and symmetric function: $S_0(-\omega)=S_0(\omega)$.

It has to be emphasized that the stochastic process $F(t)$ is also termed *oscillatory process* since it possesses evolutionary spectrum belonging to the family of the oscillatory functions $\mathcal{F}_q$ defined as $\mathcal{F}_q=\left\{\exp(i\omega t)\,a_q(\omega,t)\right\}$. The zero-mean Gaussian non-stationary random process $F(t)$ is completely defined by the knowledge of the autocorrelation function $R_{FF}(t_1,t_2)=R_{FF}(t_2,t_1)=\mathrm{E}\langle F(t_1)F(t_2)\rangle$ which is a real symmetric function given as:

$$\begin{aligned}R_{FF}(t_1,t_2)&=\int_{-\infty}^{\infty}\exp\left[\mathrm{i}\omega(t_1-t_2)\right]a(\omega,t_1)\,a^{*}(\omega,t_2)\,S_0(\omega)\,\mathrm{d}\omega=\\ &=\int_{-\infty}^{\infty}\exp\left[\mathrm{i}\omega(t_1-t_2)\right]S_{FF}(\omega,t_1,t_2)\,\mathrm{d}\omega.\end{aligned} \tag{2.7}$$

In the evolutionary process analysis (Priestley 1999), the function:

$$S_{FF}(\omega,t)=\left|a(\omega,t)\right|^2 S_0(\omega) \tag{2.8}$$

is called *EPSD* function of the non-stationary process $F(t)$. In the previous equation the symbol $|\bullet|$ denotes the modulus of the function in brackets. The processes characterized by the *EPSD* function $S_{FF}(\omega,t)$, are called *fully non-stationary* random process, since both time and frequency content change. If the modulating function is a real time dependent function, $a(\omega,t) \equiv a(t)$, the non-stationary process is called *quasi-stationary* (or *uniformly modulated*) random process.

In the stochastic analysis the one-sided *EPSD* function is generally used; the latter, in the Priestley representation, can be suitably defined by the following relationships:

$$G_{FF}(\omega,t_1,t_2) = \begin{cases} a(\omega,t_1)\,a^*(\omega,t_2)G_0(\omega) \equiv 2S_{FF}(\omega,t_1,t_2)\,, & \omega \geq 0; \\ 0\,, & \omega < 0, \end{cases} \quad (2.9)$$

where $G_0(\omega)$ $\left(G_0(\omega) = 2S_0(\omega),\ \omega \geq 0;\ G_0(\omega) = 0,\ \omega < 0\right)$ is the one-sided *PSD* function of the stationary counterpart of input process $F(t)$.

2.3.2 Models of the non-stationary random process

1) *Normalized exponential type I modulating function*

Among the modulating functions that are herein considered, the simplest one, $a_1(t)$, that defines an uniformly modulated random process, has been proposed by Hsu and Bernard (1978):

$$a_1(t) = \varepsilon_1 t \exp\left(-\alpha_1 t\right) \quad (2.10)$$

where

$$\varepsilon_1 = \alpha_1 \exp(1). \tag{2.11}$$

The constant ε_1 normalizes the exponential modulating function so that the maximum of the real function $a_1(t)$ is unity.

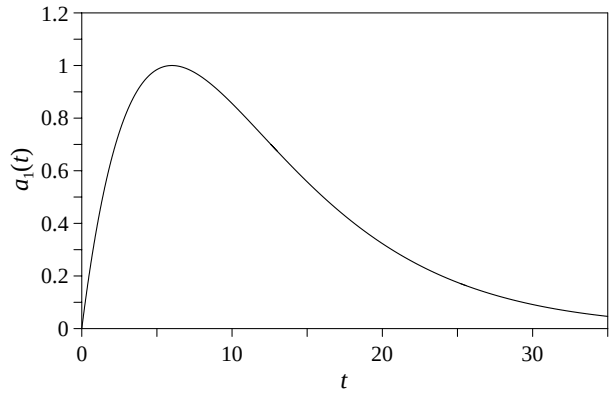

Figure 2. 7 Hsu and Bernard (1978) modulating function, $\alpha_1 = 1/6$.

2) *Normalized exponential type II modulating function*

Another time modulating function, among the most used in literature, $a_2(t)$ has been proposed by Shinozuka and Sato (1967):

$$a_2(t) = \varepsilon_2 \left[\exp(-\alpha_2 t) - \exp(-\alpha_3 t) \right]. \tag{2.12}$$

The constant ε_2 normalizes the exponential modulating function so that the maximum of the real function $a_2(t)$ is unity; it can be evaluated as:

$$\varepsilon_2 = \frac{\alpha_2}{\alpha_3 - \alpha_2} \exp\left[\frac{\alpha_3}{\alpha_3 - \alpha_2} \ln\left(\frac{\alpha_3}{\alpha_2} \right) \right]. \tag{2.13}$$

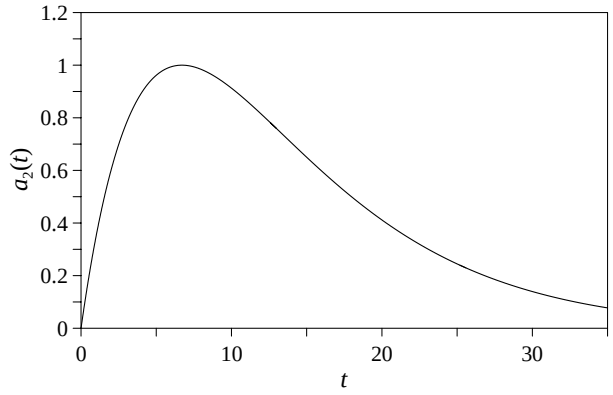

Figure 2. 8 Shinozuka and Sato (1967) modulating function, $\alpha_2 = 0.045\,\pi, \alpha_3 = 0.05\,\pi$ **.**

3) *Normalized Jennings et al. type modulating function*

This modulating real function initially increases parabolically (up to time t_1), remains constant between times t_1 and t_2, and then decreases exponentially. This was proposed by Amin and Ang (1968) and by Jennings et al. (1969). The normalized to unity expression can be written as:

$$a_3(t) = \frac{t^2}{t_1^2}\,\mathbb{W}(0,t_1) + \mathbb{W}(t_1,t_2) + \exp\left[-\alpha_4\left(t-t_2\right)\right]\mathbb{U}(t-t_2) \qquad (2.14)$$

where $\mathbb{W}(t_i,t_j)$ and $\mathbb{U}(t)$ are the *window* and the *unit-step functions* defined as:

$$\mathbb{W}(t_i,t_j) = \begin{cases} 1, & t_i < t \le t_j; \\ 0, & t \le t_i, t > t_j; \end{cases} \quad \mathbb{U}(t-t_0) = \begin{cases} 0, & t \le t_0; \\ 1, & t > t_0. \end{cases} \qquad (2.15)$$

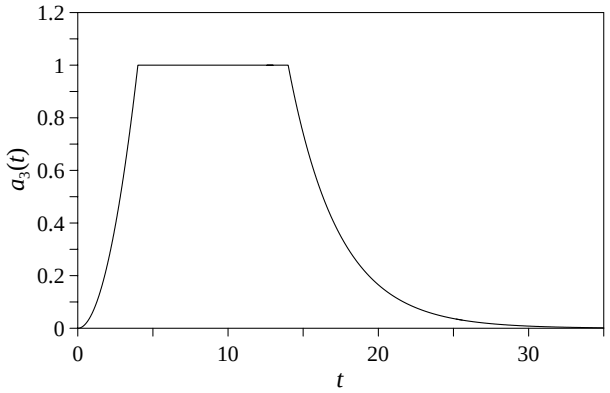

Figure 2. 9 Jennings et al. (1969) modulating function, $t_1 = 4s, t_2 = 14s, \alpha_4 = 0.3$.

4) *Normalized Spanos and Solomos model of the fully non-stationary process*

In order to take into account the main features of seismic ground motion, that is the "build-up" and the "die off" segments as well as a decreasing dominant frequency, Spanos and Solomos (1983) proposed the following time-frequency modulating function, $a_4(\omega,t)$:

$$a_4(\omega,t) = \varepsilon_4(\omega)\, t \exp\left[-\alpha_5(\omega)\, t\right] \tag{2.16}$$

with the parameter $\varepsilon_4(\omega)$ that normalizes the time-frequency modulating function so that the maximum of the real function $a_4(\omega,t)$ is unity.

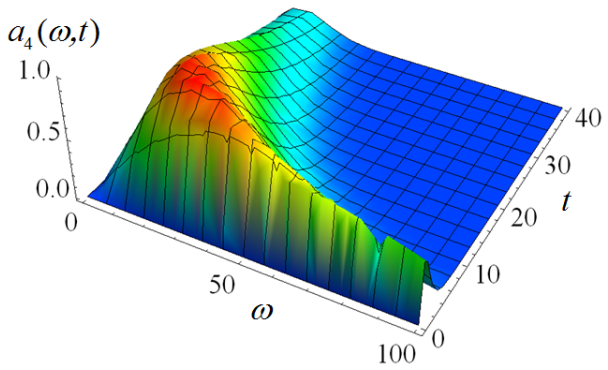

Figure 2. 10 Spanos and Solomos (1983) modulating function, $\varepsilon_4(\omega)=\frac{1}{a_{\max}}\frac{\omega\sqrt{2}}{5\pi}$, $\alpha_5(\omega)=\frac{1}{2}\left(0.15+\frac{\omega^2}{500\pi^2}\right)$, $a_{\max}=6.007$.

2.4 Wavelet analysis

In order to identify and preserve the non-stationarity of the real earthquakes, a powerful tool is represented by the wavelet analysis. In fact, the use of wavelets permits a joint time–frequency signal representation.

The wavelet transform gives a time-frequency representation of a signal $F(t)$, belonging to the family of finite energy functions:

$$E=\int_{-\infty}^{\infty}\left|F(t)\right|^2\mathrm{d}t<\infty \tag{2.17}$$

by a double series of basis functions called "wavelets" $\psi_{u,s}(t)$. Each wavelet is a local function of time, it possesses a certain frequency content and it is generated by scaling, by the parameter $s\in\mathbb{R}^+$ (controlling the frequency distribution), and shifting, by the parameter $u\in\mathbb{R}$ (localising the function at around the time instant $t=u$) a single "mother function" $\psi(t)$ (Cecini and Palmeri 2015).

The continuous wavelet transform of the signal $F(t)$, at scale *s* and position *u* is given by:

$$a_{u,s} = \int_{-\infty}^{+\infty} F(t)\,\psi_{u,s}^{*}(t)\,\mathrm{d}t \tag{2.18}$$

where the asterisk denotes the complex conjugate and

$$\psi_{u,s} = \frac{1}{\sqrt{s}}\,\psi\left(\frac{t-u}{s}\right). \tag{2.19}$$

The signal $F(t)$ will be obtained from the inverse continuous wavelet transform:

$$F(t) = \frac{1}{C}\int_{-\infty}^{+\infty}\int_{0}^{+\infty}\frac{1}{s^2}\,a_{u,s}\psi_{u,s}(t)\,\mathrm{d}s\mathrm{d}u \tag{2.20}$$

in which *C* is a normalizing constant.

Unfortunately the wavelet is a decaying function, so it is impossible to localize it in time. However families of wavelets can be conveniently generated in a way to form an orthogonal basis, so that the wavelet transform is bijective, giving a unique representation. Among the proposed models, Newland (1994) introduced a class of harmonic wavelets, having a box-shaped band limited spectrum. Later, the filtered harmonic wavelet scheme was presented by the same author (Newland 1999) incorporating a Hanning window function in the frequency domain to improve the time localization capabilities of the harmonic wavelet transform in the wavelet mean square map for a given frequency resolution

(Newland 1999, Spanos et al. 2005). In this case, the wavelet function of scale (*m*, *n*) and position (*k*) in the frequency domain takes the form:

$$\Psi_{\{m,n\},k}(\omega)=\begin{cases}\dfrac{1}{n-m}\left(1-\cos\left(\dfrac{\omega-m2\pi}{n-m}\right)\right), & m2\pi\le\omega\le n2\pi;\\ 0, & \text{elsewhere.}\end{cases} \tag{2.21}$$

By applying the inverse Fourier transform it is possible to obtain the complex-valued time domain counterpart, having magnitude

$$\left|\psi_{\{m,n\},k}(t)\right|=\frac{\sin\pi\left(t-\dfrac{k}{n-m}\right)(n-m)}{\pi\left(t-\dfrac{k}{n-m}\right)\left(\left(t-\dfrac{k}{n-m}\right)^2(n-m)^2-1\right)} \tag{2.22}$$

and phase:

$$\varphi_{(m,n),k}(t)=\pi\left(t-\frac{k}{n-m}\right)(m+n). \tag{2.23}$$

The harmonic wavelet transform of the signal $F(t)$ will be given by

$$a_{(m,n),k}=(n-m)\int_{-\infty}^{+\infty}F(t)\,\psi^{*}_{(m,n),k}(t)\,\mathrm{d}t \tag{2.24}$$

and, in order to perform a time-frequency analysis, the wavelet spectrogram can be derived

$$SP(\omega,t)=\left|a_{(m,n),k}\right|^2. \tag{2.25}$$

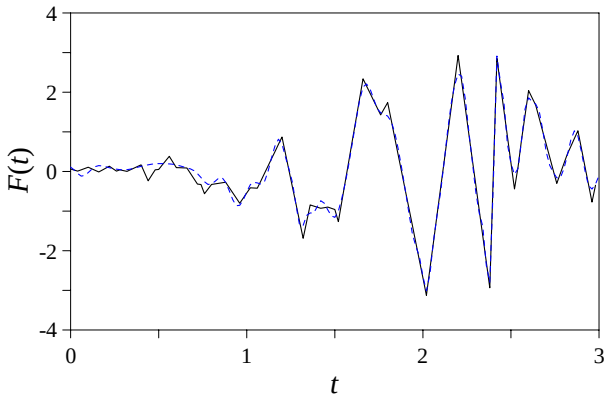

Figure 2. 11 Approximation of the first seconds of the El Centro NS recorded earthquake, 1940 (black line) with the wavelet decomposition (blue dashed line).

Figure 2.11 shows an example of approximation of a given signal $F(t)$ through the wavelets analysis.

2.5 Adaptive chirplet decomposition

In the framework of fully non-stationary processes, it is possible to use the adaptive chirplet decomposition in order to represent the forcing input. In particular the Gaussian chirplets are able to catch the modulation in frequency and in time of the signal and are suited for the decomposition of highly non-stationary signals.

For a given signal $F(t)$, Mallat and Zhang (1993) and Qian and Chen (1995), developed independently the *Matching Pursuit* (*MP*) algorithm that permits its decomposition if the following relationship is satisfied:

$$E=\int_{-\infty}^{\infty}\left|F(t)\right|^2 \mathrm{d}t<\infty \tag{2.26}$$

where E is the total energy of the signal. The *MP* provides the following decomposition of the signal:

$$F(t)=\sum_{k}A_{k}h_{k}\left(t\right) \tag{2.27}$$

where $h_{k}\left(t\right)$ is the Gaussian chirplet:

$$\begin{aligned} h_{k}\left(t\right)&=\sqrt[4]{\frac{a_{k}}{\pi}}\exp\left[-\left(a_{k}/2\right)\left(t-t_{k}\right)^{2}\right]\\ &\times\exp\left[i\left(\beta_{k}/2\right)\left(t-t_{k}\right)^{2}\right]\exp\left[i\omega_{k}\left(t-t_{k}\right)\right] \end{aligned} \tag{2.28}$$

with α_{k} that is a scaling factor, t_{k} and ω_{k} that shift in time and in frequency, respectively, the chirplet and the chirprate β_{k} that leads to a linear frequency modulation (Mann and Haykin 1995) .

The coefficients A_{k} are obtained such as the mean square error between the signal and its approximation is minimum. This leads to the solution of the optimization problem:

$$\left|A_{k}\right|^{2}=\max_{h_{k}}\left|\left\langle F_{k}\left(t\right),h_{k}\left(t\right)\right\rangle\right|^{2}=\max_{h_{k}}\left|\int_{-\infty}^{\infty}F_{k}\left(t\right)h_{k}\left(t\right)\mathrm{d}t\right|^{2}. \tag{2.29}$$

First, the original signal $F\left(t\right)=F_{k}\left(t\right)$ for $k=0$ is projected on all the functions of the dictionary and the coefficient A_{0} is determined from Eq.(2.29). Then, the residual $F_{k+1}\left(t\right)$ is determined:

$$F_{k+1}\left(t\right)=F_{k}\left(t\right)-A_{k}h_{k}\left(t\right). \tag{2.30}$$

This procedure, described above for the original signal, is repeated for the residual iteratively, and the algorithm terminates when the energy of the residual reaches a desired predefined level that obviously characterizes the quality of the approximation (Spanos et al. 2007).

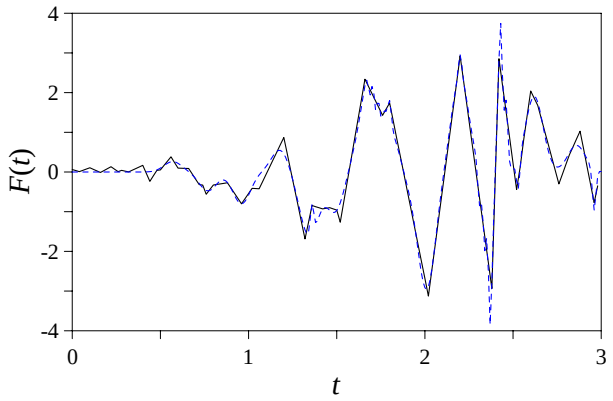

Figure 2. 12 Approximation of the firts seconds of the El Centro NS recorded earthquake, 1940 (black line) with adaptive chirplet decomposition (blue dashed line).

Applying the Wigner-Ville distribution, the adaptive spectrogram can be derived:

$$AS(t,\omega) \cong \sum_{k=0}^{K} 2A_k^2 \exp\left\{-\alpha_k (t-t_k)^2 - \left[\omega - \omega_k - \beta_k (t-t_k)\right]^2 / \alpha_k\right\} \tag{2.31}$$

and then it is possible to generate the artificial seismic waves (Yang 1986)

$$F^{(r)}(t) = \sum_{k=1}^{n} AS(t,\omega_k)\sqrt{G_0(\omega_k)\Delta\omega}\,\cos\left(\omega_k t + \theta_k^{(r)}\right) \tag{2.32}$$

where $\Delta\omega$ is the frequency increment, ω_k is the discrete frequency, $\theta_k^{(r)}$ is the random phase with uniform distribution between 0 and 2π and $G_0(\omega)$ is the one-sided *PSD* function.

2.6 Fully non-stationary spectrum compatible seismic waves

2.6.1 Simulation of the random process samples

The problem of simulating spectrum-compatible earthquake accelerograms is addressed on a probabilistic basis under the assumption that an earthquake accelerogram is considered as a sample of a random process. The samples must satisfy two exigences:

- they have to be random;
- they must describe the probabilistic characteristics of the corresponding stochastic process.

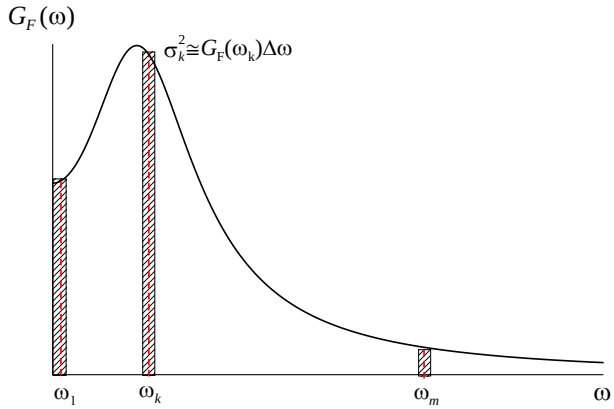

Figure 2. 13 Approximation of the one-sided *PSD* function for the generation of samples of a stationary Gaussian random process.

A zero-mean stationary Gaussian random process $F(t)$ is completely defined by the autocorrelation function $R_F(\tau)$ or by the corresponding one-sided *PSD* function $G_F(\omega)$; in order to apply the simulation technique is firstly necessary to sample this one, as shown in Figure 2.13.

It is necessary to define a *cut off frequency* $\tilde{\omega}$ such that:

$$\int_0^{\tilde{\omega}} G_F(\omega) = \tilde{\sigma}_F^2 \simeq \sigma_F^2 \tag{2.33}$$

where $G_F(\omega) = 0$ if $\omega > \tilde{\omega}$; for the ground motion acceleration process $G_F(\omega) \simeq 0$ if $\omega > 100\ [\text{rad/s}]$.

Once the cut off frequency has been chosen, the interval $[0, \tilde{\omega}]$ is divided in m_c interval of amplitude $\Delta\omega = \tilde{\omega} / m_c$, with the central point $\omega_k\ (k,1,2,\ldots,m_c)$, in such a way that the corresponding area of the sampled one-sided *PSD* function is $\sigma_k^2 = G_F(\omega_k)\Delta\omega$. So the *r*-th sample $F^{(r)}(t)$ of the zero-mean stationary Gaussian random process $F(t)$, having one-sided *PSD* function $G_F(\omega)$ and autocorrelation function $R_F(\tau)$, is defined as (Shinozuka and Jan, 1972):

$$F^{(r)}(t) = \sum_{k=1}^{m_c} \sqrt{2G_F(k\Delta\omega)\Delta\omega}\ \sin\left(k\,\Delta\omega\, t + \theta_k^{(r)}\right) \tag{2.34}$$

where $\Delta\omega$ is the frequency increment, $\theta_k^{(r)}$ is the random phase with uniform distribution between 0 and 2π.

When the process is a uniformly-modulated or fully non-stationary random process, with modulating function, respectively, $a(t)$ and $a(\omega,t)$, Eq. (2.34) is modified as:

$$\begin{aligned} F^{(r)}(t) &= \sum_{k=1}^{m_c} |a(t)| \sqrt{2G_F(k\Delta\omega)\Delta\omega}\, \sin\left(k\Delta\omega t + \theta_k^{(r)}\right) \\ F^{(r)}(t) &= \sum_{k=1}^{m_c} |a(k\Delta\omega, t)| \sqrt{2G_F(k\Delta\omega)\Delta\omega}\, \sin\left(k\Delta\omega t + \theta_k^{(r)}\right) \end{aligned} \tag{2.35}$$

Notice that the implementation of Eqs.(2.35) leads to a greater computational cost then (2.34); this is mainly due to the introduction of the modulating functions $a(t)$ and $a(\omega,t)$.

2.6.2 Stationary spectrum-compatible accelerograms

The simulation of artificial accelerograms is usually based upon a stationary stochastic zero-mean Gaussian process assumption.

Several methods for generating a spectrum-consistent *PSD* function are available in the literature (Vanmarcke and Gaparini 1977, Kaul 1978, Pfaffinger 1983, Preumont 1984, Cacciola et al. 2004).

Here the method proposed by Cacciola et al. (2004) is briefly described. This method considers the ground-acceleration as a sample of a zero-mean stationary Gaussian process. It approximates the pseudo-acceleration response spectrum as the 50% fractile of the peak maxima distribution of the response process of a Single Degree of Freedom (SDOF) oscillator subjected to the earthquake

acceleration zero-mean process, $\ddot{U}_g(t)$, whose motion is governed by the following relationship:

$$\ddot{U}(t) + 2\xi_0\omega_0\dot{U}(t) + \omega_0^2 U(t) = \ddot{U}_g(t). \tag{2.36}$$

Consequently the following very handy recursive expression of the one-sided *PSD* function of the earthquake acceleration zero-mean process, $\ddot{U}_g(t)$, compatible with the assigned pseudo-acceleration response spectrum, is obtained (Cacciola et al. 2004):

$$\begin{aligned} &G_{\ddot{U}_g}^{\mathrm{ST}}(\omega_k) = 0, \quad 0 \le \omega_k \le \omega_i; \\ &G_{\ddot{U}_g}^{\mathrm{ST}}(\omega_k) = \frac{4\xi_0}{\omega_k \pi - 4\xi_0\omega_{k-1}}\left(\frac{S_{\mathrm{pa}}^2(\omega_k,\xi_0)}{\eta_U^2(\omega_k,\xi_0)} - \Delta\omega\sum_{j=1}^{k-1} G_{\ddot{U}_g}^{\mathrm{ST}}(\omega_j)\right), \quad \omega_i \le \omega_k \le \omega_f; \end{aligned} \tag{2.37}$$

where the apex ST evidences that the one-sided *PSD* function is evaluated in the hypothesis of stationary random processes, $\omega_i \le 1(\mathrm{rad/s})$ (Cacciola et al. 2004) and ω_f are chosen as bounds of the existence domain of the one-sided *PSD* function $G_{\ddot{U}_g}^{\mathrm{ST}}(\omega)$. In Eq.(2.37) $S_{\mathrm{pa}}(\omega_k,\xi_0)$ is the target pseudo-acceleration elastic response spectrum for a given natural frequency ω_k and damping ratio $\xi_0 = 0.05$ and $\eta_U(\omega_k,\xi_0)$ is the peak factor given as (Vanmarcke 1975):

$$\eta_U(\omega_k,\xi_0)=\left\{2\ln\left\{\frac{T_s\,\omega_k}{\pi}\left(-\ln 0.5\right)^{-1}\right.\right.$$
$$\left.\left.\times\left[1-\exp\left[-\delta_U^{1.2}\sqrt{\pi\ln\left(\frac{T_s\,\omega_k}{\pi}\left(-\ln 0.5\right)^{-1}\right)}\right]\right]\right\}\right\}^{1/2}. \tag{2.38}$$

In the previous equation T_S is the time observing window, assumed equals to the strong motion phase of the ground motion process and δ_U is the bandwidth factor (see Eq. (1.21)) evaluated in the hypothesis of white noise process. The latter quantities can be written as (Vanmarcke 1972):

$$\delta_U=\left[1-\frac{1}{1-\xi_0^2}\left(1-\frac{2}{\pi}\arctan\frac{\xi_0}{\sqrt{1-\xi_0^2}}\right)^2\right]^{1/2}=0.246\quad(\xi_0=0.05). \tag{2.39}$$

Once the one-sided *PSD* function is obtained by Eq.(2.37), the *N* stationary spectrum-compatible artificial earthquake accelerograms are generated substituting $G_{\ddot{U}_g}^{ST}(\omega)$ in Eq. (2.34).

2.6.3 Non-stationary spectrum-compatible accelerograms

The main problem of the stationary model of the ground motion acceleration process is that it is unable to catch the characteristics of real earthquakes, such as the amplitude and frequency modulation of the signal. In particular it can be easily proved that the mean frequency, $\nu_{\ddot{U}_g}^{+}(t)$, which evaluates the variation in time of the mean up-crossing rate of the time axis, is a constant quantity for the stationary spectrum-compatible acceleration random process $\ddot{U}_g(t)$.

This result is in contrast with the analysis of recorded accelerograms. Furthermore, the energy, $E_{\ddot{U}_g}^{ST}(t_d)$, of the spectrum-compatible stationary acceleration random process is proportional to the variance. Indeed the following relationship holds:

$$E_{\ddot{U}_g}^{ST}(t_d) = \int_0^{t_d} \int_0^{+\infty} G_{\ddot{U}_g}^{ST}(\omega) \, d\omega \, dt = t_d \, \sigma_{\ddot{U}_g}^2, \tag{2.40}$$

where $\sigma_{\ddot{U}_g}^2 = \int_0^{\infty} G_{\ddot{U}_g}^{ST}(\omega) \, d\omega$ is the variance of the stationary spectrum-compatible stationary stochastic process $\ddot{U}_g(t)$. Moreover, Eq.(2.40) shows that the energy of the spectrum-compatible stationary acceleration random process is proportional to the duration of the process itself. This confirms that a stationary stochastic process, as well as its generic realization, possesses infinite energy. Even though this result is strictly coherent from a mathematically point of view, it is physically unrealistic.

So, the main problem of the stationary model of the ground motion acceleration process is the inability to catch the characteristics of real earthquakes. Then the most suitable model of the ground motion acceleration is the fully non-stationary process model.

The procedure proposed by Cacciola and co-workers (Cacciola 2010, Cacciola and Zentner 2012, Cacciola et al. 2014) is here extended to generate artificial spectrum-compatible fully non-stationary earthquake accelerograms. On the contrary of the stationary case the *EPSD* function cannot be defined univocally; here the following Priestley evolutionary model of the one-sided *EPSD* function of the fully non-stationary process is chosen:

$$G_{\ddot{U}_g}^{\mathrm{NST}}(\omega,t)=\left|a(\omega,t)\right|^2 G_{\ddot{U}_g}^{\mathrm{STC}}(\omega) \tag{2.41}$$

where $G_{\ddot{U}_g}^{\mathrm{STC}}(\omega)$ is the stationary counterpart of the fully non-stationary process $\ddot{U}_g(t)$ and $a(\omega,t)$ is a slowly varying deterministic time-frequency modulating function.

This method evaluates the spectrum-compatible *PSD* function of the stationary counterpart, $G_{\ddot{U}_g}^{\mathrm{STC}}(\omega)$, modifying the *PSD* function evaluated by Eq.(2.37) under the hypothesis of stationary spectrum-compatible process, $G_{\ddot{U}_g}^{\mathrm{ST}}(\omega)$, adding an additional term $\Delta G_{\ddot{U}_g}^{\mathrm{ST}}(\omega_k)$ (Cacciola 2010), namely:

$$\begin{aligned} &G_{\ddot{U}_g}^{\mathrm{STC}}(\omega_k)=0, \quad 0\le\omega_k\le\omega_i; \\ &G_{\ddot{U}_g}^{\mathrm{STC}}(\omega_k)=G_{\ddot{U}_g}^{\mathrm{ST}}(\omega_k)+\Delta G_{\ddot{U}_g}^{\mathrm{ST}}(\omega_k), \quad \omega_i\le\omega_k\le\omega_f. \end{aligned} \tag{2.42}$$

The term $\Delta G_{\ddot{U}_g}^{\mathrm{ST}}(\omega_k)$ is evaluated to reduce the gap between the target spectrum and the average one, that is:

$$\begin{aligned} &\Delta G_{\ddot{U}_g}^{\mathrm{ST}}(\omega_k)= \\ &=\frac{4\xi_0}{\omega_k\pi-4\xi_0\omega_{k-1}}\left(\frac{S_{\mathrm{pa}}^2(\omega_k,\xi_0)-\left(\varepsilon\,\overline{S}_{\mathrm{pa}}^{\mathrm{NST}}(\omega_k,\xi_0)\right)^2}{\eta_U^2(\omega_k,\xi_0)}-\Delta\omega\sum_{j=1}^{k-1}\Delta G_{\ddot{U}_g}^{\mathrm{ST}}(\omega_j)\right) \\ &\times\mathbb{U}\left(\frac{S_{\mathrm{pa}}^2(\omega_k,\xi_0)-\left(\varepsilon\,\overline{S}_{\mathrm{pa}}^{\mathrm{NST}}(\omega_k,\xi_0)\right)^2}{\eta_U^2(\omega_k,\xi_0)}-\Delta\omega\sum_{j=1}^{k-1}\Delta G_{\ddot{U}_g}^{\mathrm{ST}}(\omega_j)\right) \end{aligned} \tag{2.43}$$

where $\mathbb{U}(\bullet)$ is the unit step function defined in Eq.(2.15), $S_{\text{pa}}(\omega_k,\xi_0)$ is the target pseudo-acceleration elastic response spectrum and

$$\begin{aligned}&\varepsilon = 1 \quad \text{if} \quad S_{\text{pa}}(\omega_k,\xi_0) \geq \overline{S}_{\text{pa}}^{\text{NST}}(\omega_k,\xi_0)\\ &\text{or else}\\ &\varepsilon = \min\left\{\frac{S_{\text{pa}}(\omega_k,\xi_0)}{\overline{S}_{\text{pa}}^{\text{NST}}(\omega_k,\xi_0)}\right\}.\end{aligned} \tag{2.44}$$

Finally, in the previous equations, $\overline{S}_{\text{pa}}^{\text{NST}}(\omega_k,\xi_0)$ is the average pseudo-acceleration response spectrum obtained as the arithmetic average of the response of SDOF oscillators with natural circular frequency ω_k and damping ratio ξ_0 subjected to *N* fully non-stationary artificial earthquake accelerograms generated substituting into the second of Eqs. (2.35) the new one-sided *PSD* $G_{\ddot{U}_{\text{g}}}^{\text{STC}}(\omega)$ defined in Eq.(2.42).

Notice that, according to the Eurocode 8 (EC8) instructions (2003), the spectrum compatibility is verified if no value of the mean elastic spectrum, $\overline{S}_{\text{pa}}^{\text{NST}}(\omega,\xi_0)$, calculated from all time histories, is less than 90% of the corresponding value of the target response spectrum, $S_{\text{pa}}(\omega,\xi_0)$ in a selected range of periods. If the spectrum compatibility is not verified it is necessary to modify the stationary counterpart *PSD* function by adopting the following iterative scheme:

$$G_{\ddot{U}_{\text{g}}}^{\text{STC}\,(j)}(\omega) = G_{\ddot{U}_{\text{g}}}^{\text{STC}\,(j\text{-}1)}(\omega)\left[\frac{S_{\text{pa}}(\omega,\xi_0)}{\overline{S}_{\text{pa}}^{\text{NST}\,(j\text{-}1)}(\omega,\xi_0)}\right]^2 \tag{2.45}$$

where $G_{\ddot{U}_g}^{\mathrm{STC}\,(j-1)}(\omega)$ and $\overline{S}_{\mathrm{pa}}^{\mathrm{NST}\,(j\text{-}1)}(\omega,\xi_0)$ are the *PSD* function of the stationary counterpart and the average simulated pseudo-acceleration response spectrum, respectively, both evaluated at the $(j-1)$ iteration. Furthermore, the energy of the spectrum-compatible fully non-stationary acceleration random process is given as:

$$E_{\ddot{U}_g}^{\mathrm{NST}}(t_d)=\int_0^{t_d}\int_0^{\infty} G_{\ddot{U}_g}^{\mathrm{NST}}(\omega,t)\,\mathrm{d}\omega\,\mathrm{d}t. \tag{2.46}$$

2.7 Multi-correlated seismic input

2.7.1 Introduction

When the analysis of structures, such as long span bridges, pipelines, communication transmission systems, etc., is performed, another important problem is to correctly represent the ground motion acceleration by taking into account its spatial variability. In fact the hypothesis of uniform ground motion, that is often used in earthquake engineering to analyse conventional structures, is appropriate only when the base dimensions of the structure are small with respect to the seismic vibration wavelengths. Moreover, for long extended structures to neglect the spatial variability could mean to neglect significant additional stresses with respect to the ones resulting from the hypothesis of uniform ground motion (Saxena et al. 2000). It follows that in these cases the multi-correlated model of the seismic excitation is more appropriate (Zerva 1991). In fact it has been demonstrated that the seismic response of extended structures, is strongly influenced from the real behaviour of seismic waves by difference in arrival times of

seismic waves at different locations, loss of coherence of seismic waves due to multiple reflection and refraction as they propagate through the highly inhomogeneous soil medium and change in the amplitude and frequency content of seismic ground motion due to different local soil conditions.

In the framework of stochastic analysis, the effects of the spatial variability of the ground motion on the response have been mainly investigated assuming the multi-correlated seismic excitation as zero mean stochastic stationary Gaussian processes (see e.g. Abdel-Ghaffar and Rubin 1982, Perotti 1990, Heredia-Zavoni and Vanmarke 1994, Zerva 1994, Zanardo et al. 2002, Tubino et al. 2003, Lupoi et al. 2005, Zhang et al. 2009). To describe the fully non-stationary stochastic multi-correlated input process, two models are mainly adopted: i) the evolutionary process model (Priestley 1965, Priestley 1967); ii) the sigma-oscillatory process model (Battaglia 1979), but in the case of multivariate and/or multi-correlated fully non-stationary input processes, only the sigma-oscillatory process model is able to catch the time-dependence of the coherence function (Battaglia 1979).

2.7.2 The evolutionary process model for multi-correlated input

If the multi-correlated process model is adopted, the stochastic forcing process has to be modelled as a zero-mean Gaussian random process $\mathbf{F}(t)$ of order *N*, where *N* is the support's number of the structural system being analysed. Following the evolutionary spectral representation of non-stationary processes (Priestley 1999), this vector can be defined by the *Fourier-Stieltjes integral* as:

$$\mathbf{F}(t) = \int_{-\infty}^{+\infty} \exp(i\omega t)\,\mathbf{A}(\omega,t)\,\mathrm{d}\mathbf{N}(\omega) \tag{2.47}$$

where $\mathbf{A}(\omega,t)$ is a slowly varying complex deterministic time-frequency modulating diagonal function matrix, of order $N \times N$, which has to satisfy the condition: $\mathbf{A}(\omega,t) \equiv \mathbf{A}^{*}(-\omega,t)$; while $\mathbf{N}(\omega)$ is an orthogonal vector process (of order *N*) satisfying the following conditions:

$$\mathrm{E}\left\langle \mathrm{d}\mathbf{N}(\omega_1)\,\mathrm{d}\mathbf{N}^{*T}(\omega_2)\right\rangle = \delta(\omega_1-\omega_2)\,\mathbf{G}_0(\omega_1)\,\mathrm{d}\omega_1\mathrm{d}\omega_2 \tag{2.48}$$

where $\mathbf{G}_0(\omega)$, is an Hermitian positive definite function matrix of order $N \times N$, which describes the one-sided *PSD* function matrix of the "embedded" stationary counterpart vector process. After some algebra it can be proved that the autocorrelation function matrix of the zero-mean Gaussian non-stationary random vector process $\mathbf{F}(t)$ can be obtained as:

$$\begin{aligned}&\mathbf{R}_{\mathbf{FF}}(t_1,t_2) = \mathrm{E}\left\langle \mathbf{F}(t_1)\mathbf{F}^{T}(t_2)\right\rangle = \\ &= \int_{0}^{\infty} \exp\left[\mathrm{i}\omega(t_1-t_2)\right]\mathbf{G}_{\mathbf{FF}}(\omega,t_1,t_2)\mathrm{d}\omega\end{aligned} \tag{2.49}$$

where

$$\mathbf{G}_{\mathbf{FF}}(\omega,t_1,t_2) = \mathbf{A}(\omega,t_1)\,\mathbf{G}_0(\omega)\,\mathbf{A}^{*}(\omega,t_2). \tag{2.50}$$

Notice that the one-sided *EPSD* function matrix of the non-stationary multi-correlated process $\mathbf{F}(t)$ is obtained setting $t_1 = t_2$ in Eq.(2.50). In the framework of stochastic seismic analysis, the main distinct phenomena that give rise to the spatial variability of earthquake-induced ground motions are: (i) the incoherence effect associated to loss of coherency of seismic waves arriving from an extended source; (ii) the wave-passage effect due to difference in the arrival times of waves at separate supports; (iii) the attenuation effect due to gradual decay of wave amplitudes with distance due to energy dissipation in the ground medium; (iv) the site-response effect associated to spatially varying of the local soil profiles. For stationary excitations, these effects are well characterized by the so called coherence function, $\gamma_{0,sr}(\omega)$. It represents the one sided cross-*PSD*, $G_{0,rs}(\omega)$, of the of the motion between the two stations *r* and *s*, normalized by the square root of the corresponding one- sided auto-*PDF*s $G_{0,rr}(\omega)$ and $G_{0,ss}(\omega)$ (see e.g. Harichandran and Vanmarcke 1986, Luco and Wong 1986, Loh and Ku 1986, Zerva 1991, Der Kiureghian 1996):

$$\gamma_{0,rs}(\omega) = \frac{G_{0,rs}(\omega)}{\sqrt{G_{0,rr}(\omega)\, G_{0,ss}(\omega)}} \tag{2.51}$$

where $G_{0,rs}(\omega)$ is the *r*-th, *s*-th element of the matrix $\mathbf{G}_0(\omega)$. In general, $\gamma_{0,sr}(\omega)$ is complex valued function, whose bounded modulus is $0 \le \left|\gamma_{0,sr}(\omega)\right| \le 1$. This modulus, often called lagged coherency, gives a measure of linear statistical dependence between

the two processes. In particular, $\left|\gamma_{0,sr}(\omega)\right| = 1$ denotes perfect linear dependence between the two processes (e.g. identical and in-phase motions), whereas $\left|\gamma_{0,sr}(\omega)\right| = 0$ denotes complete lack of linear dependence. For stationary excitations, the coherence function is usually written as:

$$\gamma_{0,rs}(\omega) = \rho_{rs}(\omega)\exp\left(-\mathrm{i}\,\omega\, d_{rs}/c\right) \tag{2.52}$$

in which $\exp\left(-\mathrm{i}\,\omega\, d_{rs}/c\right)$ is a measure of the wave passage delay due to the apparent velocity of waves; c represents the velocity of the seismic waves through the ground (c decreases as the distance between the support-points increases or the soil is softer); d_{rs} is the distance between the r-th and s-th support-points and $\rho_{rs}(\omega) \equiv \left|\gamma_{0,sr}(\omega)\right|$ is usually referred as the spatial correlation function between the two support-points. Several models of the coherence function have been proposed in literature (see e.g. Harichandran and Vanmarcke 1986, Luco and Wong 1986, Loh and Ku 1986, Zerva 1991, Der Kiureghian 1996).

Notice that if the same one-sided *PSD* in every point location is considered, the one-sided cross-*PSD* of ground accelerations in a particular direction between surface points r and s, $G_{0,rs}(\omega)$, may be written as the product of the coherence function by the target one-sided *PSD* of ground acceleration $G_0(\omega)$ as follows:

$$G_{0,rs}(\omega) = \begin{cases} \gamma_{0,rs}(\omega)\, G_0(\omega), & \text{for } r \neq s \\ G_0(\omega), & \text{for } r = s. \end{cases} \tag{2.53}$$

For non-stationary excitations the coherence function for multi-correlated non-stationary vector processes, in line with Eq.(2.51), can be defined as:

$$\gamma_{F_rF_s}(\omega,t)=\frac{G_{F_rF_s}(\omega,t)}{\sqrt{G_{F_rF_r}(\omega,t)\,G_{F_rF_s}(\omega,t)}}= \\ =\frac{a_r(\omega,t)\,a_s^*(\omega,t)G_{0,rs}(\omega)}{\left|a_r(\omega,t)\right|\left|a_s(\omega,t)\right|\sqrt{G_{0,rr}(\omega)\,G_{0,ss}(\omega)}}. \tag{2.54}$$

However, in the very common hypothesis of real modulating function, the following relationship holds:

$$\gamma_{F_rF_s}(\omega,t)=\frac{G_{0,rs}(\omega)}{\sqrt{G_{0,rr}(\omega)\,G_{0,ss}(\omega)}}\equiv\gamma_{0,rs}(\omega) \tag{2.55}$$

where $\gamma_{0,rs}(\omega)$ is the coherence function for stationary excitations introduced in Eq.(2.52). Then Eq.(2.55) shows that in the evolutionary spectral analysis the coherence function of the non-stationary multi-correlated vector, $\mathbf{F}(t)$, is independent on the time and coincides with the coherence function of the stationary counterpart of the non-stationary process. This not describes correctly the phenomenon where both intensities and structural influences of each component on the others evolve in time (Battaglia 1979).

2.7.3 The sigma-oscillatory process model for multi-correlated input

2.7.3.1 The sigma-oscillatory process model

The evolutionary spectral analysis of multi-correlated stochastic processes, based on the oscillatory process model, turns out to coherence matrix independent of the time. This characteristic is a limit to the analysis of phenomenon where both intensities and frequency content of each component on the others evolves in time (Battaglia 1979). In order to overcome this drawback Battaglia (1979) introduced the *sigma-oscillatory process* as the sum of a finite number of mutually independent component oscillatory processes $X_q(t)$ $(q=1,\cdots,M$; M being the number of component oscillatory processes required by the problem). Admitting the spectral representation (2.4), a *sigma-oscillatory process* is represented as (Battaglia 1979):

$$F(t)=\sum_{q=1}^{M}X_q(t)=\sum_{q=1}^{M}\int_{-\infty}^{+\infty}\exp(\mathrm{i}\omega t)\,a_q(\omega,t)\,\mathrm{d}N_q(\omega). \tag{2.56}$$

It follows that the mean value and the mean square function of the sigma-oscillatory process $F(t)$ are given respectively as:

$$\begin{aligned}&\mathrm{E}\langle F(t)\rangle=\sum_{q=1}^{M}\mathrm{E}\langle X_q(t)\rangle=0,\quad q=1,\cdots,M;\\&\mathrm{E}\langle F^2(t)\rangle=\sum_{q=1}^{M}\mathrm{E}\langle X_q^2(t)\rangle=\sum_{q=1}^{M}\int_{0}^{+\infty}\left|a_q(\omega,t)\right|^2 G_0^{(q)}(\omega)\,\mathrm{d}\omega.\end{aligned} \tag{2.57}$$

The second of Eqs.(2.57) gives a decomposition over the frequency of the variance of the sigma-oscillatory process $F(t)$ at time *t*. Therefore, the one-sided *EPSD* function of the sigma-oscillatory process $F(t)$ can be meaningfully defined with respect to the family of the oscillatory functions $\mathcal{F}_q$ as:

$$G_{FF}(\omega,t)=\sum_{q=1}^{M}\left|a_q(\omega,t)\right|^2 G_0^{(q)}(\omega)=\sum_{q=1}^{M}G_0^{(q)}(\omega,t). \tag{2.58}$$

Notice that Eq.(2.58) shows that the sigma-oscillatory processes, $F(t)$, is a fully non-stationary process also in the case in which each component process $X_q(t)$ possesses separable one-sided *EPSD* function $G_0^{(q)}(\omega,t)=\left|a_q(t)\right|^2 G_0^{(q)}(\omega)$.

If the multi-correlated process model is adopted the stochastic forcing process has to be modelled as a zero-mean Gaussian random process $\mathbf{F}(t)$ of order *N*. It follows that the multi-correlated sigma-oscillatory process, $\mathbf{F}(t)$, can be defined as:

$$\mathbf{F}(t)=\sum_{q=1}^{M}\int_{-\infty}^{+\infty}\exp(i\omega t)\,\mathbf{A}_q(\omega,t)\,\mathrm{d}\mathbf{N}_q(\omega) \tag{2.59}$$

with $\mathbf{N}_q(\omega)$ zero-mean mutually independent, orthogonal vector process satisfying the property:

$$\mathrm{E}\left\langle \mathrm{d}\mathbf{N}_p(\omega_1)\,\mathrm{d}\mathbf{N}_q^{*T}(\omega_2)\right\rangle=\delta(\omega_1-\omega_2)\Delta_{pq}\,\mathbf{G}_0^{(p,q)}(\omega_1)\,\mathrm{d}\omega_1\mathrm{d}\omega_2;\qquad p,q=1,2\cdots M \tag{2.60}$$

where δ is the Dirac Delta function defined in Eq. (2.6) and Δ_{pq} is the Kronecker delta, defined as:

$$\Delta_{pq} = \begin{cases} 1, & p = q; \\ 0, & p \neq q. \end{cases} \tag{2.61}$$

It follows that the correlation function matrix of the multi-correlated sigma-oscillatory process $\mathbf{F}(t)$ is given as:

$$\begin{aligned} \mathbf{R}_{\mathbf{FF}}(t_1, t_2) &= \mathrm{E}\left\langle \mathbf{F}(t_1)\mathbf{F}^T(t_2) \right\rangle = \\ &= \sum_{q=1}^{M} \int_0^{\infty} \exp\left[\mathrm{i}\omega(t_1 - t_2)\right] \mathbf{A}_q(\omega, t_1)\mathbf{G}_0^{(q)}(\omega)\mathbf{A}_q^*(\omega, t_2)\,\mathrm{d}\omega = \\ &= \int_0^{\infty} \exp\left[\mathrm{i}\omega(t_1 - t_2)\right] \mathbf{G}_{\mathbf{FF}}(\omega, t_1, t_2)\mathrm{d}\omega\,. \end{aligned} \tag{2.62}$$

In this model, for $t_1 = t_2$, the one-sided *EPSD* function matrix of the non-stationary multi-correlated sigma-oscillatory process can be written as:

$$\mathbf{G}_{\mathbf{FF}}(\omega, t) = \sum_{q=1}^{M} \mathbf{A}_q(\omega, t)\mathbf{G}_0^{(q)}(\omega)\mathbf{A}_q^*(\omega, t). \tag{2.63}$$

The spectral representation in Eq.(2.63) evidences that the one-sided *EPSD* function of the sigma-oscillatory process is determined as the sum of the function $\mathbf{A}_q(\omega,t)\mathbf{G}_0^{(q)}(\omega)\mathbf{A}_q^*(\omega,t)$ associated to each component. Finally, the coherence function between the *s*-th, *r*-th element of the matrix can be written as (Battaglia 1979):

$$\gamma_{F_r F_s}(\omega,t)=\frac{\sum_{q=1}^{M} a_{r,q}(\omega,t)\,a_{s,q}^{*}(\omega,t)\,G_{0,rs}^{(q)}(\omega)}{\sqrt{\left(\sum_{q=1}^{M}\left|a_{r,q}(\omega,t)\right|^{2} G_{0,rr}^{(q)}\right)\left(\sum_{q=1}^{M}\left|a_{s,q}(\omega,t)\right|^{2} G_{0,ss}^{(q)}\right)}}. \tag{2.64}$$

Moreover, if the one-sided cross-*PSD* function of ground accelerations, in a particular direction between surface points *r* and *s*, $G_{0,rs}^{(q)}(\omega)$, may be written as the product of the coherence function by the one-sided *PSD* functions of ground acceleration at two supports, that is:

$$G_{0,rs}^{(q)}(\omega)=\begin{cases}\gamma_{0,rs}(\omega)\sqrt{G_{0,rr}^{(q)}(\omega)G_{0,ss}^{(q)}(\omega)}, & \text{for } r\neq s\\ G_{0,rr}^{(q)}(\omega), & \text{for } r=s\end{cases} \tag{2.65}$$

it follows that Eq.(2.64) can be rewritten as:

$$\gamma_{F_r F_s}(\omega,t)=\gamma_{0,rs}(\omega)\,\gamma'_{rs}(\omega,t) \tag{2.66}$$

where $\gamma_{0,rs}(\omega)$ is the coherence function for stationary excitations introduced in Eq.(2.52) and

$$\gamma'_{rs}(\omega,t)=\frac{\sum_{q=1}^{M} a_{r,q}(\omega,t)\,a_{s,q}^{*}(\omega,t)\,\sqrt{G_{0,rr}^{(q)}(\omega)G_{0,ss}^{(q)}(\omega)}}{\sqrt{\left(\sum_{q=1}^{M}\left|a_{r,q}(\omega,t)\right|^{2} G_{0,rr}^{(q)}\right)\left(\sum_{q=1}^{M}\left|a_{s,q}(\omega,t)\right|^{2} G_{0,ss}^{(q)}\right)}}. \tag{2.67}$$

Equations (2.66) and (2.67) show that, if the sigma-oscillatory process model is adopted, the coherence function of the non-

stationary multi-correlated vector, $\mathbf{F}(t)$, depends on both the time and circular frequency, on the contrary of the evolutionary process model.

2.7.3.2 The Conte and Peng sigma-oscillatory process model

In order to consider the time-frequency variation of non-stationary stochastic ground motion, Conte and Peng (1997) proposed a sigma-oscillatory process model in the case of mono-correlated input; this process model, here described in the original version, can be obviously extended in the case of multi-correlated input.

The authors (Conte and Peng 1997) modelled the seismic acceleration as the sum of a finite number, *N*, of zero-mean, independent, uniformly modulated Gaussian sub-processes $X_q(t)$. Each uniformly modulated process consists of the product of a real deterministic time modulating function, $a_q(\omega,t)$, and a stationary Gaussian sub-process, having one-sided *PSD* function $G_q(\omega)$. Thus, this model of fully non-stationary process is a particular sigma-oscillatory Gaussian process whose one-sided *EPSD* function is expressed as (Conte and Peng 1997):

$$G_{FF}(\omega,t)=\sum_{q=1}^{M}\left|a_q(t)\right|^2 G_q(\omega) \tag{2.68}$$

where

$$a_q(t)=\varepsilon_q\,(t-t_q)^{r_q}\,e^{-\alpha_q(t-t_p)}\,\mathbb{U}(t-t_q);\qquad q=1,...,M \tag{2.69}$$

and

$$G_q(\omega)=\frac{\nu_q}{\pi}\left[\frac{1}{\nu_q^2+(\omega+\eta_q)^2}+\frac{1}{\nu_q^2+(\omega-\eta_q)^2}\right];\quad q=1,...,M. \quad (2.70)$$

In the previous equations α_q and ε_q are positive constants; r_q is a positive integer; t_q is the arrival time of the sub-process $X_q(t)$; ν_q and η_q are two free parameters representing the frequency bandwidth and the circular mean frequency of the *q*-th stationary sub-process, respectively. Moreover, since the *q*-th sub-process $X_q(t)$ possesses real part of autocorrelation function $R_{X_qX_q}(\tau)=\exp(-\nu_q|\tau|)\cos(\eta_q\tau)$, it can be viewed as the linear combination of the displacement and velocity response processes of an oscillator subjected to two statistically independent Gaussian white noise processes.

The one-sided *EPSD* function (2.68) describes simultaneously the time-varying intensity and the time-varying frequency content. It follows that the excitation $F(t)$ is not separable (i.e. fully-non stationary) although its component processes are individually separable (i.e., uniformly modulated). Each uniformly modulated component process, $X_q(t)$, is characterized by a unimodal *PSD* function in the frequency domain and a unimodal mean square function in the time domain (Conte and Peng 1997).

2.7.4 Simulation of non-stationary stochastic multi-correlated sigma-oscillatory vector processes

The time-varying frequency content together with the spatial variability of the seismic acceleration input where firstly included in *Monte Carlo Simulation* (*MCS*) by Shinozuka (1971). Then several methods have been proposed in literature (see e.g. Shinozuka and Deodatis 1988, Vanmarcke et al. 1993, Deodatis 1996a, Deodatis 1996b, Di Paola and Zingales 2000, Cacciola and Deodatis 2011). Since the main drawback of the *MCS* is the calculation time, in this section it is firstly looked for the most convenient method among the ones proposed in literature, in the framework of multi-correlated stationary stochastic seismic excitations. The attention is focused on the methods proposed by Shinozuka (1971) after improved by Deodatis (1996a) and the alternative one proposed by Di Paola and Zingales (2000). Both methods require the decomposition of the one-sided *PSD* function matrix $\mathbf{G}_0(\omega)$.

In particular, in the methods proposed by Shinozuka (1971) and Deodatis (1996a) the decomposition of $\mathbf{G}_0(\omega)$ is performed by the Cholesky's decomposition (see Figure 2.14) while in the Di Paola and Zingales (2000) method the decomposition is performed once an associated frequency dependent eigenproblem is solved (see Figure 2.15).

It has been proved that, analysing the computation times for the generation of a set of artificial stationary multi-correlated accelerograms, the ratio between the calculation time of the Di Paola and Zingales (2000) method and Deodatis (1996a) method is about 1/269. Notice that in comparing the computational times, according to the main purpose of the thesis, the ergodic property of the sample has not been used.

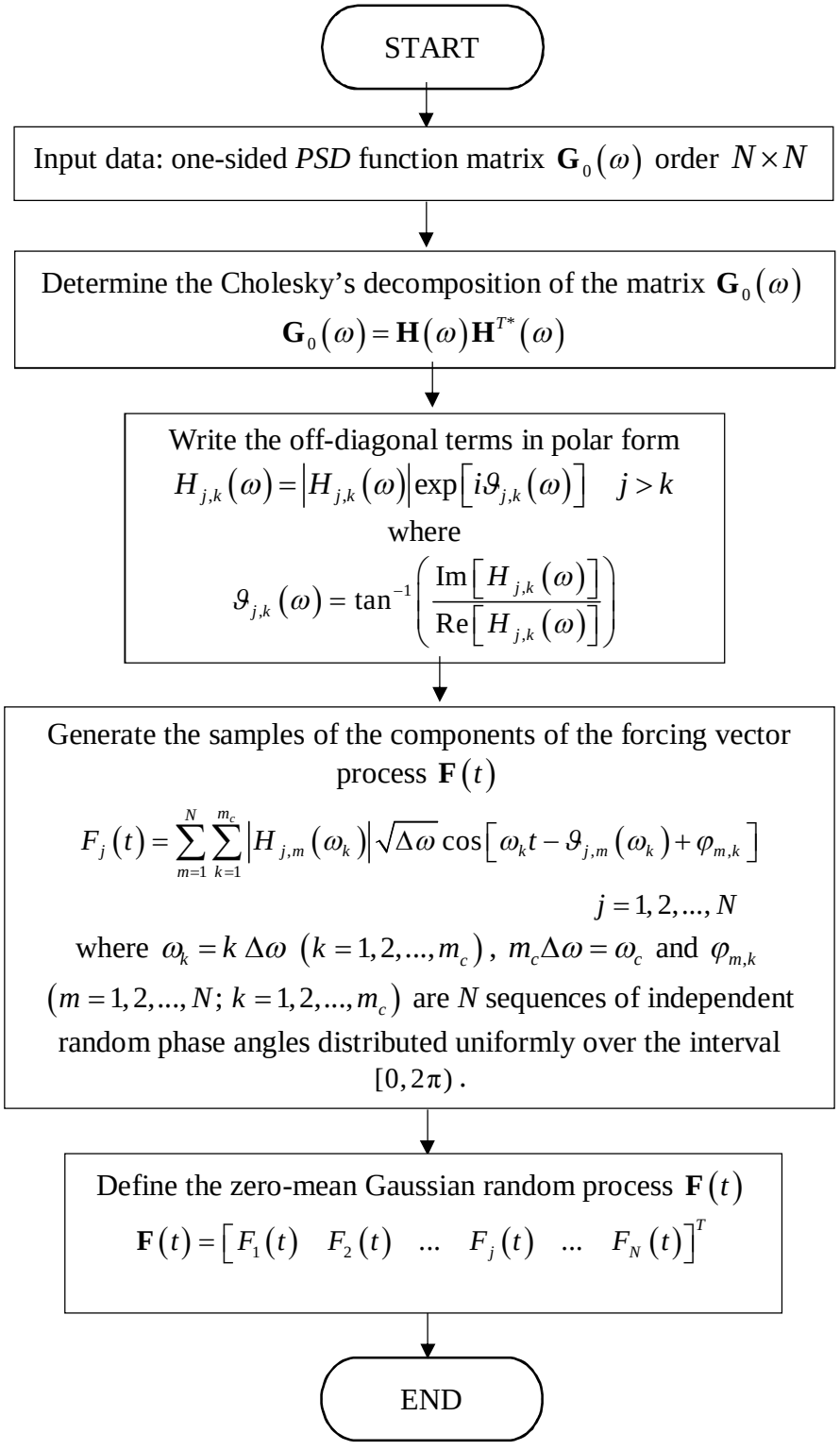

Figure 2. 14 Flow chart of the method proposed by Deodatis (1996a) for the generation of multi-correlated stationary ground motion stochastic vector process.

START

Input data: one-sided *PSD* function matrix $\mathbf{G}_0(\omega)$ of order $N \times N$

Compute the eigenproblem associated with the matrix $\mathbf{G}_0(\omega)$, satisfying the relationships:

$$\boldsymbol{\Psi}^{*\mathbf{T}}(\omega)\boldsymbol{\Psi}(\omega) = \mathbf{I}_{\hat{N}}$$

$$\boldsymbol{\Psi}^{*\mathbf{T}}(\omega)\mathbf{G}_0(\omega)\boldsymbol{\Psi}(\omega) = \boldsymbol{\Lambda}(\omega)$$

where $\boldsymbol{\Psi}(\omega)$ is a matrix of order $N \times \hat{N}$ $\left(\hat{N} \le N\right)$ whose columns are the corresponding eigenvectors $\boldsymbol{\psi}_j(\omega)$ and $\boldsymbol{\Lambda}(\omega)$ is a diagonal matrix whose elements are the eigenvalues $\lambda_j(\omega)$.

Decompose the zero-mean multi-correlated Gaussian random process $\mathbf{F}(t)$ as the sum of $\hat{N}$ fully coherent and independent each other vector processes

$$\mathbf{F}(t) \cong \sum_{j}^{\hat{N}} \mathbf{F}_j(t)$$

Generate the samples of the component vector processes $\mathbf{F}_j(t)$

$$\mathbf{F}_j(t) = \sum_{k=1}^{m_c} \left\{ \sqrt{\lambda_j(\omega_k)\Delta\omega} \left[\boldsymbol{\rho}_j(\omega_k) \left(R_k^{(j)} \cos(\omega_k t) - I_k^{(j)} \sin(\omega_k t) \right) \right] \right.$$

$$\left. - \sqrt{\lambda_j(\omega_k)\Delta\omega} \left[\boldsymbol{\chi}_j(\omega_k) \left(I_k^{(j)} \cos(\omega_k t) - R_k^{(j)} \sin(\omega_k t) \right) \right] \right\}$$

where $\omega_k = k\,\Delta\omega$ $(k = 1, 2, ..., m_c)$, $m_c \Delta\omega = \omega_c$, $\boldsymbol{\rho}_j(\omega_k)$ and $\boldsymbol{\chi}_j(\omega_k)$ are the real and imaginary part, respectively, of the eigenvector $\boldsymbol{\psi}_j(\omega)$, $R_k^{(j)}$ and $I_k^{(j)}$ are the real and imaginary parts of $P_k^{(j)}$, that are complex, normally distributed, zero mean random variables, obeying the following condition:

$$E\left\langle P_k^{(j)} P_r^{(s)*} \right\rangle = \Delta_{kr}\Delta_{rs}, \quad P_{-k}^{(j)} = P_k^{(j)*}$$

END

Figure 2. 15 Flow chart of the method proposed by Di Paola and Zingales (2000) for the generation of multi-correlated stationary ground motion stochastic vector process.

Then, since the Di Paola and Zingales (2000) method, originally formulated for the stationary case, is more convenient from a computational point of view, it has been herein extended to non-stationary multi-correlated random processes for both evolutionary and sigma-oscillatory processes.

In particular, the proposed *MCS* technique, for the sigma-oscillatory stochastic process, requires preliminarily the spectral decomposition of the matrices $\mathbf{G}_0^{(q)}$, which are Hermitian positive definite matrices, by solving the following eigenproblem:

$$\mathbf{G}_0^{(q)}(\omega)\boldsymbol{\Psi}^{(q)}(\omega)=\boldsymbol{\Psi}^{(q)}(\omega)\boldsymbol{\Lambda}^{(q)}(\omega), \qquad q=1,\cdots M. \tag{2.71}$$

As in the classical modal analysis, often only the first $\hat{N} \le N$ eigenproperties are sufficient to decompose accurately the *PSD* matrices $\mathbf{G}_0^{(q)}(\omega)$. In this case $\boldsymbol{\Psi}^{(q)}(\omega)$ becomes a $N \times \hat{N}$ matrix, whose columns are the corresponding eigenvectors, $\boldsymbol{\psi}_j^{(q)}(\omega)$, being $\boldsymbol{\rho}_j^{(q)}(\omega_k)$ and $\boldsymbol{\chi}_j^{(q)}(\omega_k)$ their real and imaginary parts, respectively; while $\boldsymbol{\Lambda}^{(q)}(\omega)$ is a $\hat{N} \times \hat{N}$ diagonal matrix, of order $\hat{N} \times \hat{N}$, whose elements are the eigenvalues $\lambda_j^{(q)}(\omega)$. Notice that, since the matrices $\mathbf{G}_0^{(q)}$ are Hermitian positive definite matrices, all eigenvalues $\lambda_j^{(q)}(\omega)$ are real and positive while the eigenvectors $\boldsymbol{\psi}_j^{(q)}(\omega)$ are complex vectors. Normalizing the eigenvectors in respect to the identity matrix $\mathbf{I}_{\hat{N}}$, the following relationships hold:

$$\begin{aligned}&\boldsymbol{\Psi}^{(q)*\mathbf{T}}(\omega)\boldsymbol{\Psi}^{(q)}(\omega)=\mathbf{I}_{\hat{N}}\\&\mathbf{G}_0^{(q)}(\omega)=\boldsymbol{\Psi}^{(q)}(\omega)\boldsymbol{\Lambda}^{(q)}(\omega)\boldsymbol{\Psi}^{(q)*\mathbf{T}}(\omega).\end{aligned}\tag{2.72}$$

Then, the zero-mean Gaussian random vector process $\mathbf{F}(t)$, of order N, can be decomposed as a summation of $\hat{N} \le N$ fully coherent and independent each other vector processes:

$$\mathbf{F}(t)\cong\sum_{j=1}^{\hat{N}}\mathbf{F}_j(t).\tag{2.73}$$

For the sigma-oscillatory stochastic process subdividing the frequency axis in m_c small intervals one can write:

$$\begin{aligned}\mathbf{F}_j(t)=\sum_{k=1}^{m_c}\sum_{q=1}^{M}&\left|\mathbf{A}^{(q)}(\omega_k,t)\right|\left\{\sqrt{\lambda_j^{(q)}(\omega_k)\Delta\omega}\right.\\&\times\left[\boldsymbol{\rho}_j^{(q)}(\omega_k)\left(R_k^{(j)}\cos(\omega_k t)-I_k^{(j)}\sin(\omega_k t)\right)\right]\\&\left.-\sqrt{\lambda_j^{(q)}(\omega_k)\Delta\omega}\left[\boldsymbol{\chi}_j^{(q)}(\omega_k)\left(I_k^{(j)}\cos(\omega_k t)-R_k^{(j)}\sin(\omega_k t)\right)\right]\right\}.\end{aligned}\tag{2.74}$$

In the previous equation $m_c\Delta\omega=\omega_c$ is the cut-off frequency, $R_k^{(j)}$ and $I_k^{(j)}$ are the real and imaginary parts of $P_k^{(j)}$, that are complex, normally distributed, zero-mean random variables, obeying the following condition:

$$E\left\langle P_k^{(j)}P_r^{(s)*}\right\rangle=\Delta_{kr}\Delta_{rs},\quad P_{-k}^{(j)}=P_k^{(j)*}.\tag{2.75}$$

Furthermore $\left|\mathbf{A}^{(q)}\left(\omega_k,t\right)\right|$ $\left(q=1,...,M\right)$ is the deterministic time-frequency modulating diagonal function matrix, whose elements are the corresponding moduli of the elements of the matrix $\mathbf{A}^{(q)}\left(\omega_k,t\right)$.

From Eq.(2.74) it is possible to derive, as a particular case, the generation formula for evolutionary multi-correlated stochastic vector processes:

$$\begin{aligned}\mathbf{F}_j\left(t\right)=\sum_{k=1}^{m_c}&\left|\mathbf{A}\left(\omega_k,t\right)\right|\left\{\sqrt{\lambda_j\left(\omega_k\right)\Delta\omega}\right.\\&\times\left[\boldsymbol{\rho}_j\left(\omega_k\right)\left(R_k^{(j)}\cos\left(\omega_k t\right)-I_k^{(j)}\sin\left(\omega_k t\right)\right)\right]\\&\left.-\sqrt{\lambda_j\left(\omega_k\right)\Delta\omega}\left[\boldsymbol{\chi}_j\left(\omega_k\right)\left(I_k^{(j)}\cos\left(\omega_k t\right)-R_k^{(j)}\sin\left(\omega_k t\right)\right)\right]\right\}.\end{aligned}\tag{2.76}$$

Notice that the calculation times for the generation of a set of artificial non-stationary multi-correlated accelerograms is almost comparable with the times required for the generation of the same numbers of sample vectors in the stationary case; this is fundamentally due to the introduction of the matrix $\left|\mathbf{A}^{(q)}\left(\omega_k,t\right)\right|$ (see Figure 2.15) that does not significantly influence the computational cost.

2.8 Numerical Applications

2.8.1 Fully non-stationary spectrum-compatible artificial earthquakes

In order to verify the procedure described in Section 2.6.3, to generate fully non-stationary artificial spectrum-compatible earthquake time histories, the set of accelerograms recorded in the

Imperial Valley (California-USA) is analysed (see Figure 2.4). Since all the events, except the one recorded at the station "El Centro Array #2" at the date of 15/10/1979, have a magnitude superior than 5.5 (see Table 2.II) and according to the EC8 instructions (2003) a spectrum of Type I is chosen as target spectrum. The *PGA* is assumed equal to the average of the *PGA* of the recorded events $a_g = 2.483\left[\mathrm{m/s^2}\right]$ and, following the values of the parameters describing the recommended Type I elastic response spectra (EC8 2003) for the type "C" of soil, the parameters $S = 1.15$, $T_B = 0.2$ [s] $T_C = 0.6$ [s] and $T_D = 2.0$ [s] are selected.

Following the iterative procedure described before the spectrum-compatible *PSD* function $G_{\ddot{U}_g}^{\mathrm{STC}}(\omega)$ of the stationary counterpart of the fully non-stationary process $\ddot{U}_{\mathrm{g}}(t)$ is obtained, for the Spanos and Solomos (1983) modulating function defined in Eq.(2.16) and for a new modulating function, obtained modifying the Spanos and Solomos (1983) model, that is:

$$\begin{aligned} a(\omega,t) &= \varphi(t)\,\varepsilon(\omega)\exp\left[-\frac{1}{2}\left(0.15+\frac{\omega^2}{500\pi^2}\right)t\right]; \\ \varepsilon(\omega) &= \frac{1}{a_{\max}}\frac{\omega\sqrt{2}}{5\pi} \end{aligned} \tag{2.77}$$

with $\varphi(t)$ a piecewise function, which models the time-amplitude variation of the non-stationary accelerograms, here assumed step-wise as in the Jennings et al. (1969) model:

$$\varphi(t) = t\left[\left(\frac{t}{\overline{t}_{0.05}}\right)^2 \mathbb{W}(0,\overline{t}_{0.05}) + \mathbb{W}(\overline{t}_{0.05},\overline{t}_{0.95}) + \exp\left[-\alpha\left(t-\overline{t}_{0.95}\right)\right]\mathbb{U}(t-\overline{t}_{0.95})\right] \tag{2.78}$$

where $\mathbb{W}(t_i,t_j)$ and $\mathbb{U}(t)$ are the window and the unit-step functions defined in Eq. (2.15).

In Eq.(2.77) the parameter $a_{\max}$ normalizes the exponential modulating function so that the maximum is unity, while the parameter α, in Eq.(2.78), is an adjustable parameter which has to be chosen to match the mean duration of the recorded accelerograms. This parameter is here assumed $\alpha = 0.13$.

In Figure 2.16 $G_{\ddot{U}_g}^{\mathrm{STC}}(\omega)$ is then compared (in logarithmic scale) with the *PSD* $G_{\ddot{U}_g}^{\mathrm{ST}}(\omega)$ evaluated by Eq.(2.37) under the hypothesis of stationary spectrum-compatible process.

From the analysis of the Figure 2.16 it is evident that at the lower frequencies the spectrum-compatible one-sided *PSD* function of the stationary counterpart, $G_{\ddot{U}_g}^{\mathrm{STC}}(\omega)$, is bigger than the stationary spectrum-compatible one-sided *PSD* function, $G_{\ddot{U}_g}^{\mathrm{ST}}(\omega)$, on the contrary of the higher frequencies.

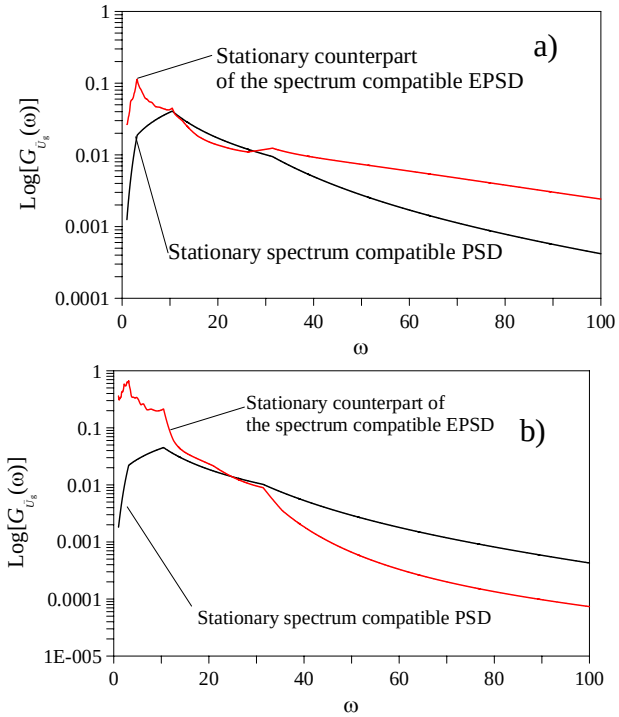

Figure 2. 16 One-sided spectrum-compatible *PSD*s $\left[m^2/s^3\right]$. Stationary assumption (black line) and stationary counterpart in the fully non-stationary assumption (red line), a) Spanos and Solomos (1983) model, b) modified Spanos and Solomos model.

The one-sided *EPSD* function of the spectrum-compatible fully non-stationary process evaluated by Eq.(2.41) is depicted in Figure 2.17.

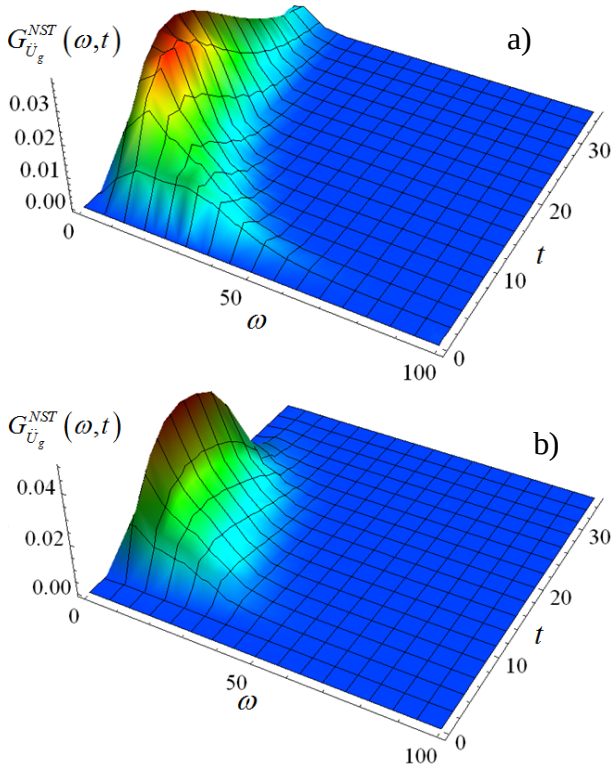

Figure 2. 17 One-sided *EPSD* function of the spectrum-compatible fully non-stationary process $\ddot{U}_g(t)$ a) Spanos and Solomos (1983) model, b) modified Spanos and Solomos model.

Figure 2.18 shows the comparison between the target spectrum $S_{pa}(T,\xi_0)$ and the average spectrum $\overline{S}_{pa}^{NST\,(j\text{-}1)}(T,\xi_0)$ derived from the 1000 artificial spectrum-compatible fully non-stationary accelerograms.

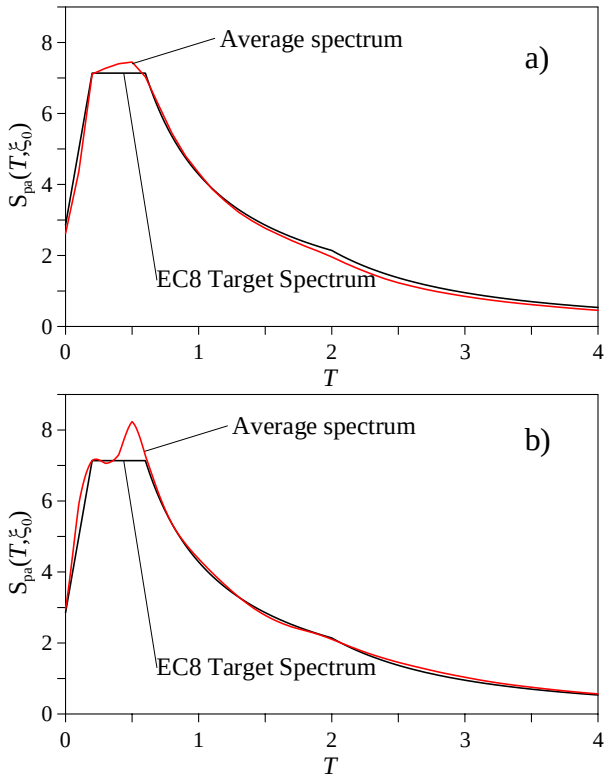

Figure 2. 18 Comparison between the selected EC8 target pseudo-acceleration spectrum $S_{pa}(T,\xi_0)$ (black line) and the average of 1000 pseudo-acceleration spectra $\overline{S}_{pa}^{NST}(T,\xi_0)$ (red line): a) Spanos and Solomos (1983) model, b) modified Spanos and Solomos model.

The arithmetic average of the up-crossing time axis rate $\overline{\nu}^{+}_{\ddot{U}_g}(t)$ is also obtained from the 1000 artificial spectrum-compatible fully non-stationary accelerograms and compared, in Figure 2.19, with the average of the up-crossing time axis rate derived from the set of the recorded time histories. From the analysis of this figure it is evident that the described model is able to catch both the time-varying amplitude and frequency content of actual accelerogram records. It is important to notice that the gap between the average mean frequency of the real accelerograms and of the artificial set cannot be regained because it depends on the spectrum compatible *PSD* function of the stationary counterpart.

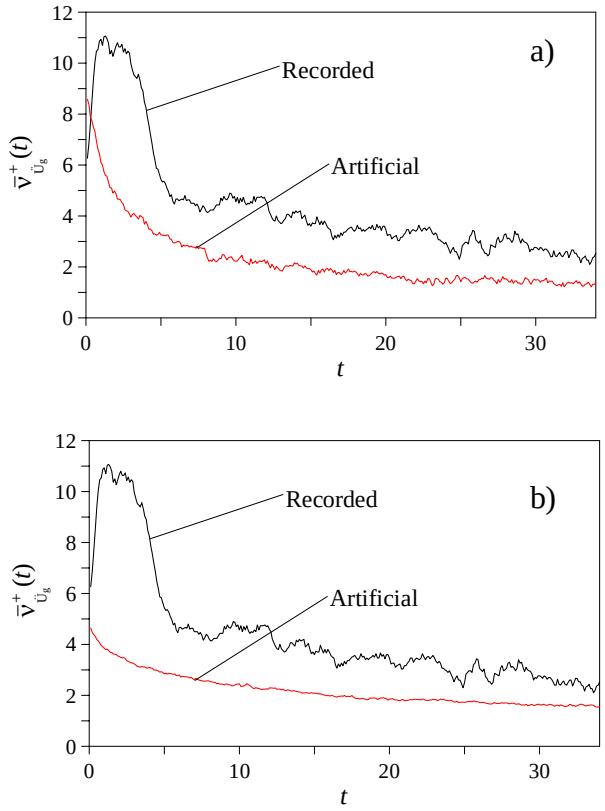

Figure 2. 19 Comparison between the average mean frequency (black line) and the average mean frequency of the artificial spectrum-compatible fully non-stationary accelerograms (red line): a) Spanos and Solomos (1983) model, b) modified Spanos and Solomos model.

Finally, in Table 2.III the following quantities are reported: the average of the energy, $2g\overline{I}_A/\pi$, evaluated as a function of the average of Arias intensity, $\overline{I}_A$, of the recorded accelerograms in the Imperial Valley; the average energy of the 1000 artificial earthquakes, $\overline{E}^{\mathrm{NST}}_{\ddot{U}_g}(t_d)$, as well as the average energy, $\overline{E}^{\mathrm{ST}}_{\ddot{U}_g}(t_d)$, of a set of 1000 spectrum-compatible stationary acceleration random process.

Table 2. III Energy characteristics $\left[m^2/s^3\right]$ of the set of accelerograms and of the stationary and fully non-stationary spectrum compatible acceleration processes

Recorded accelerograms		Artificial accelerograms					
		Spanos & Solomos spectrum compatible model		Modified spectrum compatible model		Stationary spectrum compatible model	
Total mean energy	Standard deviation	Total mean energy	Standard deviation	Total mean energy	Standard deviation	Total mean energy	Standard deviation
$\frac{2g}{\pi}\bar{I}_A$	$\frac{2g}{\pi}\sigma_{I_A}$	$\bar{E}^{\mathrm{NST}}_{\dot{U}_g}(t_d)$	$\sigma_{\bar{E}^{\mathrm{NST}}_{\dot{U}_g}(t_d)}$	$\bar{E}^{\mathrm{NST}}_{\dot{U}_g}(t_d)$	$\sigma_{\bar{E}^{\mathrm{NST}}_{\dot{U}_g}(t_d)}$	$\bar{E}^{\mathrm{ST}}_{\dot{U}_g}(t_d)$	$\sigma_{\bar{E}^{\mathrm{ST}}_{\dot{U}_g}(t_d)}$
5.54	4.88	14.11	1.2	13.02	1.45	27.31	1.32

From the analysis of the results reported in this Table it is evident that the energy associated to the spectrum-compatible stationary model is much higher than the energy evaluated by applying the other ones. On the contrary the spectrum-compatible fully non-stationary process model is able to catch also the energetic aspects of the recorded earthquakes.

2.8.2 Multi-correlated seismic input

In this section in order to verify the validity of the theory explained in Section 2.7, a four span continuous deck bridge is analysed (Lupoi et al. 2005). The deck is over three cantilever piers and the four spans are all 50 [m] long, for a total length of the bridges equal to 200 [m] (Figure 2.20).

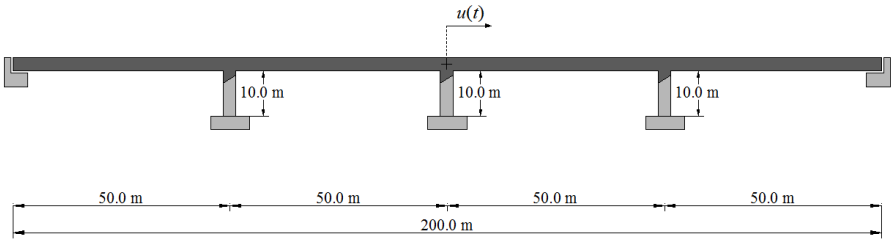

Figure 2. 20 Reference four span continuous deck bridge structure.

The concrete long span bridge is assumed classically damped with damping ratio equal to $\xi_0 = 0.05$. The area and the transverse inertia of the deck and of the piers are, respectively, equal to $A_d = 9.5\left[\mathrm{m}^2\right], I_d = 156\left[\mathrm{m}^4\right]$ and $A_p = 2\left[\mathrm{m}^2\right], I_p = 1\left[\mathrm{m}^4\right]$. The mass, *M*, is obtained taking into account the structure's own weight and is equal to *M* = 36375 [t]. The natural period of the structure is $T_0 = 2.37\left[\mathrm{s}\right]$ and the corresponding natural circular frequency is $\omega_0 = 2.65\left[\mathrm{rad/s}\right]$.

The structure undergoes to non-uniform base excitation modelled by a zero mean tri-variate Gaussian non-stationary process; the multi-variate input is obtained assuming that for the three support points the seismic acceleration possesses equal one-sided *PSD* and different modulating functions. The velocity of the seismic waves through the ground, *c*, is herein assumed $c \to \infty$, so that the coherence functions (see Eq.(2.51)) $\gamma_{0,rs}(\omega)$ become real function, as shown in Figure 2.21. Then $\gamma_{0,rs}(\omega)$ are equal to the spatial correlation function between the *r*-th and *s*-th support-points, $\rho_{rs}(\omega)$, for which the Hanrichandran and Vanmarcke (1986) model is adopted :

$$\rho_{rs}(\omega) \equiv \gamma_{0,rs} = a \exp\left[-\frac{2d_{rs}}{\alpha\theta(\omega)}(1-a+\alpha a)\right] + (1-a)\exp\left[-\frac{2d_{rs}}{\theta(\omega)}(1-a+\alpha a)\right]. \tag{2.79}$$

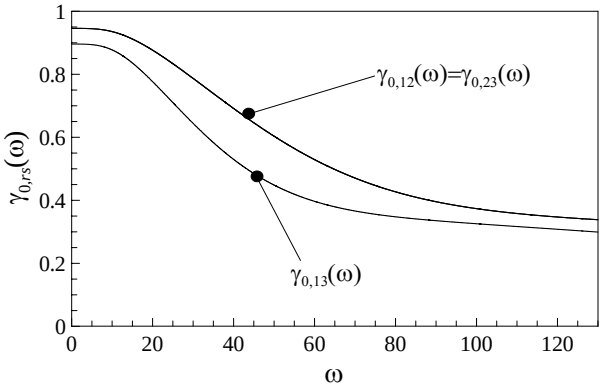

Figure 2. 21 Prescribed coherence functions $\gamma_{0,rs}(\omega)$ $(r,s=1,2,3;\ r\neq s)$.

In the previous equation it is assumed: $a=0.626$, $\alpha=0.022$, $\theta(\omega)=19700\left[1+(\omega/12.692)^{3.47}\right]^{-1/2}$ and $d_{12}=d_{23}=50\,[\mathrm{m}]$ and $d_{13}=100\,[\mathrm{m}]$ (see Figure 2.20).

In order to confirm the generality of the proposed approach, in the framework of the evolutionary process model, two cases have been analysed: the quasi-stationary (or uniformly modulated) random process model, if only the time content of the modulating function changes, and the fully non-stationary random process, when both time and frequency content change. The first model is obtained taking into account the Hsu and Bernard (1978) time-dependent modulating function while the Spanos and Solomos (1983) time-frequency dependent modulating function has been selected for the fully non-stationary model. These modulating

functions differ at each support in the time instant, $t_{\max}$, in which they take their maximum value. The Hsu and Bernard (1978) normalized to one modulating function at the *v*-th support point is written as:

$$a_v(t) = \alpha_v \exp(1) t \exp(-\alpha_v t)\, \mathbb{U}(t) \quad (v = 1,2,3) \tag{2.80}$$

where $\mathbb{U}(t)$ is the unit step function defined in Eq.(2.15). Furthermore in Eq.(2.80) it has been assumed $t_{\max,v} = 1/\alpha_v$, with $\alpha_1 = 1/6;\ \alpha_2 = 1/7;\ \alpha_3 = 1/8$ for the three support points, respectively.

The normalized to one evolutionary modulating function proposed by Spanos and Solomos (1983) assumes the following representation:

$$a_v(\omega,t) = \varepsilon_v(\omega) t \exp(-\alpha_v(\omega) t)\, \mathbb{U}(t) \quad (v = 1,2,3). \tag{2.81}$$

For the three support points the following parameters have been selected: $\varepsilon_v(\omega) = \omega\sqrt{2}/5\pi a_{\max,v}$, with $\alpha_1(\omega) = 0.15/2 + \varepsilon_1{}^2(\omega)/4$, $\alpha_2(\omega) = 0.20/2 + \varepsilon_2{}^2(\omega)/4$, $\alpha_3(\omega) = 0.25/2 + \varepsilon_3{}^2(\omega)/4$; then the normalizing to one coefficients are $a_{\max,1} = 1.34$, $a_{\max,2} = 1.16$, $a_{\max,3} = 1.04$. The unitary maximum is reached at $\omega_1 = 1.94\pi\,[\text{rad/s}]$ and $t_1 = 6.67\,[\text{s}]$, $\omega_2 = 2.24\pi\,[\text{rad/s}]$ and $t_2 = 7.02\,[\text{s}]$, $\omega_3 = 2.50\pi\,[\text{rad/s}]$ and $t_3 = 4.00\,[\text{s}]$.

The target one-sided *PSD* of ground acceleration $G_0(\omega)$ (see Eq.(2.8)) is modelled by the Clough and Penzien (1975) acceleration spectrum:

$$G_0(\omega) = G_g \frac{\left(1+4\xi_g^2\left(\omega/\omega_g\right)^2\right)}{\left(1-\left(\omega/\omega_g\right)^2\right)^2+4\xi_g^2\left(\omega/\omega_g\right)^2} \times \frac{\left(\omega/\omega_f\right)^4}{\left(1-\left(\omega/\omega_f\right)^2\right)^2+4\xi_f^2\left(\omega/\omega_f\right)^2} \tag{2.82}$$

with $\omega_g = 8\pi\left[\text{rad/s}\right]$, $\xi_f = \xi_g = 0.6$, $\omega_f = 0.1\omega_g$ and $G_g = 0.01246\left[\text{m}^2/\text{s}^3\right]$.

In Figure 2.22 the coherence functions of the non-stationary multi-correlated vector, $\mathbf{F}(t)$, are shown. This Figure shows that, for the evolutionary model of multi-correlated seismic actions, the coherence function depend only on the circular frequency.

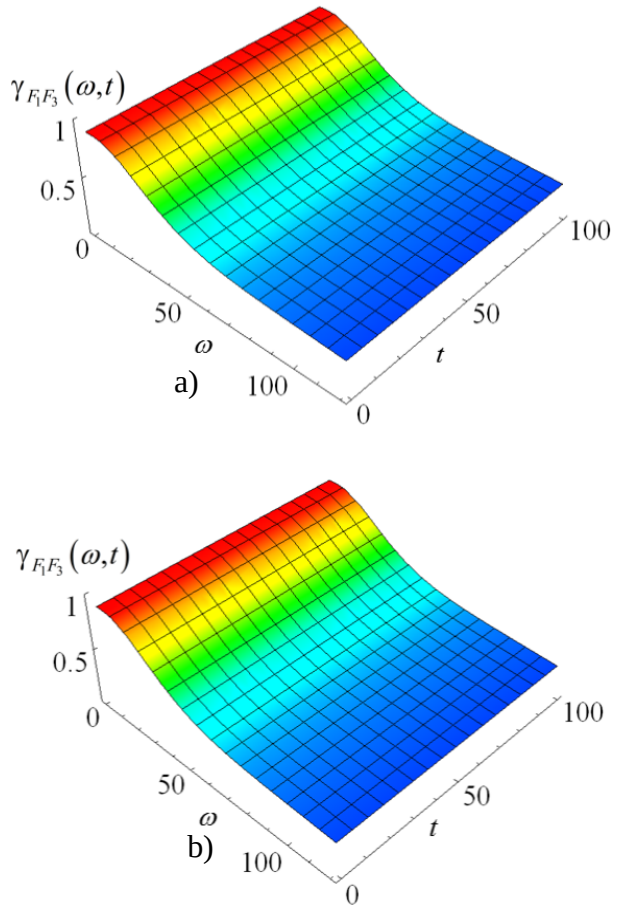

Figure 2. 22 Coherence functions $\gamma_{F_1F_3}(\omega,t)$: a) Hsu and Bernard (1978) modulating function; b) Spanos and Solomos (1983) modulating function.

In order to obtain a multi-correlated sigma-oscillatory process model, the Fourier transform of the El Centro 1940 earthquake has been decomposed in five non-overlapping frequency intervals: $0 \le \Delta\omega_1 < \omega_1$, $\omega_1 \le \Delta\omega_2 < \omega_2$, $\omega_2 \le \Delta\omega_3 < \omega_3$, $\omega_3 \le \Delta\omega_1 < \omega_4$ and $\omega_4 \le \Delta\omega_1 < \omega_5$ with $\omega_1 = 10\left[\text{rad/s}\right]$, $\omega_2 = 20\left[\text{rad/s}\right]$, $\omega_3 = 40\left[\text{rad/s}\right]$, $\omega_4 = 60\left[\text{rad/s}\right]$ and $\omega_5 = 100\left[\text{rad/s}\right]$, in such a way that the total energy of the modelled accelerogram is the same of the recorded one. Moreover, the target one-sided *PSD* of the five

component evolutionary processes is chosen following the philosophy of the Conte and Peng (1997) approach, obtaining:

$$G_0^{(q)}(\omega)=\frac{\nu_q}{\pi}\left[\frac{1}{\nu_q^2+(\omega+\eta_q)^2}+\frac{1}{\nu_q^2+(\omega-\eta_q)^2}\right] \quad (q=1,\cdots,5) \qquad (2.83)$$

where $\nu_q=2$ and $\eta_q=\omega_{q-1}+\left(\omega_q-\omega_{q-1}\right)\big/2$ are two parameters representing the frequency bandwidth and the central mean frequency of the *q*-th stationary counterpart component process, respectively $(q=1,2,\ldots,5)$. The time variation is taken into account by the Shinozuka and Sato (1967) model of the modulating function:

$$a_{v,q}(t)=\varepsilon_{v,q}\left[\exp\left(-\alpha_{1,v,q}\,t\right)-\exp\left(-\alpha_{2,v,q}\,t\right)\right]\mathbb{U}(t), \qquad q=1,\cdots,5;\quad v=1,2,3 \qquad (2.84)$$

where

$$\varepsilon_{v,q}=\mu_{v,q}\frac{\alpha_{1,v,q}}{\alpha_{2,v,q}-\alpha_{1,v,q}}\exp\left[\frac{\alpha_{2,v,q}}{\alpha_{2,v,q}-\alpha_{1,v,q}}\ln\left(\frac{\alpha_{2,v,q}}{\alpha_{1,v,q}}\right)\right], \qquad q=1,\cdots,5;\quad v=1,2,3. \qquad (2.85)$$

The parameters $\alpha_{2,v,q}>\alpha_{1,v,q}$ and $\mu_{v,q}$ are selected in such a way that the total energy of the modelled accelerogram is the same of the recorded one. The set of selected parameters are collected in Table 2.IV. They characterize the sigma-oscillatory process for each of the three support points of the bridge.

Table 2. IV Parameters of the Shinozuka and Sato (1967) modulating functions adopted in modeling the sigma-oscillatory multi-correlated process.

q	$\mu_{1,q}$	$\alpha_{1,1,q}$	$\alpha_{2,1,q}$	$\mu_{2,q}$	$\alpha_{1,2,q}$	$\alpha_{2,2,q}$	$\mu_{3,q}$	$\alpha_{1,3,q}$	$\alpha_{2,3,q}$
1	66.545	0.119	0.30 π	58.475	0.097	0.20 π	51.310	0.072	0.16 π
2	95.772	0.271	0.27 π	76.847	0.165	0.19 π	65.478	0.114	0.15 π
3	76.518	0.191	0.24 π	64.478	0.134	0.17 π	57.064	0.107	0.13 π
4	40.893	0.204	0.23 π	34.623	0.149	0.16 π	30.752	0.121	0.12 π
5	22.015	0.254	0.20 π	19.304	0.166	0.15 π	16.528	0.156	0.10 π

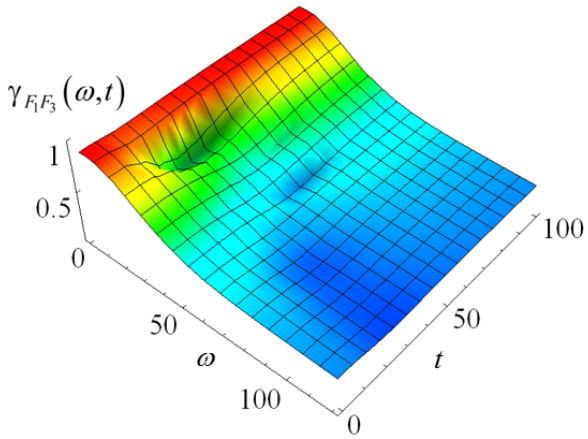

Figure 2. 23 Coherence function $\gamma_{F_1F_3}(\omega,t)$ for the sigma-oscillatory process model (Battaglia 1979).

Figure 2.23 shows that the coherence function of the non-stationary multi-correlated vector, $\mathbf{F}(t)$, depends on both the time and circular frequency, if the sigma-oscillatory process model is adopted on the contrary of the evolutionary process model analysis.

2.9 Summary and conclusions

This Chapter focuses on the characterization of the ground motion acceleration as a non-stationary random process; in fact, starting from an analysis of a set of real earthquakes, it has been shown that the stationary model of the seismic acceleration input process fails to

reproduce the typical characteristics of real recorded ground-motion time history, such as the amplitude and frequency modulation of the signal.

Then different strategies to model the ground motion acceleration stochastic process have been considered; firstly the non-stationary model of the mono-correlated input process has been done following the evolutionary spectral representation (Priesley 1965, Priesley 1967). In this framework four models of modulating functions, for both the quasi-stationary and fully non-stationary process, amongst the most common present in literature, have been presented. Other powerful strategies to analyse the evolutionary frequency content, here analysed, are based on the wavelet analysis (Spanos and Failla 2004, Spanos et al. 2005, Mallat 2009) and on the adaptive decomposition of the signal on a Gaussian chirplet set of functions (Yin et al. 2002, Politis et al. 2006, Spanos et al. 2007).

Furthermore, in order to follow the prescriptions of the building codes, a procedure to generate artificial fully non-stationary spectrum-compatible accelerograms has been proposed; a numerical application, where the non-stationary input process has been chosen coherently with the characteristics of a set of recorded earthquakes, has confirmed the proposed procedure.

In order to take into account the spatial variability of the ground motion acceleration process, that arises when the analysis of structures, such as long span bridges, pipelines, communication transmission systems, etc., is performed, the multi-correlated model of the seismic excitation has been analysed. To describe the fully non-stationary stochastic multi-correlated input process, two models have been adopted: i) the evolutionary process model (Priestley 1965, Priestley 1967); ii) the sigma-oscillatory process model (Battaglia 1979). In the numerical application it has been shown

that, in the case of multivariate and/or multi-correlated fully non-stationary input processes, only the sigma-oscillatory process model is able to catch the time-dependence of the coherence function. Furthermore in the framework of the generation of non-stationary stochastic multi-correlated sigma-oscillatory vector process, it has been proved that the Di Paola and Zingales (2000) method, originally formulated for the stationary case, is more convenient from a computational point of view than the traditional methods, then it has been herein extended to non-stationary multi-correlated random processes for both evolutionary and sigma-oscillatory processes.

Notice that, since the main aim of this research work is to obtain closed form solutions of the *EPSD* function of the response process, the wavelets analysis will not be further investigated whereas it is not yet possible to obtain such solutions in this case.

Chapter 3

Spectral characteristics of the response

3.1 Introduction

Once the characterization of the ground motion acceleration process is done, the second step of the structural engineering deals with the evaluation of structural response to perform the prediction of the safety of structural systems. Among the models of failure, the simplest one, which is also the most widely used in practical analyses, is based on the assumption that a structure fails as soon as the response at a critical location exits a prescribed safe domain for the first time. The probability of failure, in this case, coincides with the *first passage probability*, i.e. the probability that the absolute value of the random response process of a selected structural response (e.g. strain or stress at a critical point) will exceed a specified safety bound, *b*, within a specified time interval (Lin 1976). In random vibration theory, the problem of probabilistically predicting this event is termed *first passage problem*. Unfortunately, this is one of the most complicated problem in computational stochastic mechanics. The solution of this problem, has not been derived in exact form, even in the simplest case of the stationary response of a Single Degree of Freedom (SDOF) linear oscillator

under zero mean Gaussian white noise (Muscolino and Palmeri 2005). Hence, a large number of approximated techniques has been proposed in literature, which differ in generality, complexity and accuracy (Lutes and Sarkani 1997). These techniques require the evaluation of the reliability function of structural systems as a function of barrier crossing rates, distribution of peaks and extreme values. The latter quantities can be evaluated, for stationary input process, as a function of the well-known *Spectral Moments* (*SMs*) introduced by Vanmarcke (1972). For stationary stochastic response processes, the *SMs* are defined as the geometric moments of the one-sided *Power Spectral Density* (*PSD*) function of the response process. Application of spectral methods to non-stationary random processes is more difficult than for stationary processes, indeed for non-stationary processes the geometric approach fails (Di Paola 1985, Muscolino 1988). To solve this problem, Di Paola (1985) introduced the *Pre-Envelope Covariances* (*PECs*) as the covariances of the response of structural systems subjected to a complex-valued random process, the so-called *pre-envelope process*. The real part of this process is proportional to the original non-stationary process, while the imaginary part is an auxiliary random process related to the real part in such a way that the complex process exhibits power in the positive frequency range only. Since the use of complex pre-envelope process is not very intuitive, Michaelov et al. (1999a, 1999b) evaluated the *PECs* as a function of the *Evolutionary Power Spectral Density* (*EPSD*) function of the response and recalled them as *Non-Geometric Spectral Moments* (*NGSMs*). It has to be emphasized that the *NGSMs* contain more information than the "conventional" covariances. Indeed, the *NGSMs* have been proved to be more appropriate for describing non-stationary processes and can be effectively employed in structural reliability applications.

The *NGSMs* have been evaluated by means of the integral formulation (Di Paola and Petrucci 1990, Muscolino 1991, Michaelov et al. 1999b, Barbato and Conte 2008). Alternatively, the *NGSMs* have been derived as solution of set of first-order linear differential equations, for white (Caddemi and Muscolino 1998) and non-white uniformly modulated input process (Langley 1986a, Borino et al. 1988, Caddemi et al. 2004). Although the differential formulation is more suitable from a computational point of view, it is not widely applied and the integral formulation is preferred (Muscolino and Cacciola 2011). This is due to the fact that, in the differential formulation, the complex input-output covariances, which involve the Hilbert transform of both input and output, are needed in order to define the imaginary part of the complex pre-envelope input process.

This Chapter is addressed on the definition of the spectral characteristics of the response of linear *n*-degree-of-freedom, classically and non-classically damped, systems subjected to fully non-stationary excitations. After a brief analysis of the dynamic behaviour of these systems, the *NGSMs* will be obtained as elements of the pre-envelope covariance matrix and a new approach for their evaluation via the *Monte Carlo Simulation* (*MCS*) method will be presented.

3.2 Classically damped structures subjected to mono-correlated input

3.2.1 Equations of motion

Let consider a linear quiescent *n*-degree-of-freedom (*n*-DOF) classically damped structural system whose dynamic behaviour is governed by the equation of motion:

$$\mathbf{M}\,\ddot{\mathbf{u}}(t) + \mathbf{C}\dot{\mathbf{u}}(t) + \mathbf{K}\mathbf{u}(t) = \mathbf{f}(t) \tag{3.1}$$

where **M**, **C**, and **K** are the $(n\times n)$ mass, damping, and stiffness matrices of the structure; **u**(*t*) is the $(n\times 1)$ vector of displacements, having for *i*-th element $u_i(t)$ and a dot over a variable denotes differentiation with respect to time; **f**(*t*) denotes the external loads vector. Under the assumption of classically damped system the equation of motion can be decoupled by applying the modal analysis. Therefore let introduce the modal coordinate transformation:

$$\mathbf{u}(t) = \mathbf{\Phi}\,\mathbf{q}(t) = \sum_{j=1}^{m} \boldsymbol{\phi}_j q_j(t) \;\Rightarrow\; u_i(t) = \sum_{j=1}^{m} \phi_{ij}\, q_j(t). \tag{3.2}$$

In this equation, $\mathbf{\Phi} = \left[\boldsymbol{\phi}_1 \quad \boldsymbol{\phi}_2 \quad \ldots \quad \boldsymbol{\phi}_m\right]$ is the modal matrix, of order $n\times m$, collecting the m eigenvectors $\boldsymbol{\phi}_j$, normalized with respect to the mass matrix **M**, solutions of the following eigenproblem:

$$\mathbf{K}^{-1}\,\mathbf{M}\,\mathbf{\Phi} = \mathbf{\Phi}\,\mathbf{\Omega}^{-2}\;; \quad \mathbf{\Phi}^T\mathbf{M}\,\mathbf{\Phi} = \mathbf{I}_m \tag{3.3}$$

where $\mathbf{\Omega}$ is a diagonal matrix listing the undamped natural circular frequency ω_j, $\mathbf{I}_m$ is the identity matrix of order m and the superscript T denotes the transpose operator. Once the modal matrix $\mathbf{\Phi}$ is evaluated, by applying the coordinate transformations (3.2) to Eq.(3.1), the following set of decoupled second order differential equations is obtained:

$$\ddot{\mathbf{q}}(t) + \mathbf{\Xi}\,\dot{\mathbf{q}}(t) + \mathbf{\Omega}^2\mathbf{q}(t) = \mathbf{\Phi}^T\mathbf{f}\,(t) \tag{3.4}$$

in which $\boldsymbol{\Xi}$ is a the generalized damping matrix given by:

$$\boldsymbol{\Xi}=\boldsymbol{\Phi}^T\mathbf{C}\,\boldsymbol{\Phi}. \tag{3.5}$$

For classically damped structures the modal damping matrix $\boldsymbol{\Xi}$ is a diagonal matrix listing the quantities $2\xi_j\omega_j$, being ξ_j the modal damping ratio. Let's assume now that the forcing term is a mono-correlated zero-mean Gaussian random process vector that can be given by the equation:

$$\mathbf{f}(t)=\mathbf{s}F(t) \tag{3.6}$$

where $\mathbf{s}$ is the $(n\times 1)$ vector of spatial distribution of loads and $F(t)$ is a zero-mean Gaussian non-stationary random process. It follows that the *j*-th differential Eq.(3.4) can be written as:

$$\ddot{q}_j(t)+2\xi_j\omega_j\ \dot{q}_j(t)+\omega_j^2 q_j(t)=p_j\,F(t),\qquad j=1,2,...,m \tag{3.7}$$

where

$$p_j=\boldsymbol{\phi}_j^T\mathbf{s} \tag{3.8}$$

is the *j*-th participating factor.

Notice that, since the zero-mean Gaussian non-stationary random process $F(t)$ possesses one-sided *PSD*, it is a complex process whose imaginary part is a process having stationary counterpart proportional to Hilbert transform of the real part of the complex process itself (Di Paola 1985, Langley 1986a, Muscolino 1988, Di Paola and Petrucci 1990, Muscolino 1991).

3.2.2 Evaluation of *NGSMs*

The modal *NGSM*s have to be defined as the element of the modal *PEC* matrix, introduced by Di Paola and Petrucci (1990), which collects the complex covariances of the response:

$$\begin{aligned}\boldsymbol{\Sigma}_{\mathbf{yy}}(t) = \mathrm{E}\left\langle \mathbf{y}(t)\mathbf{y}^{*T}(t)\right\rangle = \begin{bmatrix} \mathrm{E}\left\langle \mathbf{q}(t)\mathbf{q}^{*}(t)\right\rangle & \mathrm{E}\left\langle \mathbf{q}(t)\dot{\mathbf{q}}^{*}(t)\right\rangle \\ \mathrm{E}\left\langle \dot{\mathbf{q}}(t)\mathbf{q}^{*}(t)\right\rangle & \mathrm{E}\left\langle \dot{\mathbf{q}}(t)\dot{\mathbf{q}}^{*}(t)\right\rangle \end{bmatrix} = \\ = \begin{bmatrix} \boldsymbol{\Lambda}_{0,\mathbf{qq}}(t) & \mathrm{i}\boldsymbol{\Lambda}_{1,\mathbf{qq}}(t) \\ -\mathrm{i}\boldsymbol{\Lambda}^{*T}_{1,\mathbf{qq}}(t) & \boldsymbol{\Lambda}_{2,\mathbf{qq}}(t) \end{bmatrix}\end{aligned} \tag{3.9}$$

where the asterisk indicates the complex conjugate quantity and where $\boldsymbol{\Lambda}_{0,\mathbf{qq}}(t)$, $\boldsymbol{\Lambda}_{1,\mathbf{qq}}(t)$ and $\boldsymbol{\Lambda}_{2,\mathbf{qq}}(t)$ are complex time-dependent matrices of $m \times m$ order collecting the modal *NGSM*s of zero-th, first and second order; moreover $\mathbf{y}(t)$ is the modal state variable vector defined as:

$$\mathbf{y}(t) = \begin{bmatrix} \mathbf{q}(t) \\ \dot{\mathbf{q}}(t) \end{bmatrix}. \tag{3.10}$$

After very simple algebra it can be proved that, by means of the coordinate transformation (3.2), the *b*-th *NGSMs*, $\lambda_{b,u_i u_i}(t)$ $(b = 0,1,2)$, of the *i*-th nodal response, $u_i(t)$, can be evaluated as function of the elements of the modal *PEC*s matrices, $\boldsymbol{\Sigma}_{k\ell}(t)$ $\left(k, \ell = 1..., m\right)$, since the following relationship holds:

$$\boldsymbol{\Sigma}_{u_i u_i}(t) = \begin{bmatrix} \lambda_{0,u_i u_i}(t) & \mathrm{i}\lambda_{1,u_i u_i}(t) \\ -\mathrm{i}\lambda^{*}_{1,u_i u_i}(t) & \lambda_{2,u_i u_i}(t) \end{bmatrix} = \sum_{k=1}^{m}\sum_{\ell=1}^{m} p_k \; p_\ell \, \phi_{ik} \, \phi_{i\ell} \, \boldsymbol{\Sigma}_{k\ell}(t). \tag{3.11}$$

Mathematically strictly speaking, as a consequence of the introduction of the one-sided *PSD*, the response processes $u_i(t)$ is a complex function. Moreover, it has to be emphasized that the zero-th *NGSM*, $\lambda_{0,u_iu_i}(t)$, and the second order *NGSM*, $\lambda_{2,u_iu_i}(t)$, are real functions that coincide with the covariance of the response in terms of displacement and velocity, respectively; while the first order *NGSM*, $\lambda_{1,u_iu_i}(t)$, is a complex quantity whose real part can be evaluated as the cross-covariance between the response process and the response velocity process of the same linear system subjected to a non-stationary input whose stationary counterpart is proportional to its Hilbert transform (Di Paola 1985, Muscolino 1988, Di Paola and Petrucci 1990, Muscolino 1991, Langley 1986a). The modal *PEC*s matrices, $\boldsymbol{\Sigma}_{k\ell}(t)$, introduced in Eq.(3.11), is defined as follows:

$$\begin{aligned}\boldsymbol{\Sigma}_{k\ell}(t) &= \begin{bmatrix} \mathrm{E}\left\langle \tilde{q}_k(t)\tilde{q}_\ell^*(t)\right\rangle & \mathrm{E}\left\langle \tilde{q}_k(t)\dot{\tilde{q}}_\ell^*(t)\right\rangle \\ \mathrm{E}\left\langle \dot{\tilde{q}}_k(t)\tilde{q}_\ell^*(t)\right\rangle & \mathrm{E}\left\langle \dot{\tilde{q}}_k(t)\dot{\tilde{q}}_\ell^*(t)\right\rangle \end{bmatrix} = \\ &= \begin{bmatrix} \lambda_{0,k\ell}(t) & \mathrm{i}\lambda_{1,k\ell}(t) \\ -\mathrm{i}\lambda_{1,k\ell}^*(t) & \lambda_{2,k\ell}(t) \end{bmatrix}\end{aligned} \tag{3.12}$$

where $\tilde{q}_j(t) = q_j(t)/p_j$ is a complex process too solution of the following differential equation:

$$\ddot{\tilde{q}}_j(t) + 2\xi_j\omega_j\,\dot{\tilde{q}}_j(t) + \omega_j^2\tilde{q}_j(t) = F(t) \tag{3.13}$$

Notice that Eq.(3.13) coincides with Eq.(3.7), with the position $p_j = 1$; namely Eq. (3.13) is the equation of the motion of a dummy

oscillator, in fact its solution is "purged" from the participating factors. It has been proved (Di Paola 1985, Langley 1986a, Muscolino 1988, Borino et al 1988, Di Paola and Petrucci 1990, Muscolino 1991, Caddemi and Muscolino 1998, Michaelov et al. 1999a, Michaelov et al. 1999b, Caddemi et al. 2004, Barbato and Conte 2008, Muscolino and Cacciola 2011) that the so called "purged" *NGSMs*, $\lambda_{b,k\ell}(t)$, can be evaluated as a function of the statistics of the response of a dummy oscillator whose motion is governed by Eq.(3.13). Indeed after some algebra, these quantities, which are complex ones, can be evaluated in time-domain, for quiescent structural systems (at time t=0) as follows (Di Paola 1985, Di Paola and Petrucci 1990, Muscolino 1991):

$$\begin{aligned}
&\lambda_{0,k\ell}(t) \equiv \mathrm{E}\left\langle \tilde{q}_k(t)\tilde{q}_\ell^*(t)\right\rangle = \int_0^t\int_0^t h_k\left(t-\tau_1\right)h_\ell\left(t-\tau_2\right)R_{FF}(\tau_1,\tau_2)\,\mathrm{d}\tau_1\mathrm{d}\tau_2;\\
&\lambda_{1,k\ell}(t) \equiv -\mathrm{i}\,\mathrm{E}\left\langle \tilde{q}_k(t)\dot{\tilde{q}}_\ell^*(t)\right\rangle = -\mathrm{i}\int_0^t\int_0^t h_k\left(t-\tau_1\right)\dot{h}_\ell\left(t-\tau_2\right)R_{FF}(\tau_1,\tau_2)\,\mathrm{d}\tau_1\mathrm{d}\tau_2;\\
&\lambda_{2,k\ell}(t) \equiv \mathrm{E}\left\langle \dot{\tilde{q}}_k(t)\dot{\tilde{q}}_\ell^*(t)\right\rangle = \int_0^t\int_0^t \dot{h}_k\left(t-\tau_1\right)\dot{h}_\ell\left(t-\tau_2\right)R_{FF}(\tau_1,\tau_2)\,\mathrm{d}\tau_1\mathrm{d}\tau_2;\\
&\qquad\qquad k=1,2,...,m;\quad \ell=1,2,...,m\,.
\end{aligned} \tag{3.14}$$

where $R_{FF}(\tau_1,\tau_2)$ is the complex autocorrelation function defined as:

$$R_{FF}\left(t_1,t_2\right) = \int_0^\infty \exp\left[\mathrm{i}\omega\left(t_2-t_1\right)\right]a(\omega,t_1)\,a^*(\omega,t_2)G_0(\omega)\mathrm{d}\omega \tag{3.15}$$

where $G_0\left(\omega\right)$ is the one-sided *PSD* function of the stationary counterpart of the input process and

$$h_j(t) = \frac{1}{\bar{\omega}_j} \exp\left(-\xi_j \omega_j t\right) \sin\left(\bar{\omega}_j t\right) \tag{3.16}$$

with $\bar{\omega}_j = \omega_j \sqrt{1-\xi_j^2}$ $(j = k, \ell)$ the damped circular frequency of the *j*-th dummy oscillator. Notice that the presence of the imaginary unit in the second term of the second of Eqs. (3.14) inverts the roles of the real and imaginary parts of $\lambda_{1,k\ell}(t)$ with respect to the cross-covariance $\lambda_{0,k\ell}(t)$ and $\lambda_{2,k\ell}(t)$; furthermore for $k = \ell$ while $\lambda_{0,k\ell}(t)$ and $\lambda_{2,k\ell}(t)$ become real quantities, $\lambda_{1,k\ell}(t)$ remains a complex one.

Moreover, by substituting the complex function $R_{FF}(t_1, t_2)$, defined in Eq.(3.15), into Eq.(3.14), after very simple algebra, it is possible to evaluate the "purged" *NGSMs* as (Di Paola and Petrucci 1990):

$$\begin{aligned}
\lambda_{0,k\ell}(t) &= \int_0^\infty \tilde{Q}_k^*(\omega,t)\tilde{Q}_\ell(\omega,t) G_0(\omega)\mathrm{d}\omega; \\
\lambda_{1,k\ell}(t) &= -\mathrm{i}\int_0^\infty \tilde{Q}_k^*(\omega,t)\dot{\tilde{Q}}_\ell(\omega,t) G_0(\omega)\mathrm{d}\omega; \\
\lambda_{2,k\ell}(t) &= \int_0^\infty \dot{\tilde{Q}}_k^*(\omega,t)\dot{\tilde{Q}}_\ell(\omega,t) G_0(\omega)\mathrm{d}\omega.
\end{aligned} \tag{3.17}$$

For $j=k, \ell$, the following positions have be made:

$$\begin{aligned}
\tilde{Q}_j(\omega,t) &= \int_0^t h_j(t-\tau)\exp(\mathrm{i}\omega\tau)a(\omega,\tau)\mathrm{d}\tau; \\
\dot{\tilde{Q}}_j(\omega,t) &= \int_0^t \dot{h}_j(t-\tau)\exp(\mathrm{i}\omega\tau)a(\omega,\tau)\mathrm{d}\tau.
\end{aligned} \tag{3.18}$$

Remarkably, since the integrals (3.18) are convolution integrals of Duhamel's type, they can be interpreted as the response, in terms of state variables, of the quiescent *j*-th dummy oscillator subjected to the deterministic complex function $f(\omega,t)=\exp(\mathrm{i}\omega t)a(\omega,t)$. Moreover, introducing the state variable, of the response of the *j*-th dummy oscillator:

$$\mathbf{Y}_j(\omega,t)=\begin{bmatrix}\tilde{Q}_j(\omega,t)\\ \dot{\tilde{Q}}_j(\omega,t)\end{bmatrix};\qquad j=k,\ell \tag{3.19}$$

the relationships (3.17) can be rewritten in compact form as follows:

$$\mathbf{\Sigma}_{k\ell}(t)\equiv\int_0^\infty \mathbf{G}_{k\ell}(\omega,t)\mathrm{d}\omega \tag{3.20}$$

where $\mathbf{G}_{k\ell}(\omega,t)$ is the one-sided *EPSD* function matrix of the "purged" modal response, in state variable, given as:

$$\mathbf{G}_{k\ell}(\omega,t)=G_0(\omega)\,\mathbf{Y}_k^*(\omega,t)\mathbf{Y}_\ell^T(\omega,t). \tag{3.21}$$

It follows that, by applying the coordinate transformation (3.2), the one-sided *EPSD* function matrix of the nodal response is given as:

$$\mathbf{G}_{u_iu_i}(t)=\sum_{k=1}^{m}\sum_{\ell=1}^{m}p_k\;p_\ell\,\phi_{ik}\,\phi_{i\ell}\mathbf{G}_{k\ell}(t). \tag{3.22}$$

It has to be emphasized that the vector function introduced in Eq. (3.19), $\mathbf{Y}_j(\omega,t)$, is herein defined as the *modal Time-Frequency*

Varying Response (*TFR*) *vector function* in terms of state variables. Indeed, its first element, $\tilde{Q}_j(\omega,t)$, is the so-called *evolutionary frequency response function* of the *j*-th modal oscillator $(j=k,\ell)$ (Li and Chen 2009).

Finally, taking into account Eq. (3.11), the *b*-th *NGSMs*, $\lambda_{b,u_iu_i}(t)$ ($b=0,1,2$), of the *i*-th nodal response, $u_i(t)$, is given as a function of modal *NGSMs* $\lambda_{b,k\ell}(t)$, $b=0,1,2$, "purged" by p_j factors as follows:

$$\begin{aligned}
\lambda_{0,u_iu_i}(t) &\equiv \mathrm{E}\left\langle u_i(t)u_i^*(t)\right\rangle = \sum_{k=1}^{m}\sum_{\ell=1}^{m} p_k p_\ell \phi_{ik}\phi_{i\ell}\lambda_{0,k\ell}(t);\\
\lambda_{1,u_iu_i}(t) &\equiv -\mathrm{i}\,\mathrm{E}\left\langle u_i(t)\dot{u}_i^*(t)\right\rangle = \sum_{k=1}^{m}\sum_{\ell=1}^{m} p_k p_\ell \phi_{ik}\phi_{i\ell}\lambda_{1,k\ell}(t);\\
\lambda_{2,u_iu_i}(t) &\equiv \mathrm{E}\left\langle \dot{u}_i(t)\dot{u}_i^*(t)\right\rangle = \sum_{k=1}^{m}\sum_{\ell=1}^{m} p_k p_\ell \phi_{ik}\phi_{i\ell}\lambda_{2,k\ell}(t).
\end{aligned} \tag{3.23}$$

3.2.3 Stationary *SMs*

Let us assume now the modulating function $a(\omega,t)=\mathbb{U}(t)$. In this case, starting from this non-stationary formulation it is possible to deduce the formulation in the case of stationary input. This result is obtained by setting $t\to\infty$ into Eq.(3.19). So operating the following time independent relationship is obtained:

$$\lim_{t\to\infty}\mathbf{Y}_j(\omega,t)=\left\{\begin{array}{c}\exp(\mathrm{i}\omega t)H_j(\omega)\\ \mathrm{i}\omega\exp(\mathrm{i}\omega t)H_j(\omega)\end{array}\right\} \tag{3.24}$$

where $H_j(\omega)$ ($j=k,\ell$) is the transfer function of the *j*-th oscillator:

$$H_j(\omega) = \int_0^\infty h_j(\tau)\exp(-\mathrm{i}\omega\tau)\,\mathrm{d}\tau = \frac{1}{\omega_j^2 - \omega^2 + \mathrm{i}\,2\xi_j\omega_j\omega}. \tag{3.25}$$

By substituting Eq. (3.24) into Eq.(3.21) and the results into Eq.(3.20), the elements of this matrix are the well-known Vanmarcke (1972) *SMs*, between the k, ℓ-th dummy oscillators:

$$\begin{aligned}
\lambda_{0,k\ell} &= \int_0^\infty H_k^*(\omega)\,H_\ell(\omega)\,G_0(\omega)\mathrm{d}\omega\,; \\
\lambda_{1,k\ell} &= \int_0^\infty \omega\,H_k^*(\omega)\,H_\ell(\omega)\,G_0(\omega)\mathrm{d}\omega; \\
\lambda_{2,k\ell} &= \int_0^\infty \omega^2 H_k^*(\omega)\,H_\ell(\omega)\,G_0(\omega)\mathrm{d}\omega.
\end{aligned} \tag{3.26}$$

3.3 Classically damped structures subjected to multi-correlated input

3.3.1 Equations of motion

Let consider a linear quiescent classically damped structural system with n unconstrained degree-of-freedom (n-DOF) subjected to N–support motion. In the hypothesis that the seismic motion has only one component per each support point, so N is also the number of DOF of the support points, the dynamic behaviour of the structural system is governed by the following equation of motion:

$$\mathbf{M}\,\ddot{\mathbf{u}}(t) + \mathbf{C}\dot{\mathbf{u}}(t) + \mathbf{K}\mathbf{u}(t) = -\mathbf{M}\,\mathbf{B}\,\mathbf{F}(t) \tag{3.27}$$

where $\mathbf{u}(t)$ is the vector of order $n\times 1$ collecting the displacements of the *n*-DOF of the structure with respect to the *N*–support points, having for *i*-th element $u_i(t)$. Furthermore, in Eq.(3.27) $\mathbf{F}(t)$ is the $N\times 1$ order vector containing the base input accelerations and $\mathbf{B}$ is the influence matrix, of order $n\times N$, given as:

$$\mathbf{B} = -\mathbf{K}^{-1}\mathbf{K}_{\mathrm{sb}} \tag{3.28}$$

where $\mathbf{K}_{\mathrm{sb}}$ is the $n\times N$ order coupling stiffness matrix between the *n* unconstrained DOF of the structure and the *N* support DOF. It follows that the *k*-th column of the influence matrix, represents the displacements at the unconstrained DOF of the structure when the *k*-th support DOF is displaced by a unit amount, while all other support DOF remain fixed.

Under the assumption of classically damped systems the equation of motion can be decoupled by applying the modal analysis, by introducing the modal coordinate transformation (3.2) to Eq.(3.27), the following set of decoupled second order differential equations is obtained:

$$\ddot{\mathbf{q}}(t) + \mathbf{\Xi}\dot{\mathbf{q}}(t) + \mathbf{\Omega}^2\mathbf{q}(t) = \mathbf{P}\,\mathbf{F}(t) \tag{3.29}$$

where

$$\mathbf{P} = -\mathbf{\Phi}^T\,\mathbf{M}\mathbf{B}. \tag{3.30}$$

The *k*-th differential Eq.(3.29) can be written as:

$$\ddot{q}_k(t)+2\xi_k\omega_k\,\dot{q}_k(t)+\omega_k^2\,q_k(t)=\sum_{r=1}^{N}p_{kr}\,F_r(t),\quad k=1,2,...,m;\ (3.31)$$

where p_{kr} is the *k*-th, *r*-th element of the matrix $\mathbf{P}$ and $F_r(t)$ is the *r*-th element of the of vector $\mathbf{F}(t)$.

Notice that, since the zero-mean Gaussian non-stationary random process $\mathbf{F}(t)$ possesses one-sided *PSD*, it is a complex process whose imaginary part is a process having stationary counterpart proportional to Hilbert transform of the real part of the complex process itself.

3.2.2 Evaluation of the *NGSMs*

The modal *NGSM*s have to be defined as the element of the modal *PEC* matrix introduced by Di Paola and Petrucci (1990). Indeed the following relationship holds:

$$\begin{aligned}\boldsymbol{\Sigma}_{\mathbf{yy}}(t)=\mathrm{E}\left\langle\mathbf{y}(t)\mathbf{y}^{*T}(t)\right\rangle=\begin{bmatrix}\mathrm{E}\left\langle\mathbf{q}(t)\mathbf{q}^{*}(t)\right\rangle & \mathrm{E}\left\langle\mathbf{q}(t)\dot{\mathbf{q}}^{*}(t)\right\rangle\\ \mathrm{E}\left\langle\dot{\mathbf{q}}(t)\mathbf{q}^{*}(t)\right\rangle & \mathrm{E}\left\langle\dot{\mathbf{q}}(t)\dot{\mathbf{q}}^{*}(t)\right\rangle\end{bmatrix}=\\ =\begin{bmatrix}\boldsymbol{\Lambda}_{0,\mathbf{qq}}(t) & \mathrm{i}\boldsymbol{\Lambda}_{1,\mathbf{qq}}(t)\\ -\mathrm{i}\boldsymbol{\Lambda}_{1,\mathbf{qq}}^{*T}(t) & \boldsymbol{\Lambda}_{2,\mathbf{qq}}(t)\end{bmatrix}\end{aligned}\qquad(3.32)$$

where $\boldsymbol{\Lambda}_{0,\mathbf{qq}}(t)$, $\boldsymbol{\Lambda}_{1,\mathbf{qq}}(t)$ and $\boldsymbol{\Lambda}_{2,\mathbf{qq}}(t)$ are complex time-dependent matrices of $m\times m$ order collecting the modal *NGSM*s of zero-th, first and second order; moreover $\mathbf{y}(t)$ is the modal state variable vector defined as:

$$\mathbf{y}(t)=\begin{bmatrix}\mathbf{q}(t)\\ \dot{\mathbf{q}}(t)\end{bmatrix}.\qquad(3.33)$$

After very simple algebra it can be shown that, by means of the coordinate transformation (3.2), the *b*-th *NGSMs*, $\lambda_{b,u_iu_i}(t)$ $(b=0,1,2)$, of the *i*-th nodal displacement response, $u_i(t)$, are evaluated as function of the modal *PEC*s matrices $\mathbf{\Sigma}_{k\ell rs}(t)$ $(k,l=1,\ldots,m;\, r,s=1,\ldots N)$ by the following relationships:

$$\begin{aligned}\mathbf{\Sigma}_{u_iu_i}(t) &= \begin{bmatrix} \lambda_{0,u_iu_i}(t) & \mathrm{i}\lambda_{1,u_iu_i}(t) \\ -\mathrm{i}\lambda^{*}_{1,u_iu_i}(t) & \lambda_{2,u_iu_i}(t) \end{bmatrix} = \\ &= \sum_{k=1}^{m}\sum_{\ell=1}^{m}\sum_{r=1}^{N}\sum_{s=1}^{N} p_{kr}\, p_{\ell s}\, \phi_{ik}\, \phi_{i\ell}\, \mathbf{\Sigma}_{k\ell rs}(t)\end{aligned} \tag{3.34}$$

where p_{jv} is the *j*-th, *v*-th element of the matrix $\mathbf{P}$ $(j=k,\ell;\, v=r,s)$. Once again it has to be emphasized that the zero-th *NGSM*, $\lambda_{0,u_iu_i}(t)$, and the second order *NGSM*, $\lambda_{2,u_iu_i}(t)$, are real functions that coincide with the variances of the response in terms of displacement and velocity, respectively; while the first order *NGSM*, $\lambda_{1,u_iu_i}(t)$, is a complex quantity . The modal *PEC* matrix, $\mathbf{\Sigma}_{k\ell rs}(t)$, introduced in Eq.(3.34), is defined as:

$$\begin{aligned}\mathbf{\Sigma}_{k\ell rs}(t) &= \begin{bmatrix} \mathrm{E}\left\langle \tilde{q}_{kr}(t)\tilde{q}^{*}_{\ell s}(t)\right\rangle & \mathrm{E}\left\langle \tilde{q}_{kr}(t)\dot{\tilde{q}}^{*}_{\ell s}(t)\right\rangle \\ \mathrm{E}\left\langle \dot{\tilde{q}}_{kr}(t)\tilde{q}^{*}_{\ell s}(t)\right\rangle & \mathrm{E}\left\langle \dot{\tilde{q}}_{kr}(t)\dot{\tilde{q}}^{*}_{\ell s}(t)\right\rangle \end{bmatrix} = \\ &= \begin{bmatrix} \lambda_{0,k\ell rs}(t) & \mathrm{i}\lambda_{1,k\ell rs}(t) \\ -\mathrm{i}\lambda^{*}_{1,k\ell rs}(t) & \lambda_{2,k\ell rs}(t) \end{bmatrix}\end{aligned} \tag{3.35}$$

where $\tilde{q}_{jv}(t) = q_j(t)/p_{jv}$ is a complex process too, solution of the following differential equation:

$$\ddot{\tilde{q}}_{jv}(t) + 2\xi_j \omega_j \, \dot{\tilde{q}}_{jv}(t) + \omega_j^2 \tilde{q}_{jv}(t) = F_v(t). \tag{3.36}$$

As already done for the classically damped systems subjected to mono-correlated input, the "purged" *NGSMs* $\lambda_{b,k\ell rs}(t)$, among the surface points *r* and *s*, can be evaluated as a function of the statistics of the response of a dummy oscillator whose motion is governed by Eq. (3.36). Indeed after some algebra, these quantities, which are complex ones, can be evaluated in time-domain, for quiescent structural systems (at time *t*=0) as follows (Di Paola 1985, Di Paola and Petrucci 1990, Muscolino 1991):

$$\begin{aligned}
&\lambda_{0,k\ell rs}(t) \equiv \mathrm{E}\left\langle \tilde{q}_{kr}(t)\tilde{q}^*_{\ell s}(t)\right\rangle = \\
&\qquad = \int_0^t\int_0^t h_k\left(t-\tau_1\right) h_\ell\left(t-\tau_2\right) R_{F_rF_s}(\tau_1,\tau_2)\,\mathrm{d}\tau_1\mathrm{d}\tau_2; \\
&\lambda_{1,k\ell rs}(t) \equiv -\mathrm{i}\,\mathrm{E}\left\langle \tilde{q}_{kr}(t)\dot{\tilde{q}}^*_{\ell s}(t)\right\rangle = \\
&\qquad = -\mathrm{i}\int_0^t\int_0^t h_k\left(t-\tau_1\right) \dot{h}_\ell\left(t-\tau_2\right) R_{F_rF_s}(\tau_1,\tau_2)\,\mathrm{d}\tau_1\mathrm{d}\tau_2; \\
&\lambda_{2,k\ell rs}(t) \equiv \mathrm{E}\left\langle \dot{\tilde{q}}_{kr}(t)\dot{\tilde{q}}^*_{\ell s}(t)\right\rangle = \\
&\qquad = \int_0^t\int_0^t \dot{h}_k\left(t-\tau_1\right) \dot{h}_\ell\left(t-\tau_2\right) R_{F_rF_s}(\tau_1,\tau_2)\,\mathrm{d}\tau_1\mathrm{d}\tau_2; \\
&\qquad k=1,2,...,m;\quad \ell=1,2,...,m;\quad r=1,2,...,N;\quad s=1,2,...,N
\end{aligned} \tag{3.37}$$

where $R_{F_rF_s}(\tau_1,\tau_2)$ is the complex autocorrelation function at the two stations *r* and *s* defined as:

$$R_{F_rF_s}\left(t_1,t_2\right) = \int_0^\infty \exp\left[\mathrm{i}\omega\left(t_2-t_1\right)\right] a_r(\omega,t_1)\, a_s^{\,*}(\omega,t_2) G_{0,rs}(\omega)\mathrm{d}\omega \tag{3.38}$$

where $G_{0,rs}(\omega)$ is the *r*-th, *s*-th element of the matrix $\mathbf{G}_0(\omega)$, $a_v(\omega,t)$ $(v=r,s)$ is the *v*-th, element of the diagonal matrix $\mathbf{A}(\omega,t)$ and with $h_j(t)$ the function defined in Eq.(3.16). Notice that the presence of the imaginary unit in the second term of the second of Eqs. (3.37) inverts the roles of the real and imaginary parts of $\lambda_{1,k\ell rs}(t)$ with respect to the cross-covariance $\lambda_{0,k\ell rs}(t)$ and $\lambda_{2,k\ell rs}(t)$.

Moreover, by substituting the complex function defined in Eq.(3.38), into Eq.(3.37), after very simple algebra, it is possible to evaluate the "purged" *NGSMs* as:

$$\begin{aligned}
\lambda_{0,k\ell rs}(t) &= \int_0^\infty \tilde{Q}_{kr}^*(\omega,t)\tilde{Q}_{\ell s}(\omega,t)G_{0,rs}(\omega)\mathrm{d}\omega;\\
\lambda_{1,k\ell rs}(t) &= -\mathrm{i}\int_0^\infty \tilde{Q}_{kr}^*(\omega,t)\dot{\tilde{Q}}_{\ell s}(\omega,t)G_{0,rs}(\omega)\mathrm{d}\omega;\\
\lambda_{2,k\ell rs}(t) &= \int_0^\infty \dot{\tilde{Q}}_{kr}^*(\omega,t)\dot{\tilde{Q}}_{\ell s}(\omega,t)G_{0,rs}(\omega)\mathrm{d}\omega;
\end{aligned} \tag{3.39}$$

For $j=k,\ell$ and $v=r,s$, the following positions have be made:

$$\begin{aligned}
\tilde{Q}_{jv}(\omega,t) &= \int_0^t h_j(t-\tau)\exp(\mathrm{i}\omega\tau)a_v(\omega,\tau)\mathrm{d}\tau;\\
\dot{\tilde{Q}}_{jv}(\omega,t) &= \int_0^t \dot{h}_j(t-\tau)\exp(\mathrm{i}\omega\tau)a_v(\omega,\tau)\mathrm{d}\tau.
\end{aligned} \tag{3.40}$$

Remarkably, since the integrals (3.40) are convolution integrals of Duhamel's type, they can be interpreted as the response, in terms of state variables, of the quiescent *j*-th dummy oscillator at the *v*-th surface point subjected to the deterministic complex function

$f_v(\omega,t)=\exp(\mathrm{i}\omega t)a_v(\omega,t)$. Introducing the state variable of the response of the *j*-th dummy oscillator at the *v* surface point:

$$\mathbf{Y}_{jv}(\omega,t)=\begin{bmatrix}\tilde{Q}_{jv}(\omega,t)\\ \dot{\tilde{Q}}_{jv}(\omega,t)\end{bmatrix};\qquad j=k,\ell\qquad v=r,\mathrm{s} \tag{3.41}$$

the relations (3.39) can be written in compact form as:

$$\mathbf{\Sigma}_{k\ell rs}(t)\equiv\int_0^\infty \mathbf{G}_{k\ell rs}(\omega,t)\mathrm{d}\omega \tag{3.42}$$

where $\mathbf{\Sigma}_{k\ell rs}(t)$ is the covariance function matrix and $\mathbf{G}_{k\ell rs}(\omega,t)$ is the one-sided *EPSD* function matrix between the *k*-th and ℓ-th modal "purged" response processes and among the surface points *r* and *s*. This matrix can be written as:

$$\mathbf{G}_{k\ell rs}(\omega,t)=\mathbf{Y}^*_{kr}(\omega,t)G_{0,rs}(\omega)\mathbf{Y}^T_{\ell s}(\omega,t). \tag{3.43}$$

By means of the modal transformation (3.2), the nodal one-sided *EPSD* function matrix of the displacement response, $u_i(t)$, can be evaluated, after very simple algebra as follows:

$$\mathbf{G}_{u_iu_i}(t)=\sum_{k=1}^{m}\sum_{\ell=1}^{m}\sum_{r=1}^{N}\sum_{s=1}^{N}p_{kr}\,p_{\ell s}\,\phi_{ik}\,\phi_{i\ell}\,\mathbf{G}_{k\ell rs}(t) \tag{3.44}$$

Finally, by taking into account Eq.(3.34), the nodal *NGSMs* can be evaluated as a function of $\lambda_{b,k\ell rs}(t)$, $b=0,1,2$, which are the so-

called time-dependent modal *NGSMs* "purged" by p_{jv} factors as follows:

$$\begin{aligned}
\lambda_{0,u_i u_i}(t) &= \sum_{k=1}^{m}\sum_{\ell=1}^{m}\sum_{r=1}^{N}\sum_{s=1}^{N} p_{kr}\; p_{\ell s}\, \phi_{ik}\, \phi_{i\ell}\, \lambda_{0,k\ell rs}(t);\\
\lambda_{1,u_i u_i}(t) &= \sum_{k=1}^{m}\sum_{\ell=1}^{m}\sum_{r=1}^{N}\sum_{s=1}^{N} p_{kr}\; p_{\ell s}\, \phi_{ik}\, \phi_{i\ell}\, \lambda_{1,k\ell rs}(t);\\
\lambda_{2,u_i u_i}(t) &= \sum_{k=1}^{m}\sum_{\ell=1}^{m}\sum_{r=1}^{N}\sum_{s=1}^{N} p_{kr}\; p_{\ell s}\, \phi_{ik}\, \phi_{i\ell}\, \lambda_{2,k\ell rs}(t).
\end{aligned} \tag{3.45}$$

3.4 Non-Classically damped structures subjected to mono-correlated input

3.4.1 Equations of motion

When the structural system is assumed non-classically damped it follows that the mass, damping and stiffness matrices do not satisfy the Caughey-O'Kelly (1966) condition. In this case the modal damping matrix $\boldsymbol{\Xi}$ is not a diagonal matrix. It follows that, the equation of motion in modal subspace Eq.(3.4) are coupled. To solve Eq.(3.1) the vector $\mathbf{z}(t)$ of state variables have to be introduced:

$$\dot{\mathbf{z}}(t) = \mathbf{D}\,\mathbf{z}(t) + \mathbf{w}F(t) \tag{3.46}$$

where $\mathbf{z}(t)$ is the 2*n*-state vector variable while the matrix **D** and the vector **w** are defined as:

$$\mathbf{z}(t) = \begin{bmatrix} \mathbf{u}(t) \\ \dot{\mathbf{u}}(t) \end{bmatrix}; \quad \mathbf{D} = \begin{bmatrix} \mathbf{0} & \mathbf{I}_m \\ -\mathbf{M}^{-1}\mathbf{K} & -\mathbf{M}^{-1}\mathbf{C} \end{bmatrix}; \quad \mathbf{w} = \begin{bmatrix} \mathbf{0} \\ -\boldsymbol{\tau} \end{bmatrix}. \tag{3.47}$$

It has been proved that from a computational point of view it is more convenient to decouple the set of first order differential equations given in Eq.(3.46) by applying the *complex modal analysis*. According to this analysis the following coordinate transformation is introduced:

$$\mathbf{z}(t) = \boldsymbol{\Psi}\, \mathbf{x}(t). \tag{3.48}$$

If m is the number of modes selected for the analysis, $\mathbf{x}(t)$ is a complex vector of order $2m$ and the complex matrix $\boldsymbol{\Psi}$, of order $(2n \times 2m)$, collects the complex eigenvectors solutions of the following eigenproblem:

$$\mathbf{D}^{-1}\boldsymbol{\Psi} = \boldsymbol{\Psi}\, \boldsymbol{\Lambda}^{-1}; \quad \boldsymbol{\Psi}^T \mathbf{A}\, \boldsymbol{\Psi} = \mathbf{I}_{2m} \tag{3.49}$$

with $\boldsymbol{\Lambda}$ the diagonal matrix collecting the $2m$ complex eigenvalues and

$$\mathbf{A} = \begin{bmatrix} \mathbf{C} & \mathbf{M} \\ \mathbf{M} & \mathbf{0} \end{bmatrix}. \tag{3.50}$$

Since the structural systems are usually underdamped, both eigenvalues, λ_j, and eigenvectors, $\boldsymbol{\psi}_j$, appear in complex-conjugated pairs. Then the corresponding matrices can be written as:

$$\begin{aligned} \boldsymbol{\Psi} &= \begin{bmatrix} \boldsymbol{\psi}_1 & \boldsymbol{\psi}_2 & \cdots & \boldsymbol{\psi}_m & \boldsymbol{\psi}_1^* & \boldsymbol{\psi}_2^* & \cdots & \boldsymbol{\psi}_m^* \end{bmatrix}; \\ \boldsymbol{\Lambda} &= \mathrm{Diag}\begin{bmatrix} \lambda_1 & \lambda_2 & \cdots & \lambda_m & \lambda_1^* & \lambda_2^* & \cdots & \lambda_m^* \end{bmatrix}. \end{aligned} \tag{3.51}$$

The asterisk over a variable denotes complex conjugate quantity and $\mathrm{Diag}[\cdots]$ represents a diagonal matrix. In the previous matrices the eigenvalues and the associate eigenvectors are ordered in such a way that $|\lambda_1| \le |\lambda_2| \le \cdots \le |\lambda_m|$. The symbol $|\bullet|$ denotes the modulus of the function in brackets. Once the complex matrix $\boldsymbol{\Psi}$ is evaluated, by applying the coordinate transformations Eq. (3.48) to Eq.(3.46), the following set of $2m$ complex decoupled first order differential equations is obtained:

$$\dot{\mathbf{x}}(t) = \boldsymbol{\Lambda}\,\mathbf{x}(t) + \mathbf{v}\,F(t); \qquad \mathbf{x}(0) = \mathbf{0} \tag{3.52}$$

with

$$\mathbf{v} = \boldsymbol{\Psi}^T \mathbf{A}\,\mathbf{w}. \tag{3.53}$$

Finally the nodal response can be evaluated by the coordinate transformation (3.48).

3.4.2 Evaluation of the *NGSMs*

In the case of non-classically damped systems the nodal *NGSMs* are evaluated directly as the b,b element of the matrices $\boldsymbol{\Lambda}_{i,\mathbf{uu}}(t)$. These matrices can be evaluated in compact form by introducing the *PEC* matrix. This matrix is a $2n \times 2n$ Hermitian that for non-classically damped systems can be evaluated as (Muscolino 1991):

$$\begin{aligned}\boldsymbol{\Sigma}_{\mathbf{zz}}(t) = \mathrm{E}\left\langle \mathbf{z}(t)\mathbf{z}^{*T}(t)\right\rangle = \begin{bmatrix} \mathrm{E}\left\langle \mathbf{u}(t)\mathbf{u}^{*}(t)\right\rangle & \mathrm{E}\left\langle \mathbf{u}(t)\dot{\mathbf{u}}^{*}(t)\right\rangle \\ \mathrm{E}\left\langle \dot{\mathbf{u}}(t)\mathbf{u}^{*}(t)\right\rangle & \mathrm{E}\left\langle \dot{\mathbf{u}}(t)\dot{\mathbf{u}}^{*}(t)\right\rangle \end{bmatrix} = \\ = \begin{bmatrix} \boldsymbol{\Lambda}_{0,\mathbf{uu}}(t) & \mathrm{i}\boldsymbol{\Lambda}_{1,\mathbf{uu}}(t) \\ -\mathrm{i}\boldsymbol{\Lambda}_{1,\mathbf{uu}}^{*T}(t) & \boldsymbol{\Lambda}_{2,\mathbf{uu}}(t) \end{bmatrix}\end{aligned} \tag{3.54}$$

where $\mathbf{z}(t)$ is the nodal state variable vector defined in Eq.(3.47). After some algebra, these matrices, can be evaluated in time-domain, for quiescent structural systems (at time t=0) as follows (Di Paola 1985, Di Paola and Petrucci 1990, Muscolino 1991):

$$\mathbf{\Sigma_{zz}}(t) = \int_0^t \int_0^t \mathbf{\Theta}(t-\tau_1)\,\mathbf{w}\mathbf{w}^T\,\mathbf{\Theta}^T(t-\tau_2)\,R_{FF}(\tau_1,\tau_2)\,\mathrm{d}\tau_1\,\mathrm{d}\tau_2 \tag{3.55}$$

where $\mathbf{w}$ has been defined in Eq. (3.47), $R_{FF}(\tau_1,\tau_2)$ is the complex autocorrelation function defined in Eq.(3.15), and $\mathbf{\Theta}(t)$ is the transition matrix defined as (Borino and Muscolino 1986, Muscolino 1996):

$$\mathbf{\Theta}(t) = \exp(\mathbf{D}t) = \mathbf{\Psi}\exp(\mathbf{\Lambda}t)\mathbf{\Psi}^T\mathbf{A} \equiv \mathbf{\Psi}^*\exp(\mathbf{\Lambda}^* t)\mathbf{\Psi}^{*T}\mathbf{A} \tag{3.56}$$

in which $\mathbf{D}$ has been defined in Eq.(3.47), $\mathbf{\Lambda}$ and $\mathbf{\Psi}$, are the matrices that collect its eigenvalues and eigenvectors, respectively, defined in Eq.(3.51). By substituting the transition matrix (3.56) into Eq.(3.55), the nodal *PEC* matrix can be written as:

$$\mathbf{\Sigma_{zz}}(t) = \\ = \mathbf{\Psi}^* \left\{ \int_0^t \int_0^t \exp\left[\mathbf{\Lambda}^*(t-\tau_1)\right]\mathbf{v}^*\mathbf{v}^T \exp\left[\mathbf{\Lambda}(t-\tau_2)\right] R_{FF}(\tau_1,\tau_2)\,\mathrm{d}\tau_1\,\mathrm{d}\tau_2 \right\} \mathbf{\Psi}^T \tag{3.57}$$

where the position (3.53) has been used. By substituting the autocorrelation function defined in Eq.(3.15) into Eq.(3.57), it is possible to evaluate the *PEC* matrix (3.54) as:

$$\mathbf{\Sigma_{zz}}(t) = \mathbf{\Psi}^*\,\mathbf{\Sigma_{xx}}(t)\mathbf{\Psi}^T \tag{3.58}$$

where $\mathbf{\Sigma}_{\mathbf{xx}}(t)$ is the *PEC* matrix in the complex state space defined as:

$$\mathbf{\Sigma}_{\mathbf{xx}}(t) = \int_0^{\infty} \mathbf{G}_{\mathbf{xx}}(\omega, t)\, \mathrm{d}\,\omega. \tag{3.59}$$

In the previous equation $\mathbf{G}_{\mathbf{xx}}(\omega, t)$ is the one-sided *EPSD* matrix function of the complex response, that is:

$$\mathbf{G}_{\mathbf{xx}}(\omega, t) = G_0(\omega)\, \mathbf{X}^{*}(\omega, t)\, \mathbf{X}^{T}(\omega, t) \tag{3.60}$$

where $G_0(\omega)$ is the one-sided *PSD* function of the stationary counterpart of the input process and $\mathbf{X}(\omega, t)$ is the *TFR* vector of the complex response, given by:

$$\mathbf{X}(\omega, t) = \int_0^{t} \exp\left[\mathbf{\Lambda}(t - \tau_1)\right] \mathbf{v} \exp(\mathrm{i}\omega\tau)\, a(\omega, \tau)\, \mathrm{d}\tau. \tag{3.61}$$

Since coordinate transformation (3.48) holds, the following coordinate transformation holds too:

$$\mathbf{Z}(\omega, t) = \mathbf{\Psi}\, \mathbf{X}(\omega, t) \tag{3.62}$$

where $\mathbf{Z}(\omega, t)$ is the *TFR* vector of the complex response. Then Eq. (3.58) can be alternatively written as:

$$\boldsymbol{\Sigma}_{\mathbf{zz}}(t) = \boldsymbol{\Psi}^{*}\left[\int_{0}^{\infty} G_0(\omega)\,\mathbf{X}^{*}(\omega,t)\,\mathbf{X}^{T}(\omega,t)\,\mathrm{d}\,\omega\right]\boldsymbol{\Psi}^{T} = \\ = \int_{0}^{\infty} G_0(\omega)\,\mathbf{Z}^{*}(\omega,t)\,\mathbf{Z}^{T}(\omega,t)\,\mathrm{d}\,\omega. \tag{3.63}$$

Notice that by means of the proposed approach the computational effort is sensitively reduced; in fact, by mean of the second of Eqs.(3.63) the *NGSMs* of the nodal response are evaluated directly as the diagonal element of submatrices of the nodal *PEC* matrix. This means that it is necessary to calculate only $3n$ integrals, without the necessity of the evaluation of the *NGSMs* in the complex state space, that is equivalent to $3m^2$ integrals.

3.5 Monte Carlo simulation for the evaluation of *NGSMs*

In order to make a validation of the models that will be proposed, the *NGSMs* evaluated by the analytical approach have to be compared with the ones obtained with the *MCS*. This method, proposed in 1944 by Von Neumann e Ulam, in fact permits to evaluate the statistics of the response process, once the samples of the input process have been generated. It is well known that the *MCS* technique is still the only universal method that can provide accurate solution even when nonlinearities and input uncertainties are involved. In fact the main advantage of this method is to provide accurate results for all the problems in which the deterministic solution, analytic or numeric, is known; the main defect is the computational effort, that is necessary to obtain solutions that are statistically significant.

In this section a new approach for the evaluation of the *NGSMs* via the *MCS* method will be presented; by means of this new method the computation of any Hilbert transforms of the generated samples of the response is avoided.

3.5.1 Classically damped structures subjected to mono-correlated input

In the framework of classically damped systems subjected to mono-correlated stochastic process, since the samples of the input stochastic process, $F^{(i)}(t)$, are chosen in such a way that the input process, $F(t)$, possess one-sided *EPSD* function, $G_{FF}(\omega,t)$ (see Eq.(2.9). In orded to do this the non-stationary input process has to be a complex process having stationary counterpart of the imaginary part proportional to Hilbert transform of the real stationary counterpart part itself. Then, for the evaluation of the *NGSMs* via the *MCS*, it is necessary to define the real and imaginary part of the input process; this requires the computation of the Hilbert transform of the samples of the stationary counterpart of the stochastic process $F(t)$. Since the Hilbert transform is very arduous from a computational point of view, a new procedure to evaluate the *NGSMs* via the *MCS* is herein proposed. Notice that, doing so, the computation of any Hilbert transform is avoided.

The "purged" *NGSMs* of the complex output process have to be evaluated by means of the following relationships (Di Paola 1985, Langley 1986a, Muscolino 1988, Di Paola and Petrucci 1990, Muscolino 1991):

$$\mathrm{Re}\left\{\lambda_{0,k\ell}(t)\right\}=\frac{1}{N}\sum_{i=1}^{N}\left[\mathrm{Re}\left\{\tilde{q}_k^{(i)}(t)\right\}\mathrm{Re}\left\{\tilde{q}_l^{(i)}(t)\right\}+\mathrm{Im}\left\{\tilde{q}_k^{(i)}(t)\right\}\mathrm{Im}\left\{\tilde{q}_l^{(i)}(t)\right\}\right];$$

$$\mathrm{Re}\left\{\lambda_{1,k\ell}(t)\right\}=\frac{1}{N}\sum_{i=1}^{N}\left[\mathrm{Re}\left\{\tilde{q}_k^{(i)}(t)\right\}\mathrm{Im}\left\{\dot{\tilde{q}}_l^{(i)}(t)\right\}-\mathrm{Im}\left\{\tilde{q}_k^{(i)}(t)\right\}\mathrm{Re}\left\{\dot{\tilde{q}}_l^{(i)}(t)\right\}\right];$$

$$\mathrm{Re}\left\{\lambda_{2,k\ell}(t)\right\}=\frac{1}{N}\sum_{i=1}^{N}\left[\mathrm{Re}\left\{\dot{\tilde{q}}_k^{(i)}(t)\right\}\mathrm{Re}\left\{\dot{\tilde{q}}_l^{(i)}(t)\right\}+\mathrm{Im}\left\{\dot{\tilde{q}}_k^{(i)}(t)\right\}\mathrm{Im}\left\{\dot{\tilde{q}}_l^{(i)}(t)\right\}\right] \tag{3.64}$$

where $\mathrm{Re}\left\{\tilde{q}_k^{(i)}(t)\right\}$ is the response of the dummy oscillator, whose motion is governed by the differential equation (3.13) subjected to the forcing function $\mathrm{Re}\left\{F^{(i)}(t)\right\}$, whose generic sample, according to Eq.(2.35), can be evaluated as:

$$\mathrm{Re}\left\{F^{(i)}(t)\right\}=\frac{\sqrt{2}}{2}\sum_{r=1}^{m_c}\sqrt{2G_{FF}\left(t,r\,\Delta\omega\right)\Delta\omega}\,\sin\left(r\,\Delta\omega t+\theta_r^{(i)}\right) \tag{3.65}$$

while $\mathrm{Im}\left\{\tilde{q}_k^{(i)}(t)\right\}$ is the response of the dummy oscillator (3.13) subjected to the forcing function $\mathrm{Im}\left\{F^{(i)}(t)\right\}$, whose generic sample, according to Eq. (2.35), can be evaluated as:

$$\mathrm{Im}\left\{F^{(i)}(t)\right\}=\frac{\sqrt{2}}{2}\sum_{r=1}^{m_c}\sqrt{2G_{FF}\left(t,r\,\Delta\omega\right)\Delta\omega}\,\cos\left(r\,\Delta\omega t+\theta_r^{(i)}\right). \tag{3.66}$$

Notice that in Eq. (3.66) the introduction of the function $\cos(\bullet)$, instead of $\sin(\bullet)$ is equivalent to carry out the Hilbert transform of the stationary counterpart of the input process, but it is not equivalent form a computational point of view. In fact, by mean of this procedure, the computational effort is sensitively reduced.

In Eqs.(3.65) and (3.66) $\Delta\omega = \omega_c / m_c = 0.1$ is the frequency increment; $\omega_c = 100\ \mathrm{rad/s}$ is the adopted upper cut-off circular frequency; $m_c = 1000$ and $\theta_r^{(i)}$ are random phase angles uniformly distributed over the interval $[0 - 2\pi)$. Notice that, in order to rightly apply Eqs.(3.64), the samples of random phase angles have to be generated at the same time in Eqs.(3.65) and (3.66).

3.5.2 Classically damped structures subjected to multi-correlated input

When the stochastic input is modelled as a multi-correlated fully non-stationary process, the "purged" *NGSMs* of the complex output process have to be evaluated by means of the following relationships:

$$\begin{aligned}
\mathrm{Re}\left\{\lambda_{0,k\ell rs}(t)\right\} &= \frac{1}{N}\sum_{i=1}^{N}\left[\mathrm{Re}\left\{\tilde{q}_{kr}^{(i)}(t)\right\}\mathrm{Re}\left\{\tilde{q}_{ls}^{(i)}(t)\right\} + \mathrm{Im}\left\{\tilde{q}_{kr}^{(i)}(t)\right\}\mathrm{Im}\left\{\tilde{q}_{ls}^{(i)}(t)\right\}\right];\\
\mathrm{Re}\left\{\lambda_{1,k\ell rs}(t)\right\} &= \frac{1}{N}\sum_{i=1}^{N}\left[\mathrm{Re}\left\{\tilde{q}_{kr}^{(i)}(t)\right\}\mathrm{Im}\left\{\dot{\tilde{q}}_{ls}^{(i)}(t)\right\} - \mathrm{Im}\left\{\tilde{q}_{kr}^{(i)}(t)\right\}\mathrm{Re}\left\{\dot{\tilde{q}}_{ls}^{(i)}(t)\right\}\right];\\
\mathrm{Re}\left\{\lambda_{2,k\ell rs}(t)\right\} &= \frac{1}{N}\sum_{i=1}^{N}\left[\mathrm{Re}\left\{\dot{\tilde{q}}_{kr}^{(i)}(t)\right\}\mathrm{Re}\left\{\dot{\tilde{q}}_{ls}^{(i)}(t)\right\} + \mathrm{Im}\left\{\dot{\tilde{q}}_{kr}^{(i)}(t)\right\}\mathrm{Im}\left\{\dot{\tilde{q}}_{ls}^{(i)}(t)\right\}\right]
\end{aligned} \tag{3.67}$$

where $\mathrm{Re}\left\{\tilde{q}_{jv}^{(i)}(t)\right\}$ and $\mathrm{Im}\left\{\tilde{q}_{jv}^{(i)}(t)\right\}$ are the response of the *j*-th dummy oscillator at the *v*-support, whose motion is governed by the differential equation (3.36) subjected, respectively, to the forcing function $\mathrm{Re}\left\{F_v^{(i)}(t)\right\}$ and $\mathrm{Im}\left\{F_v^{(i)}(t)\right\}$.

The generic sample of the input process, according to the flow chart in Figure 2.15, can be evaluated as the *v*-th element of the vector:

$$\begin{aligned}\mathrm{Re}\left\{\mathbf{F}^{(i)}(t)\right\} &\cong \sum_{j=1}^{\hat{N}} \mathrm{Re}\left\{\mathbf{F}_j^{(i)}(t)\right\};\\ \mathrm{Im}\left\{\mathbf{F}^{(i)}(t)\right\} &\cong \sum_{j=1}^{\hat{N}} \mathrm{Im}\left\{\mathbf{F}_j^{(i)}(t)\right\};\end{aligned} \tag{3.68}$$

where

$$\begin{aligned}\mathrm{Re}\left\{\mathbf{F}_j^{(i)}(t)\right\} &= \frac{\sqrt{2}}{2}\sum_{k=1}^{m_c}\left\{\sqrt{\lambda_j(\omega_k)\Delta\omega}\right.\\ &\times\left[\boldsymbol{\rho}_j(\omega_k)\left(R_{k,j}^{(i)}\cos(\omega_k t) - I_{k,j}^{(i)}\sin(\omega_k t)\right)\right]\\ &\left.-\sqrt{\lambda_j(\omega_k)\Delta\omega}\left[\boldsymbol{\chi}_j(\omega_k)\left(I_{k,j}^{(i)}\cos(\omega_k t) - R_{k,j}^{(i)}\sin(\omega_k t)\right)\right]\right\};\end{aligned} \tag{3.69}$$

$$\begin{aligned}\mathrm{Im}\left\{\mathbf{F}_j^{(i)}(t)\right\} &= \frac{\sqrt{2}}{2}\sum_{k=1}^{m_c}\left\{\sqrt{\lambda_j(\omega_k)\Delta\omega}\right.\\ &\times\left[\boldsymbol{\rho}_j(\omega_k)\left(R_{k,j}^{(i)}\sin(\omega_k t) - I_{k,j}^{(i)}\cos(\omega_k t)\right)\right]\\ &\left.-\sqrt{\lambda_j(\omega_k)\Delta\omega}\left[\boldsymbol{\chi}_j(\omega_k)\left(I_{k,j}^{(i)}\sin(\omega_k t) - R_{k,j}^{(i)}\cos(\omega_k t)\right)\right]\right\}\end{aligned}$$

with $\Delta\omega = \omega_c/m_c = 0.1$ is the frequency increment; $\omega_c = 100$ rad/s is the adopted upper cut-off circular frequency; $m_c = 1000$, $\boldsymbol{\rho}_j(\omega_k)$ and $\boldsymbol{\chi}_j(\omega_k)$ are the real and imaginary part, respectively, of the eigenvector $\boldsymbol{\psi}_j(\omega)$ (see Figure 2.15), $R_k^{(j)}$ and $I_k^{(j)}$ are the real and imaginary parts of $P_k^{(j)}$, that are complex, normally distributed, zero mean random variables, obeying the following condition:

$$E\left\langle P_k^{(j)} P_r^{(s)*}\right\rangle = \Delta_{kr}\Delta_{rs}, \quad P_{-k}^{(j)} = P_k^{(j)*} \tag{3.70}$$

where Δ_{pq} is the Kronecker delta, defined as:

$$\Delta_{pq} = \begin{cases} 1, & p = q; \\ 0, & p \neq q. \end{cases} \tag{3.71}$$

Notice that, in order to rightly apply Eqs.(3.67), the samples of random variables have to be generated at the same time in Eqs. (3.69).

3.5.3 Non-Classically damped structures subjected to mono-correlated input

When the structure is assumed as non-classically damped, the traditional modal analysis is not still used, and the nodal *NGSMs* are evaluated directly through the relations:

$$\begin{aligned}
\mathrm{Re}\left\{\lambda_{0,u_r u_r}(t)\right\} &= \frac{1}{N}\sum_{i=1}^{N}\left[\mathrm{Re}\left\{u_r^{(i)}(t)\right\}\mathrm{Re}\left\{u_r^{(i)}(t)\right\} + \mathrm{Im}\left\{u_r^{(i)}(t)\right\}\mathrm{Im}\left\{u_r^{(i)}(t)\right\}\right]; \\
\mathrm{Re}\left\{\lambda_{1,u_r u_r}(t)\right\} &= \frac{1}{N}\sum_{i=1}^{N}\left[\mathrm{Re}\left\{u_r^{(i)}(t)\right\}\mathrm{Im}\left\{\dot{u}_r^{(i)}(t)\right\} - \mathrm{Im}\left\{u_r^{(i)}(t)\right\}\mathrm{Re}\left\{\dot{u}_r^{(i)}(t)\right\}\right]; \\
\mathrm{Re}\left\{\lambda_{2,u_r u_r}(t)\right\} &= \frac{1}{N}\sum_{i=1}^{N}\left[\mathrm{Re}\left\{\dot{u}_r^{(i)}(t)\right\}\mathrm{Re}\left\{\dot{u}_r^{(i)}(t)\right\} + \mathrm{Im}\left\{\dot{u}_r^{(i)}(t)\right\}\mathrm{Im}\left\{\dot{u}_r^{(i)}(t)\right\}\right].
\end{aligned} \tag{3.72}$$

In this case $\mathrm{Re}\left\{u_r^{(i)}(t)\right\}$ and $\mathrm{Im}\left\{u_r^{(i)}(t)\right\}$ are the response of the *r*-th nodal DOF, whose motion is governed by the state-variables differential equation (3.46) subjected to the forcing function, respectively, $\mathrm{Re}\left\{F^{(i)}(t)\right\}$, defined in Eq.(3.65), and $\mathrm{Im}\left\{F^{(i)}(t)\right\}$, defined in Eq.(3.66).

3.6 The Role of *NGSMs* in reliability analysis of structures

The *NGSMs* play a fundamental role in the reliability analysis of structures; in fact, for linear structure subjected to stationary or non-stationary Gaussian random input processes a lot of papers have been devoted to the validation of the so called *first-passage probability problem* solutions (that will be further discussed in Chapter 5) by applying the methods based on up-crossing mean rates of a given threshold and censored closures. Both methods require the evaluations of *NGSMs* which need a very cumbersome computational effort, especially for fully non-stationary input processes.

In particular, starting from the purged *NGSMs* of the modal response $\lambda_{i,kl}(t)$, it is possible to obtain the ones for the generic structural response of interest, $S_r(t)$, $\lambda_{i,S_rS_r}(t)$, by introducing an opportune influence matrix $\mathbf{E}$; in fact, taking into account Eq. (3.2), since the following transformations holds:

$$\mathbf{S}(t) = \tilde{\mathbf{R}}\mathbf{u}(t) = \tilde{\mathbf{R}}\boldsymbol{\Phi}\mathbf{u}(t) = \mathbf{E}\mathbf{q}(t) \tag{3.73}$$

where $\tilde{\mathbf{R}}$ is a transformation matrix that have to be defined specifically for the structural response of interest, consequently the *NGSMs* of $S_r(t)$ are given by the following relationships:

$$\lambda_{0,\mathrm{S}_i S_i}(t) = \sum_{k=1}^{m}\sum_{\ell=1}^{m} p_{kr}\; p_{\ell s}\, e_{ik}\, e_{i\ell}\, \lambda_{0,k\ell}(t);$$
$$\lambda_{1,\mathrm{S}_i S_i}(t) = \sum_{k=1}^{m}\sum_{\ell=1}^{m}\sum_{s=1}^{N} p_{kr}\; p_{\ell s}\, e_{ik}\, e_{i\ell}\, \lambda_{1,k\ell}(t); \qquad (3.74)$$
$$\lambda_{2,\mathrm{S}_i S_i}(t) = \sum_{k=1}^{m}\sum_{\ell=1}^{m} p_{kr}\; p_{\ell s}\, e_{ik}\, e_{i\ell}\, \lambda_{2,k\ell}(t).$$

Then in the framework of non-stationary analysis of structures, other time-dependent parameter, very useful in describing the time-variant spectral properties of the stochastic process, are: *i) the bandwidth parameter*, $\delta_S(t)$, that measures the variation in the time of the narrowness of the stochastic process $S(t)$; ii) the mean frequency, $\nu_S^+(t)$, which evaluates the variation in time of the mean up-crossing rate of the time axis; iii) the central frequency, $\omega_{\mathrm{C,S}}(t)$, which scrutinizes the variation of the frequency content of the stochastic process with respect to time. The three functions introduced before can be evaluated as a function of *NGSMs* and have been defined, respectively, as (Michaelov et al 1999a, Michaelov et al 1999b):

$$\delta_S(t) = \sqrt{1 - \frac{\mathrm{Re}\left\{\lambda_{1,S}(t)\right\}^2}{\lambda_{0,S}(t)\lambda_{2,S}(t)}};$$
$$\nu_S^+(t) = \frac{1}{2\pi}\sqrt{\frac{\lambda_{2,S}(t)}{\lambda_{0,S}(t)}}; \qquad (3.75)$$
$$\omega_{\mathrm{C},S}(t) = \frac{\mathrm{Re}\left\{\lambda_{1,S}(t)\right\}}{\lambda_{0,S}(t)}.$$

The problem of the reliability analysis of structures subjected to non-stationary input process and the importance of the *NGSMs* in this framework will be further discussed in Chapter 5.

3.7 Summary and conclusions

Once the characterization of the ground motion acceleration is done, aim of this Chapter is the definition of the spectral characteristics of the response of linear *n*-degree-of-freedom systems, according to three different scenarios:

- classically damped structures subjected to mono-correlated input;
- classically damped structures subjected to multi-correlated input;
- non-classically damped structures subjected to mono-correlated input.

After a brief analysis of the dynamic behaviour of these structures, the *NGSMs* are be obtained as elements of the pre-envelope covariance matrix. Notice that for the classically damped systems the nodal *NGSMs* are obtained as a function of the modal *NGSMs*, while for the non-classically damped systems the nodal NGSMs are obtained directly in the nodal state space; in the last case the computational effort is sensitively reduced, because there isn't the necessity of the evaluation of the *NGSMs* in the complex state space.

Furthermore, in order to make a validation of the proposed procedure, the *NGSMs* evaluated by the analytical approach have to be compared with the ones obtained with the *MCS*. Then, in this Chapter a new approach for the *MCS* of the *NGSMs* has been presented; this new method, takes into account that the non-stationary input process has to be a complex process having

stationary counterpart of the imaginary part proportional to Hilbert transform of the real stationary counterpart part itself. By means of this new procedure the computational effort is sensitively reduced since the computation of any Hilbert transforms of the generated samples of the stationary counterpart of the input process is avoided.

Chapter 4

Closed form solutions of the *EPSD* function matrix of the response

4.1 Introduction

In the framework of stochastic analysis of linear Multi-Degree of Freedom (MDOF) structures, closed-form or explicit solutions are very useful especially if the structural reliability analysis is performed. Spanos and Solomos (1983) derived analitycal expressions for the joint and the marginal probability densities of the response amplitude for a lightly damped Single-Degree of Freedom (SDOF) oscillator subjected to zero-mean stochastic excitation modelled as non-stationary excitation. Explicit or closed-form solutions have been presented by Iwan and Hou (1989) for the evaluation of the cross-covariance functions of an oscillator subjected to uniformly modulated white noise and by Conte and Peng (1996) for the evaluation of correlation and the *Evolutionary Power Spectral Density* (*EPSD*) matrices of the response of classically damped linear MDOF system subjected to uniformly modulated random process. Afterwards closed form solutions have been presented by Peng and Conte (1998) for fully non-stationary

earthquake excitation modelled by the Conte and Peng (1997) sigma-oscillatory process. In the case of uniformly modulated random process: Jangid (2004) derived closed form expressions for the time-varying frequency response function; Falsone and Settineri (2011) derived the correlation matrix and the *EPSD* matrix of the response of linear structural systems subjected to random multi-correlated processes for an exponential type of the modulating function.

In literature, approximate explicit form solutions of the *Non-Geometric Spectral Moments* (*NGSMs*) have been determined by Michaelov et al. (1999b) for linear oscillators subjected to uniformly modulated white noise processes, while closed form solutions of the *NGSMs* have been obtained, for both classically and non-classically damped linear systems, by Barbato and Conte (2008) for non-stationary white noise input processes and by Barbato and Vasta (2010) for uniformly modulated non-stationary coloured input process. Barbato and Conte (2015) derived closed-form solutions for the *NGSMs* of non-stationary stochastic processes representing the response of linear elastic structural models subjected to fully non-stationary excitation earthquake ground motion processes.

In this Chapter a novel procedure to obtain closed form solutions of the *EPSD* function matrix of the response of linear, classically and non-classically damped, structural systems subjected to the seismic input, modelled as a fully non-stationary random process is proposed. The effectiveness of the proposed procedure will be tested with several numerical applications where the results will be compared with the *Monte Carlo Simulation* (*MCS*).

Explicit solutions of the *EPSD* function matrix for particular modulating functions, among the most used in literature, are proposed in Appendix A.

4.2 Closed form solution of the *EPSD* matrix

4.2.1 Closed form solutions for classically damped structures subjected to mono-correlated input

In this section closed-form solutions of the *EPSD* function matrix of the response of classically damped systems subjected to mono-correlated input are proposed. According to Eq. (3.22) the one-sided *EPSD* function matrix of the nodal response is given as:

$$\mathbf{G}_{u_i u_i}(t) = \sum_{k=1}^{m}\sum_{\ell=1}^{m} p_k \; p_\ell \, \phi_{ik} \, \phi_{i\ell} \mathbf{G}_{k\ell}(t) \tag{4.1}$$

where $\mathbf{G}_{k\ell}(\omega,t)$ is the one-sided *EPSD* function matrix of the "purged" modal response, that can be evaluated as a function of the *modal Time-Frequency varying Response* (*TFR*) *vector function* $\mathbf{Y}_i\left(\omega,t\right)\left(i=k,l\right)$ (see Eq(3.19)):

$$\mathbf{G}_{k\ell}(\omega,t) = G_0(\omega)\, \mathbf{Y}_k^*\left(\omega,t\right) \mathbf{Y}_\ell^T\left(\omega,t\right) \tag{4.2}$$

where the asterisk indicates the complex conjugate quantity and $G_0(\omega)$ is the one-sided *PSD* function of the stationary counterpart of the input process. According to Eqs.(3.18), the vector $\mathbf{Y}_j\left(\omega,t\right)$ can be written in integral form as:

$$\mathbf{Y}_j\left(\omega,t\right) = \int_{t_0}^{t} \mathbf{\Theta}_j\left(t-\tau\right) \exp\left(\mathrm{i}\omega\tau\right) a(\omega,\tau)\, \mathbf{v}\, \mathrm{d}\tau; \qquad j=k,\ell \tag{4.3}$$

where $\mathbf{\Theta}_j(t)$ is the transition matrix of the *j*-th modal oscillator defined as (Borino and Muscolino 1986):

$$\mathbf{\Theta}_j(t)=\exp\left(\mathbf{D}_j\,t\right)=\begin{bmatrix}-\omega_j^2 g_j(t) & h_j(t)\\ -\omega_j^2 h_j(t) & \dot{h}_j(t)\end{bmatrix} \tag{4.4}$$

with

$$\begin{aligned} g_j(t)&=-\frac{1}{\omega_j^2}\exp\left(-\xi_j\omega_j t\right)\left[\cos(\bar{\omega}_j t)+\frac{\xi_j\omega_j}{\bar{\omega}_j}\sin(\bar{\omega}_j t)\right];\\ h_j(t)&=\dot{g}_j(t)=\frac{1}{\bar{\omega}_j}\exp\left(-\xi_j\omega_j t\right)\sin(\bar{\omega}_j t);\\ \dot{h}_j(t)&=\exp\left(-\xi_j\omega_j t\right)\left[\cos(\bar{\omega}_j t)-\frac{\xi_j\omega_j}{\bar{\omega}_j}\sin(\bar{\omega}_j t)\right]. \end{aligned} \tag{4.5}$$

Notice that Eq.(4.3) represent the integral form of the response, in state variable, of the *j*-th quiescent dummy oscillator (3.13), at time $t=t_0$, subjected to the force $f(\omega,t)=\exp(i\omega t)a(\omega,t)$. Eq. (4.3) can be also obtained as the solution of the following first order differential equation:

$$\dot{\mathbf{Y}}_j(\omega,t)=\mathbf{D}_j\,\mathbf{Y}_j(\omega,t)+\mathbf{v}\,f(\omega,t)\mathbb{U}(t);\quad \mathbf{Y}_j(\omega,t_0)=\mathbf{Y}_{0,j} \tag{4.6}$$

where $\mathbb{U}(t)$ is the *unit step function* defined as

$$\mathbb{U}(t-t_0)=\begin{cases}0, & t\le t_0;\\ 1, & t>t_0,\end{cases} \tag{4.7}$$

and

$$\mathbf{D}_j = \begin{bmatrix} 0 & 1 \\ -\omega_j^2 & -2\xi_j\omega_j \end{bmatrix}; \quad \mathbf{v} = \begin{bmatrix} 0 \\ 1 \end{bmatrix}. \tag{4.8}$$

Eq.(4.6) represents the differential equation of motion, in state variable, of the *j*-th dummy oscillator (3.13), with initial conditions $\mathbf{Y}_j(\omega, t_0) = \mathbf{Y}_{0,j}$ at time $t = t_0$, subjected to a pseudo-force $f(\omega, t)$. If the particular solution of this equation, $\mathbf{Y}_{\mathrm{p},j}(\omega, t)$, can be determined in explicit form (Muscolino and Alderucci 2015), the *modal TFR vector function*, solution of Eq.(4.6), can be written as (Borino and Muscolino 1986,Muscolino 1996):

$$\mathbf{Y}_j(\omega, t) = \left[\mathbf{Y}_{\mathrm{p},j}(\omega, t) + \mathbf{\Theta}_j(t - t_0)\left(\mathbf{Y}_j(\omega, t_0) - \mathbf{Y}_{\mathrm{p},j}(\omega, t_0) \right) \right] \mathbb{U}(t). \tag{4.9}$$

Notice that the differential formulation (4.9) is valid also when the *j*-th dummy oscillator is not quiescent at time time $t = t_0$, on the contrary of the integral formulation (4.6). Furthermore, the contribution of the last term in the right member of Eq.(4.9) decreases in the time because of the transition matrix satisfies the following condition:

$$\lim_{t \to \infty} \mathbf{\Theta}_j(t) = \mathbf{0}. \tag{4.10}$$

The analytical expression of the particular solution vector $\mathbf{Y}_{\mathrm{p},j}(\omega, t)$, which appears in Eq.(4.9), can be easily obtained in closed form for the most common models of modulating function $a(\omega, t)$ proposed in literature.

In particular almost the totality of modulating functions proposed in literature (see e.g. Shinozuka and Sato 1967, Amin and Ang 1968,

Iyengar and Iyengar 1969, Jennings et al. 1969, Hsu and Bernard 1978, Spanos and Solomos 1983, Iwan and Hou 1989, Conte and Peng 1997) can be evaluated as linear combinations of the following function:

$$a(\omega,t) = \varepsilon(\omega)\,(t-t_0)^b\,\exp\left[-\alpha(\omega)(t-t_0)\right]\;\mathbb{U}(t-t_0); \tag{4.11}$$

where $\mathbb{U}(t-t_0)$ is the unit step function (4.7), r is an integer real number, while $\varepsilon(\omega)$ and $\alpha(\omega)$ could be complex functions which have to be chosen to satisfy the condition: $a(\omega,t) \equiv a^*(-\omega,t)$. It follows that the particular solution vector of the differential equations of the j-th oscillator with initial conditions $\mathbf{Y}_j(\omega,t_0) = \mathbf{Y}_{0,j}$ at time $t = t_0$, forced by the function $\exp\left[\mathrm{i}\omega(t-t_0)\right]a(\omega,t)$, can be evaluated in closed form as follows (Muscolino and Alderucci 2015):

$$\mathbf{Y}_{\mathrm{p},\,j}(\omega,t) = \\ = -\varepsilon(\omega)\exp\left[-\beta(\omega)(t-t_0)\right]\left[\sum_{s=0}^{b}\frac{b!}{s!}(t-t_0)^s\,\mathbf{B}_j^{b-s+1}(\omega)\right]\mathbf{v}\,\mathbb{U}(t-t_0); \tag{4.12}$$

with

$$\beta(\omega) = \alpha(\omega) - \mathrm{i}\omega; \\ \mathbf{B}_j(\omega) = \left[\mathbf{D}_j + \beta(\omega)\mathbf{I}_2\right]^{-1} = \chi_j(\omega)\begin{bmatrix}\beta(\omega)-2\xi_j\omega_j & -1\\ \omega_j^2 & \beta(\omega)\end{bmatrix}; \tag{4.13}$$

and

$$\chi_j(\omega)=\frac{1}{\beta(\omega)^2-2\xi_j\omega_j\beta(\omega)+\omega_j^2}. \tag{4.14}$$

Substituting the vector $\mathbf{Y}_{\mathrm{p},j}(\omega,t)$ into Eq.(4.9), the solution vector, $\mathbf{Y}_j(\omega,t)$, of the *j*-th oscillator in state variable, can be evaluated in closed-form solution as:

$$\mathbf{Y}_j(\omega,t)=-\varepsilon(\omega)\,b!\left\{\exp\left[-\beta(\omega)(t-t_0)\right]\left[\sum_{s=0}^{b}\frac{(t-t_0)^s}{s!}\mathbf{B}_j^{b-s+1}(\omega)\right]\right.$$
$$\left.-\mathbf{\Theta}_j(t-t_0)\mathbf{B}_j^{b+1}(\omega)\right\}\mathbf{v}\,\mathbb{U}(t-t_0); \tag{4.15}$$

where the conditions $\mathbf{Y}_j(\omega,t_0)=\mathbf{0}$ has been considered. It has to be emphasized that this very remarkable result is obtained because of the state variable formulation has been adopted.

Notice that if the modulating function is assumed equals to *unit step function*, $a(\omega,t)=\mathbb{U}(t)$, with $\mathbb{U}(t)$ defined in Eq.(4.7), and taking the limit as $t\to\infty$, the first of element of Eq.(4.15) leads to:

$$\lim_{t\to\infty}\tilde{Q}_j(\omega,t)=\exp(\mathrm{i}\,\omega t)H_j(\omega) \tag{4.16}$$

where $H_j(\omega)$ is the *frequency response function* of the *j*-th modal oscillator:

$$H_j(\omega)=\frac{1}{\omega_j^2-\omega^2+\mathrm{i}\,2\xi_j\omega_j\omega}. \tag{4.17}$$

Finally, substituting Eq. (4.15) in Eq. (4.2) and the result in Eq. (4.1) the one-sided *EPSD* function matrix of the nodal response is obtained.

4.2.2 Closed form solutions for classically damped structures subjected to multi-correlated input

In this section closed-form solutions of the *EPSD* function matrix of the response of classically damped systems subjected to multi-correlated input are proposed, for both the evolutionary process model and sigma-oscillatory process model of the stochastic input. In this case this matrix, according to Eq. (3.44), can be written as:

$$\mathbf{G}_{u_i u_i}(t) = \sum_{k=1}^{m}\sum_{\ell=1}^{m}\sum_{r=1}^{N}\sum_{s=1}^{N} p_{kr}\, p_{\ell s}\, \phi_{ik}\, \phi_{i\ell}\, \mathbf{G}_{k\ell rs}(t) \tag{4.18}$$

where $\mathbf{G}_{k\ell rs}(\omega,t)$ is the is the one-sided *EPSD* function matrix of the "purged" modal response between the two stations *r* and *s*.

4.2.2.1 Evolutionary process model

In the case of multi-correlated input the one-sided *EPSD* function matrix of the "purged" modal response between the two stations *r* and *s* is obtained as:

$$\mathbf{G}_{k\ell rs}(\omega,t) = \mathbf{Y}^{*}_{kr}(\omega,t)\, G_{0,rs}(\omega)\, \mathbf{Y}^{T}_{\ell s}(\omega,t). \tag{4.19}$$

In the previous equation $G_{0,rs}(\omega)$ is the *r*-th, *s*-th element of the matrix $\mathbf{G}_0(\omega)$; the modal *TFR* vector function, $\mathbf{Y}_{jv}(\omega,t)$, for

quiescent systems at time $t = t_0$, taking into account Eq.(2.47), can be evaluated as:

$$\mathbf{Y}_{jv}(\omega,t) = \int_{t_0}^{t} \mathbf{\Theta}_j(t-\tau)\,\mathbf{v}\exp(\mathrm{i}\omega\tau)\,a_v(\omega,\tau)\,\mathrm{d}\tau; \quad j = k,\ell; \quad v = r,s. \tag{4.20}$$

Notice that Eq.(4.20) represent the integral form of the response, in state variable, of the *j*-th quiescent dummy oscillator (3.36), at time $t = t_0$, subjected to the force $f_v(\omega,t) = \exp(i\omega t)\,a_v(\omega,t)$, in which $a_v(\omega,t)$ is the modulating function of the evolutionary process, *v*-th, element $(v = r,s)$ of the diagonal matrix $\mathbf{A}(\omega,t)$.

As recently proposed by Alderucci and Muscolino (2015), the *modal TFR vector functions* $\mathbf{Y}_{jv}(\omega,t)$, for the commonly adopted expressions of the time-frequency varying modulating functions, $a_v(\omega,t)$, can be obtained in closed form solution as the solution of the following first order differential equations, given as:

$$\dot{\mathbf{Y}}_{jv}(\omega,t) = \mathbf{D}_j\,\mathbf{Y}_{jv}(\omega,t) + \mathbf{v}\exp(\mathrm{i}\omega t)\,a_v(\omega,t); \; \mathbf{Y}_{jv}(\omega,t_0) = \mathbf{Y}_{0,jv} \tag{4.21}$$

If the particular solution of this equation, $\mathbf{Y}_{\mathrm{p},\,jv}(\omega,t)$, can be determined in explicit form, the solution of Eq.(4.21), can be written respectively as (Borino and Muscolino 1986, Muscolino 1996):

$$\mathbf{Y}_{jv}(\omega,t) = \mathbf{Y}_{\mathrm{p},\,jv}(\omega,t) + \mathbf{\Theta}_j(t-t_0)\left[\mathbf{Y}_{jv}(\omega,t_0) - \mathbf{Y}_{\mathrm{p},\,jv}(\omega,t_0)\right]. \tag{4.22}$$

Notice that the differential formulation (4.21) is valid also when the *j*-th dummy oscillator is not quiescent at time time $t = t_0$, on the contrary of the integral formulation (4.20). Furthermore, the contribution of the last term in the right member of Eq.(4.22) decreases in the time because of the transition matrix, defined in Eq.(4.4) satisfies the condition (4.10).

Almost the totality of modulating functions proposed in literature (see e.g. Shinozuka and Sato 1967, Amin and Ang 1968, Iyengar and Iyengar 1969, Jennings et al. 1969, Hsu and Bernard 1978, Spanos and Solomos 1983, Iwan and Hou 1989, Conte and Peng 1997) can be evaluated as linear combinations of the following function:

$$a_v(\omega,t) = \varepsilon_v(\omega)(t-t_0)^{b_v} \exp\left[-\alpha_v(\omega)(t-t_0)\right]\mathbb{U}(t-t_0); \quad v = 1,...,N; \tag{4.23}$$

where $\mathbb{U}(t-t_0)$ is the unit step function defined as (4.7), r is an integer real number, while $\varepsilon_v(\omega)$ and $\alpha_v(\omega)$ could be complex functions which have to be chosen to satisfy the condition: $a_v(\omega,t) \equiv a_v^*(\omega,t)$. It follows that the particular solution vector of the differential equations of the *j*-th oscillator with initial conditions $\mathbf{Y}_{jv}(\omega,t_0) = \mathbf{Y}_{0,jv}$ at time $t = t_0$, forced by the function $\exp\left[\mathrm{i}\omega\left(t-t_0\right)\right]a_v(\omega,t)$, can be evaluated in closed form as follows (Alderucci and Muscolino 2015):

$$\begin{aligned}\mathbf{Y}_{\mathrm{p},\,jv}(\omega,t) &= -\varepsilon_v(\omega)\exp\left[-\beta_v(\omega)(t-t_0)\right] \\ &\times\left[\sum_{s=0}^{b_v}\frac{b_v!}{s!}(t-t_0)^s\,\mathbf{B}_{jv}^{b_v-s+1}(\omega)\right]\mathbf{v}\;\mathbb{U}(t-t_0);\end{aligned} \tag{4.24}$$

with

$$\begin{aligned}&\beta_v(\omega)=\alpha_v(\omega)-\mathrm{i}\omega; \\ &\mathbf{B}_{jv}(\omega)=\left[\mathbf{D}_j+\beta_v(\omega)\mathbf{I}_2\right]^{-1}=\chi_{jv}(\omega)\begin{bmatrix}\beta_v(\omega)-2\xi_j\omega_j & -1\\ \omega_j^2 & \beta_v(\omega)\end{bmatrix}\end{aligned} \tag{4.25}$$

and

$$\chi_{jv}(\omega)=\frac{1}{\beta_v(\omega)^2-2\xi_j\omega_j\,\beta_v(\omega)+\omega_j^2}. \tag{4.26}$$

Substituting the vector $\mathbf{Y}_{\mathrm{p},\,jv}(\omega,t)$ into Eq.(4.22), the solution vector, $\mathbf{Y}_{jv}(\omega,t)$, of the *j*-th oscillator in state variable, can be evaluated in closed-form solution as:

$$\begin{aligned}\mathbf{Y}_{jv}(\omega,t) &= -\varepsilon_v(\omega)\,b_v!\Big\{\exp\left[-\beta_v(\omega)(t-t_0)\right] \\ &\times\left[\sum_{s=0}^{b_v}\frac{(t-t_0)^s}{s!}\mathbf{B}_{jv}^{b_v-s+1}(\omega)\right]-\boldsymbol{\Theta}_j(t-t_0)\mathbf{B}_{jv}^{b_v+1}(\omega)\Big\}\mathbf{v}\;\mathbb{U}(t-t_0);\end{aligned} \tag{4.27}$$

where the condition $\mathbf{Y}_{jv}(\omega,t_q)=\mathbf{0}$ has been considered. It has to be emphasized that this very remarkable result is obtained because of the state variable formulation has been adopted.

Finally, substituting Eq. (4.27) in Eq. (4.19) and the result in Eq. (4.18) the one-sided *EPSD* function matrix of the nodal response is obtained.

4.2.2.2 Sigma-oscillatory process model

When the sigma-oscillatory process is used as model of the multi-correlated input the one-sided *EPSD* function matrix of the "purged" modal response is given as:

$$\mathbf{G}_{k\ell rs}(\omega,t)=\sum_{q=1}^{N}\mathbf{Y}^{*}_{krq}\left(\omega,t\right)G^{(q)}_{0,rs}\left(\omega\right)\mathbf{Y}^{T}_{lsq}\left(\omega,t\right) \tag{4.28}$$

where $G^{(q)}_{0,rs}\left(\omega\right)$ is the one-sided cross-*PSD* function of ground accelerations, in a particular direction between surface points *r* and *s*. In this case the modal *TFR* vector function, $\mathbf{Y}_{jvq}\left(\omega,t\right)$, for quiescent systems at time $t=t_0$, taking into account Eq.(2.59), can be evaluated as:

$$\mathbf{Y}_{jvq}\left(\omega,t\right)=\int_{t_q}^{t}\mathbf{\Theta}_j\left(t-\tau\right)\mathbf{v}\exp\left(\mathrm{i}\omega\tau\right)a_{v,q}(\omega,\tau)\,\mathrm{d}\tau;\quad j=k,\ell;\quad v=r,s. \tag{4.29}$$

Notice that Eq.(4.29) represent the integral form of the response, in state variable, of the *j*-th quiescent dummy oscillator (3.36), at time $t=t_q$, subjected to the force $f_{v,q}\left(\omega,t\right)=\exp\left(i\omega t\right)a_{v,q}\left(\omega,t\right)$, in which $a_{v,q}(\omega,t)$ is the modulating function of the *q*-th component of the sigma-

oscillatory process, *v*-th, element $(v = r, s)$ of the diagonal matrix $\mathbf{A}_q(\omega, t)$.

As recently proposed by Alderucci and Muscolino (2015), the modal *TFR* vector functions $\mathbf{Y}_{jvq}(\omega, t)$, for the commonly adopted expressions of the time-frequency varying modulating functions $a_{v,q}(\omega, t)$, can be obtained in closed form solution as the solution of the following first order differential equations, given as:

$$\dot{\mathbf{Y}}_{jvq}(\omega, t) = \mathbf{D}_j \mathbf{Y}_{jvq}(\omega, t) + \mathbf{v} \exp(\mathrm{i}\omega t)\, a_{v,q}(\omega, t); \quad \mathbf{Y}_{jvq}(\omega, t_q) = \mathbf{Y}_{0,jvq}. \tag{4.30}$$

If the particular solution of this equation, $\mathbf{Y}_{\mathrm{p},jvq}(\omega, t)$, can be determined in explicit form, the solution of Eq.(4.30), can be written as (Borino and Muscolino 1986, Muscolino 1996):

$$\mathbf{Y}_{jvq}(\omega, t) = \mathbf{Y}_{\mathrm{p},jvq}(\omega, t) + \mathbf{\Theta}_j(t - t_0)\left[\mathbf{Y}_{jvq}(\omega, t_0) - \mathbf{Y}_{\mathrm{p},jvq}(\omega, t_0)\right]. \tag{4.31}$$

Notice that the differential formulation (4.21) is valid also when the *j*-th dummy oscillator is not quiescent at time $t = t_q$, on the contrary of the integral formulation (4.20). Furthermore, the contribution of the last term in the right member of Eq.(4.31) decreases in the time because of the transition matrix, defined in Eq.(4.4) satisfies the condition (4.10).

Almost the totality of modulating functions proposed in literature (see e.g. Shinozuka and Sato 1967, Amin and Ang 1968, Iyengar and Iyengar 1969, Jennings et al. 1969, Hsu and Bernard 1978, Spanos and Solomos 1983, Iwan and Hou 1989, Conte and Peng

1997) for the sigma-oscillatory stochastic processes can be evaluated as linear combinations of the following function:

$$a_{v,q}(\omega,t)=\varepsilon_{vq}(\omega)(t-t_q)^{b_{vq}}\exp\left[-\alpha_{vq}(\omega)(t-t_q)\right]\mathbb{U}(t-t_q);\quad v=1,...,N,\ q=1,...,M \tag{4.32}$$

where $\mathbb{U}(t-t_q)$ is the unit step function defined as (4.7), r is an integer real number, while $\varepsilon_{vq}(\omega)$ and $\alpha_{vq}(\omega)$ could be complex functions which have to be chosen to satisfy the condition: $a_{v,q}(\omega,t)\equiv a^{*}_{v,q}(\omega,t)$. It follows that the particular solution vector of the differential equations of the *j*-th oscillator with initial conditions $\mathbf{Y}_{jv}\left(\omega,t_q\right)=\mathbf{Y}_{0,jv}$ at time $t=t_q$, forced by the function $\exp\left[\mathrm{i}\omega\left(t-t_q\right)\right]a_{v,q}(\omega,t)$, can be evaluated in closed form as follows (Alderucci and Muscolino 2015):

$$\mathbf{Y}_{\mathrm{p},\,jvq}\left(\omega,t\right)=-\varepsilon_{vq}(\omega)\exp\left[-\beta_{vq}\left(\omega\right)(t-t_q)\right]\times\left[\sum_{s=0}^{b_{vq}}\frac{b_{vq}!}{s!}(t-t_q)^{s}\,\mathbf{B}_{jvq}^{b_{vq}-s+1}\left(\omega\right)\right]\mathbf{v}\ \mathbb{U}(t-t_q); \tag{4.33}$$

with

$$\beta_{vq}\left(\omega\right)=\alpha_{vq}\left(\omega\right)-\mathrm{i}\omega;$$
$$\mathbf{B}_{jvq}\left(\omega\right)=\left[\mathbf{D}_j+\beta_{vq}\left(\omega\right)\mathbf{I}_2\right]^{-1}=\chi_{jvq}\left(\omega\right)\begin{bmatrix}\beta_{vq}\left(\omega\right)-2\xi_j\omega_j & -1\\ \omega_j^2 & \beta_{vq}\left(\omega\right)\end{bmatrix}; \tag{4.34}$$

and

$$\chi_{jvq}(\omega)=\frac{1}{\beta_{vq}(\omega)^2-2\xi_j\omega_j\,\beta_{vq}(\omega)+\omega_j^2}. \tag{4.35}$$

Substituting the vector $\mathbf{Y}_{\mathrm{p},jvq}(\omega,t)$ into Eq.(4.31), the solution vector, $\mathbf{Y}_{jvq}(\omega,t)$, of the *j*-th oscillator in state variable, can be evaluated in closed-form solution, respectively, as:

$$\begin{aligned}\mathbf{Y}_{jvq}(\omega,t)=&-\varepsilon_{vq}(\omega)b_{vq}!\Big\{\exp\left[-\beta_{vq}(\omega)(t-t_q)\right]\\&\times\left[\sum_{s=0}^{b_{vq}}\frac{(t-t_q)^s}{s!}\mathbf{B}_{jvq}^{b_{vq}-s+1}(\omega)\right]-\mathbf{\Theta}_j(t-t_q)\mathbf{B}_{jvq}^{b_{vq}+1}(\omega)\Big\}\mathbf{v}\mathbb{U}(t-t_q)\end{aligned} \tag{4.36}$$

where the condition $\mathbf{Y}_{jvq}(\omega,t_q)=\mathbf{0}$ has been considered. It has to be emphasized that this very remarkable result is obtained because of the state variable formulation has been adopted.

Finally, substituting Eq. (4.36) in Eq. (4.28) and the result in Eq. (4.18) the one-sided *EPSD* function matrix of the nodal response is obtained.

4.2.3 Closed form solutions for non-classically damped structures subjected to mono-correlated input

In this section closed-form solutions of the *EPSD* function matrix of the response of non-classically damped systems subjected to mono-correlated input are proposed.

The one-sided *EPSD* matrix function of the nodal response $\mathbf{G}_{\mathbf{ZZ}}(\omega,t)$ is, given by:

$$\mathbf{G}_{\mathbf{ZZ}}(\omega,t)=G_0(\omega)\,\mathbf{Z}^*(\omega,t)\mathbf{Z}^T(\omega,t) \tag{4.37}$$

where $G_0(\omega)$ is the one-sided PSD function of the stationary counterpart of input process $F(t)$ and $\mathbf{Z}(\omega,t)$ is the *TFR* vector of the nodal response. If the system is assumed as non-classically damped, the vector $\mathbf{Z}(\omega,t)$ can be written in integral form as:

$$\mathbf{Z}(\omega,t)=\int_{t_0}^{t}\mathbf{\Theta}(t-\tau)\exp(\mathrm{i}\omega\tau)a(\omega,\tau)\mathbf{v}\,\mathrm{d}\tau;\qquad j=k,\ell \tag{4.38}$$

where $\mathbf{\Theta}(t)$ is the transition matrix defined as (Borino and Muscolino 1986):

$$\mathbf{\Theta}(t)=\exp(\mathbf{D}t)=\mathbf{\Psi}\exp(\mathbf{\Lambda}t)\mathbf{\Psi}^{T}\mathbf{A} \tag{4.39}$$

where $\mathbf{D}$ has been defined in Eq.(3.47). Notice that Eq.(4.38) represent the integral form of the solution of Eq. (3.46), when the system is assumed quiescent, at time $t=t_0$, and subjected to the force $f(\omega,t)=\exp(i\omega t)a(\omega,t)$. $\mathbf{Z}(\omega,t)$ can be also evaluated as the solution of the following set of 2*n* first order differential equation (Muscolino and Alderucci, 2015):

$$\dot{\mathbf{Z}}(\omega,t)=\mathbf{D}\,\mathbf{Z}(\omega,t)+\mathbf{w}\,f(\omega,t)\mathbb{U}(t);\qquad \mathbf{Z}(\omega,\mathrm{t}_0)=\mathbf{Z}_0 \tag{4.40}$$

subjected to pseudo-force $f(\omega,t)=\exp(-\mathrm{i}\omega t)a(\omega,t)$. In the previous equations $\mathbf{w}$ has been defined in Eq.(3.47). Since the following coordinate transformation holds:

$$\mathbf{Z}(\omega,t)=\mathbf{\Psi}\,\mathbf{X}(\omega,t) \tag{4.41}$$

It follows that the first order differential equation (4.40) can be rewritten as a set of 2*m* decoupled first order differential equations:

$$\begin{aligned}&\dot{\mathbf{X}}(\omega,t)=\mathbf{\Lambda}\,\mathbf{X}(\omega,t)+\mathbf{v}\,f(\omega,t)\mathbb{U}(t);\\&\mathbf{X}_0\equiv\mathbf{X}(\omega,t_0)=\mathbf{\Psi}^T\mathbf{A}\;\;\mathbf{Z}_0\end{aligned}\tag{4.42}$$

This equation represents the differential equation of motion, in state variable, of a dynamical system at with initial conditions $\mathbf{X}(\omega,t_0)=\mathbf{X}_0$ at time $t=t_0$, subjected to a pseudo-force $f(\omega,t)$. If the particular solution of Eq.(4.42), $\mathbf{X}_{\mathrm{p}}(\omega,t)$, can be determined in explicit form, the *TFR* vector function can be written as (Borino and Muscolino, 1986; Muscolino 1996):

$$\mathbf{X}(\omega,t)=\left\{\mathbf{X}_{\mathrm{p}}(\omega,t)+\exp(\mathbf{\Lambda}t)\left[\mathbf{X}(\omega,t_0)-\mathbf{X}_{\mathrm{p}}(\omega,t_0)\right]\right\}\mathbb{U}(t)\tag{4.43}$$

Notice that the differential formulation (4.43) is valid also when the dynamical system is not quiescent at time time $t=t_0$, on the contrary of the integral formulation(4.38). Then, according to Eq.(4.41), the solution of Eq.(4.40) can be written as:

$$\begin{aligned}&\mathbf{Z}(\omega,t)=\mathbf{\Psi}\;\mathbf{X}(\omega,t)=\\&=\mathbf{\Psi}\left\{\mathbf{X}_{\mathrm{p}}(\omega,t)+\exp(\mathbf{\Lambda}t)\left[\mathbf{X}(\omega,t_0)-\mathbf{X}_{\mathrm{p}}(\omega,t_0)\right]\right\}\mathbb{U}(t)=\\&=\left\{\mathbf{Z}_{\mathrm{p}}(\omega,t)+\mathbf{\Theta}(t)\left[\mathbf{Z}(\omega,t_0)-\mathbf{Z}_{\mathrm{p}}(\omega,t_0)\right]\right\}\mathbb{U}(t).\end{aligned}\tag{4.44}$$

The analytical expression of the particular solution vector $\mathbf{Z}_{\mathrm{p}}(\omega,t)=\mathbf{\Psi}\mathbf{X}_{\mathrm{p}}(\omega,t)$, can be easily obtained in closed form for the

most common models of modulating function $a(\omega,t)$ proposed in literature.

Then the particular solution vector of non-classically damped structural system, forced by the function $f(\omega,t)=\exp(i\omega t)a(\omega,t)$, can be evaluated in closed form as:

$$\begin{aligned}\mathbf{Z}_{\mathrm{p}}(\omega,t) &= -\varepsilon(\omega)\exp\left[-\beta(\omega)(t-t_0)\right] \\ &\times\boldsymbol{\Psi}\left[\sum_{s=0}^{b}\frac{b!}{s!}(t-t_0)^s\,\boldsymbol{\Gamma}^{b-s+1}(\omega)\right]\boldsymbol{\Psi}^T\mathbf{A}\,\mathbf{w}\,\mathbb{U}(t)\end{aligned} \tag{4.45}$$

where $\beta(\omega)=\alpha(\omega)-\mathrm{i}\omega$ and $\boldsymbol{\Gamma}(\omega)$ is a diagonal matrix defined as:

$$\boldsymbol{\Gamma}(\omega)=\left[\boldsymbol{\Lambda}+\beta(\omega)\mathbf{I}_{2m}\right]^{-1} \tag{4.46}$$

whose *j*-th element is

$$\gamma_j(\omega)=\frac{1}{\lambda_j+\beta(\omega)} \tag{4.47}$$

being γ_j the *j*-th element of diagonal matrix $\boldsymbol{\Gamma}$. Finally, substituting $\mathbf{Z}_{\mathrm{p}}(\omega,t)$ into Eq.(4.44) the solution vector $\mathbf{Z}(\omega,t)$ can be evaluated in closed-form solution as:

$$\begin{aligned}\mathbf{Z}(\omega,t) &= -\varepsilon(\omega)b!\Big\{\exp\left(-\beta(\omega)(t-t_0)\right) \\ &\times\boldsymbol{\Psi}\left[\sum_{s=0}^{b}\frac{(t-t_0)^s}{s!}\boldsymbol{\Gamma}^{b-s+1}(\omega)\right]\boldsymbol{\Psi}^T\mathbf{A}\;-\boldsymbol{\Theta}(t-t_0)\boldsymbol{\Gamma}^{b+1}(\omega)\Big\}\mathbf{w}\,\mathbb{U}(t)\end{aligned} \tag{4.48}$$

where the condition $\mathbf{Z}(\omega,t_0)=\mathbf{0}$ has been considered. Notice that if all complex modes have been considered in the analysis and the modulating function is assumed equals to *unit step function*, $a(\omega,t)=\mathbb{U}(t)$, by taking the limit as $t\to\infty$, the *TFR* vector function, $\mathbf{Z}(\omega,t)$, leads to:

$$\lim_{t\to\infty}\mathbf{Z}(\omega,t)=\exp(\mathrm{i}\omega t)\boldsymbol{\Psi}\boldsymbol{\Gamma}(\omega)\boldsymbol{\Psi}^T\mathbf{A}\ \mathbf{w}\mathbb{U}(t)= \\ =\exp(\mathrm{i}\omega t)\begin{bmatrix}\mathbf{H}(\omega)\\ \mathrm{i}\omega\mathbf{H}(\omega)\end{bmatrix}\mathbf{w}\mathbb{U}(t) \tag{4.49}$$

where $\mathbf{H}(\omega)$ is the *frequency response function* matrix in the nodal space:

$$\mathbf{H}(\omega)=\left[\mathbf{K}-\omega^2\mathbf{M}+\mathrm{i}\omega\,\mathbf{C}\right]^{-1}. \tag{4.50}$$

Finally, substituting Eq. (4.45) in Eq. (4.44) and the result in Eq. (4.37) the one-sided *EPSD* function matrix of the nodal response is obtained.

4.3 Numerical applications

4.3.1 Classically damped systems subjected to mono correlated input

4.3.1.1 SDOF system

In order to validate the proposed procedure when the forcing input is represented by the chirplets, a SDOF system, with different damping ratios has been analysed. These three SDOF systems are

subjected to a ground motion acceleration, modelled as the adaptive spectrogram (2.31), with the target one-sided *PSD* of ground acceleration $G_0(\omega)$ modelled by the Clough and Penzien (1975) acceleration spectrum defined as:

$$G_0(\omega) = G_g \frac{\left(1+4\xi_g^2\left(\omega/\omega_g\right)^2\right)}{\left(1-\left(\omega/\omega_g\right)^2\right)^2+4\xi_g^2\left(\omega/\omega_g\right)^2} \times \frac{\left(\omega/\omega_f\right)^4}{\left(1-\left(\omega/\omega_f\right)^2\right)^2+4\xi_f^2\left(\omega/\omega_f\right)^2} \tag{4.51}$$

with $\omega_g = 8\pi\,[\text{rad/s}]$, $\xi_f = \xi_g = 0.6$, $\omega_f = 0.1\omega_g$ and $G_g = 0.01246\left[\text{m}^2/\text{s}^3\right]$.

The Figures 4.1, 4.2 shows the comparison between the between the first *NGSM* $\lambda_{0,uu}(t)$ and the validation with the *MCS* (1000 samples).

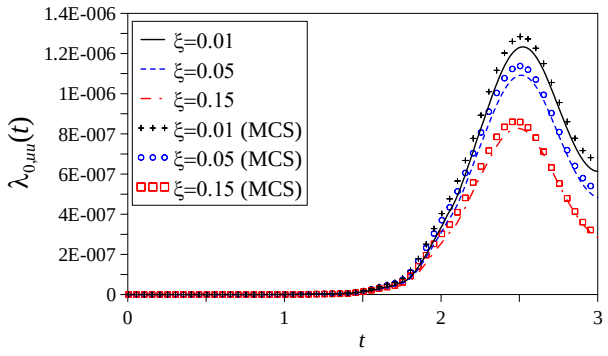

Figure 4. 1 Comparison of closed-form solutions and *MCS* of spectral characteristics $\lambda_{0,uu}(t)$ $\left[\text{m}^2\right]$ for SDOF systems with natural period $T = 2\,[\text{s}]$ and varying damping ratio $(\xi = 0.01, \xi = 0.05, \xi = 0.15)$.

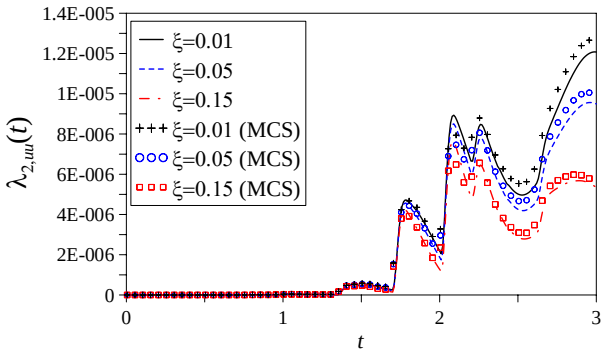

Figure 4. 2 Comparison of closed-form solutions and *MCS* of spectral characteristics $\lambda_{2,uu}(t)$ $\left[\mathrm{m}^2/\mathrm{s}^2\right]$ for SDOF systems with natural period $T=2\,[\mathrm{s}]$ and varying damping ratio $(\xi=0.01, \xi=0.05, \xi=0.15)$.

Figure 4.3 show the one-sided *EPSD* function of the response of the three SDOF systems, evaluated according to Eq.(4.1); closed form solution of the *EPSD* function when the input is represented by the chirplets are given in the Appendix A.

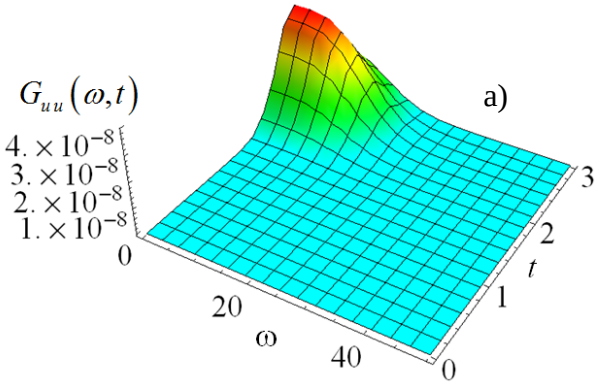

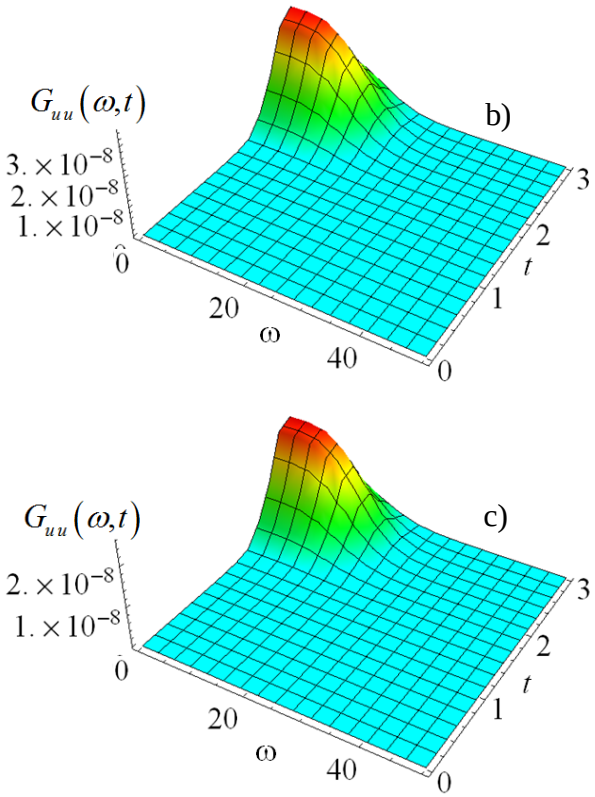

Figure 4. 3 One-sided *EPSD* functions of the response $G_{uu}(\omega,t)$ $\left[\mathrm{m^2\,s}\right]$ of SDOF systems with natural period $T=2\left[\mathrm{s}\right]$ and varying damping ratio: a) $\xi=0.01$; b) $\xi=0.05$; c) $\xi=0.15$.

4.3.1.2 MDOF system

In this section the benchmark quiescent classically damped linear MDOF (Muscolino and Alderucci 2015), composed by a three-story one-bay steel shear-frame, is considered. This frame has a uniform story height $H=320\left[\mathrm{cm}\right]$ and a bay width $L=600\left[\mathrm{cm}\right]$, as shown in Figure 4.4. The steel columns are made of European HE340A wide flange beams with moment of inertia along the strong axis $I=27690\left[\mathrm{cm^4}\right]$. The steel material is modelled as linear elastic with Young's modulus $E=200\left[\mathrm{GPa}\right]$. The beams are considered rigid to enforce a typical shear building behaviour. Under this

assumptions, the shear-frame is modelled as a three DOF linear system.

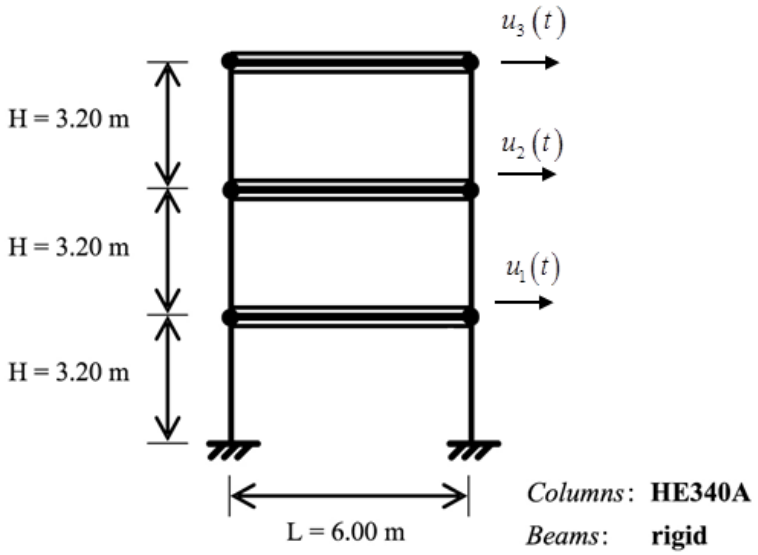

Figure 4. 4 Geometric configuration of benchmark three-story one-bay shear-type frame.

The frame described above is assumed to be part of a building structure with a distance between frames $L_0 = 600[\text{cm}]$. The tributary mass per story, *M*, is obtained assuming a distributed gravity load of $q = 8\ [\text{kN/m}^2]$, accounting for the structure's own weight, as well as for permanent and live loads, and is equal to $M = 28800[\text{kg}]$. The modal periods of the linear elastic undamped shear-frame are $T_1 = 0.376[\text{s}]$, $T_2 = 0.134[\text{s}]$ and $T_3 = 0.093[\text{s}]$, with corresponding effective modal mass ratios of 91.41%, 7.45% and 1.10% respectively. The damping ratio $\xi = 0.05$ is assumed equal for the three modes of vibration.

The benchmark structural model is subjected to a stochastic earthquake base excitation. The ground acceleration is modelled as either time or time-frequency modulated functions. The one-sided *PSD* of the "embedded" stationary countpart stochastic process is defined by the so-called Kanai (1957)-Tajimi (1960) model:

$$G_0(\omega) = G_{\mathrm{W}} \frac{4\,\xi_{\mathrm{K}}^2\,\omega_{\mathrm{K}}^2\,\omega^2 + \omega_{\mathrm{K}}^4}{\left(\omega_{\mathrm{K}}^2 - \omega^2\right)^2 + 4\,\xi_{\mathrm{K}}^2\,\omega_{\mathrm{K}}^2\,\omega^2} \tag{4.52}$$

where ω_{K}=19 rad/s is the filter frequency that determines the dominant input frequency and ξ_{K}= 0.65 is the filter damping coefficient that indicates the sharpness of the one-sided *PSD* function. In Eq.(4.52), in order to compare the responses evaluated by adopting different models, the one-sided *PSD* of the ideal white noise, G_{W}, is normalized in such a way that the "total ground motion acceleration energy" of the analysed non-stationary ground acceleration model is the same as that of Conte and Peng (1997) model, that is:

$$E_{\mathrm{W}} = \int_0^{\infty} \int_0^{t_f} G_{FF}\left(\omega,\tau\right) \mathrm{d}\tau\, \mathrm{d}\omega \tag{4.53}$$

where $G_{FF}\left(\omega,t\right)$ is the one-sided *EPSD* function of the input process introduced in Eq.(2.9) and $(0,t_f]$ is the time interval in which the ground motion possesses significant values.

In this section, four different models of the non-stationary earthquake ground acceleration are considered. The first two processes, that is the normalized exponential type II modulating

function (see Eq. (2.12)) (Shinozuka and Sato 1967) and Jennings et al. (1969) type modulating function (see Eq.(2.14)), represent uniformly modulated processes; while the last two, Spanos and Solomos model (1983) (see Eq.(2.16)) and Conte and Peng model (1997) (see Eq.(2.68) to Eq.(2.70)), represent fully non-stationary random processes. The parameters selected for the normalized exponential type II modulating function (Shinozuka and Sato 1967), see Eq.(2.12), are: $\alpha_2 = 0.045\pi$, $\alpha_3 = 0.05\pi$; while the ones for the Jennings et al. (1969), see Eq.(2.78), are: $t_1 = 4[\mathrm{s}]$, $t_2 = 14[\mathrm{s}]$, and $\alpha_4 = 0.3$. The parameters selected for Spanos and Solomos (1983) type modulating function are:

$$\alpha_5(\omega) = \frac{1}{2}\left(0.15 + \frac{\omega^2}{25\pi^2}\right); \quad \varepsilon_5(\omega) = \frac{\omega}{5\pi}\sqrt{2}. \tag{4.54}$$

Finally, the parameters selected for the Conte and Peng (1997) model are the ones estimated for the N-S accelerogram component of the Imperial Valley earthquake of May 18, 1940, recorded at the El Centro site (Conte and Peng 1997). These parameters are reported in Table 4.I.

Table 4. I Parameters for the non-stationary ground motion of the Conte and Peng (1997) model, corresponding to the NS accelerogram component recorded to El Centro (May, 18 1940).

q	ε_q	r_q	α_q	t_q [s]	ν_q	η_q [rad/s]
1	37.2434	8	2.7283	- 0.5918	1.4553	6.7603
2	104.0241	8	2.9549	- 0.9857	2.4877	11.0857
3	31.9989	8	2.6272	1.7543	3.3024	7.3688
4	43.8375	9	3.1961	1.6860	2.1968	13.5917

5	33.1958	9	3.1763	- 0.0781	3.1241	14.3825
6	41.3111	9	3.1214	- 0.7096	6.7335	25.1532
7	4.2234	10	2.9904	- 0.9464	2.6905	48.0612
8	19.9802	6	1.8950	1.4020	7.2086	37.6163
9	2.4884	10	2.6766	5.3123	6.1101	19.4612
10	24.1474	10	3.3493	8.8564	1.9862	9.040
11	2.5916	2	0.2240	3.2558	2.4201	9.3381
12	2.2733	3	0.5285	16.2065	1.5244	14.1067
13	24.2732	3	1.0361	17.5331	1.7141	24.0444
14	41.0734	2	0.7511	22.3717	5.9541	27.7953
15	1.3697	10	2.5936	21.6830	1.9362	12.9198
16	15.4646	2	0.7044	27.2979	1.7897	12.0205
17	0.0174	10	1.8451	- 2.4168	4.9373	98.6280
18	2.9646	10	3.1137	1.5751	1.9726	61.8316
19	0.0007	10	1.3686	2.5173	3.2479	43.9075
20	0.8092	4	0.5969	6.4396	3.6749	26.3365
21	16.7115	2	0.7294	12.4930	1.7075	37.1139

The corresponding "total ground motion acceleration energy" is: $E_W = 107734\left[\mathrm{cm}^2/\mathrm{s}^2\right]$. It follows that the $G_{\mathrm{W}} = 157.3\left[\mathrm{cm}^2/\mathrm{s}^3\right]$ for the normalized exponential type II quasi-stationary model (Shinozuka and Sato 1967), $G_{\mathrm{W}} = 155.4\left[\mathrm{cm}^2/\mathrm{s}^3\right]$ for the Jennings et al. (1969) quasi-stationary type model and $G_{\mathrm{W}} = 418\left[\mathrm{cm}^2/\mathrm{s}^3\right]$ for the Spanos and Solomos (1983) fully non-stationary type model.

In Figures 4.5 and 4.6 the one-sided *EPSD* functions, $G_{FF}(\omega,t)$, and the central frequency functions, $\omega_{C,F}(t)$, of the input processes associated to the four modulating functions herein considered are depicted. Analysing these Figures the different behaviour of these functions for the four models here studied is evident. In particular for the first two models, which represent *quasi-stationary* random processes, the central frequency is constant while for the last two

models, which describe *fully non-stationary* random processes, the central frequency is time-variant.

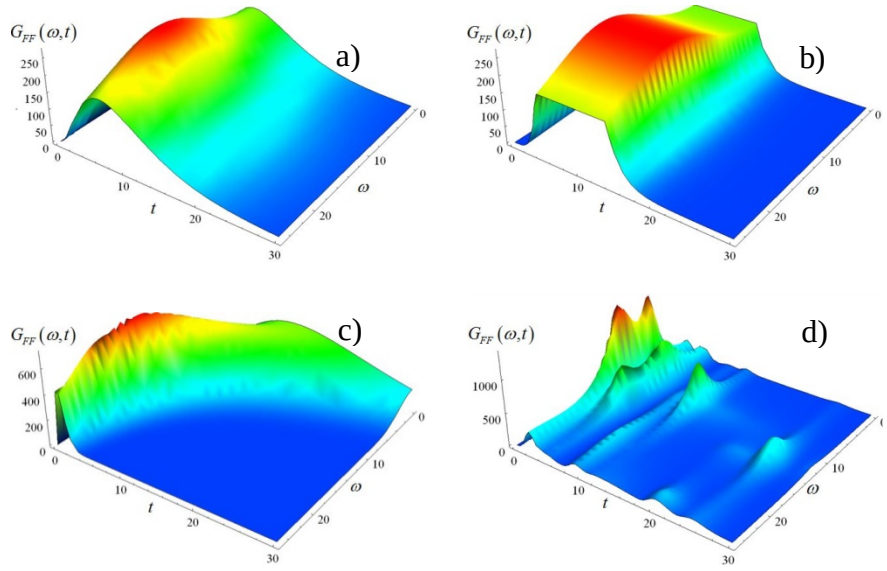

Figure 4. 5 One-sided *EPSD* of the input process $G_{FF}(\omega,t)\left[\mathrm{cm}^2/\mathrm{s}^3\right]$ for the four analysed non-stationary models: a) Shinozuka and Sato model (1967); b) Jennings et al. model (1969); c) Spanos and Solomos model (1983); d) Conte and Peng model (1997).

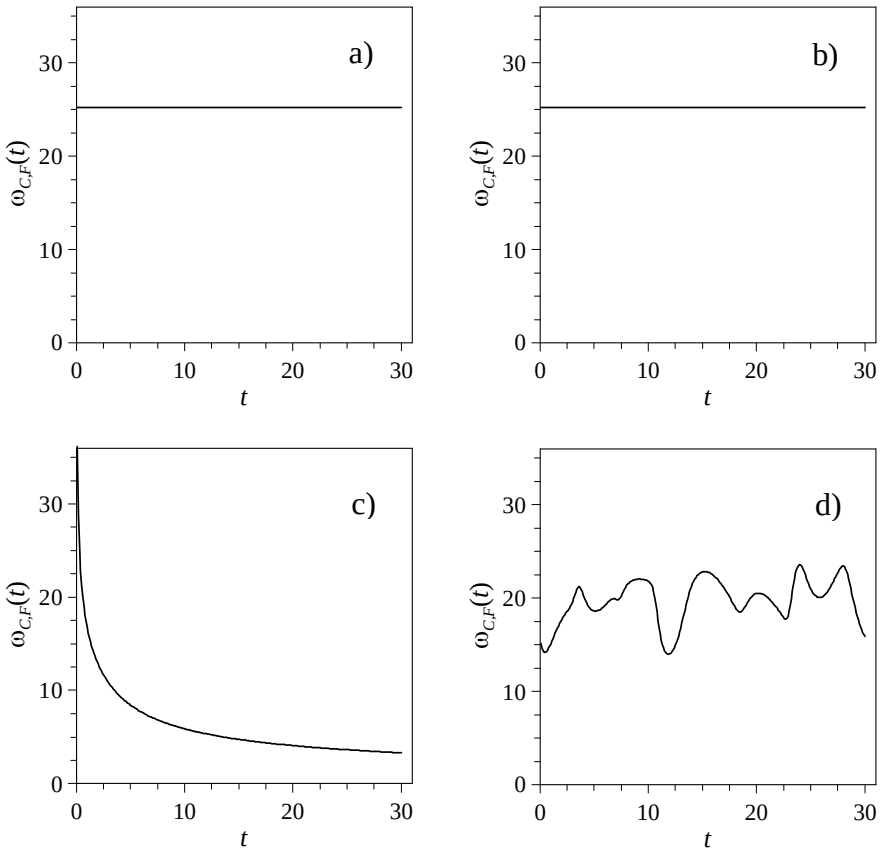

Figure 4. 6 Time-variant central frequency $\omega_{C,F}(t)$ [rad/s] of the input process for the four analysed non-stationary models: a) Shinozuka and Sato model (1967); b) Jennings et al. model (1969); c) Spanos and Solomos model (1983); d) Conte and Peng model (1997).

Figures 4.7-4.9 show the absolute value of the components of the modal *TFR* vector functions, $\mathbf{Y}_j(\omega,t)(j=1,2,3)$, that are the evolutionary frequency response function, $\tilde{Q}_j(\omega,t)$, and its time derivative $\dot{\tilde{Q}}_j(\omega,t)$, for the first three models of the non-stationary earthquake ground acceleration (Shinozuka and Sato (1967) model, Jennings et al. (1969) model, Spanos and Solomos (1983) model).

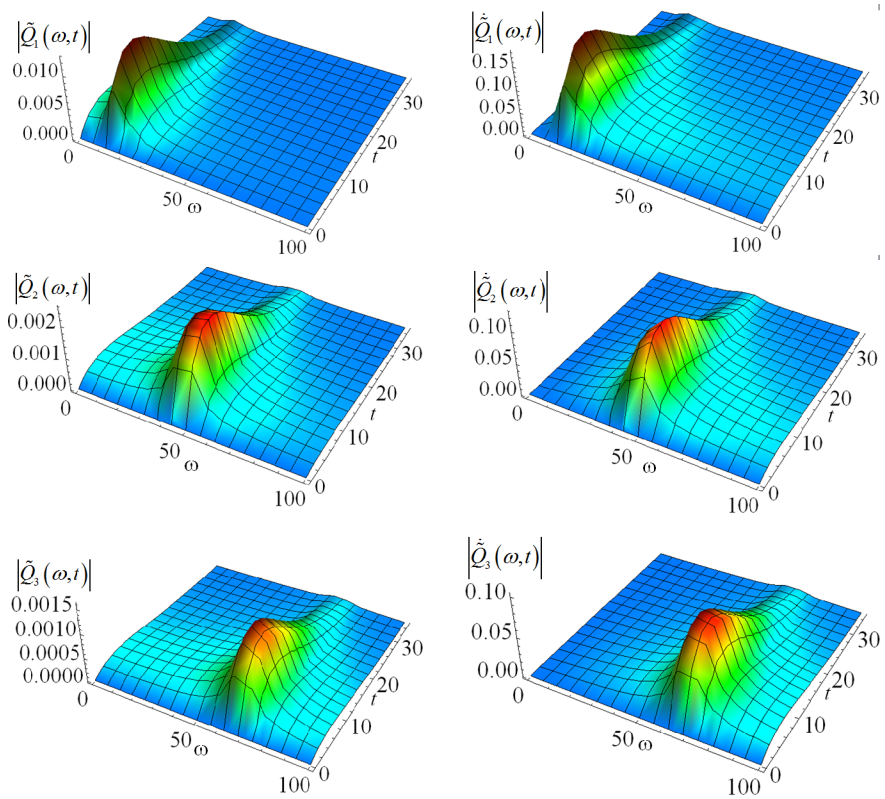

Figure 4. 7 Absolute value of the modal evolutionary frequency response function, $|\tilde{Q}_i(\omega,t)|$ $(i=1,2,3)$, and of its time derivative, $|\dot{\tilde{Q}}_i(\omega,t)|$ $(i=1,2,3)$, for the Shinozuka and Sato model (1967) of the non-stationary input process

From the analysis of this Figures it is evident that for the first two models, that are quasi-stationary input model, the shape of this function is sensitively influenced from the corresponding circular frequency, while in the Spanos and Solomos model of the fully non-stationary input process their aspect is substantially due to the frequency varying content of the modulating function.

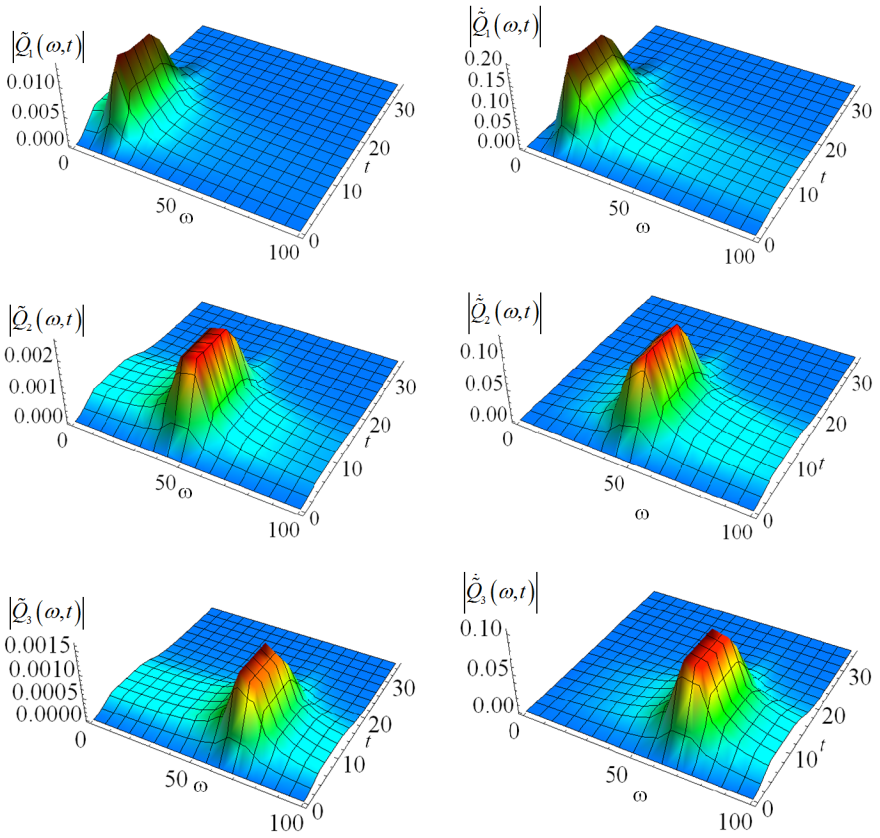

Figure 4. 8 Absolute value of the modal evolutionary frequency response function, $|\tilde{Q}_i(\omega,t)|$ $(i=1,2,3)$, and of its time derivative, $|\dot{\tilde{Q}}_i(\omega,t)|$ $(i=1,2,3)$, for the Jennings et al. model (1969) of the non-stationary input process

Notice that the same quantities are not depicted for the Conte and Peng (1997) model since, in this case, the *TFR* vector functions have to be defined for each component of the sigma-oscillatory process. For this reason the meaning of these quantities is difficult to interpret.

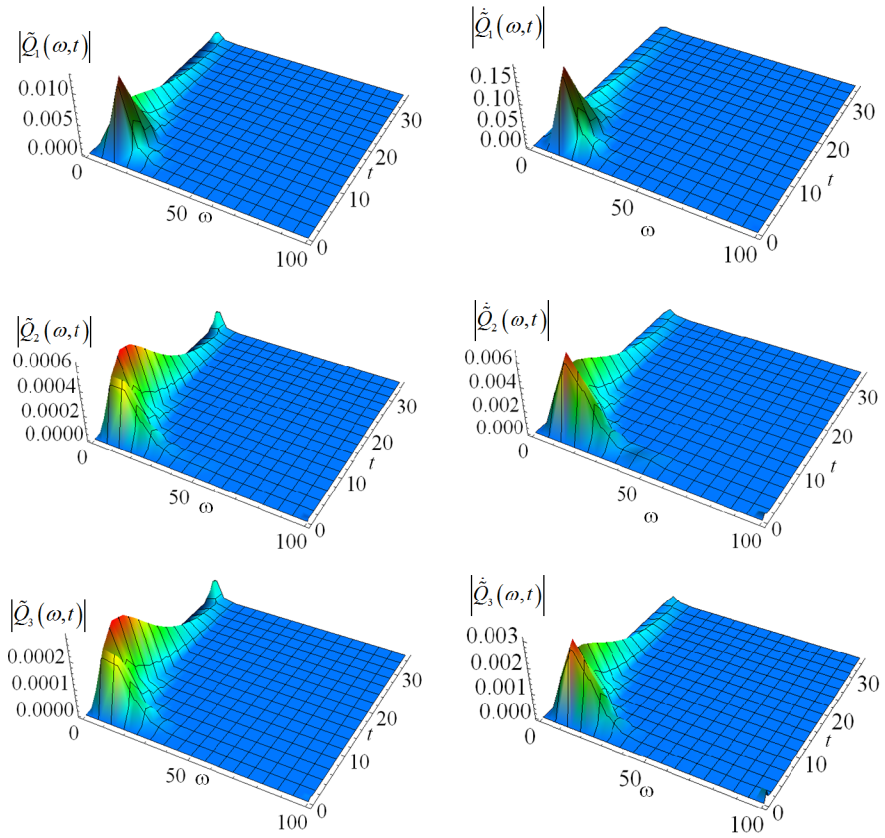

Figure 4. 9 Absolute value of the modal evolutionary frequency response function, $|\tilde{Q}_i(\omega,t)|$ $(i=1,2,3)$, and of its time derivative, $|\dot{\tilde{Q}}_i(\omega,t)|$ $(i=1,2,3)$, for the Spanos and Solomos model (1983) of the non-stationary input process

In Figure 4.10-4.12 the time histories of the relative to ground displacement *NGSMs* of the three floors for the four modulating functions, herein analysed, are depicted; it can be easily observed that the shape of the modulating function influences significantly the response configuration of spectral moments. In order to verify the proposed procedure the time-variant *NGSMs* evaluated by the proposed analytical approach are compared with the ones obtained by *MCS*. To obtain the *MCS* results, $N=5000$ samples of input the random process have been generated.

Notice that the imaginary part of the first order *NGSM*, $\mathrm{Im}\left\{\lambda_{1,u_i u_i}\right\}$, has not been here depicted since it is not necessary for the evaluation of the spectral characteristics of the response.

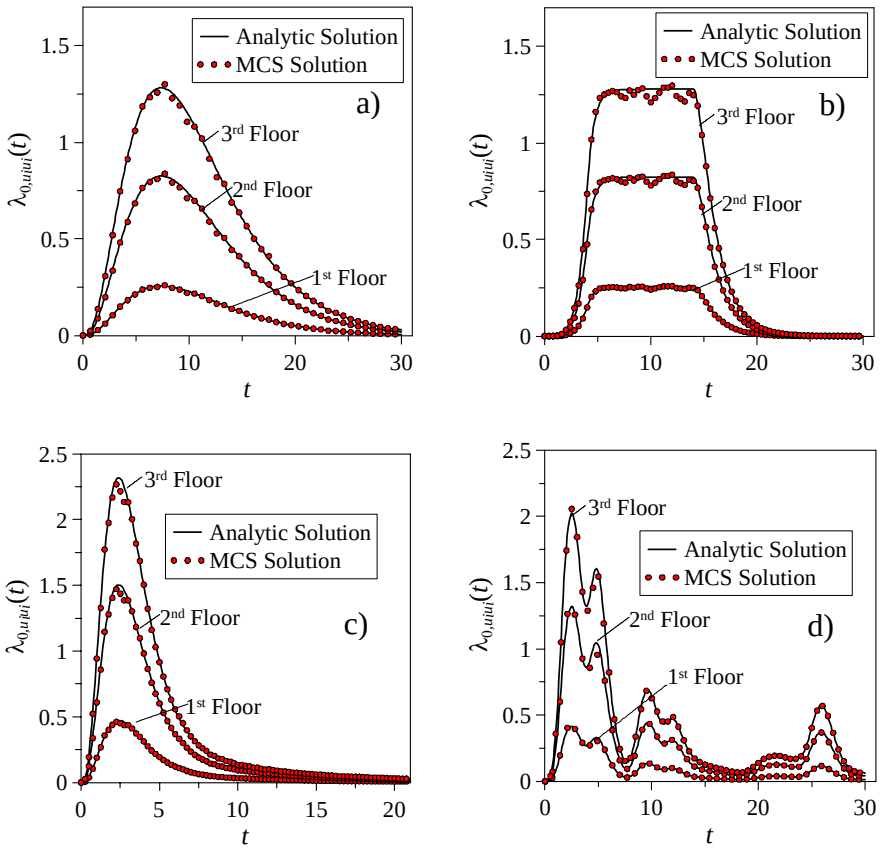

Figure 4. 10 Comparison between the time-variant histories of the $\lambda_{0,u_i u_i}(t)$ *NGSMs* $\left[\mathrm{cm}^2\right]$, of the three relative to ground floor displacements, evaluated by applying the proposed analytical solution and the *MCS* for the four analysed models of non-stationary input process a) Shinozuka and Sato model (1967); b) Jennings et al. model (1969); c) Spanos and Solomos model (1983); d) Conte and Peng model (1997).

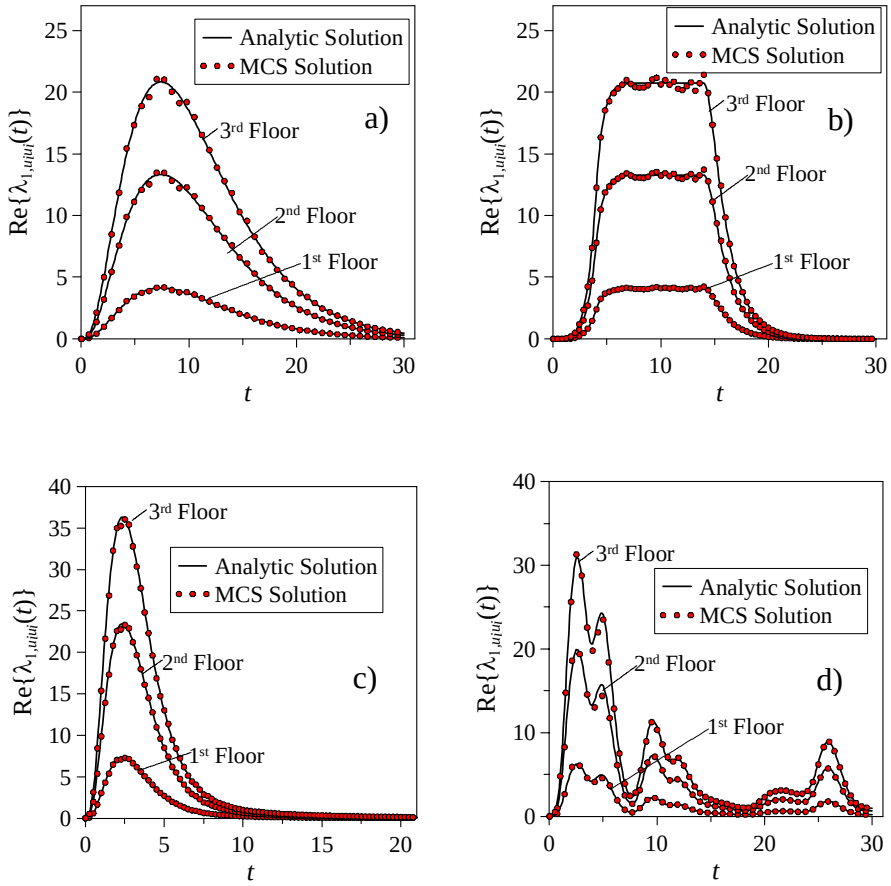

Figure 4. 11 Comparison between the time-variant histories of the $\mathrm{Re}\{\lambda_{1,u_iu_i}(t)\}$ ***NGSMs*** $[\mathrm{cm}^2/\mathrm{s}]$**, of the three relative to ground floor displacements, by applying the proposed analytical solution and the *MCS* for the four analysed models of non-stationary input process : a) Shinozuka and Sato model (1967); b) Jennings et al. model (1969); c) Spanos and Solomos model (1983); d) Conte and Peng model (1997).**

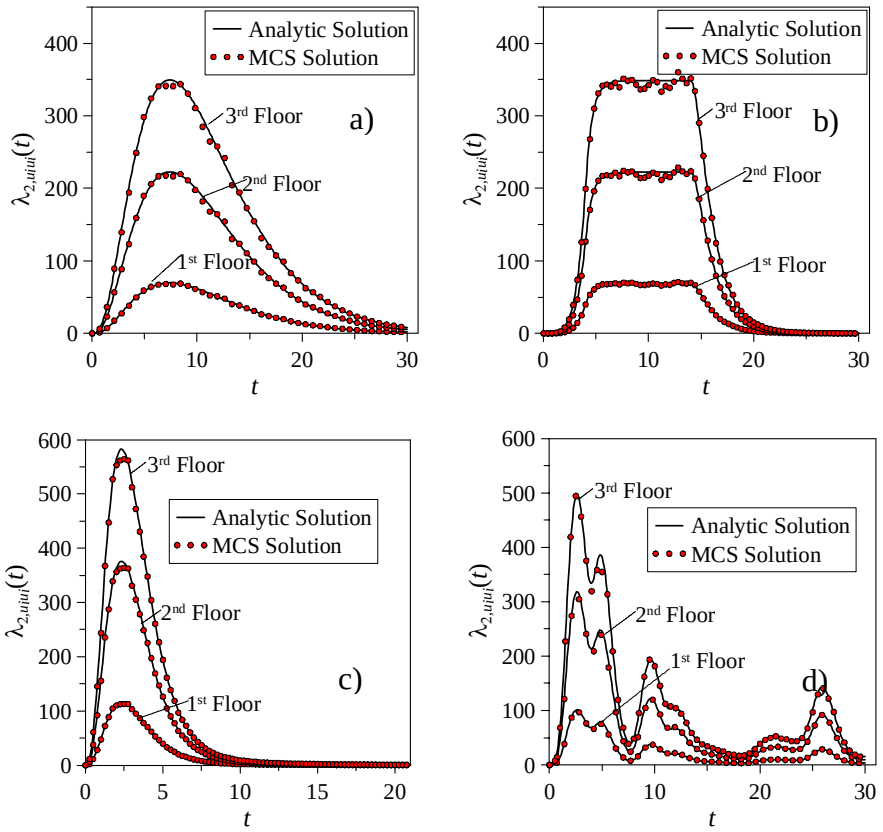

Figure 4. 12 Comparison between the time-variant histories of the $\lambda_{2,u_iu_i}(t)$ *NGSMs* $\left[\mathrm{cm}^2/\mathrm{s}^2\right]$, of the three relative to ground floor displacements, evaluated by applying the proposed analytical solution and the *MCS* for the four analysed models of non-stationary input process : a) Shinozuka and Sato model (1967); b) Jennings et al. model (1969); c) Spanos and Solomos model (1983); d) Conte and Peng model (1997).

In Figure 4.13 the bandwidth parameters, $\delta_{u_iu_i}(t)$, of the relative to ground floor displacements are depicted. These Figures show that, for the uniformly modulated models as well as for the Spanos and Solomos (1983) model, the bandwidth parameters decrease rapidly from a value close to 0.6 (corresponding to a broadband process) to a value close to 0.2 (corresponding to a much narrower band process). On the contrary for the Conte and Peng (1997) model, this parameter is always almost equals to 0.2.

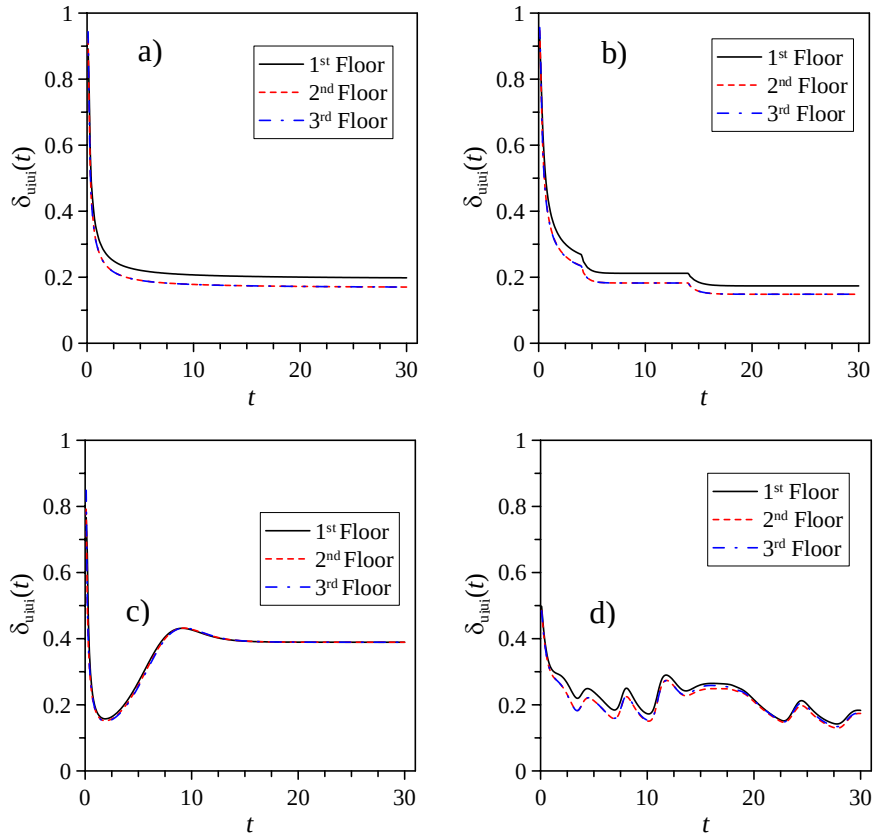

Figure 4. 13 Bandwidth parameter $\delta_{u_i u_i}(t)$ of the three floors for the four analysed models of non-stationary input process : a) Shinozuka and Sato model (1967); b) Jennings et al. model (1969); c) Spanos and Solomos model (1983); d) Conte and Peng model (1997).

To synthetically describe the time-variant spectral properties of the generic real-valued non-stationary processes, in Figures 4.14 and 4.15 the mean frequencies, $\nu^{+}_{u_i,u_i}(t)$, and the central frequencies, $\omega_{C,u_i u_i}(t)/\omega_1$ normalized by the first mode natural circular frequency, of the three relative to ground floor displacements are depicted. For the first two models these quantities get to an asymptotic value, that, in Figure 4.15, is very close to the natural frequency of the structural system; it means that the response process is dominated by the first mode of vibration of the structure. This

behaviour is different for the last two models, corresponding to non-separable processes; in Figures 4.14c and 4.15c the mean frequencies and the central frequencies decrease in time while in Figures 4.14d and 4.15d the same quantities oscillate through a mean value. In addition the time histories of time-variant spectral parameters for the three floors are almost coincident.

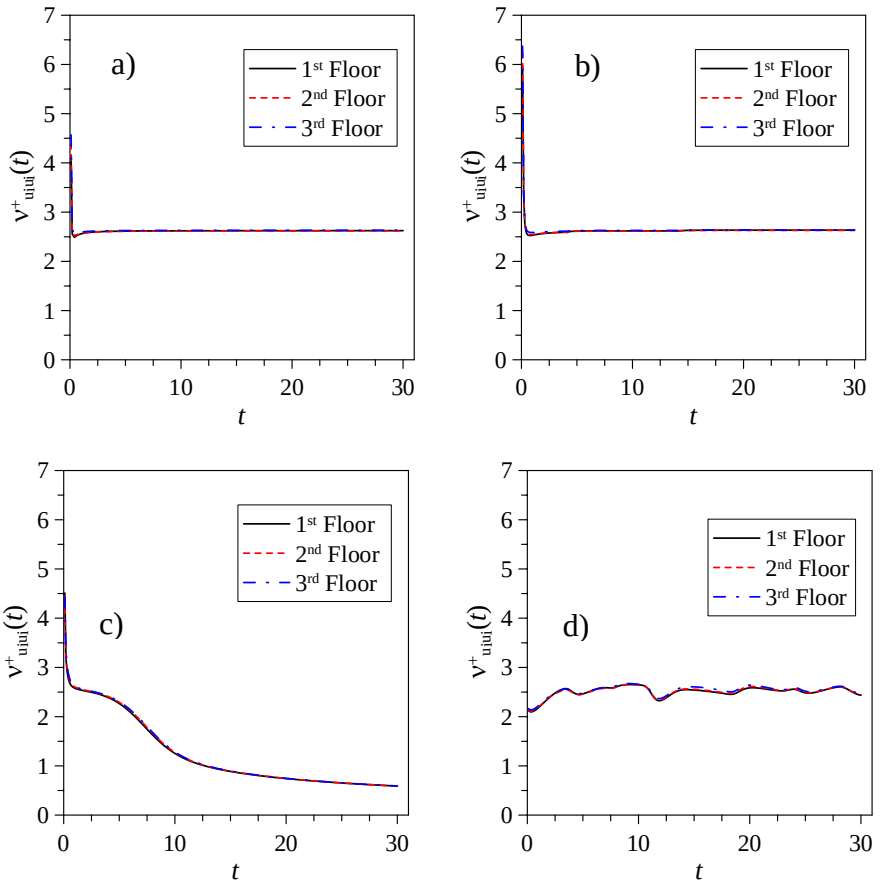

Figure 4. 14 Mean frequency $\nu^+_{u_i,u_i}(t)$ of the three floors for the four analysed models of non-stationary input process : a) Shinozuka and Sato model (1967); b) Jennings et al. model (1969); c) Spanos and Solomos model (1983); d) Conte and Peng model (1997).

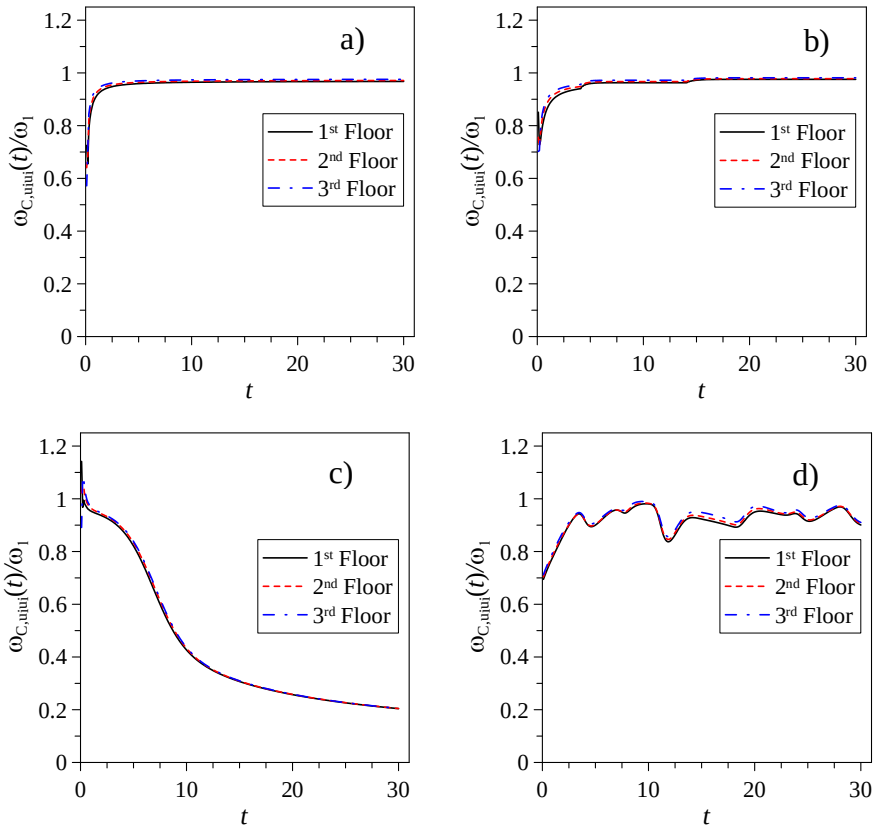

Figure 4. 15 Central frequencies of the three floors normalized by the first mode natural frequency $\omega_{C,u_iu_i}(t)/\omega_1$ for the four analysed models of non-stationary input process: a) Shinozuka and Sato model (1967); b) Jennings et al. model (1969); c) Spanos and Solomos model (1983); d) Conte and Peng model (1997).

Once again, according to Eq.(4.1), it is possible to obtain the one-sided *EPSD* function of the response of the third floor as shown in Figure 4.16; closed form solution of the *EPSD* function for the four analysed non stationary models are given in the Appendix A.

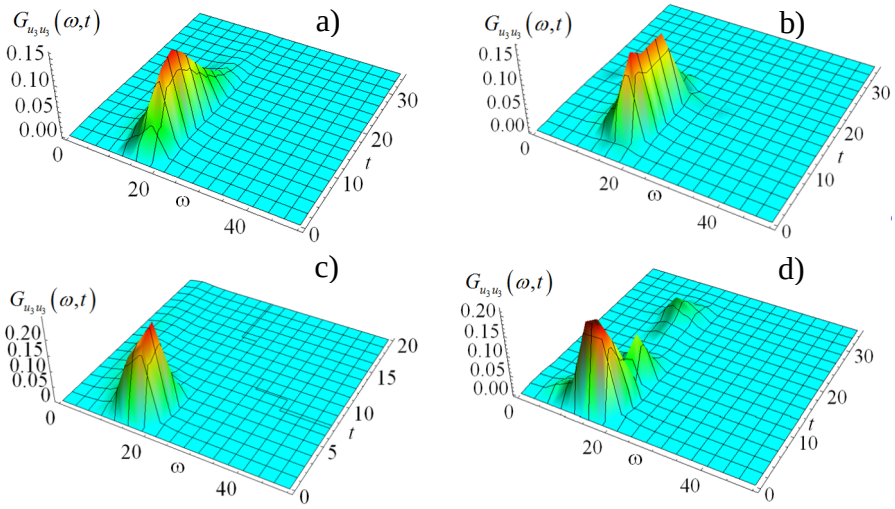

Figure 4.16 One-sided *EPSD* of the response process of the third floor $G_{u_3u_3}(\omega,t)\left[\mathrm{cm^2\,s}\right]$ for the four analysed non-stationary models: a) Shinozuka and Sato model (1967); b) Jennings et al. model (1969); c) Spanos and Solomos model (1983); d) Conte and Peng model (1997).

4.3.2 Classically damped systems subjected to multi-correlated input

4.3.4.1 Four span continuous deck

The accuracy of the proposed method if verified comparing the between the first *NGSM* of the bridge deck (see Figure 2.19) response, $\lambda_{0,uu}(t)$, evaluated by means of the proposed procedure with the one obtained by *MCS* (2500 samples). In particular, in Figures 4.17, as well as the validation with the *MCS*, the first *NGSM* of the response of the bridge obtained by taking into account the spatial variability of the ground motion and the ones which are the result of the hypothesis of uniform ground motion, are compared for the two analysed models of non-stationary multi-correlated input process: Hsu e Bernard model (1978) and Spanos and Solomos

model (1983). The parameters of these modulating functions are the same of Section 2.8.2.

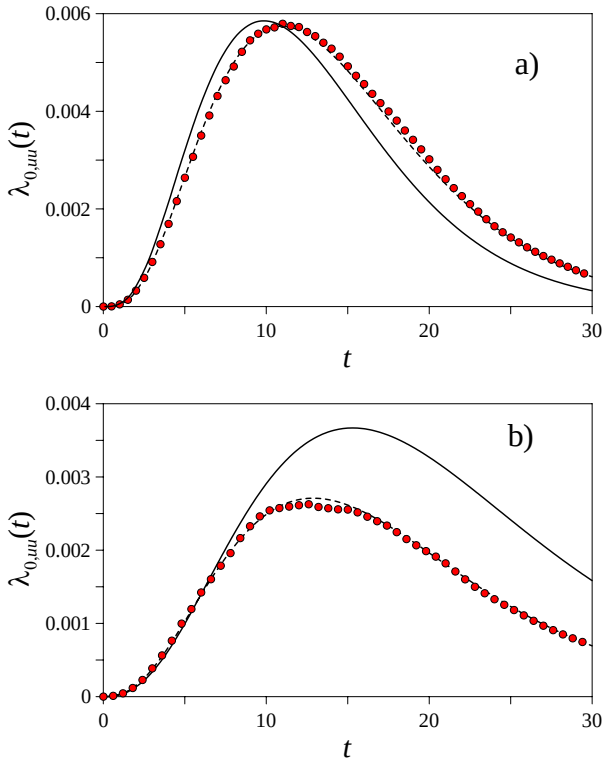

Figure 4. 17 Time-variant histories of the $\lambda_{0,uu}(t)$ *NGSMs* $\left[\mathrm{m}^2\right]$ obtained by taking into account the spatial variability of the ground motion (dashed line), under the hypothesis of uniform ground motion (continuous line) and comparison with the *MCS* (red dots) for the two analysed models of non-stationary input process: a) Hsu e Bernard model (1978); b) Spanos and Solomos model (1983).

Then figure 4.18 shows the comparison between the first *NGSM* of the response of the bridge obtained by taking into account the spatial variability of the ground motion and the one in the hypothesis of uniform ground motion, when the input is modelled as a sigma-oscillatory process, as explained in Section 2.8.2. In the same Figure the validation with the *MCS* (2500 samples) is shown.

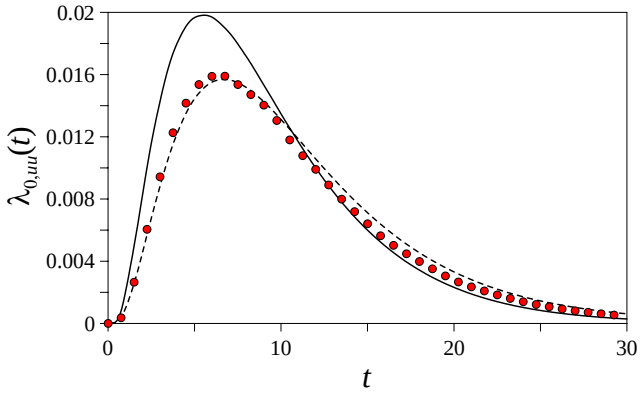

Figure 4. 18 Time-variant histories of the variance of the $\lambda_{0,uu}(t)$ *NGSMs* $\left[\mathrm{m}^2\right]$ obtained by taking into account the spatial variability of the ground motion (dashed line), under the hypothesis of uniform ground motion (continuous line) and comparison with the *MCS* (red dots) for the sigma-oscillatory process model.

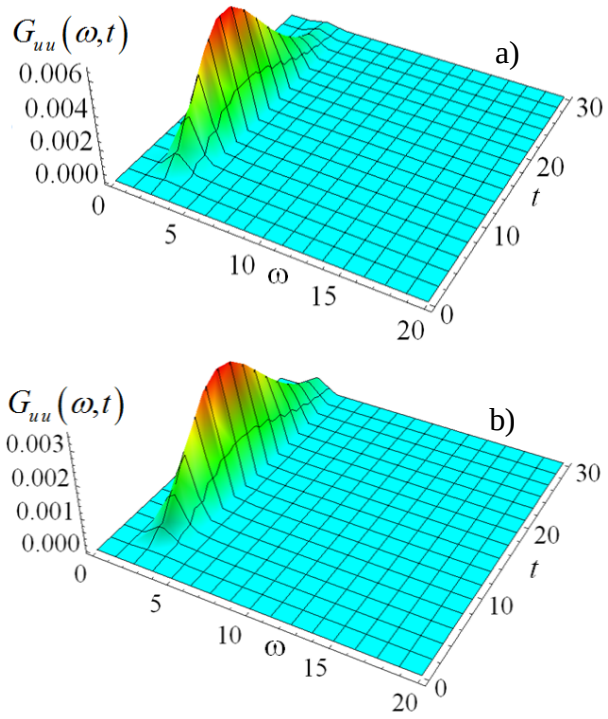

Figure 4. 19 One-sided *EPSD* functions of the response $G_{uu}(\omega,t)$ $\left[\mathrm{m}^2\,\mathrm{s}\right]$ for the two analysed models of non-stationary input process: a) Hsu e Bernard model (1978); b) Spanos and Solomos model (1983).

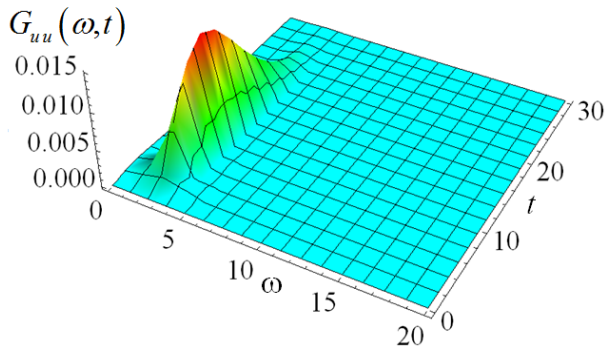

Figure 4. 20 One-sided *EPSD* functions of the response $G_{uu}(\omega,t)$ $\left[\mathrm{m^2\,s}\right]$ for the sigma-oscillatory process model (Battaglia 1979)

For both the evolutionary and sigma-oscillatory models of stochastic input the *EPSD* function of the response (see Eq. (4.18)) are obtained as function of the *TFR* vector functions (see Figures 4.19 and 4.20).

4.3.4.2 Truss structure bridge

The proposed procedure is also applied to the 43-bar truss structure (Cacciola and Muscolino 2011) shown in Figure 4.21.

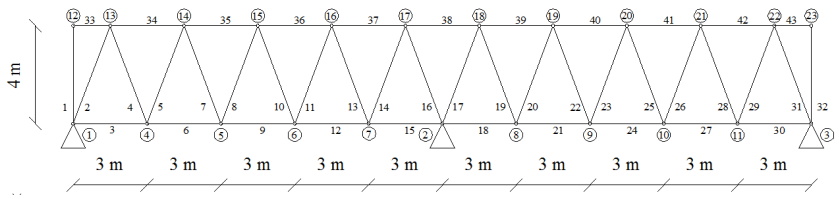

Figure 4. 21 Reference truss structure.

All the elements have the same cross section area, $A_i = 0.004265\left[\mathrm{m^2}\right]$, and nominal Young's modulus, $E_i = 2\times10^{11}\left[\mathrm{N/m^2}\right]$, while the lengths L_i are specified in Figure

4.21 $(i = 1, 2, \ldots, 43)$; the lumped mass at each node is summarized in Table 4.II, while the first ten periods and circular frequencies are written in Table 4.III. The truss structure is assumed classically damped with damping ratio equal to $\xi = 0.02$

Table 4. II Lumped mass at each node of the truss-structure

n	Mass [kg]	n	Mass [kg]	n	Mass [kg]	n	Mass [kg]
1	156.55	7	10212.69	13	187.58	19	212.69
2	10212.69	8	10212.69	14	212.69	20	212.69
3	156.55	9	10212.69	15	212.69	21	212.69
4	10212.69	10	10212.69	16	212.69	22	187.58
5	10212.69	11	10212.69	17	212.69	23	75.31
6	10212.69	12	75.31	18	212.69		

Table 4. III First ten periods and circular frequencies of the truss-structure.

i	ω_i [rad/s]	T_i [s]
1	45.89	0.1369
2	47.90	0.1311
3	90.04	0.0698
4	94.98	0.0661
5	114.62	0.0548
6	118.00	0.0532
7	142.09	0.0442
8	142.33	0.0441
9	171.39	0.0366
10	171.40	0.0366

The structure, quiescent at time $t = 0$, is subjected to the a non-uniform base excitation modelled by a zero mean tri-variate Gaussian non-stationary process. The multi-variate input is assumed equal to the one defined in the previous subsection, obtained

substituting in Eq. (2.79) the distances $d_{12} = d_{23} = 15[\mathrm{m}]$ and $d_{13} = 30[\mathrm{m}]$ (see Figure 4.21).

For both the evolutionary and sigma-oscillatory models of stochastic input the *EPSD* function of the response (see Eq. (4.18)) are obtained as function of the *TFR* vector functions.

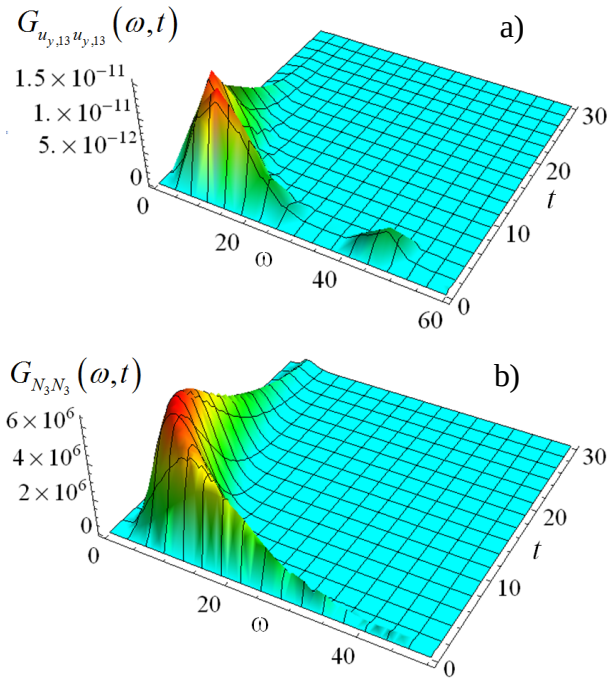

Figure 4. 22 One-sided *EPSD* functions for the Spanos and Solomos model (1983) : a) nodal vertical displacement of the node n°13, $G_{u_{y,13}u_{y,13}}(\omega,t)\ \left[\mathrm{m^2\,s}\right]$**; b) normal stress of the bar n°3,** $G_{N_3N_3}(\omega,t)\ \left[\mathrm{N^2\,s}\right]$**.**

For the Spanos and Solomos model (1983) of the stochastic input the one-sided *EPSD* functions of the normal stress of the bar n°3 and of the vertical displacement of the node n°13 (see Figure 4.21) are depicted in Figures 4.22, respectively. In Figures 4.23 the same functions are shown for the sigma-oscillatory model (Battaglia 1979) of the stochastic input.

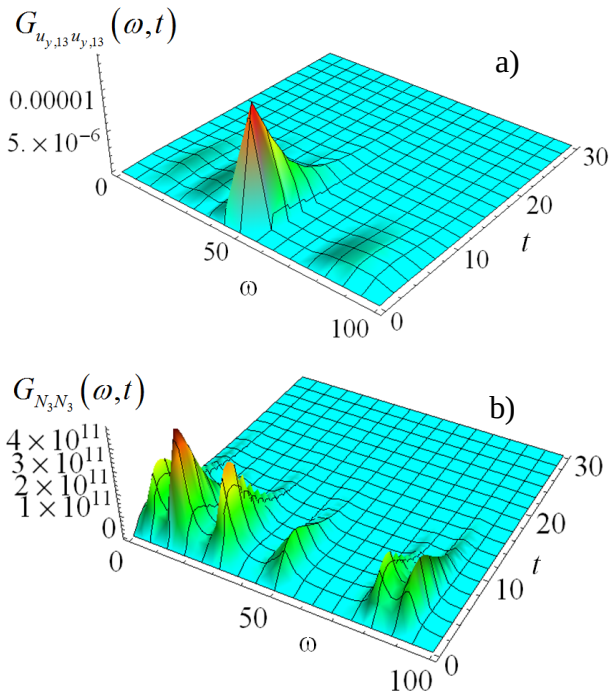

Figure 4. 23 One-sided *EPSD* functions for the sigma-oscillatory model (Battaglia 1979): a) nodal vertical displacement of the node n°13, $G_{u_{y,13}u_{y,13}}(\omega,t)\left[\mathrm{m^2\,s}\right]$**; b) normal stress of the bar n°3,** $G_{N_3N_3}(\omega,t)\left[\mathrm{N^2\,s}\right]$**.**

Notice that the one-sided *EPSD* of the nodal response have been evaluated according to Eq. (4.18).

4.3.3 Non-classically damped system subjected to mono-correlated input

4.3.3.1 Shear type frame

In this section in order to verify the accuracy of the proposed procedure when the system is assumed non-classically damped the benchmark quiescent linear MDOF of Section 4.3.1 is analysed.

In this case the structure presents viscous dampers of coefficient $c=200\left[\mathrm{kNs/m}\right]$ across the second and third stories and a proportional damper of coefficient ηc across the first story, as

shown in Figure 4.24 a). When $\eta = 1$ the structure is classically damped. The elements out of the diagonal can be considered as a measure of the non-classicity of the system. A method to define this value request the introduction of the "coupling index" (Claret and Venancio Filho 1991):

$$\rho = \max\left[\Xi_{i,j}^2 \Big/ \left(\Xi_{i,i}\Xi_{j,j}\right)\right] \quad (i,j=1,2,\ldots,n) \quad i \neq j \quad 0 \leq \rho < 1 \quad (4.55)$$

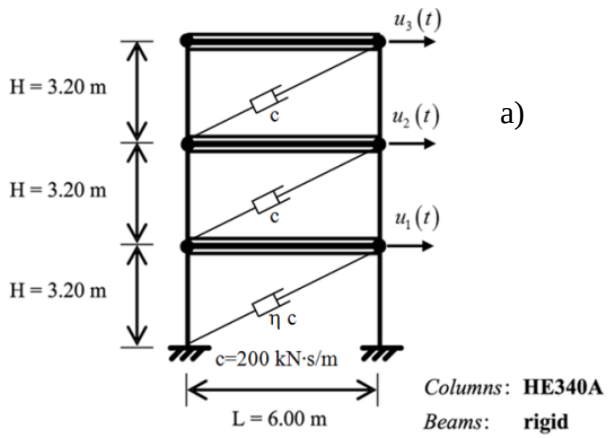

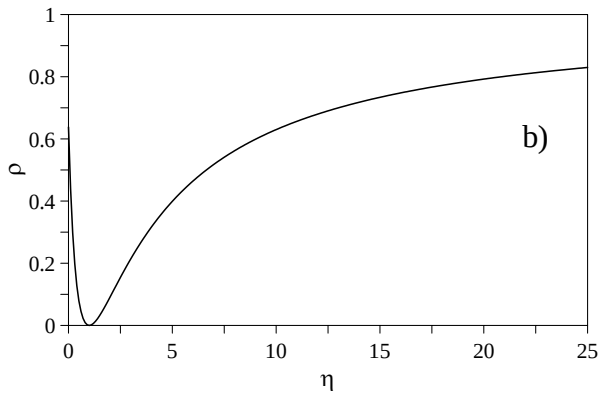

Figure 4. 24 a) Geometric configuration of benchmark three-story one-bay shear-type frame; b) Coupling index

As shown in Figure 4.24 b), when $\eta = 1$ the coefficient $\rho = 0$ and the frame is classically damped.

Table 4. IV Periods, natural frequencies and complex eigenvalues of the shear-type frame, $\eta = 1$

Mode	Circular frequency $\omega[\text{rad/s}]$	Period $T[\text{s}]$	Eigenvalue λ
1	16.701	0.376	-0.688+16.688 i
2	49.797	0.134	-5.399+46.485 i
3	67.624	0.093	-11.274+66.677 i

By applying the complex modal analisys (see Eqs.(3.48) to (3.51)) it is possible to obtain the complex eigenvalues of the system (Eq. (3.51)). In particular, if $\eta = 1$, since the system is classically damped, the natural frequencies of the structure are coincident with the modulus of the complex eigenvalue.

If $\eta = 10$ the system becomes non-classically damped and the complex eigenvalues change:

Table 4. V Complex eigenvalues of the shear-type frame, $\eta = 10$ **.**

Mode	Eigenvalue λ
1	-4.025+17.730 i
2	-32.099+35.469 i
3	-12.487+59.476 i

When $\eta > 13$ the eigenvalues becomes positive and real, so the system is overcritically-damped and it is not possible to apply the proposed procedure.

The benchmark structural model undergoes to a stochastic earthquake base excitation, modelled by a zero mean Gaussian spectrum-compatible fully non-stationary process, as explained in section 2.8.1, with the Spanos and Solomos (1983) modulating function.

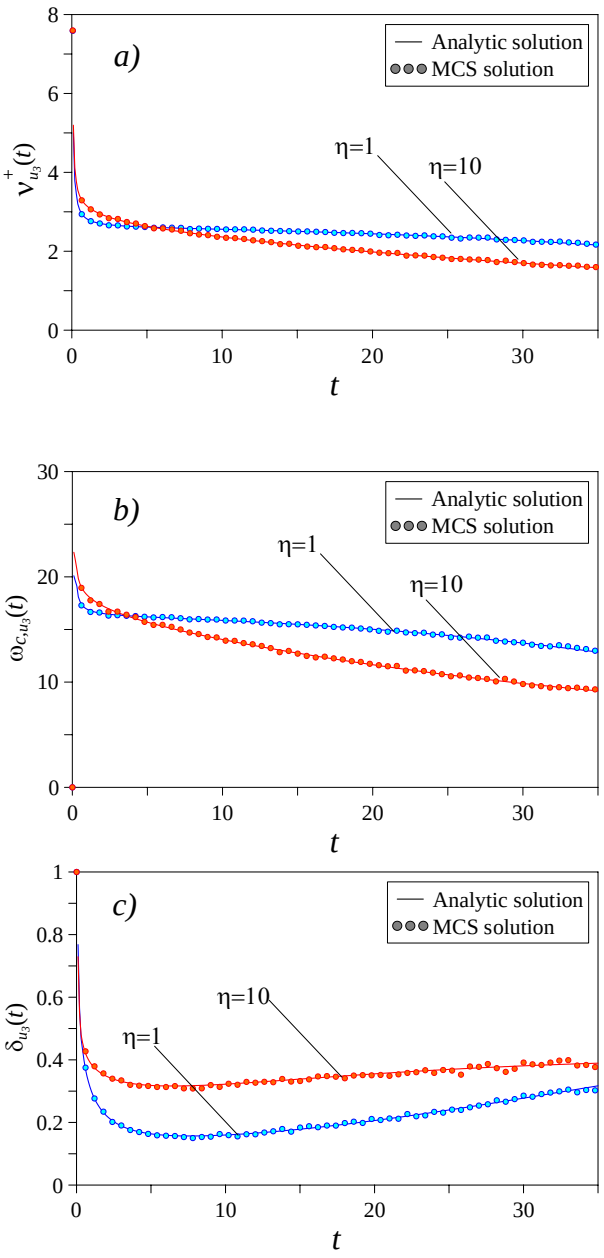

Figure 4. 25 Comparison between the time-variant histories of a) the mean frequency $\nu^{+}_{u_3}(t)$, b) the central frequency $\omega_{C,u_3}(t)$ and c) the bandwidth parameter $\delta_{u_3}(t)$, of the third relative to ground floor displacement, by applying the proposed analytical solution and the *MCS*.

Figures 4.25 show the time histories of the mean frequency, the central frequency and the bandwidth parameter of the third floor for

$\eta = 1$ and $\eta = 10$, evaluated by the proposed analytical approach and compared with the ones obtained by Monte Carlo Simulation (1000 samples of input).

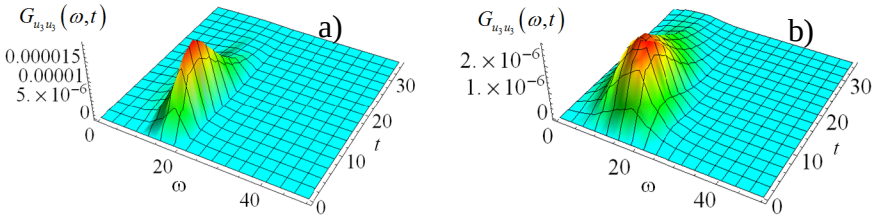

Figure 4.26 One-sided *EPSD* of the response process of the third floor $G_{u_3u_3}(\omega,t)$ $\left[\mathrm{m}^2\,\mathrm{s}\right]$**: a)** $\eta = 1$**; b)** $\eta = 10$**.**

Figure 4.26 shows one-sided *EPSD* function of the response of the third floor, obtained according to Eq.(4.37).

4.3.3.2 External viscous dampers in the 2-D structure

In this section the quiescent linear MDOF depicted in Figure 4.27 is analysed; differently from the previous application in this case the viscous dampers are outside the structure and considered as fixed to a rigid support. It is important to notice that this configuration doesn't modify the stiffness matrix of the structure.

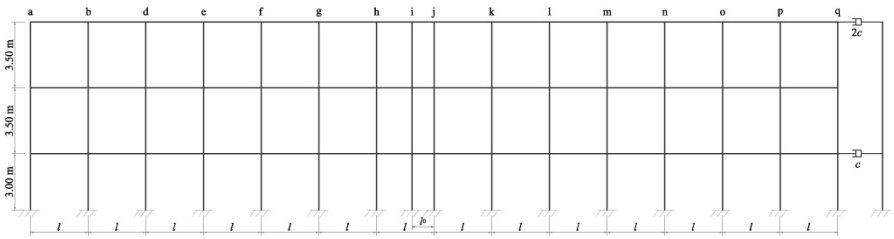

Figure 4. 27 Five-story plane frame structure, $l = 3.07\left[\mathrm{m}\right]$, $l_0 = 1.18\left[\mathrm{m}\right]$**.**

The geometric configuration is reported in Figure 4.27. The columns are made of concrete, modelled as linear elastic with Young's modulus $E = 28000\,[\mathrm{MPa}]$. The beams are considered rigid to enforce a typical shear building behaviour. Under this assumptions, the shear-frame is modelled as a three DOF linear system. The geometrical properties of the columns are reported in Table 4.VI and are the same for each floor.

Table 4. VI Geometric configuration of the 2-D frame

Columns: *a, q* [cm]	**Columns**: *b, c, d, e, f, g, h, j, k, l, m, n, o* [cm]	**Column**: *i* [cm]
20×50	60×60	20×40

The frame described above is assumed to be part of a building structure with a distance between frames $L_0 = 835\,[\mathrm{cm}]$. The tributary mass per story, M_i, are obtained assuming a distributed load, accounting for the structure's own weight, as well as for permanent and live loads, and are reported in Table 4.VII.

Table 4. VII Tributary mass per story

Floor	Mass [kg]
1	212230
2	230845
3	104213

The three natural circular frequencies and periods of vibration are reported in Table 4.VIII.

Table 4. VIII Periods and natural frequencies of the 2-D frame

Mode	Circular frequency $\omega[\text{rad/s}]$	Period $T[\text{s}]$
1	14.230	0.441
2	38.224	0.164
3	47.771	0.131

The structure presents viscous dampers of coefficient $c = 2700[\text{kNs/m}]$ outside the first and the third stories, as shown in Figure 4.27. The elements out of the diagonal of the generalized damping matrix $\boldsymbol{\Xi}$ can be considered as a measure of the non-classicity of the system; in fact for this structure the coupling index defined in Eq.(4.55) is equal to $\rho = 0.76$, so the system cannot be considered classically damped.

The three complex eigenvalues (see Eq.(3.51)) are reported in Table 4.IX.

Table 4. IX Complex eigenvalues of the 2-D frame

Mode	Eigenvalue λ
1	-17.99+5.33 i
2	-11.93+28.36 i
3	-7.37+44.42 i

The structural model undergoes to a stochastic earthquake base excitation, modelled by a zero mean Gaussian fully non-stationary process. The time-frequency modulating function is assumed coherently to Eq.(2.77), with:

$$\begin{aligned} &a_{\max} = 6.007; \\ &t_1 = 5.04\ [\mathrm{s}]; \\ &t_2 = 19.44\ [\mathrm{s}]; \\ &\alpha = 0.13. \end{aligned} \tag{4.56}$$

The target one-sided PSD of ground acceleration $G_0(\omega)$ (see Eq.(2.8)) is modelled by the Clough and Penzien (1975) acceleration spectrum (see Eq.(4.51)).

The following Figures show the time histories of the *NGSMs* with or without the contribution of the viscous dampers and the comparison with the results of the *MCS* (1000 samples).

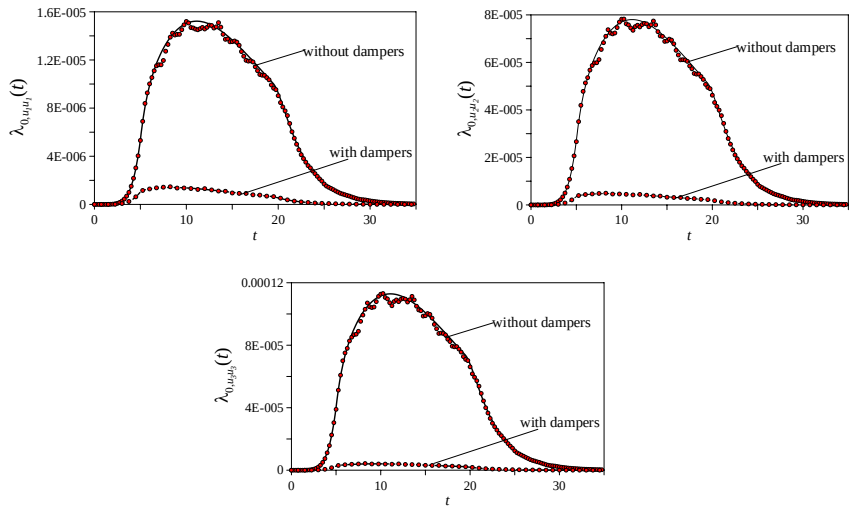

Figure 4. 28 Comparison between the time-variant histories of the $\lambda_{0,u_iu_i}(t)$ *NGSMs* $\left[\mathrm{m}^2\right]$, of the three relative to ground floor displacements, by applying the proposed analytical solution and the *MCS*.

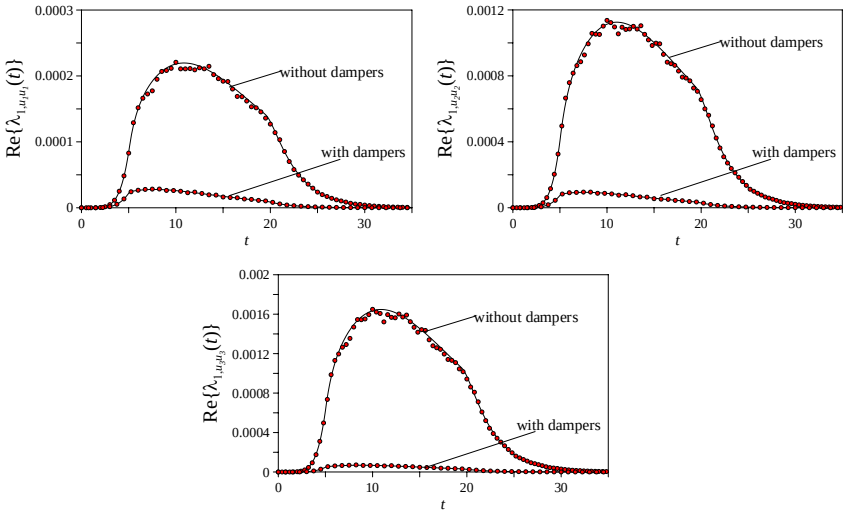

Figure 4. 29 Comparison between the time-variant histories of the $\mathrm{Re}\left\{\lambda_{1,u_i u_i}(t)\right\}$ ***NGSMs*** $\left[\mathrm{m}^2/\mathrm{s}\right]$**, of the three relative to ground floor displacements, by applying the proposed analytical solution and the *MCS*.**

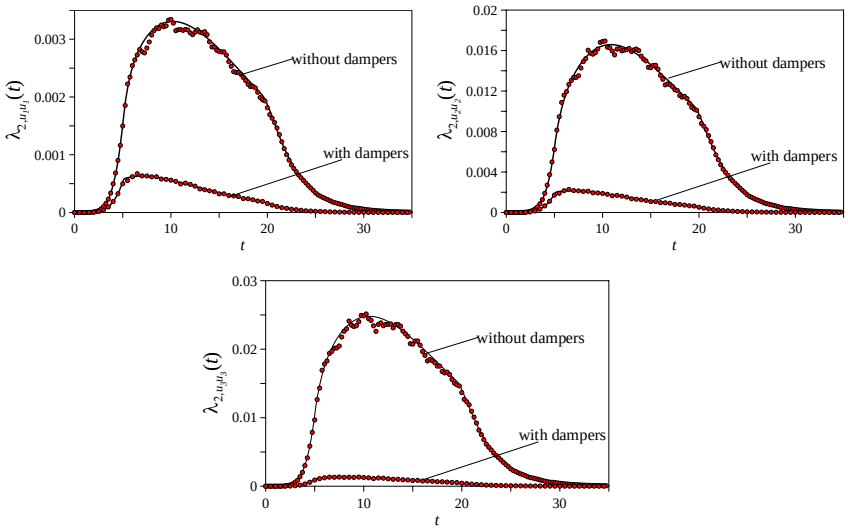

Figure 4. 30 Comparison between the time-variant histories of the $\lambda_{2,u_i u_i}(t)$ ***NGSMs*** $\left[\mathrm{m}^2/\mathrm{s}^2\right]$**, of the three relative to ground floor displacements, by applying the proposed analytical solution and the *MCS*.**

From the analysis of Figures 4.28-4.30 it is evident the influence of the dampers, in terms of reduction of the spectral characteristics of the response.

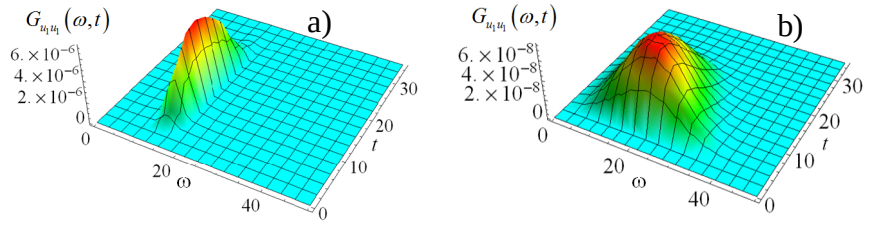

Figure 4. 31 One-sided *EPSD* of the response process of the first floor $G_{u_3u_3}(\omega,t)$ $\left[\mathrm{m}^2\,\mathrm{s}\right]$**: a) without dampers; b)with dampers.**

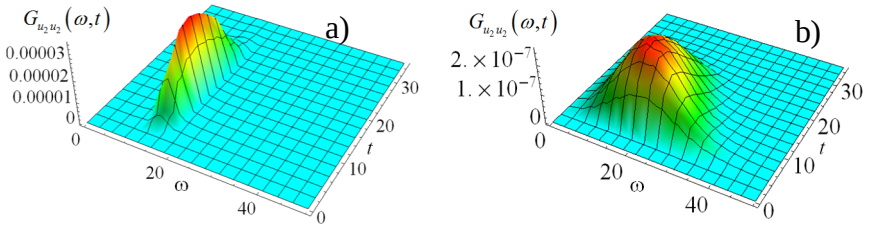

Figure 4. 32 One-sided *EPSD* of the response process of the second floor $G_{u_3u_3}(\omega,t)$ $\left[\mathrm{m}^2\,\mathrm{s}\right]$**: a) without dampers; b)with dampers.**

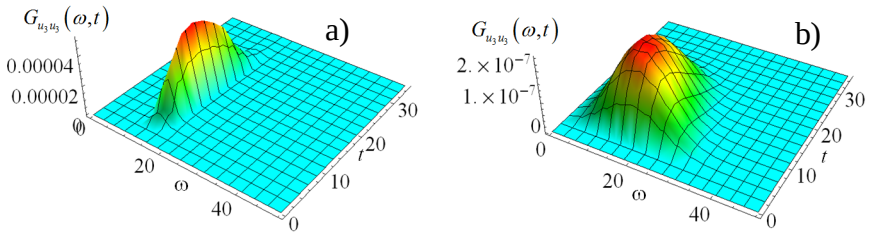

Figure 4. 33 One-sided *EPSD* of the response process of the third floor $G_{u_3u_3}(\omega,t)$ $\left[\mathrm{m}^2\,\mathrm{s}\right]$**: a) without dampers; b)with dampers.**

Figures 4.31, 4.32 and 4.33 show the one-sided *EPSD* function of the response of each floor, obtained according to Eq.(4.37), with or without dampers. Notice that the presence of the dampers influences the shape of the *EPSD* function.

4.3.3.3 External viscous dampers in the 3-D structure

The effectiveness of the proposed procedure is assessed also in the case of a five-story spatial frame, depicted in Figure 4.34 subjected to seismic excitation in the *x* direction.

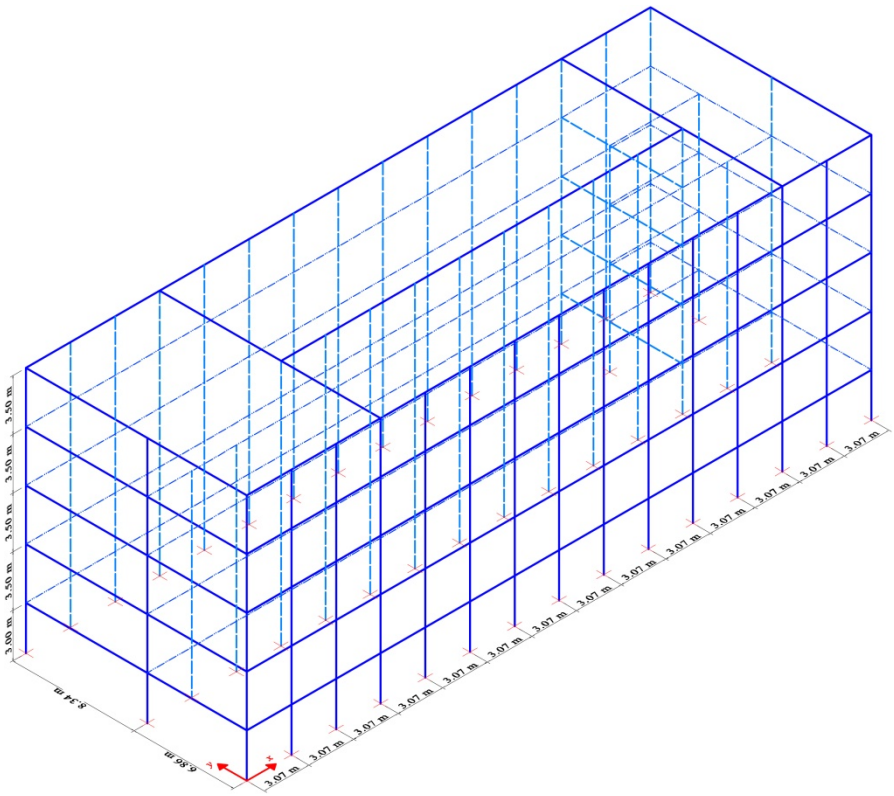

Figure 4. 34 Five-story frame structure: 3D model.

The columns are made of concrete, modelled as linear elastic with Young's modulus $E = 28000\,[\mathrm{MPa}]$. The beams are considered rigid to enforce a typical shear building behaviour. The 3D-frame is modelled as a 15- DOF linear system.

The mass matrix **M,** obtained assuming a distributed load, accounting for the structure's own weight, as well as for permanent and live loads, and the stiffness matrix **K** of the structural system are here reported:

$$\mathbf{M} = \begin{bmatrix} \mathbf{M}_x & \mathbf{0} & \mathbf{0} \\ \mathbf{0} & \mathbf{M}_y & \mathbf{0} \\ \mathbf{0} & \mathbf{0} & \mathbf{I}_p \end{bmatrix}; \tag{4.57}$$

with

$$\mathbf{M}_x = \mathbf{M}_y = \begin{bmatrix} 856282 & 0 & 0 & 0 & 0 \\ 0 & 865612 & 0 & 0 & 0 \\ 0 & 0 & 865612 & 0 & 0 \\ 0 & 0 & 0 & 855976 & 0 \\ 0 & 0 & 0 & 0 & 658690 \end{bmatrix};$$

$$\mathbf{I}_p = \begin{bmatrix} 1.78\times10^8 & 0 & 0 & 0 & 0 \\ 0 & 1.80\times10^8 & 0 & 0 & 0 \\ 0 & 0 & 1.80\times10^8 & 0 & 0 \\ 0 & 0 & 0 & 1.77\times10^8 & 0 \\ 0 & 0 & 0 & 0 & 1.37\times10^8 \end{bmatrix} \tag{4.58}$$

and

$$\mathbf{K} = \begin{bmatrix} \mathbf{K}_{xx} & \mathbf{K}_{xy} & \mathbf{K}_{x\vartheta} \\ \mathbf{K}_{xy}^{T} & \mathbf{K}_{yy} & \mathbf{K}_{y\vartheta} \\ \mathbf{K}_{x\vartheta}^{T} & \mathbf{K}_{y\vartheta}^{T} & \mathbf{K}_{\vartheta\vartheta} \end{bmatrix} \tag{4.59}$$

with

$$\mathbf{K}_{xx} = \begin{bmatrix} 2.83\times10^{9} & -1.09\times10^{9} & 0 & 0 & 0 \\ -1.09\times10^{9} & 2.19\times10^{9} & -1.09\times10^{9} & 0 & 0 \\ 0 & -1.09\times10^{9} & 2.19\times10^{9} & -1.09\times10^{9} & 0 \\ 0 & 0 & -1.09\times10^{9} & 1.93\times10^{9} & -8.40\times10^{8} \\ 0 & 0 & 0 & -8.40\times10^{8} & 8.40\times10^{8} \end{bmatrix}$$

$$\mathbf{K}_{yy} = \begin{bmatrix} 3.48\times10^{9} & -1.34\times10^{9} & 0 & 0 & 0 \\ -1.34\times10^{9} & 2.70\times10^{9} & -1.34\times10^{9} & 0 & 0 \\ 0 & -1.34\times10^{9} & 2.70\times10^{9} & -1.34\times10^{9} & 0 \\ 0 & 0 & -1.34\times10^{9} & 2.51\times10^{9} & -1.17\times10^{9} \\ 0 & 0 & 0 & -1.17\times10^{9} & 1.17\times10^{9} \end{bmatrix};$$

$$\mathbf{K}_{xy} = \mathbf{0};$$

$$\mathbf{K}_{x\theta} = \begin{bmatrix} -2.74\times10^{9} & 1.05\times10^{9} & 0 & 0 & 0 \\ 1.05\times10^{9} & -2.10\times10^{9} & 1.05\times10^{9} & 0 & 0 \\ 0 & 1.05\times10^{9} & -2.10\times10^{9} & 1.08\times10^{9} & 0 \\ 0 & 0 & 1.05\times10^{9} & -1.49\times10^{9} & 3.88\times10^{8} \\ 0 & 0 & 0 & 4.10\times10^{8} & 3.88\times10^{8} \end{bmatrix};$$

$$\mathbf{K}_{y\theta} = \begin{bmatrix} 9.44\times10^{9} & -3.62\times10^{9} & 0 & 0 & 0 \\ -3.65\times10^{9} & 7.24\times10^{9} & -3.62\times10^{9} & 0 & 0 \\ 0 & -3.62\times10^{9} & 7.24\times10^{9} & -3.77\times10^{9} & 0 \\ 0 & 0 & -3.62\times10^{9} & 4.51\times10^{9} & -6.58\times10^{8} \\ 0 & 0 & 0 & -7.34\times10^{8} & 6.57\times10^{8} \end{bmatrix};$$

$$\mathbf{K}_{\theta\theta} = \begin{bmatrix} 9.42\times10^{11} & -3.64\times10^{11} & 0 & 0 & 0 \\ -3.64\times10^{11} & 7.28\times10^{11} & -3.64\times10^{11} & 0 & 0 \\ 0 & -3.64\times10^{11} & 7.28\times10^{11} & -3.64\times10^{11} & 0 \\ 0 & 0 & -3.64\times10^{11} & 6.65\times10^{11} & -3.08\times10^{11} \\ 0 & 0 & 0 & -3.08\times10^{11} & -3.08\times10^{11} \end{bmatrix};$$

(4.60)

Table 4. X Periods and natural frequencies of the 3-D frame

Mode	Circular frequency $\omega[\text{rad/s}]$	Period $T[\text{s}]$
1	11.279	0.557
2	12.046	0.521
3	14.835	0.423
4	31.720	0.198

The first four natural circular frequencies and periods of vibration are reported in Table 4.X.

The structure presents viscous dampers of coefficient $c = 5100[\text{kNs/m}]$ in the x direction, distributed outside every story, as shown in Figure 4.35.

Figure 4. 35 Five-story frame structure with dampers configuration.

The elements out of the diagonal of the generalized damping matrix $\boldsymbol{\Xi}$ can be considered as a measure of the non-classicity of the system; in fact for this structure the coupling index defined in Eq.(4.55) is equal to $\rho = 0.62$, so the system cannot be considered

classically damped. The fifteen complex eigenvalues (see Eq.(3.51) are reported in Table 4.XI.

The structural model undergoes to a stochastic earthquake base excitation, modelled by a zero mean Gaussian fully non-stationary process, as explained in Section 4.2.3.2.

Table 4. XI Complex eigenvalues of the 3-D frame

Mode	Eigenvalue λ
1	-1.07+12.19 i
2	-12.30+1.59 i
3	-2.19+13.33 i
4	-13.82+30.34 i
5	-2.40+34.42 i
6	-4.81+38.87 i
7	-12.76+48.62 i
8	-3.40+52.96 i
9	-7.02+60.40 i
10	-12.55+60.07 i
11	-4.17+66.06 i
12	-15.15+68.89 i
13	-4.65+72.77 i
14	-8.19+77.54 i
15	-9.41+87.47 i

The following Figures show the time histories of the *NGSMs* with or without the contribution of the viscous dampers and the comparison with the results of the *MCS* (1000 samples).

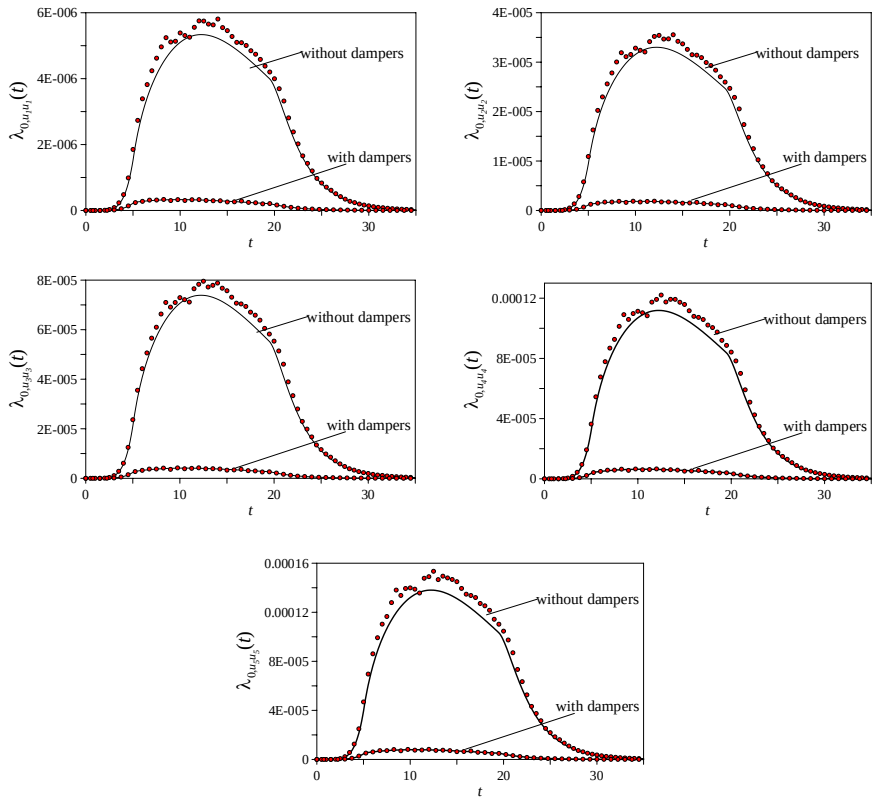

Figure 4. 36 Comparison between the time-variant histories of the $\lambda_{0,u_iu_i}(t)$ *NGSMs* $\left[\mathrm{m}^2\right]$, of the three relative to ground floor displacements, by applying the proposed analytical solution and the *MCS*.

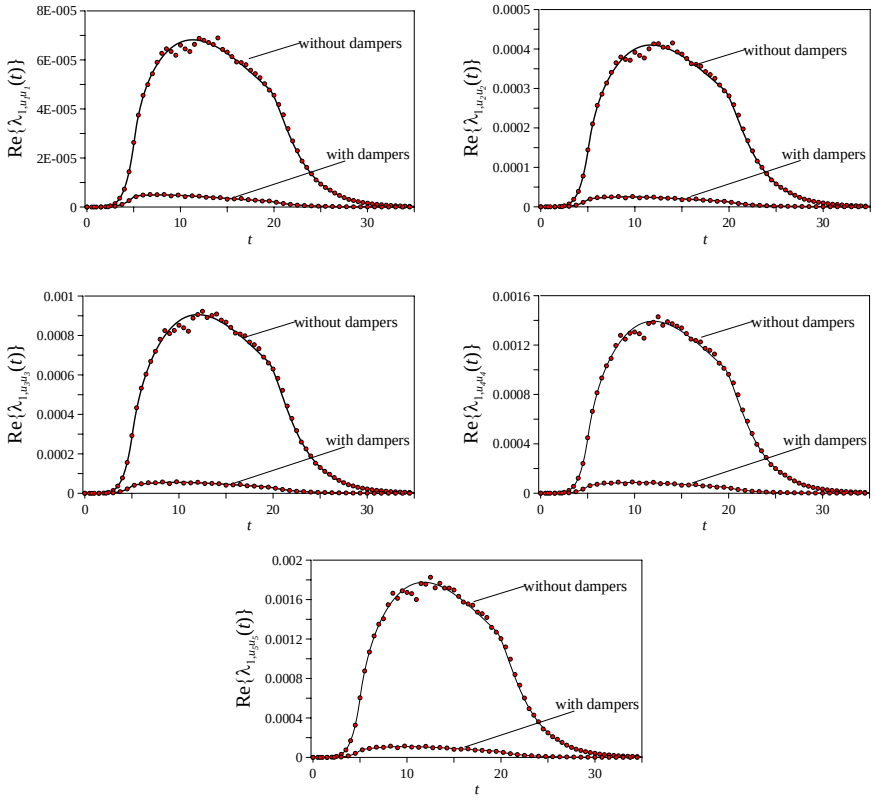

Figure 4. 37 Comparison between the time-variant histories of the $\mathrm{Re}\{\lambda_{1,u_i u_i}(t)\}$ ***NGSMs*** $\left[\mathrm{m}^2/\mathrm{s}\right]$**, of the three relative to ground floor displacements, by applying the proposed analytical solution and the *MCS*.**

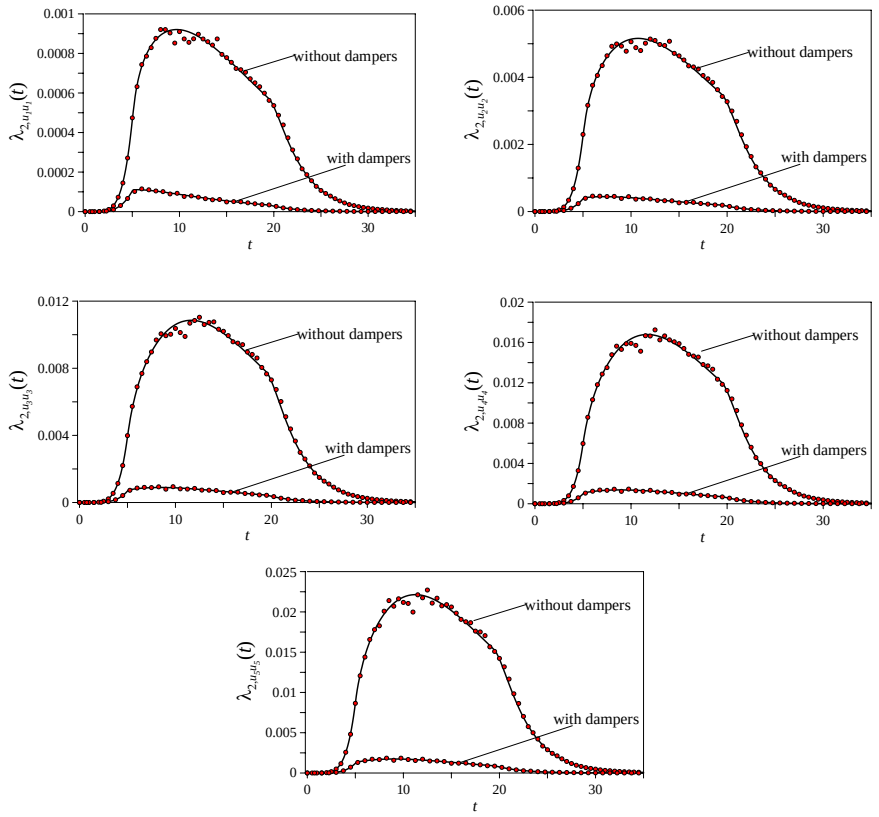

Figure 4. 38 Comparison between the time-variant histories of the $\lambda_{2,u_i u_i}(t)$ *NGSMs* $\left[\mathrm{m}^2/\mathrm{s}^2\right]$, of the three relative to ground floor displacements, by applying the proposed analytical solution and the *MCS*.

From the analysis of Figures 4.36-4.38 it is evident the influence of the dampers, in terms of reduction of the spectral characteristics of the response.

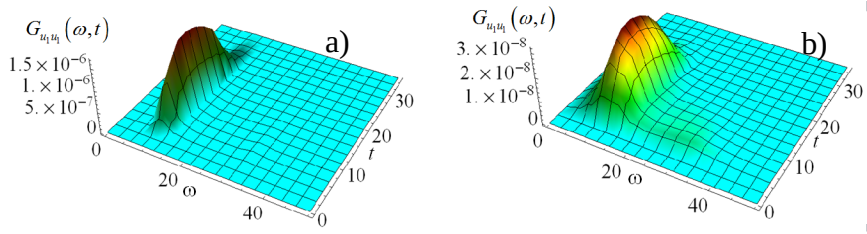

Figure 4. 39 One-sided *EPSD* of the response process of the first floor $G_{u_1 u_1}(\omega,t)$ $\left[\mathrm{m}^2\,\mathrm{s}\right]$: a) without dampers; b)with dampers.

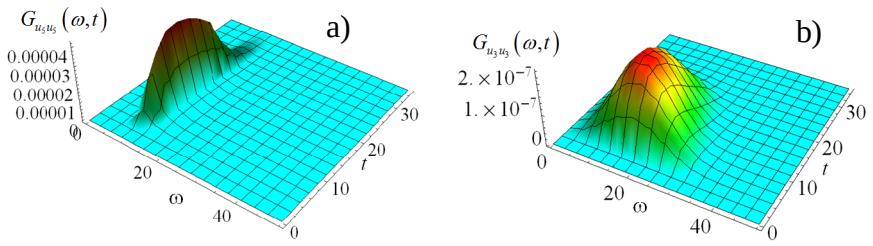

Figure 4. 40 One-sided *EPSD* of the response process of the fifth floor $G_{u_3u_3}(\omega,t)$ $\left[\mathrm{m}^2\,\mathrm{s}\right]$**: a) without dampers; b)with dampers.**

Figure 4.39 and 4.40 show the one-sided *EPSD* function of the response of the first and fifth floor, obtained according to Eq.(4.37), with or without dampers. Notice that the presence of the dampers influences the shape of the *EPSD* function.

4.4 Summary and conclusions

In this Chapter a new, very handy, procedure to evaluate the spectral characteristics of the structural response for both classically and non-classically damped systems, in the cases of mono-correlated and multi-correlated stochastic input process, is proposed. In fact, by mean of closed form solutions of the *TFR* vector function it is possible to evaluate the *EPSD* matrix function of the structural response. The main steps of the proposed approach are:

i) the use of modal analysis, or the complex modal analysis, to decouple the equation of motion;

ii) the introduction of the modal state variable in order to evaluate the *NGSM*s, in the time domain, as element of the *pre-envelope covariance* matrix;

iii) the determination, in state variable, by very handy explicit closed-form solutions, of the *TFR vector functions* and of the *EPSD* matrix function of the structural response for the most common adopted models of the seismic input in the framework of stochastic analysis;

iv) the evaluation of the spectral characteristics of the stochastic response by adopting the closed-form expression of the *EPSD* matrix function.

Several numerical applications, where the comparison with the *MCS* has been done, have confirmed the generality and the effectiveness of the proposed procedure.

Chapter 5

First passage probability problem

5.1 Introduction

Structural systems are conceived and designed to survive natural actions. If the excitations are modeled as random processes, the dynamic response is described by a random process too and the structural safety needs to be evaluated in a probabilistic sense.

In many dynamic applications of structural systems subjected to stochastic excitation, it is important to determine the probability that the maximum absolute value of a selected structural response of interest, $S(t)$ (e.g. strain or stress at a critical point), will not exceed in magnitude, for the first time, its relative limit state level, $b(t)$, within an assigned time interval $[0,t]$:

$$\mathcal{R}_{S_{\max}}(t) = \Pr\langle S_{\max}(\tau) \le b(\tau); \quad 0 \le \tau \le t \rangle \tag{5.1}$$

where $\mathcal{R}_{S_{\max}}(t)$ is the so-called *reliability function* and $S_{\max}(t)$ is the *extreme value random response process* of a selected structural response of interest $S(t)$ defined as:

$$S_{\max}(t) = \max_{0 \le \tau \le t} \left| S(\tau) \right|. \tag{5.2}$$

In the previous equations, the symbol $|\bullet|$ denotes absolute value, while $\Pr\langle \bullet \rangle$ gives the probability associated with the event into angle brackets. This problem is known in literature as the *first-passage probability problem* (Lutes and Sarkani 1997, Li and Chen 2009). This is based on the assumption that a structure fails once *the extreme value random response process* of interest, $S(t)$, at a critical location, exits a prescribed safe domain for the first time. Unfortunately, the prediction of the probability of success is one of the most complicated problems in random vibration theory. Indeed, the solution of this problem has not been derived in exact form, even in the simplest case of the stationary response of a *Single-Degree-of-Freedom* (SDOF) linear oscillator under zero-mean Gaussian white noise (Lutes and Sarkani 1997, Li and Chen 2009). Hence, a large number of approximate techniques has been proposed in the literature, which differ in generality, complexity and accuracy (see e.g. Muscolino and Palmeri 2005, Li and Chen 2009, Pradlwarter and Schueller 2010). In this context solution of first-passage probability problem has been performed by diffusion methods which require the solution of a first order partial differential equation to obtain the evolution of the *Probability Density Function* (*PDF*) of extreme value random process (see e.g. Langley 1988, Li and Chen 2009) or by numerical procedures which determine the stochastic input and response processes in terms of the Karhunen–Loève representation while the extreme value random process statistics are estimated by a line sampling procedure (Pradlwarter and Schueller 2010).

The most adopted methods, which lead to analytical solutions, are based on simplified assumptions in which structural failures are associated to up-crossing mean rate of a given threshold (Corotis et al. 1972, Yang 1972, Corotis and Marshall 1977). Alternatively, the first-passage probability problem has been approached by solving, in approximate form, the highly non-linear first order differential equation governing the time evolution of the non-stationary extreme value random response process (Suzuki and Minai 1980). Since the usual tools of the non-linear stochastic analysis cannot solve this differential equation, approximate solution has been obtained by means of Gaussian and non-Gaussian censored closures (Suzuki and Minai 1980, Suzuki and Minai 1985, Senthilnathan and Lutes 1991, Muscolino and Palmeri 2005). In this context, more recently, Muscolino and Palmeri (2005), proposed an *Advanced Censored gumbel Closure* (*ACC*) approach to evaluate the statistics of the extreme value random process for linear systems excited by zero-mean Gaussian random processes. This procedure, very efficient from a computational point of view, requires, as well as the methods based on the knowledge of up-crossing mean rates of given thresholds, the evaluation of the first three *Non-Geometric Spectral Moments* (*NGSMs*) of the structural response of interest, which need a very cumbersome computational effort, especially for fully non-stationary input processes. Indeed, only in the paper by He (2010) the reliability function has been estimated for a fully non-stationary excitation, under the little bit realistic hypothesis of filtered white noise random process excitation. Moreover, no results exist in literature about the validation of the two methods for the most general case of non-filtered fully non-stationary input processes. This is especially due to the difficulties in the evaluation of the *NGSMs* for such input processes.

Thanks' to the procedure recently proposed by Muscolino and Alderucci (2015) it is possible to evaluate the *NGSMs* of the structural response of interest by evaluating simple integrals in the frequency domain for both separable and non-separable non-stationary excitations. It follows that the approximate solution of the first-passage probability problem can be performed very efficiently for fully non-stationary input processes too.

The evaluation of the *reliability function* and the subsequent *survival probability* of Multi-Degree-of-Freedom (MDOF) structural systems subjected to fully non-stationary excitations is an open problem in the framework of stochastic analysis, especially from a computational point of view. In my opinion this is due to the lack of computational efficiency of the simplest and intuitive methods before described requiring the mean up-crossing rate of given thresholds or censored closures.

Aim of the last Chapter of this Ph.D. thesis is to evidence that once the *Evolutionary Power Spectral Density* (*EPSD*) function, of a generic structural response of interest, is evaluated in closed form solutions by means of the approach here proposed, the *reliability function* as well as the *survival probability* can be evaluated very efficiently. In order to do this, after a short summary of the preliminary concepts on the first-passage probability problem, the main equations useful to evaluate the *survival probability* of linear structural systems with material having strength described by a Gaussian *PDF* are presented.

Furthermore, in the numerical applications section, the approximated formulation has been tested for the prediction of maximum response statistics and of the reliability functions of two different oscillators, with different damping ratios, and of a MDOF system. The comparison between the classical and the *ACC*

(Muscolino and Palmeri 2005) approach has been performed and the validation has been done thanks to the *Monte Carlo Simulation* (*MCS*).

5.2 First passage probability problem: preliminary concepts

5.2.1 Methods requiring the mean up-crossing rate of given thresholds

The *first-passage probability problem* permits to define the probability of success as a function of the probability that the maximum absolute value of a selected structural response of interest, $S(t)$ (e.g., strain or stress at a critical point), will not exceed in magnitude, for the first time, its relative limit state level, b, within an assigned time interval $[0,t]$.

As said before, this problem is one of the most complicated problems in random vibration theory and only approximate solutions have been derived. In the framework of approximate methods, for linear structures subjected to zero-mean Gaussian random processes, the *reliability function*, $\mathcal{R}_{S_{\max}}(t)$, of the *extreme value random response process*, $S_{\max}(t)$ defined in Eq.(5.2), of the selected structural response of interest, $S(t)$, can be expressed as (see e.g. Lutes and Sarkani 1997, Muscolino and Palmeri 2005, Li and Chen 2009):

$$\begin{aligned}\mathcal{R}_{S_{\max}}(t) &\equiv L_{S_{\max}}(b;t) = \Pr\langle S_{\max}(t) \le b(t)\rangle \equiv \\ &\equiv \Pr\langle T_S^1(b) > t\rangle \approx \Pr\langle S_{\max}(0) \le b(0)\rangle \exp\left[-\int_0^t \alpha_S(b;\tau)\,\mathrm{d}\tau\right]\end{aligned} \tag{5.3}$$

where $L_{S_{\max}}(b;t)$ is the *Cumulative Distribution Function* (*CDF*) of the random process $S_{\max}(t)$; $\alpha_S(b;t)$ is the so-called *hazard function* and represents the limiting decay rate of the first passage probability; $T_S^1(b)$ is a random variable describing the instant at which the random process $S_{\max}(t)$ firstly crosses the threshold $b(t) \geq 0$ with positive slope; finally $\Pr\langle S_{\max}(0) \leq b(0)\rangle$ is the probability of success at time $t = 0$ which, for quiescent structural systems, is equal to unity. Various definitions have been proposed for the hazard function for zero-mean Gaussian random process. The first one assumes that successive up-crossing of the level *b* are independent and constitute a Poisson process, in this case the hazard function is evaluated as:

$$\alpha_S(b;t) \equiv 2\nu_S^+(b;t) \tag{5.4}$$

where

$$\nu_S^+(b;t) = \int_0^\infty \dot{s}\, p_{S\dot{S}}(b,\dot{s};t)\,\mathrm{d}\dot{s} \tag{5.5}$$

is the mean up-crossing rate of level $b(t)$ by the random process $S(t)$ (Rice 1945), while $p_{S\dot{S}}(s,\dot{s};t)$ is the joint Gaussian *PDF* between the response random process of interest, $S(t)$, and its time differentiation.

The second approximation assumes the hypothesis that the crossings occur in clumps (Vanmarcke 1975); in this approximation the hazard

function for non-stationary processes can be written as (Corotis et al 1972, Yang 1972):

$$\alpha_S(b;t) \equiv 2\nu_S^+(b;t)\,\beta_S(b;t) \tag{5.6}$$

where

$$\beta_S(b;t) = \left\{ \frac{1-\exp\left[-\dfrac{\nu_A^+(b;t)}{2\nu_S^+(b;t)}\right]}{1-\dfrac{\nu_S^+(b;t)}{\nu_S^+(0,t)}} \right\} \tag{5.7}$$

and

$$\nu_A^+(b;t) = \int_0^\infty \dot{a}\, p_{A\dot{A}}(b,\dot{a};t)\,\mathrm{d}\dot{a} \tag{5.8}$$

is the mean up-crossing rate of level $b(t)$ by the random envelope process $A(t)$ defined as follows (Cramer and Leadbetter 1967):

$$A(t) = \sqrt{S^2(t) + \hat{S}^2(t)}. \tag{5.9}$$

In Eq.(5.8) $p_{A\dot{A}}(a,\dot{a};t)$ is the joint *PDF* between the envelope response process and its time differentiation. In Eq.(5.9) $\hat{S}(t)$ is the Hilbert transform of $S(t)$ defined as:

$$\hat{S}(t)=\frac{1}{\pi}\int_{-\infty}^{\infty}\frac{S(\rho)}{t-\rho}\mathrm{d}\rho. \tag{5.10}$$

Explicit expressions with different level of accuracy were derived in literature to evaluate $\nu_A^+(b;t)$ (Yang 1972, Langley 1986b, Muscolino 1988). It has to be emphasized that $\beta_S(b,t)$ in Eq.(5.7) can be seen as a corrective term of the hazard function, given in Eq.(5.4), obtained considering the up-crossing of barrier *b* constituting a Poisson process. In order to evaluate the mean up-crossing rates $\nu_S^+(b;t)$ and $\nu_A^+(b;t)$, assuming negligible the correlation coefficient between the response process and its time derivative, the following approximate relationships have been derived for the up-crossing rates (Langley 1986b):

$$\begin{aligned}\nu_S^+(b;t)&\cong\frac{1}{2\pi}\sqrt{\frac{\lambda_{2,S}(t)}{\lambda_{0,S}(t)}}\exp\left[-\frac{b^2(t)}{2\lambda_{0,S}(t)}\right]\\ \nu_A^+(b;t)&\cong\sqrt{\frac{\lambda_{2,S}(t)}{2\pi}}\frac{b(t)\,\delta_S(t)}{\lambda_{0,S}(t)}\exp\left[-\frac{b^2(t)}{2\lambda_{0,S}(t)}\right]\end{aligned} \tag{5.11}$$

where $\delta_S(t)$ is the bandwidth parameter defined in the first of Eq. (3.75) and the functions $\lambda_{j,S}(t)$ ($i=0,1,2$) are the *NGSMs* defined in Eq.(3.74). Substituting Eqs.(5.11) into Eq.(5.6) the following approximate expression is derived for the hazard function (Corotis et al. 1972, Corotis and Marshall 1977):

$$\alpha_S(b;t) \cong 2\nu_S^+(b;t)\,\beta_S(b;t) = \\ = \frac{1}{\pi}\sqrt{\frac{\lambda_{2,S}(t)}{\lambda_{0,S}(t)}}\left\{\frac{1-\exp\left[-b(t)\,\delta_S(t)\sqrt{\dfrac{\pi}{2\lambda_{0,S}(t)}}\right]}{\exp\left[\dfrac{b^2(t)}{2\lambda_{0,S}(t)}\right]-1}\right\} \tag{5.12}$$

where the function $\beta_S(b;t)$, introduced in Eq.(5.7), takes the following approximate form:

$$\beta_S(b;t) = \left\{\frac{1-\exp\left[-b(t)\,\delta_S(t)\sqrt{\dfrac{\pi}{2\lambda_{0,S}(t)}}\right]}{1-\exp\left[-\dfrac{b^2(t)}{2\lambda_{0,S}(t)}\right]}\right\}. \tag{5.13}$$

Substituting the hazard function given in Eq.(5.12) into Eq.(5.3) the *CDF* $L_{S_{\max}}(b;t)$ of extreme value random process is determined. Then, the mean value, $\mu_{S_{\max}}(t)$, and standard deviation, $\sigma_{S_{\max}}(t) = \sqrt{m_{2,S_{\max}}(t) - \mu^2_{S_{\max}}(t)}$, of the random process $S_{\max}(t)$ can be obtained once the following quantities are numerically evaluated:

$$\mu_{S_{\max}}(t) \equiv m_{1,S_{\max}}(t) = \int_0^\infty b(t)\,p_{S_{S_{\max}}}(b;t)\,\mathrm{d}b \\ m_{2,S_{\max}}(t) = \int_0^\infty b^2(t)\,p_{S_{S_{\max}}}(b;t)\,\mathrm{d}b \tag{5.14}$$

where

$$p_{S_{S_{\max}}}(b;t) = \frac{\partial L_{S_{S_{\max}}}(b;t)}{\partial b} \tag{5.15}$$

is the *PDF* of the extreme value random process.

5.2.2 Methods requiring censored closures

In the previous section the approximate reliability function was derived assuming that the up-crossing rate of given thresholds are independent or occur in clumps. In literature the first-passage probability problem has been approached alternatively by solving, in approximate form, the highly non-linear first order differential equation governing the time evolution of the non-stationary extreme value random response process $S_{\max}(t)$ (Suzuki and Minai 1980):

$$\begin{aligned} S_{\max}(t) &= g\left[S(t), \dot{S}(t), S_{\max}(t)\right]\mathrm{d}t = \\ &= \left[\dot{S}(t)\,\mathbb{U}\left(S(t)\,\dot{S}(t)\right)\mathbb{U}\left(|S(t)| - S_{\max}(t)\right)\right]\mathrm{d}t \end{aligned} \tag{5.16}$$

$\mathbb{U}(\bullet)$ being the unit step function continuous from the right, that is:

$$\mathbb{U}(t - t_0) = \begin{cases} 0, & t < t_0; \\ 1, & t \geq t_0. \end{cases} \tag{5.17}$$

Eq.(5.16) allows to derive the non-linear differential equation governing the time evolution of the *i*-th statistical moment of $S_{\max}(t)$ as follows:

$$\dot{m}_{i,S_{\max}}(t) = i\,\mathrm{E}\left\langle S_{\max}^{i-1}(t)\; g\left[S(t), \dot{S}(t), S_{\max}(t)\right]\right\rangle. \tag{5.18}$$

Notice that, for $i = 1, 2, \ldots, n$, Eq.(5.18) implicitly involves higher-order moments, the latter constitutes an infinite hierarchy of equations, which has to be closed with expedient techniques. Doing so, statistical moments of order greater than *n* are expressed as functions of those of a given order up to *n* (closure order), and the first *n* moment equations can be solved in approximated form. Unfortunately, classical closures, e.g. the simplest Gaussian closure (in which $n = 2$), do not apply, because an inconsistency exists, which brings theoretical and computational difficulties. In fact, by virtue of Eq. (5.16), the non-stationary random process $S_{\max}(t)$ has a positive increment at time *t* if and only if $\text{sign}\left[S(t)\right] = \text{sign}\left[\dot{S}(t)\right]$ and $\left|S(t)\right| \geq S_{\max}(t)$. However, by the definition of stochastic process $S_{\max}(t)$, given in Eq.(5.2), the latter condition can be satisfied just by the equivalence, $S_{\max}(t) \equiv \left|S(t)\right|$.

A simple way to circumvent this evident discrepancy is to consider a censored distribution for the random process $S_{\max}(t)$. Namely the probability mass associated with the impossible event $S_{\max}(t) < \left|S(t)\right|$ is removed and conveniently lumped at the limiting position where $S_{\max}(t) = \pm S(t)$ (Suzuki and Minai 1980, Suzuki and Minai 1985, Senthilnathan and Lutes 1991, Muscolino and Palmeri 2005). Doing so, the condition $\left|S(t)\right| \geq S_{\max}(t)$ is satisfied associating a finite probability with the limit event $S_{\max}(t) = \pm S(t)$. As a finite probability cannot be directly included in any continuous model, the analytical counterpart of this arrangement is the introduction of two Dirac delta functions in the joint *PDF* between the random processes $S_{\max}(t)$ and $S(t)$. The latter are centered at

$S_{\max}(t) = \pm S(t)$, i.e. where $S_{\max}(t)$ reaches a barrier of level $b(t) = |S(t)|$ (Muscolino and Palmeri 2005).

The main drawback of this approach is that the joint *PDF* should be known in order to center the Dirac deltas. This drawback has been overcome introducing a *guest PDF* for the extreme value random process (Suzuki and Minai 1980, Suzuki and Minai 1985, Senthilnathan and Lutes 1991, Muscolino and Palmeri 2005). In order to do this Muscolino and Palmeri (2005) introduced the following hypotheses: i) the random processes $\dot{S}(t)$ and $S_{\max}(t)$ are treated as independent; ii) the *guest PDF* is of Gumbel type; iii) the response bandwidth is accounted for a consistent *censorship factor*, $0 \le \chi_{S_{\max}}(t) \le 1$, which governs the distribution of the Dirac delta functions introduced in the joint *PDF* of $S(t)$ and $S_{\max}(t)$. Under these hypothesis the time evolution of the first two statistical moment of the extreme value random response process can be evaluated as:

$$\begin{aligned} \dot{m}_{1,S_{\max}}(t) \equiv \dot{\mu}_{S_{\max}}(t) = f_1(t) = 2\,\chi_{S_{\max}}(t) \int_0^\infty v_S^+(b;t)\, L_{S_{\max}}^G(b;t)\,\mathrm{d}b \\ \dot{m}_{2,S_{\max}}(t) = f_2(t) = 4\,\chi_{S_{\max}}(t) \int_0^\infty b(t)\, v_S^+(b;t)\, L_{S_{\max}}^G(b;t)\,\mathrm{d}b \end{aligned} \tag{5.19}$$

where $L_{S_{\max}}^G(b;t)$ is the *guest CDF* of the random processes $S_{\max}(t)$ assumed of the Gumbel type:

$$L_{S_{\max}}^G(b;t) = \exp\left\{\exp\left[-\frac{\eta_{S_{\max}}(t) - b(t)}{\kappa_{S_{\max}}(t)}\right]\right\} \tag{5.20}$$

with

$$\kappa_{S_{\max}}(t)=\frac{\sqrt{6}}{\pi}\sigma_{S_{\max}}(t)=\frac{1}{\pi}\sqrt{6\left[m_{2,S_{\max}}(t)-m_{1,S_{\max}}^{2}(t)\right]};$$
$$\eta_{S_{\max}}=m_{1,S_{\max}}(t)-\gamma\,\kappa_{S_{\max}}(t) \tag{5.21}$$

$\gamma\cong 0.5772$ being the Euler number. It has been proved that the *censorship factor* $\chi_{S_{\max}}(t)$ introduced in Eq.(5.19) can be evaluated as (Muscolino and Palmeri 2005):

$$\chi_{S_{\max}}(t)=\int_{0}^{\infty}\beta_S\left(b;t\right)p_{S_{\max}}\left(b;t\right)\mathrm{d}b \tag{5.22}$$

where $\beta_S\left(\rho,t\right)$ is the coefficient introduced in Eq.(5.13) and $p_{S_{S_{\max}}}\left(b;t\right)$ is the *PDF* of the extreme value process given as:

$$p_{S_{\max}}\left(b;t\right)=\left\{p_{S_{\max}}^{G}\left(b;t\right)\left[2L_S\left(b;t\right)-1\right]+2L_{S_{\max}}^{G}\left(b;t\right)p_S\left(b;t\right)\right\}\mathbb{U}\left(b\right) \tag{5.23}$$

with $p_S\left(b;t\right)$ the Gaussian *Power Spectral Density* (*PSD*) function of the response process $S(t)$, $L_S\left(b;t\right)$ its *CDF* and $p_{S_{\max}}^{G}\left(b;t\right)$ the *guest PDF* of Gumbel type:

$$p_{S_{\max}}^{G}\left(b;t\right)=\frac{\partial L_{S_{\max}}^{G}\left(b;t\right)}{\partial b}=$$
$$=\frac{1}{\kappa_{S_{\max}}(t)}\exp\left\{\frac{\eta_{S_{\max}}(t)-b(t)}{\kappa_{S_{\max}}(t)}-\exp\left[\frac{\eta_{S_{\max}}(t)-b(t)}{\kappa_{S_{\max}}(t)}\right]\right\}. \tag{5.24}$$

The solution of the problem must be numerically obtained with the second-order Runge–Kutta method, after the subdivision of the time axis into small intervals of equal width Δt. Since at the time step $[t_k, t_{k+1}]$ the *NGSMs* statistics of the response process $S(t)$ can be evaluated independently, the statistical moments of the random process $S_{\max}(t)$ at the left endpoint $t_k = k\Delta t$ are also known from the previous step. Then the approximate first two statistical moments at the right endpoint, $t_{k+1} = t_k + \Delta t$, can be evaluated as (Muscolino and Palmeri 2005):

$$\begin{aligned} m_{1,S_{\max}}(t_{k+1}) &= m_{1,S_{\max}}(t_k) + f_1(t_k)\,\Delta t \\ m_{2,S_{\max}}(t_{k+1}) &= m_{2,S_{\max}}(t_k) + f_2(t_k)\,\Delta t \end{aligned} \tag{5.25}$$

where

$$\begin{aligned} f_1(t_k) &= 2\,\chi_{S_{\max}}(t_k)\int_0^\infty \nu_S^+(b;t_k)\,L_{S_{\max}}^G(b;t_k)\,\mathrm{d}b \\ f_2(t_k) &= 4\,\chi_{S_{\max}}(t_k)\int_0^\infty b(t_k)\,\nu_Y^+(b;t_k)\,L_{S_{\max}}^G(b;t_k)\,\mathrm{d}b. \end{aligned} \tag{5.26}$$

Then the mean value, $\mu_{S_{\max}}(t_{k+1}) \equiv m_{1,S_{\max}}(t_{k+1})$, and standard deviation, $\sigma_{S_{\max}}(t_{k+1}) = \sqrt{m_{2,S_{\max}}(t_{k+1}) - \mu_{S_{\max}}^2(t_{k+1})}$, of extreme value random of the random process $S_{\max}(t)$ at time instant t_{k+1}, can be derived. Finally the reliability function can be evaluated as (Muscolino and Palmeri 2005):

$$\mathcal{R}_{S_{\max}}(t) \equiv L_{S_{\max}}(b;t) = \left[2L_S(b;t) - 1\right] L_{S_{\max}}^G(b;t)\,\mathbb{U}(b). \tag{5.27}$$

5.3 Reliability assessment

In structural engineering, once the *CDF* of the extreme value process $S_{\max}(t)$ is determined, the next step is to provide a measure of the risk in terms of *probability of failure*, $\mathcal{P}_{\mathcal{F}}$, and a measure of the success in terms of *probability of success* or *survival probability*, $\mathcal{P}_{\mathcal{S}} = 1 - \mathcal{P}_{\mathcal{F}}$.

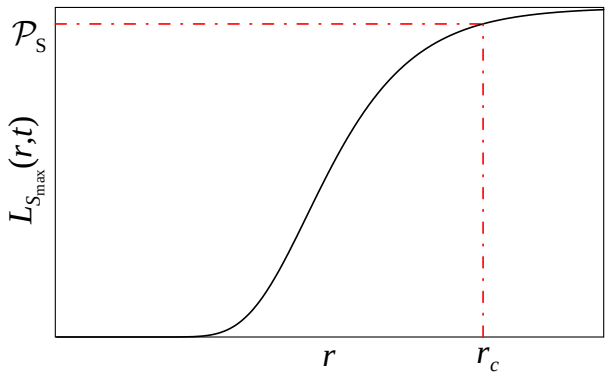

Figure 5. 1 System reliability.

For convenience, but without loss of generality, only the safety of the selected structural element of interest , $S(t)$ (e.g., strain or stress at a critical point), is considered here and the structural element is considered to have failed if its resistance, *R*, is less than the *extreme value*, $S_{\max}(t)$, acting on it. In particular, if it is required that the extreme value random response process, $S_{\max}(t)$, of a structural response of interest will not exceed in magnitude, for the first time, the deterministic limit state level, r_c, in the time interval $[0,t]$, the *survival probability* can be evaluated as:

$$\mathcal{P}_{\mathcal{S},S_{\max}}\left(r_c,t\right)=\Pr\langle S_{\max}(\tau)\le r_c;\quad 0\le\tau\le t\rangle=$$
$$=\int_0^{r_c} p_{S_{\max}}\left(b;t\right)\mathrm{d}b\equiv L_{S_{\max}}\left(r_c,t\right). \tag{5.28}$$

Often it is assumed that the resistance of the structural element is a Gaussian random variable, *R*, characterized by the *PDF*, $p_R(r)$, having mean-value μ_R and standard deviation σ_R. In this case the *survival probability* can be evaluated as:

$$\mathcal{P}_{\mathcal{S},S_{\max}}\left(r;t\right)=\int_{-\infty}^{\infty}\int_0^{b=r} p_R(r)\; p_{S_{\max}}\left(b;t\right)\mathrm{d}b\;\mathrm{d}r=$$
$$=\int_{-\infty}^{\infty} p_R(r)\,L_{S_{\max}}\left(r;t\right)\mathrm{d}r \tag{5.29}$$

where $p_{S_{\max}}\left(r;t\right)$ and $L_{S_{\max}}\left(r;t\right)$ are the *PDF* and *CDF* of the extreme value random response process, $S_{\max}(t)$, derived in the previous sections under the assumption that up-crossings of a specified threshold of the analysed structural quantity occur in clumps or by applying the advanced censored Gumbel closure approach. Finally, the so-called failure function (Melchers 1999) can be derived from the argument of the integral in Eq.(5.29) as follows:

$$\mathcal{F}_{S_{\max}}\left(r;t\right)=p_R(r)\left[1-L_{S_{\max}}\left(r;t\right)\right]. \tag{5.30}$$

It follows that the *probability of failure* is given as:

$$\mathcal{P}_{\mathcal{F},S_{\max}}(r;t) = \Pr\langle S_{\max}(\tau) > r_c; \quad 0 \le \tau \le t\rangle = \\ = \int_{-\infty}^{\infty}\int_{b=r}^{\infty} p_R(r)\; p_{S_{\max}}(b;t)\,\mathrm{d}b\,\mathrm{d}r = \int_{-\infty}^{\infty} \mathcal{F}_{S_{\max}}(r;t)\,\mathrm{d}r. \tag{5.31}$$

Another useful parameter in reliability analysis is the *reliability index,* I_S, given by:

$$I_S = \frac{\mu_E}{\sigma_E} \tag{5.32}$$

where

$$\mu_E = \mu_R - \mu_S \\ \sigma_E^2 = \sigma_S^2 + \sigma_R^2. \tag{5.33}$$

Notice that much more higher is the reliability index much more lower is the failure probability.

5.4 Numerical Applications

5.4.1 Single-Degree of Freedom systems

In order to validate the procedures previously described, the formulations have been implemented firstly for the prediction of maximum response statistics and of the reliability functions of two different oscillators, with different damping ratios. The excitation consists in a fully non-stationary process, modelled as the Spanos and Solomos (1983) model first and then as the Conte and Peng (1996) one.

For the evolutionary modulating function proposed by Spanos and Solomos (1983) (see Eq. (2.16)) the following parameters have been selected: $\varepsilon(\omega)=\omega\sqrt{2}/5\pi$ and $\alpha(\omega)=0.15/2+\varepsilon^{2}(\omega)/4$. The maximum is reached at $\omega=1.94\pi\left[\text{rad/s}\right]$ and $t=6.67\left[\text{s}\right]$. The target one-sided *PSD* function of the "embedded" stationary counterpart $G_0(\omega)$ is modelled by the Clough and Penzien (1975) acceleration spectrum:

$$G_0(\omega)=G_g\frac{\left(1+4\xi_g^2\left(\omega/\omega_g\right)^2\right)}{\left(1-\left(\omega/\omega_g\right)^2\right)^2+4\xi_g^2\left(\omega/\omega_g\right)^2}\times\frac{\left(\omega/\omega_f\right)^4}{\left(1-\left(\omega/\omega_f\right)^2\right)^2+4\xi_f^2\left(\omega/\omega_f\right)^2} \tag{5.34}$$

where in order to simulate the El Centro earthquake (1940) the following parameters have been selected:

$$\begin{aligned}&G_g=0.5656\left[\text{m}^2/\text{s}^3\right];\\&\omega_g=19.0\left[\text{rad/s}\right];\\&\xi_g=0.65;\\&\omega_f=2.0\left[\text{rad/s}\right];\\&\xi_f=0.6.\end{aligned} \tag{5.35}$$

The selected parameters for the Conte and Peng (1996) model (see Eq. (2.68) to Eq.(2.70)) are the ones estimated for the N-S accelerogram component of the Imperial Valley earthquake of May 18, 1940, recorded at the El Centro site (Table 4.I).

In order to compare the responses evaluated by adopting different models, the one-sided *PSD* of the ideal white noise, G_g, is normalized in such a way that the "total ground motion acceleration energy" (see Eq. (4.53)) of the analysed non-stationary ground acceleration model is the same as that of Conte and Peng (1996) model.

Then, in order to check the accuracy of classical approximations, that are the Poisson model and the Corotis et al. (1972) model, and censored closures (Muscolino and Palmeri 2005), the results were compared with those of *MCS*, performed with 2,500 samples.

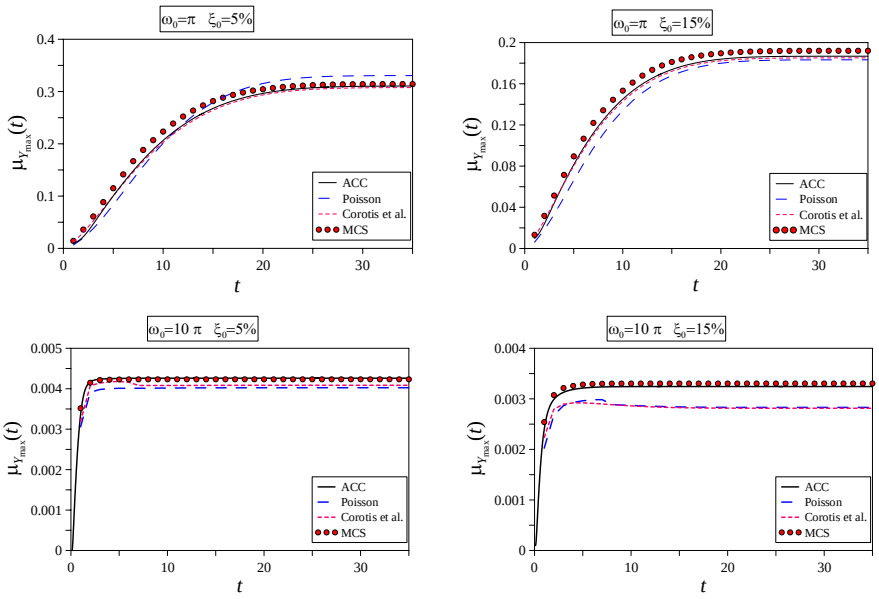

Figure 5. 2 Comparison between classical and *ACC* (Muscolino and Palmeri 2005) approaches with *MCS* of the mean value for the Spanos and Solomos (1983) model.

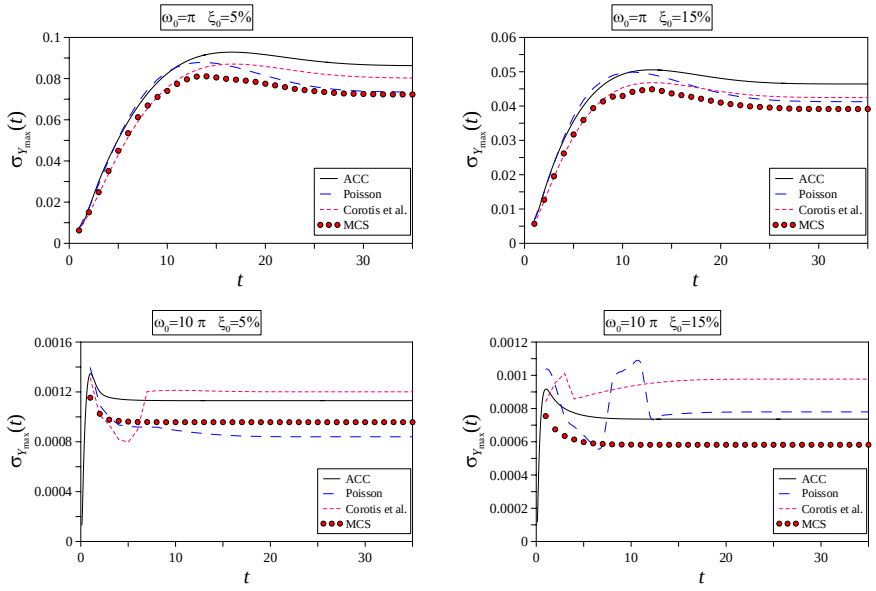

Figure 5. 3 Comparison between classical and *ACC* (Muscolino and Palmeri 2005) approaches with *MCS* of the standard deviation for the Spanos and Solomos (1983) model.

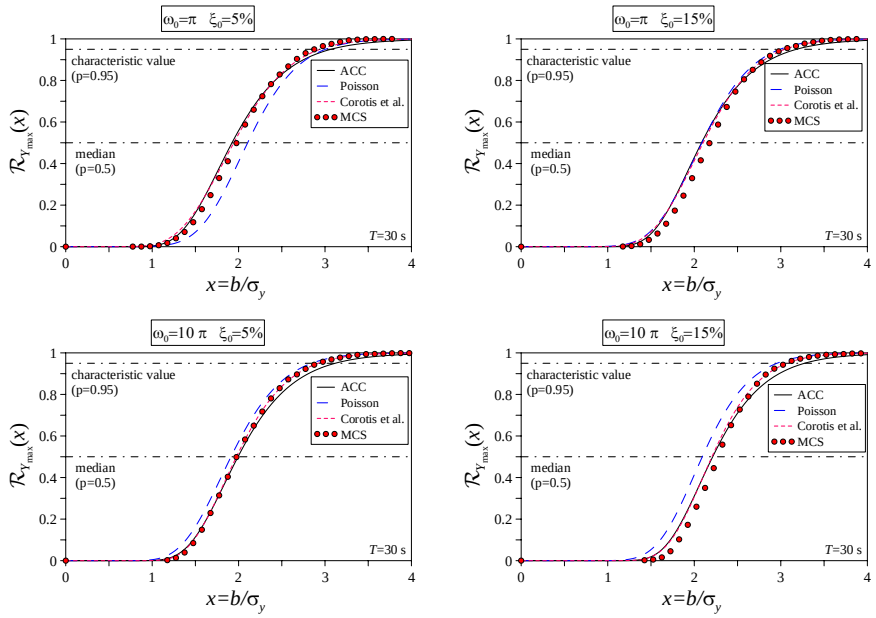

Figure 5. 4 Comparison between classical and *ACC* (Muscolino and Palmeri 2005) approaches with *MCS* of the reliability function at time T=30 s for the Spanos and Solomos (1983) model.

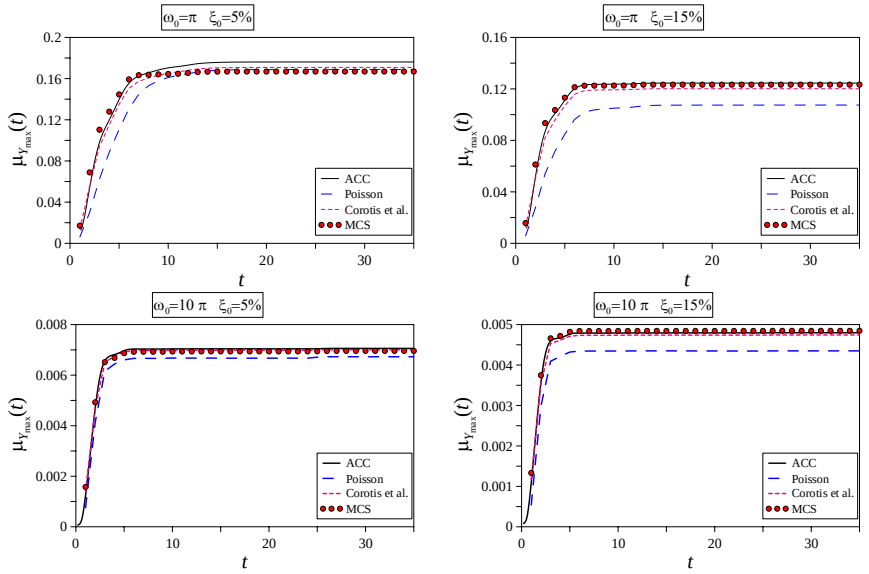

Figure 5. 5 Comparison between classical and *ACC* (Muscolino and Palmeri 2005) approaches with *MCS* of the mean value for the Conte and Peng (1996) model.

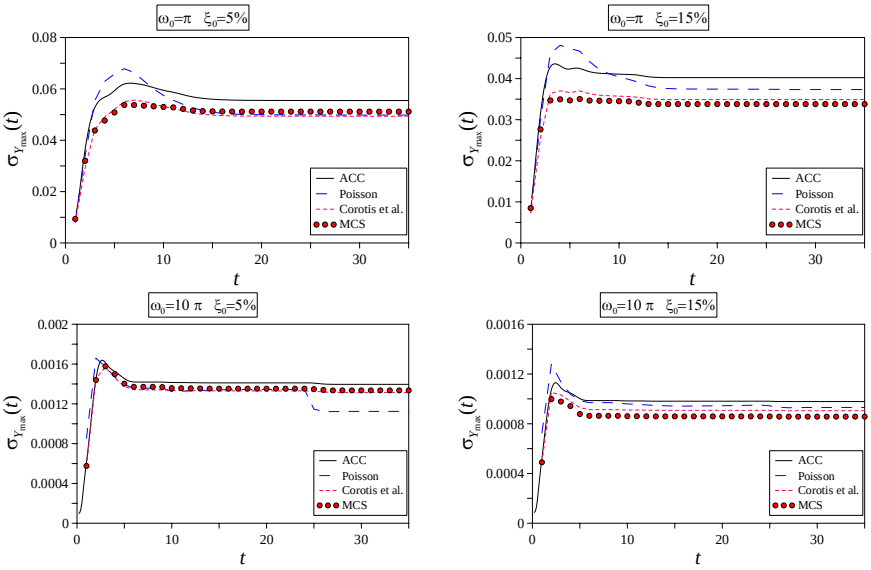

Figure 5. 6 Comparison between classical and *ACC* (Muscolino and Palmeri 2005) approaches with *MCS* of the standard deviation for the Conte and Peng (1996) model.

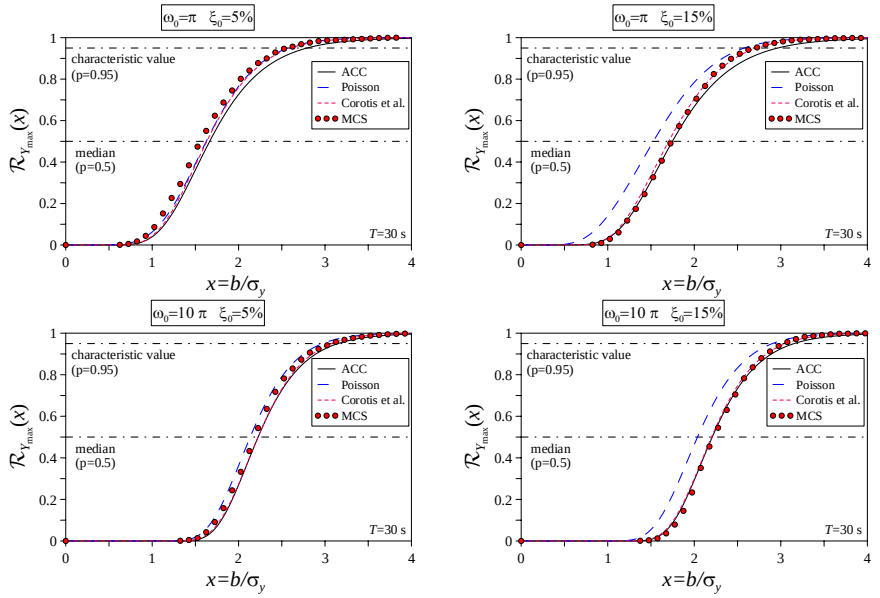

Figure 5. 7 Comparison between classical and *ACC* (Muscolino and Palmeri 2005) approaches with *MCS* of the reliability function at time T=30 s for the Conte and Peng (1996) model.

As evident from the analysis of the Figures 5.2 and 5.5, the *ACC* model (Muscolino and Palmeri 2005) is able to catch with accuracy the mean value of the oscillators at higher frequencies as well as the Corotis et al. (1972) model, while in Figures 5.3 and 5.6 both the classical and *ACC* approach are not always able to obtain the standard deviation.

The reliability functions, plotted in Figure 5.4 and 5.6 as a function of $x = b/\sigma_y$, where $\sigma_y = \sqrt{\max_{0\le\tau\le t_f}|\lambda_0(\tau)|}$, show that the Poisson model fails and the *ACC* approach is confirmed from the analysis of the comparison with the *MCS*. Furthermore from the analysis the same Figures it can be shown that the Corotis et al. (1972) model can be suitably used in reliability analysis of structures subjected to fully non-stationary input.

5.4.2 Multi-Degrees of Freedom systems

A reliability analysis is herein performed for a MDOF system. The structural model is the same of Section 4.3.3.3, considered without dampers and with a damping ratio equal for all modes $\xi = 0.05$.

To perform reliability assessment of the structure, the attention is focused on the relative displacement components (the so-called drift) along the *x*-direction of the first frame, as evidenced in Fig 5.8.

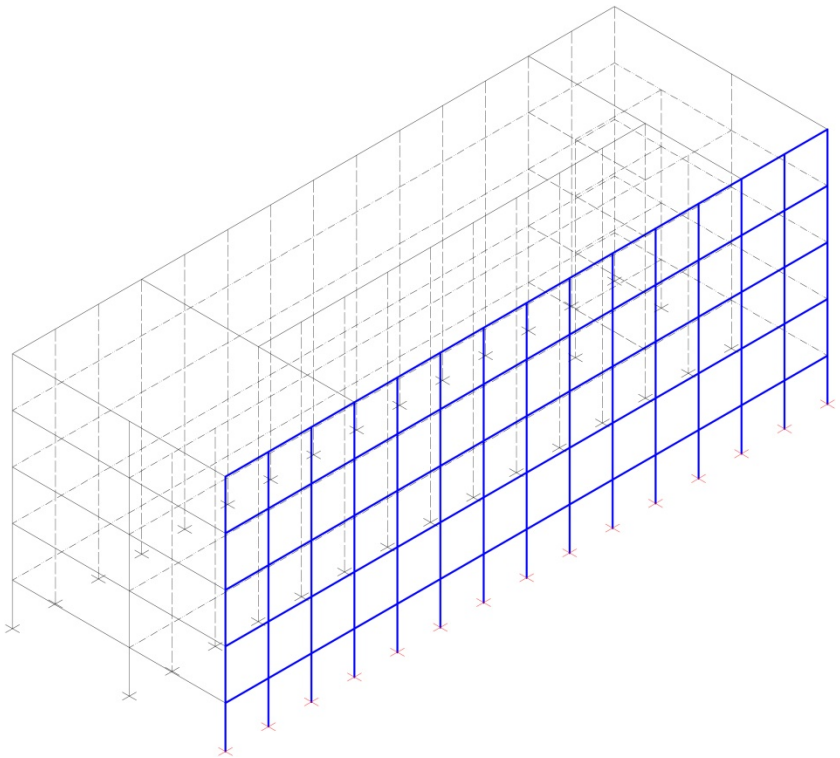

Figure 5. 8 Five-story frame structure.

Notice that in order to obtain the *NGSMs* in terms of drift of the first frame, it is necessary to introduce a first coordinate transformation; in fact, in order to obtain the displacement of the first frame along the *x* direction, $\mathbf{u}^{(f)}(t)$, as a function of the

displacement of the barycenter at each floor, $\mathbf{u}^{(g)}(t)$, and according to the modal coordinate transformation $\mathbf{u}(t)=\mathbf{\Phi q}(t)$ the following relationship olds:

$$\mathbf{u}^{(f)}(t)=\mathbf{T}\mathbf{u}^{(g)}(t)=\mathbf{T}\mathbf{\Phi}\mathbf{q}^{(g)}(t) \tag{5.36}$$

where **T** is defined as:

$$\mathbf{T}=\begin{pmatrix} 1 & 0 & 0 & 0 & 0 & 0 & 0 & 0 & 0 & 0 & y_1^{(g)} & 0 & 0 & 0 & 0 \\ 0 & 1 & 0 & 0 & 0 & 0 & 0 & 0 & 0 & 0 & 0 & y_2^{(g)} & 0 & 0 & 0 \\ 0 & 0 & 1 & 0 & 0 & 0 & 0 & 0 & 0 & 0 & 0 & 0 & y_3^{(g)} & 0 & 0 \\ 0 & 0 & 0 & 1 & 0 & 0 & 0 & 0 & 0 & 0 & 0 & 0 & 0 & y_4^{(g)} & 0 \\ 0 & 0 & 0 & 0 & 1 & 0 & 0 & 0 & 0 & 0 & 0 & 0 & 0 & 0 & y_5^{(g)} \end{pmatrix} \tag{5.37}$$

in which $y_i^{(g)}(i=1,2,...,5)$ are the coordinate of the barycenter with respect to the coordinate system along the *y* axis. Then, a second coordinate transformation must be introduced in order to obtain the drifts along the *x*-direction of the first frame, $\mathbf{Y}(t)$, as a function of the displacement of the first frame along the *x* direction, $\mathbf{u}^{(f)}(t)$; the transformation matrix $\tilde{\mathbf{R}}$ is given by:

$$\tilde{\mathbf{R}}=\begin{pmatrix} 0 & 0 & 0 & -1 & 1 \\ 0 & 0 & -1 & 1 & 0 \\ 0 & -1 & 1 & 0 & 0 \\ -1 & 1 & 0 & 0 & 0 \\ 1 & 0 & 0 & 0 & 0 \end{pmatrix}. \tag{5.38}$$

According to Eq. (3.73) the drift of the first frame $\mathbf{Y}(t)$ are obtained thanks' to the formula:

$$\mathbf{Y}(t)=\tilde{\mathbf{R}}\mathbf{u}^{(f)}(t)=\tilde{\mathbf{R}}\mathbf{T}\mathbf{u}^{(g)}(t)=\tilde{\mathbf{R}}\mathbf{T}\boldsymbol{\Phi}\mathbf{q}^{(g)}(t)=\mathbf{E}\mathbf{q}^{(g)}(t) \tag{5.39}$$

By mean of the influence matrix **E** it is possible to evaluate the *NGSMs* in terms of drift starting by the purged *NGSMs* of the modal response, according to Eq. (3.74).

The structure undergoes to a spectrum compatible input process (see Section 3.6), modelled as stationary input process, quasi-stationary input process, with the Hsu and Bernard (1978) modulating function (see Eq.(2.10)), and fully-non stationary input process, with the Spanos and Solomos (1983) modulating function (see Eq.(2.16)).

According to the EC8 instructions (2003) a spectrum of Type I is chosen as target spectrum, following the values for the type "C" of soil, the parameters $S=1.15$, $T_B=0.2$ [s] $T_C=0.6$ [s] and $T_D=2.0$ [s] are selected. The peak ground acceleration is assumed equal to $a_g=1.647\left[\mathrm{m/s^2}\right]$, considering a strategic structure with a nominal life of 100 years and the damage limit state.

In Table 5.I the energy, $E_{\ddot{U}_g}^{\mathrm{ST}}(t_d)$ and $E_{\ddot{U}_g}^{\mathrm{NST}}(t_d)$, of the stationary and non-stationary, respectively, spectrum-compatible acceleration random process are reported; these quantities are evaluated by the relationships:

$$E_{\ddot{U}_g}^{\mathrm{ST}}(t_d)=\int_0^{t_d}\int_0^{\infty} G_{\ddot{U}_g}^{\mathrm{ST}}(\omega)\,\mathrm{d}\omega\,\mathrm{d}t;$$
$$E_{\ddot{U}_g}^{\mathrm{NST}}(t_d)=\int_0^{t_d}\int_0^{\infty} G_{\ddot{U}_g}^{\mathrm{NST}}(\omega,t)\,\mathrm{d}\omega\,\mathrm{d}t; \tag{5.40}$$

where $G_{\ddot{U}_g}^{\mathrm{ST}}(\omega)$ and $G_{\ddot{U}_g}^{\mathrm{NST}}(\omega,t)$ are, respectively, the stationary spectrum compatible *PSD* function and the stationary counterpart of the non-stationary spectrum compatible *EPSD*.

Table 5. I Total energy $\left[m^2/s^3\right]$ of the stationary, quasi-stationary and fully non-stationary spectrum compatible acceleration processes

Stationary spectrum compatible model	Hsu & Bernard spectrum compatible model	Spanos & Solomos spectrum compatible model
12.13	6.04	6.30

From the analysis of the results reported in this Table it is evident that the energy associated to the stationary spectrum-compatible model is much higher than the energy evaluated by applying the other ones.

The mean values, the variance an the reliability functions of the response have been evaluated, according to the Corotis et al. (1972) model, in the three cases of spectrum compatible input process and all the results have been compared with the *MCS* method (1000 samples).

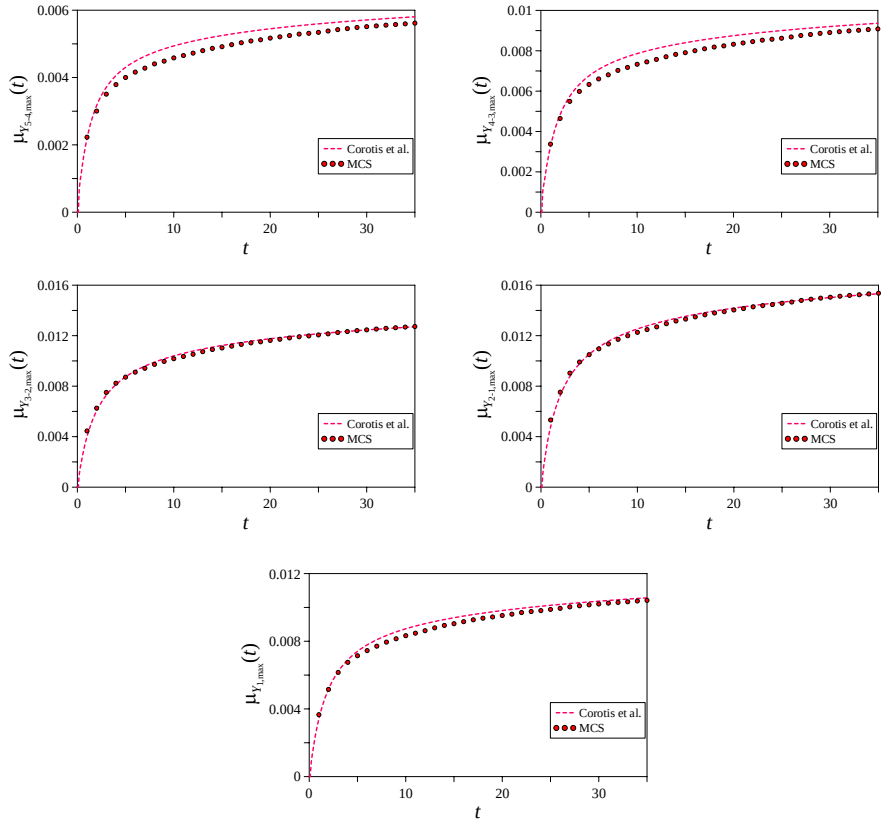

Figure 5. 9 Comparison between Corotis et al. (1972) model and *MCS* of the mean value of the inter-story drift for the spectrum compatible stationary model.

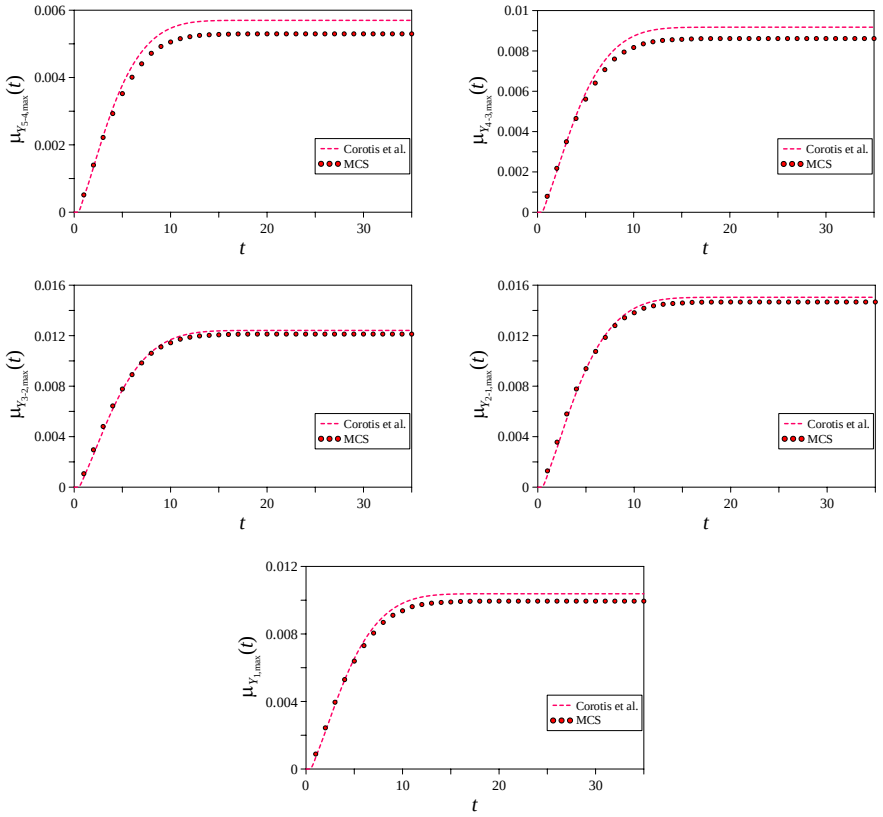

Figure 5. 10 Comparison between Corotis et al. (1972) model and *MCS* of the mean value of the inter-story drift for the spectrum compatible quasi-stationary model.

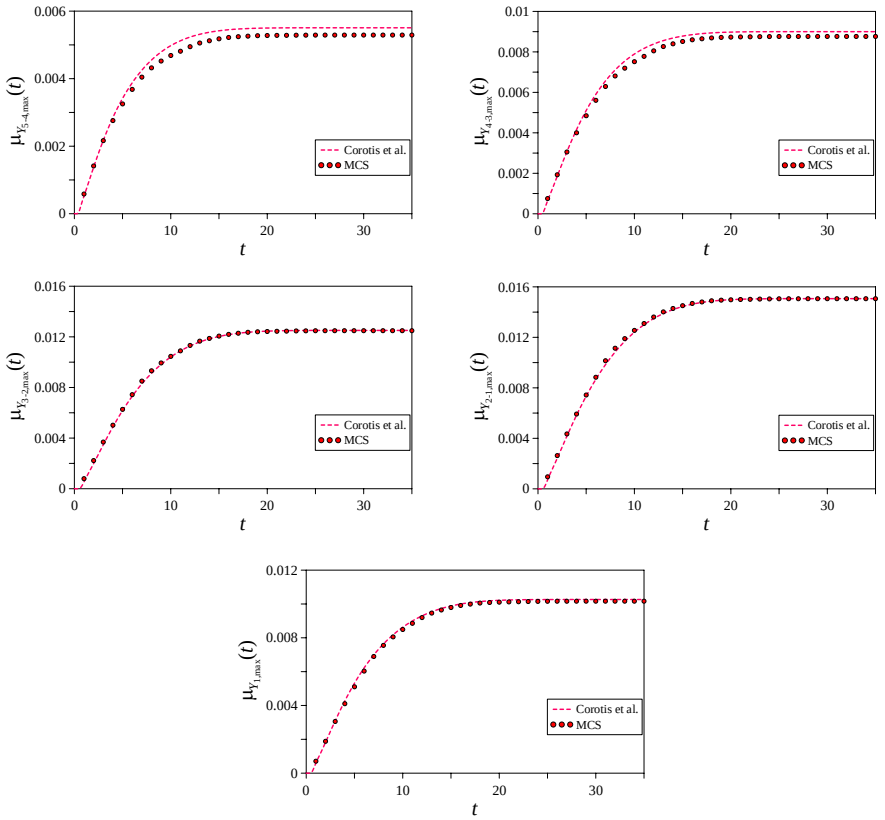

Figure 5. 11 Comparison between Corotis et al. (1972) model and *MCS* of the mean value of the inter-story drift for the spectrum compatible fully non-stationary model.

Figures 5.9, 5.10 and 5.11 plot the mean value of the peak response of the inter-story drift $\mu_{Y_{i-j,\max}}(t)$ along the *x*-direction as a function of the time, *t*. The Corotis et al. (1972) model is in good agreement with the results of the *MCS* when the input is modelled as a non-stationary random process.

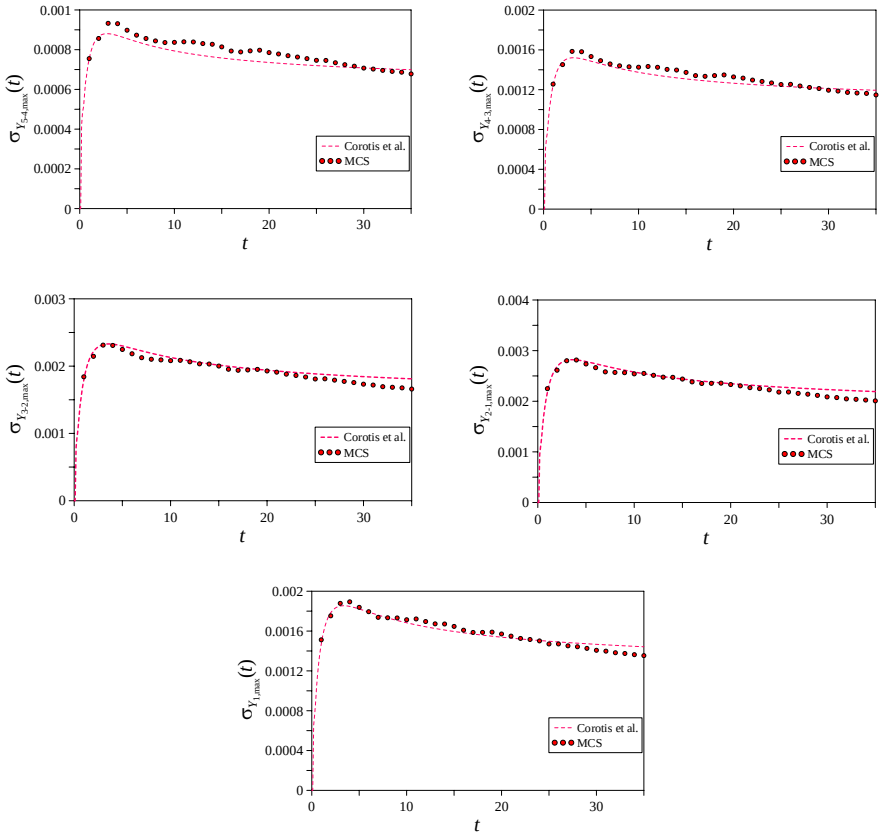

Figure 5. 12 Comparison between Corotis et al. (1972) model and *MCS* of the standard deviation of the inter-story drift for the spectrum compatible stationary model.

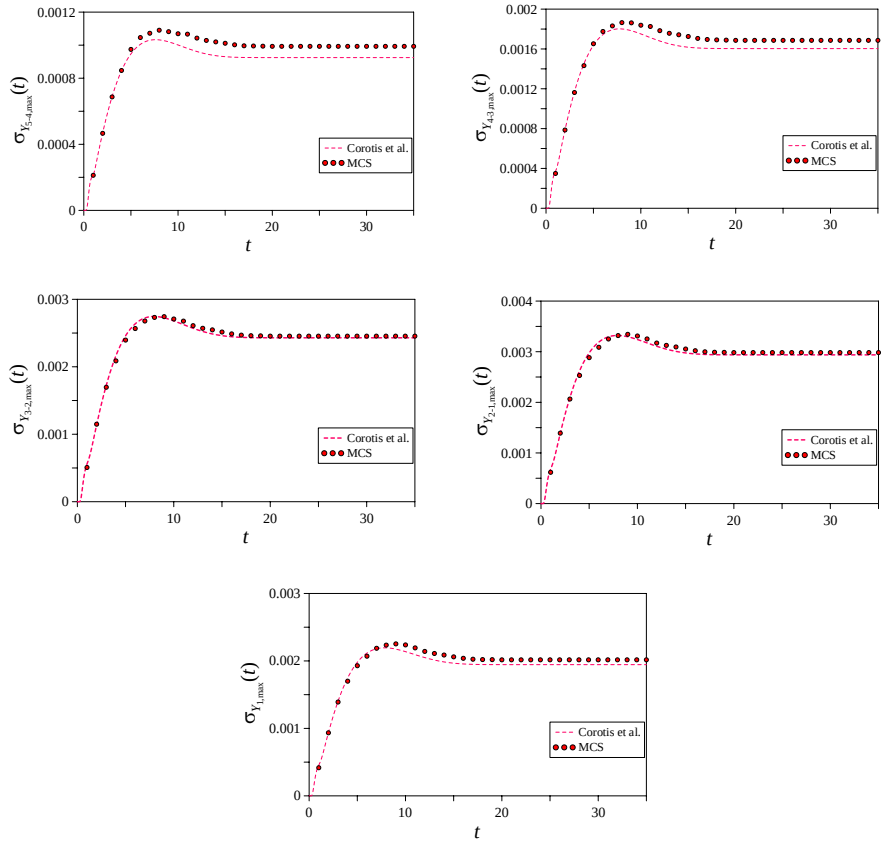

Figure 5. 13 Comparison between Corotis et al. (1972) model and *MCS* of the standard deviation of the inter-story drift for the spectrum compatible quasi-stationary model.

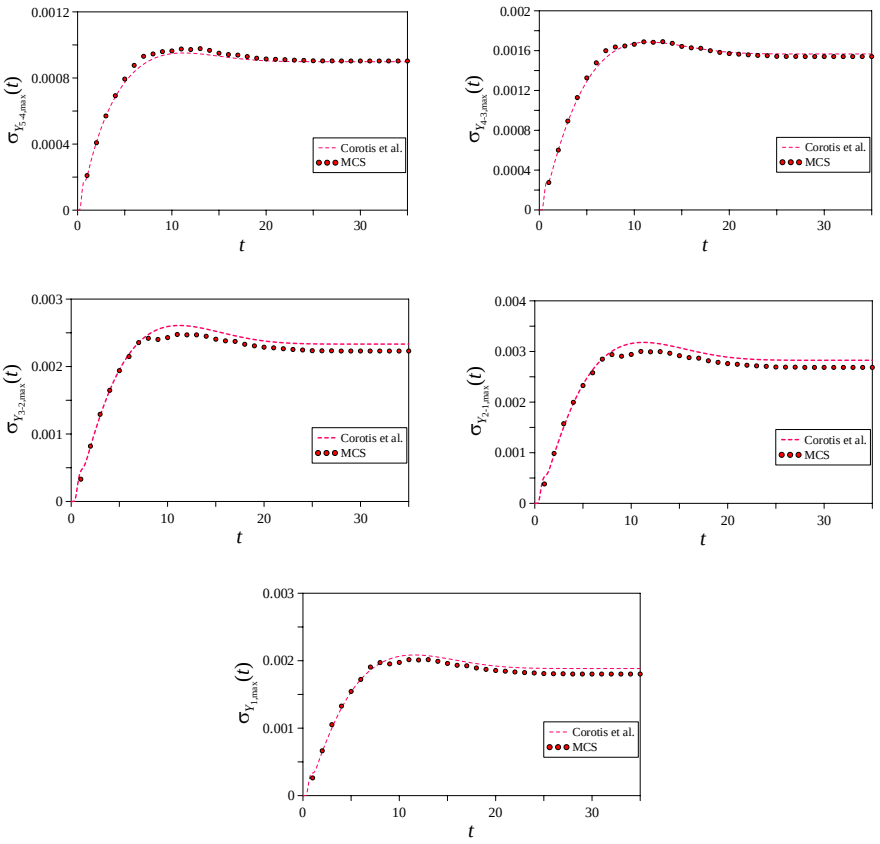

Figure 5. 14 Comparison between Corotis et al. (1972) model and *MCS* of the standard deviation of the inter-story drift for the spectrum compatible fully non-stationary model

The accuracy of the Corotis et al. (1972) model is confirmed also for the standard deviation of the peak response of the inter-story drift $\sigma_{Y_{i-j,\max}}(t)$ along the *x*-direction, as shown in Figures 5.12, 5.13 and 5.14.

Another comparison with the *MCS* can be done from the analysis of the reliability index, given in Eq. (5.32).

Table 5. II The reliability index of the inter-story drifts for the stationary spectrum compatible input.

drift	Corotis et al. (1972) model	MCS	Err%
5-4	7.23459	7.82092	7.49694
4-3	2.59175	2.80798	7.70078
3-2	4.58210	4.98686	8.11655
2-1	9.74390	10.3882	6.20251
1	21.7345	10.3882	4.23157

Table 5. III The reliability index of the inter-story drifts for the quasi-stationary spectrum compatible input.

drift	Corotis et al. (1972) model	MCS	Err%
5-4	5.45901	5.48283	0.434547
4-3	2.02867	2.12346	4.464100
3-2	3.53385	3.61602	2.272590
2-1	7.37268	7.34547	0.370374
1	16.5459	15.8156	4.617810

Table 5. IV The reliability index of the inter-story drifts for the fully non-stationary spectrum compatible input.

drift	Corotis et al. (1972) model	MCS	Err%
5-4	5.69891	6.01186	5.20556
4-3	2.10008	2.2125	5.08109
3-2	3.63936	3.81761	4.66917
2-1	7.66117	7.94568	3.58065
1	17.2463	17.3986	0.87528

From the analysis of Tables 5.II, 5.III, 5.IV it is evident that the Corotis et al. (1972) model is in good agreement with the *MCS*, in fact the percentage error is always lower than 10%. An interesting result is that the reliability index in the stationary case is always

bigger than in the non-stationary case, that means that the stationary process model gives non-conservative results.

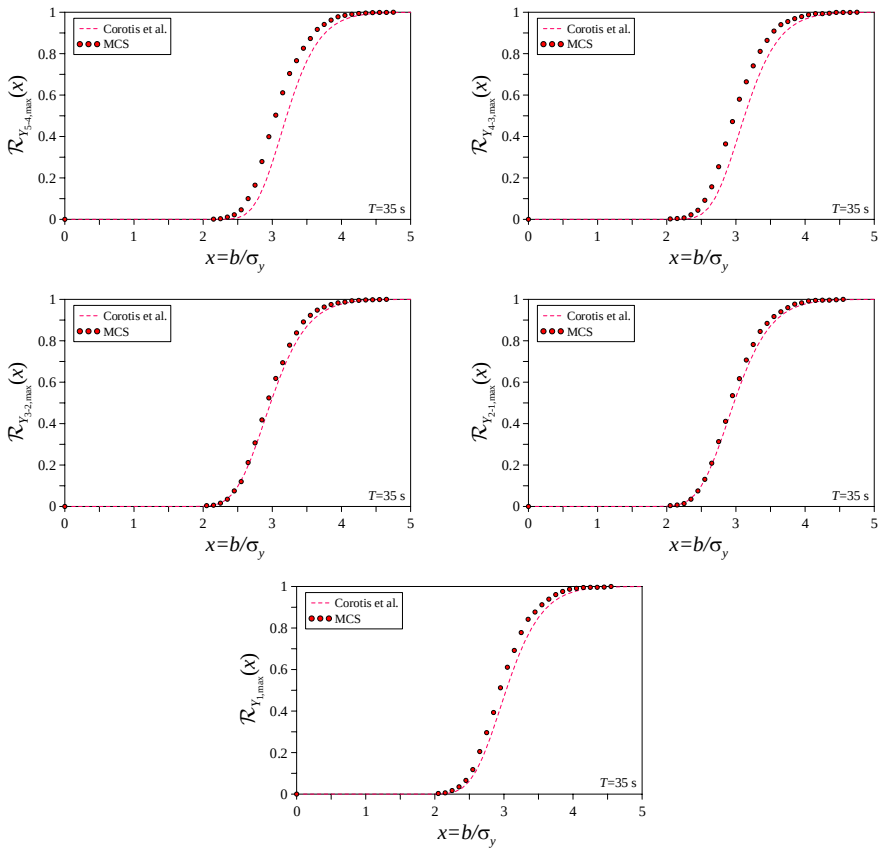

Figure 5. 15 Comparison between Corotis et al. (1972) model and *MCS* of the reliability function at time T=35 [s] of the inter-story drift for the spectrum compatible stationary model.

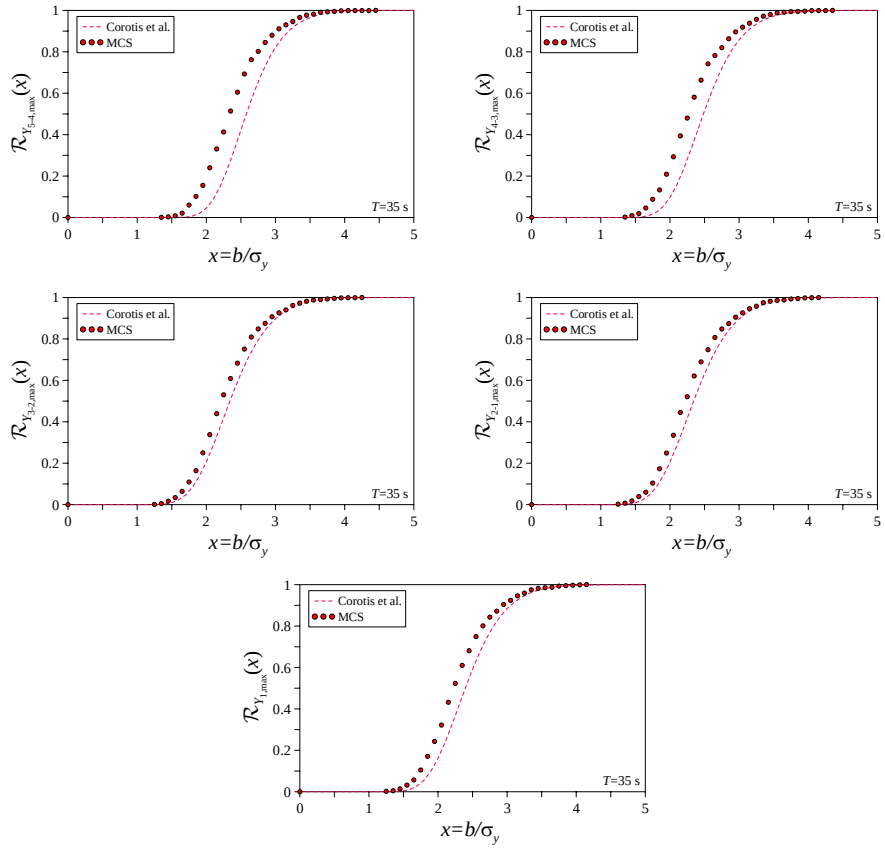

Figure 5. 16 Comparison between Corotis et al. (1972) model and *MCS* of the reliability function at time T=35 [s] of the inter-story drift for the spectrum compatible quasi-stationary model.

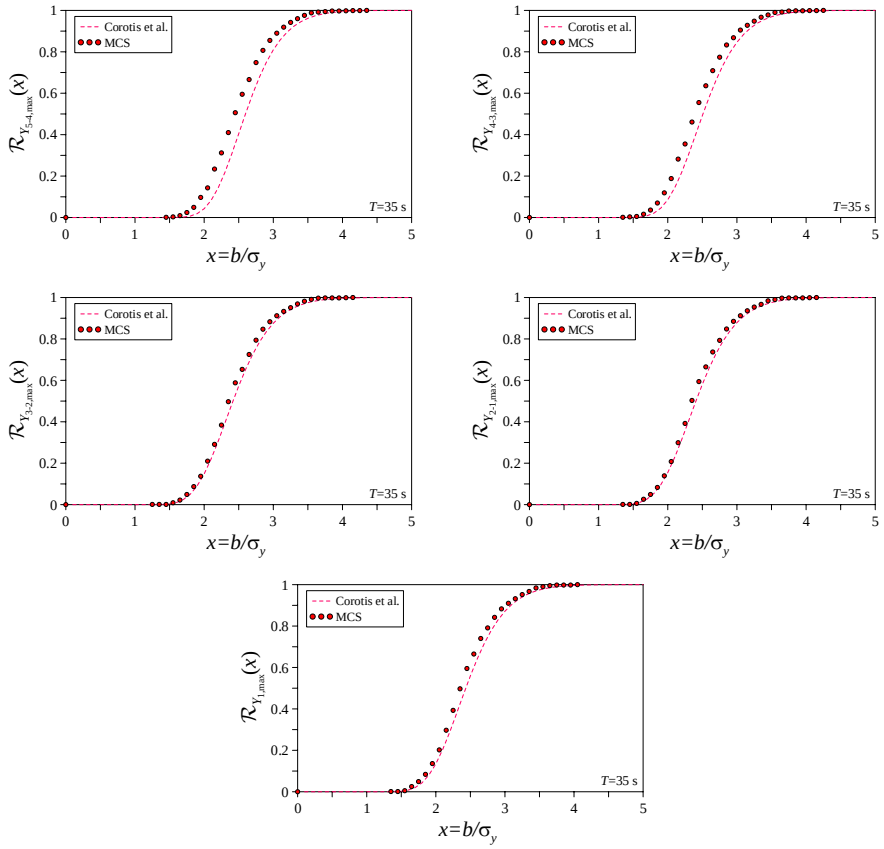

Figure 5. 17 Comparison between Corotis et al. (1972) model and *MCS* of the reliability function at time T=35 [s] of the inter-story drift for the spectrum compatible fully non-stationary model.

From an analysis of the reliability function, see Figures. 5.15, 5.16, 5.17, a reliability assessment can be done. In particular the survival probability is considered for a critical level of the inter-story drift assumed equal to the 0.6% of the inter-story height. In this case the safety check is represented from the relation:

$$\mathcal{P}_{\mathcal{F}} \le \bar{\mathcal{P}}_{\mathcal{F}} = 10^{-\alpha} \tag{5.41}$$

where $\bar{\mathcal{P}}_{\mathcal{F}}$ is the limit probability of failure and α is the security measure, here assumed $\alpha = 2$.

Table 5. V The failure probability of the inter-story drifts for the stationary spectrum compatible input.

drift	$\mathcal{P}_{\mathcal{F}}$
5-4	0
4-3	0
3-2	0.0003103980
2-1	0.0137624000
1	0

Table 5. VI The failure probability of the inter-story drifts for the quasi-stationary spectrum compatible input.

drift	$\mathcal{P}_{\mathcal{F}}$
5-4	0
4-3	0
3-2	0.0025108600
2-1	0.0353412000
1	0.0000451103

Table 5. VII The failure probability of the inter-story drifts for the fully non-stationary spectrum compatible input.

drift	$\mathcal{P}_{\mathcal{F}}$
5-4	0
4-3	0
3-2	0.0020935500
2-1	0.0316602000
1	0.0000246434

Tables 5.II, 5.III, 5.IV lists the probability of failure for the critical level of the $x_c = b_c / \sigma_y$ of each story along the *x*-direction. It is seen that the largest probability of failure of the stories, for which the safety check is not verified, occurs in the second floor, not in the first, for all the models of the input process. Notice that, in general, the stationary process model gives non-conservative results; in fact

the probability of failure is in general lower than the non-stationary models despite that the energy associated to the stationary spectrum-compatible model is much higher than the energy evaluated by applying the non-stationary model of the input process.

5.5 Summary and conclusions

The last Chapter of this research work deals with the reliability assessment of linear structural systems subjected to fully non-stationary stochastic excitations. To this aim the traditional methods for the first passage probability problem, that require the evaluation of the mean up-crossing rate of given thresholds, considered independent or occurring in clumps, have been compared with the method requiring censored closures of the non-stationary extreme value random response process. Thanks' to the proposed procedure, that permits the evaluation of the *NGSM*s of the structural response of interest by evaluating simple integrals in the frequency domain for both separable and non-separable non-stationary excitations, the approximate solution of the first-passage probability problem can be performed very efficiently for fully non-stationary input processes too.

In the Numerical Applications Section it has been demonstrated, thanks' to the comparison of the results with the MCS, that the *ACC* model (Muscolino and Palmeri 2005) is able to catch with accuracy the mean value of the extreme value random response process as well as the Corotis et al. (1972) model, while both the classical and *ACC* approach are not always able to obtain the standard deviation. From the analysis of the reliability functions, it has been shown that the Poisson model fails, on the contrary of the *ACC* model and Corotis et al. model. Furthermore it has been shown that the Corotis

et al. (1972) model can be suitably used in reliability analysis of structures subjected to fully non-stationary input.

Finally it has been evidenced that, in general, the stationary process model gives non-conservative results, despite that the energy associated to the stationary spectrum-compatible model is much higher than the energy evaluated by applying the non-stationary model of the input process.

Conclusions

The probabilistic analysis of structural systems subjected to the ground acceleration process requires the spectral characterization of both the input excitation and the structural response. Into this framework, in this Ph.D. thesis a novel procedure to obtain closed form solutions of the spectral characteristics of the response of linear structural systems subjected to seismic acceleration modelled as stochastic processes has been presented.

After a short review of the preliminary definitions of the probability theory in Chapter 1, Chapter 2 focuses on the characterization of the ground motion acceleration as a non-stationary random process; in fact, starting from an analysis of a set of real earthquakes, it has been shown that the stationary model of the seismic acceleration input process fails to reproduce the typical characteristics of real recorded ground-motion time history. Then different strategies to model the ground motion acceleration stochastic process have been considered, for both the mono-correlated an multi-correlated input process. Furthermore, in order to follow the prescriptions of the building codes, a procedure to generate artificial fully non-stationary spectrum-compatible accelerograms has been proposed.

Once the characterization of the ground motion acceleration is done, it is possible to analyse the safety of structural systems subjected to those excitations. Unfortunately the characterization of the output processes can be extremely complex, when non-stationary input processes are involved. In this framework a new, very handy, procedure to evaluate the spectral characteristics of the structural response, summarized in Chapter 3, is proposed thanks' to closed form solutions of the *Time-Frequency varying Response* (*TFR*) vector function, that are obtained in Chapter 4 for both classically an non-classically damped systems, in the cases of mono-correlated and multi-correlated stochastic input process. In fact, by mean of this function it is possible to evaluate the *Evolutionary Power Spectral Density* (*EPSD*) matrix function of the structural response. The main steps of the proposed approach are: i) the use of modal analysis, or the complex modal analysis, to decouple the equation of motion; ii) the introduction of the modal state variable in order to evaluate the *Non-Geometric Spectral Moments* (*NGSM*s), in the time domain, as element of the *pre-envelope covariance* matrix; iii) the determination, in state variable, by very handy explicit closed-form solutions, of the *TFR vector functions* and of the *EPSD* matrix function of the structural response for the most common adopted models of the seismic input in the framework of stochastic analysis; iv) the evaluation of the spectral characteristics of the stochastic response by adopting the closed-form expression of the *EPSD* matrix function.

The last Chapter of this research work deals with the reliability assessment of linear structural systems subjected to fully non-stationary stochastic excitations. To this aim the traditional methods for the first passage probability problem, that require the evaluation

of the mean up-crossing rate of given thresholds, considered independent or occurring in clumps, have been compared with the methods requiring censored closures of the non-stationary extreme value random response process. Thanks' to the proposed procedure, that permits the evaluation of the *NGSM*s of the structural response of interest by evaluating simple integrals in the frequency domain for both separable and non-separable non-stationary excitations, the approximate solution of the first-passage probability problem can be performed very efficiently for fully non-stationary input processes too. Furthermore it has been evidenced that, in general, the stationary process model gives non-conservative results, despite that the energy associated to the stationary spectrum-compatible model is much higher than the energy evaluated by applying the non-stationary model of the input process.

In conclusion the proposed method is a powerful tool in the analysis of both classically and non-classically damped systems, subjected to mono-correlated and multi correlated stochastic input. In fact, by mean of the closed form solutions of the *TFR* vector function it is possible to obtain closed-form solution of the *EPSD* matrix function of the response, that permits a simple and speedy evaluation of the *NGSMs*. It has been evidenced that the proposed procedure reduces the computational times with respect to the methods that are present in literature, so it can be efficiently used in reliability assessment problems.

Appendix A

TFR vector functions

A.1 Evolutionary process model

A.1.1 General solution

In this section the general solution of Eq. (4.6), given in Eq.(4.15) , which represents the equation of motion, in state variable, of the *j*-th quiescent dummy oscillator (3.13), at time t=0, subjected to the pseudo-force $f(\omega,t)=\varepsilon(\omega)\,t^{r}\exp\left[-\alpha(\omega)t\right]\exp\left[\mathrm{i}\omega t\right]\equiv\varepsilon(\omega)\,t^{r}\exp\left[-\beta(\omega)t\right]$ is first derived. After very simple algebra it can be proved that the particular solution of Eq. (4.6). can be written as:

$$\mathbf{Y}_{\mathrm{p},j}(\omega,t)=\exp\left[-\beta(\omega)t\right]\left[\sum_{s=0}^{r}t^{s}\,\mathbf{b}_{j,s}(\omega)\right],\quad t>0\,; \tag{A.1}$$

where

$$\mathbf{b}_{j,s}(\omega)=-\varepsilon(\omega)\frac{r!}{s!}\,t^{s}\,\mathbf{B}_{j}^{r-s+1}(\omega)\,\mathbf{v} \tag{A.2}$$

with the positions given in Eqs.(4.13) and (4.14). Substituting Eq.(A.1) into Eq.(4.9) the general solution, given in Eq.(4.15), is obtained.

An explicit close solution of the *Time-Frequency varying Response* (*TFR*) vector function and of the *Evolutionary Power Spectral Density* (*EPSD*) function matrix of the response is herein given for the most common modulating functions used in literature.

A.1.2 Normalized exponential type I modulating function

For the Hsu and Bernard (1978) model of the modulating function of the non-stationary zero-mean Gaussian process,

$$a_1(t) = \varepsilon_1 t \exp\left(-\alpha_1 t\right) \tag{A.3}$$

where

$$\varepsilon_1 = \alpha_1 \exp(1), \tag{A.4}$$

according to Eq. (4.12), the particular solution vector of Eq.(4.6), forced by the function $f(\omega,t) = \exp\left(\mathrm{i}\omega t\right) a_1(t)$, can be evaluated in closed form as (Muscolino and Alderucci 2015):

$$\mathbf{Y}_{\mathrm{p},j}\left(\omega,t\right) = -\varepsilon_1 \exp\left(-\beta_1\left(\omega\right)t\right)\left[\mathbf{B}_j\left(\omega\right) + t\,\mathbf{I}_2\right]\mathbf{B}_j\left(\omega\right)\mathbf{v}\,\mathbb{U}(t); \tag{A.5}$$

where the matrix $\mathbf{B}_j\left(\omega\right)$ has been defined in Eq.(4.13), with $\beta\left(\omega\right) \equiv \beta_1\left(\omega\right) = \alpha_1 - \mathrm{i}\omega$, where $\mathbf{I}_2$ is the identity matrix of order 2 and where $\mathbb{U}(t)$ is the unit step function defined as:

$$\mathbb{U}(t-t_0)=\begin{cases}0, & t\le t_0;\\ 1, & t>t_0.\end{cases} \tag{A.6}$$

It follows that, according to Eq.(4.9) the state variable *TFR vector function* $\mathbf{Y}_j(\omega,t)$, of the quiescent *j*-th dummy oscillator (at time $t=0$), can be evaluated as:

$$\begin{aligned}\mathbf{Y}_j(\omega,t)=&-\varepsilon_1\Big\{\exp\Big(-\beta_1(\omega)t\Big)\Big[\mathbf{B}_j(\omega)+t\,\mathbf{I}_2\Big]\\ &-\boldsymbol{\Theta}_j(t)\mathbf{B}_j(\omega)\Big\}\mathbf{B}_j(\omega)\,\mathbf{v}\,\mathbb{U}(t);\end{aligned} \tag{A.7}$$

Finally, for the modulating function defined in Eq.(2.10), the one-sided *EPSD* function matrix, $\mathbf{G}_{k\ell}(\omega,t)$, between the state variable responses of the k,ℓ-th dummy oscillators can be evaluated, according to Eq.(3.21), in explicit form as:

$$\begin{aligned}\mathbf{G}_{k\ell}(\omega,t)&=G_0(\omega)\,\mathbf{Y}_k^{*}(\omega,t)\,\mathbf{Y}_\ell^{T}(\omega,t)\\ &=\varepsilon_1^2\,G_0(\omega)\Big\{\exp\Big(-\beta_1^{*}(\omega)t\Big)\Big[\mathbf{B}_k^{*}(\omega)+t\,\mathbf{I}_2\Big]-\boldsymbol{\Theta}_k(t)\mathbf{B}_k^{*}(\omega)\Big\}\mathbf{B}_k^{*}(\omega)\\ &\times\mathbf{v}\mathbf{v}^T\,\mathbf{B}_\ell^{T}(\omega)\Big\{\exp\Big(-\beta_1(\omega)t\Big)\Big[\mathbf{B}_\ell^{T}(\omega)+t\,\mathbf{I}_2\Big]-\mathbf{B}_\ell^{T}(\omega)\boldsymbol{\Theta}_\ell^{T}(t)\Big\};\end{aligned} \tag{A.8}$$

where $G_0(\omega)$ is the embedded stationary counterpart of the one-sided *EPSD* function. Substituting Eq.(A.8) into Eq.(3.20) the pre-envelope covariance matrix between the state variable responses of the k,ℓ-th dummy oscillators is obtained.

A.1.3 Normalized exponential type II modulating function

For the Shinozuka and Sato (1967) model of the modulating function of the non-stationary zero-mean Gaussian process,

$$a_2(t) = \varepsilon_2 \left[\exp\left(-\alpha_2 t\right) - \exp\left(-\alpha_3 t\right) \right] \tag{A.9}$$

where the constant ε_2 normalizes the exponential modulating function so that the maximum of the real function $a_2(t)$ is unity:

$$\varepsilon_2 = \frac{\alpha_2}{\alpha_3 - \alpha_2} \exp\left[\frac{\alpha_3}{\alpha_3 - \alpha_2} \ln\left(\frac{\alpha_3}{\alpha_2} \right) \right], \tag{A.10}$$

according to Eq. (4.12), the particular solution vector of Eq.(4.6), forced by the function $f(\omega,t) = \exp\left(\mathrm{i}\omega t\right) a_2(t)$, can be evaluated in closed form as (Muscolino and Alderucci 2015):

$$\begin{aligned} \mathbf{Y}_{\mathrm{p},j}(\omega,t) = -\varepsilon_2 \Big[& \exp\left(-\beta_2(\omega)t\right) \mathbf{B}_{2,j}(\omega) \\ & - \exp\left(-\beta_3(\omega)t\right) \mathbf{B}_{3,j}(\omega) \Big] \mathbf{v}\, \mathbb{U}(t); \end{aligned} \tag{A.11}$$

with

$$\begin{aligned} & \beta_r(\omega) = \alpha_r - \mathrm{i}\omega; \\ & \mathbf{B}_{r,j}(\omega) = \left[\mathbf{D}_j + \beta_r(\omega) \mathbf{I}_2 \right]^{-1} = \\ & \quad = \chi_{r,j}(\omega) \begin{bmatrix} \beta_r(\omega) - 2\xi_j \omega_j & -1 \\ \omega_j^2 & \beta_r(\omega) \end{bmatrix}; \qquad r = 2,3 \end{aligned} \tag{A.12}$$

and

$$\chi_{r,j}(\omega)=\frac{1}{\beta_r(\omega)^2-2\xi_j\omega_j\,\beta_r(\omega)+\omega_j^2},\quad r=2,3. \tag{A.13}$$

It follows that, according to Eq.(4.9) the state variable modal *TFR* vector function $\mathbf{Y}_j(\omega,t)$, of the quiescent *j*-th dummy oscillator (at time $t=0$), can be evaluated as:

$$\begin{aligned}\mathbf{Y}_j(\omega,t)=&-\varepsilon_2\left\{\left[\exp\left(-\beta_2(\omega)t\right)\mathbf{B}_{2,j}(\omega)-\exp\left(-\beta_3(\omega)t\right)\mathbf{B}_{3,j}(\omega)\right]\right.\\&\left.-\boldsymbol{\Theta}_j(t)\left[\mathbf{B}_{2,j}(\omega)-\mathbf{B}_{3,j}(\omega)\right]\right\}\mathbf{v}\,\mathbb{U}(t),\end{aligned} \tag{A.14}$$

Finally, for the modulating function defined in Eq.(2.12), the one-sided *EPSD* function matrix, $\mathbf{G}_{k\ell}(\omega,t)$, between the k, ℓ-th dummy oscillators, can be evaluated in explicit form as:

$$\begin{aligned}&\mathbf{G}_{k\ell}(\omega,t)=\\&=\varepsilon_2^2\,G_0(\omega)\left\{\left[\exp\left(-\beta_2^*(\omega)t\right)\mathbf{B}_{2,k}^*(\omega)-\exp\left(-\beta_3^*(\omega)t\right)\mathbf{B}_{3,k}^*(\omega)\right]\right.\\&\left.-\boldsymbol{\Theta}_k(t)\left[\mathbf{B}_{2,k}^*(\omega)-\mathbf{B}_{3,k}^*(\omega)\right]\right\}\mathbf{v}\,\mathbf{v}^T\\&\times\left\{\left[\exp\left(-\beta_2(\omega)t\right)\mathbf{B}_{2,\ell}^T(\omega)-\exp\left(-\beta_3(\omega)t\right)\mathbf{B}_{3,\ell}^T(\omega)\right]\right.\\&\left.-\left[\mathbf{B}_{2,\ell}^T(\omega)-\mathbf{B}_{3,\ell}^T(\omega)\right]\boldsymbol{\Theta}_\ell^T(t)\right\}\end{aligned} \tag{A.15}$$

where $G_0(\omega)$ is the embedded stationary counterpart of the one-sided *PSD* function. Substituting Eq.(A.15) into Eq. (3.20) the pre-envelope covariance matrix between the state variable responses of the k,ℓ-th dummy oscillators is obtained.

A.1.4 Normalized Jennings et al type modulating function

A quite different solution has to be pursued in the Jenning et al. model (1969) of the modulating function. In this case the forcing function $f(\omega,t)$ of differential equation (4.6) has to be written as the sum of three terms:

$$f(\omega,t)=\exp(\mathrm{i}\omega t)\,a_3(t)= \\ =\left[\frac{t^2}{t_1^2}\mathbb{W}(0,t_1)+\mathbb{W}(t_1,t_2)+\exp\left[-\alpha_4(t-t_2)\right]\mathbb{U}(t-t_2)\right]\exp(\mathrm{i}\omega t) \tag{A.16}$$

where $\mathbb{W}(t_j,t_i)$ is the window functions defined as:

$$\mathbb{W}(t_i,t_j)=\begin{cases}1, & t_i<t\le t_j;\\ 0, & t\le t_i,\ t>t_j.\end{cases} \tag{1.17}$$

This modulating function is a three time interval step function. It follows that in spite of the *j*-th modal oscillator is quiescent at time *t*=0 , $\mathbf{Y}_j(\omega,0)=\mathbf{0}$, the initial condition at time $t=t_1$ and $t=t_2$ are different from zero. It follows that the general solution in this case, $\mathbf{Y}_j(\omega,t)$, can be determined as (Borino and Muscolino 1986. Muscolino 1996):

$$\begin{aligned}
&\mathbf{Y}_j(\omega,t)=\mathbf{Y}_{\mathrm{p},j}^{(1)}(\omega,t)-\boldsymbol{\Theta}_j(t)\,\mathbf{Y}_{\mathrm{p},j}^{(1)}(\omega,0), \quad 0<t\le t_1;\\
&\mathbf{Y}_j(\omega,t)=\mathbf{Y}_{\mathrm{p},j}^{(2)}(\omega,t)+\boldsymbol{\Theta}_j(t-t_1)\left[\mathbf{Y}_j(\omega,t_1)-\mathbf{Y}_{\mathrm{p},j}^{(2)}(\omega,t_1)\right], \quad t_1<t\le t_2;\\
&\mathbf{Y}_j(\omega,t)=\mathbf{Y}_{\mathrm{p},j}^{(3)}(\omega,t)+\boldsymbol{\Theta}_j(t-t_2)\left[\mathbf{Y}_j(\omega,t_2)-\mathbf{Y}_{\mathrm{p},j}^{(3)}(\omega,t_2)\right], \quad t>t_2,
\end{aligned} \tag{A.18}$$

where $\mathbf{Y}_{\mathrm{p},j}^{(i)}(\omega,t)$ is the particular solution vector in the *i*-th time interval. Namely, the first vector is evaluated in the time interval $(0,t_1]$, the second in the time interval $(t_1,t_2]$ and the third for $t>t_2$ .Then, the three particular solution vectors are evaluated considering the following three pseudo-force functions, each for the corresponding time interval:

$$\begin{aligned} &f^{(1)}(\omega,t)=\exp(\mathrm{i}\omega t)\frac{t^2}{t_1^2}, \quad 0<t\le t_1;\\ &f^{(2)}(\omega,t)=\exp(\mathrm{i}\omega t), \quad t_1<t\le t_2;\\ &f^{(3)}(\omega,t)=\exp(\mathrm{i}\omega t)\exp\left[-\alpha_4(t-t_2)\right], \quad t>t_2. \end{aligned} \tag{A.19}$$

Then the particular solution vector of Eq.(4.6), forced by the function $f(\omega,t)=\exp(\mathrm{i}\omega t)a_3(t)$, can be evaluated in closed form as (Muscolino and Alderucci 2015):

$$\mathbf{Y}_{\mathrm{p},j}(\omega,t)=\begin{cases} -\dfrac{1}{t_1^2}\left[\exp(\mathrm{i}\omega t)\displaystyle\sum_{s=0}^{2}\frac{2}{s!}t^s\,\mathbf{B}_j^{2-s+1}(\omega)\mathbf{v}\right], & 0<t\le t_1;\\ -\exp(\mathrm{i}\omega t)\mathbf{B}_j(\omega)\mathbf{v}, & t_1<t\le t_2;\\ -\exp\left[-\alpha_4(t-t_2)+\mathrm{i}\omega t\right]\mathbf{B}_j(\omega)\mathbf{v}, & t>t_2. \end{cases} \tag{A.20}$$

where the matrix $\mathbf{B}_j(\omega)$ has been defined in Eq. (4.13) with $\beta(\omega)\equiv\beta_4(\omega)=\alpha_4-\mathrm{i}\omega$. It follows that, according to Eq. (4.13) the state variable vector of the modal *TFR* vector function, $\mathbf{Y}_j(\omega,t)$, of

the quiescent *j*-th dummy oscillator (at time $t = 0$), can be evaluated as:

$$\mathbf{Y}_j(\omega,t) = \begin{cases} -\dfrac{2}{t_1^2}\left\{\exp(\mathrm{i}\omega t)\sum_{s=0}^{2}\dfrac{1}{s!}t^s\,\mathbf{B}_j^{2-s}(\omega) - \boldsymbol{\Theta}_j(t)\mathbf{B}_j^2(\omega)\right\}\mathbf{B}_j(\omega)\mathbf{v}, & 0 < t \le t_1; \\ -\exp(\mathrm{i}\omega t)\mathbf{B}_j(\omega)\mathbf{v} + \boldsymbol{\Theta}_j(t-t_1) & \\ \quad\times\left[\mathbf{Y}_j(\omega,t_1) + \exp(\mathrm{i}\omega t_1)\mathbf{B}_j(\omega)\mathbf{v}\right], & t_1 < t \le t_2; \\ -\exp\left[-\alpha_4(t-t_2) + \mathrm{i}\omega t\right]\mathbf{B}_j(\omega)\mathbf{v} + \boldsymbol{\Theta}_j(t-t_2) & \\ \quad\times\left[\mathbf{Y}_j(\omega,t_2) + \exp(\mathrm{i}\omega t_2)\,\mathbf{B}_j(\omega)\mathbf{v}\right], & t > t_2. \end{cases}$$

(A.21)

Once the state variable function vector, $\mathbf{Y}_k(\omega,t)$ and $\mathbf{Y}_\ell(\omega,t)$, of the k, ℓ-th dummy oscillators are determined it is possible to evaluate in explicit form the one-sided *EPSD* function matrix $\mathbf{G}_{k\ell}(\omega,t) = G_0(\omega)\,\mathbf{Y}_k^*(\omega,t)\,\mathbf{Y}_\ell^T(\omega,t)$ as the sum of three contributions: the first in the time interval $(0,t_1]$, the second in the time interval $(t_1,t_2]$, the third for $t > t_2$. Substituting the so evaluated one-sided *EPSD* function matrix into Eq. (3.20) , the pre-envelope covariance matrix between the state variable responses of the k,ℓ-th dummy oscillators is obtained.

A.1.5 Spanos and Solomos model of the fully non-stationary process

For the Spanos and Solomos (1983) model of the modulating function of the non-stationary zero-mean Gaussian process:

$$a_4(\omega,t) = \varepsilon_4(\omega)\, t \exp\left[-\alpha_5(\omega)\, t\right] \tag{A.22}$$

with the parameter $\varepsilon_4(\omega)$ that normalizes the time-frequency modulating function so that the maximum of the real function $a_4(\omega,t)$ is unity. According to Eq. (4.12), the particular solution vector of Eq.(4.6), forced by the function $f(\omega,t) = \exp(\mathrm{i}\omega t)\, a_4(t)$, can be evaluated in closed form as (Muscolino and Alderucci 2015):

$$\begin{aligned}\mathbf{Y}_{\mathrm{p},j}(\omega,t) = &-\varepsilon_5(\omega)\exp\left[-\beta_5(\omega)t\right]\left[\mathbf{B}_j(\omega) + t\,\mathbf{I}_2\right] \\ &\times \mathbf{B}_j(\omega)\,\mathbf{v}\,\mathbb{U}(t).\end{aligned} \tag{A.23}$$

It follows that, according to Eq. (4.13) the state variable vector of the modal *TFR* vector function, $\mathbf{Y}_j(\omega,t)$, of the quiescent *j*-th dummy oscillator (at time $t = 0$), can be evaluated as

$$\begin{aligned}\mathbf{Y}_j(\omega,t) = &-\varepsilon_5(\omega)\left\{\exp\left(-\beta_5(\omega)t\right)\left[\mathbf{B}_j(\omega) + t\,\mathbf{I}_2\right] - \boldsymbol{\Theta}_j(t)\,\mathbf{B}_j(\omega)\right\} \\ &\times \mathbf{B}_j(\omega)\,\mathbf{v}\,\mathbb{U}(t)\end{aligned} \tag{A.24}$$

where the matrix $\mathbf{B}_j(\omega)$ has been defined in Eq. (4.13) with $\beta(\omega) \equiv \beta_5(\omega) = \alpha_5(\omega) - \mathrm{i}\omega$. It follows that the corresponding one-sided *EPSD* function matrix, $\mathbf{G}_{k\ell}(\omega,t)$, between the state variable

responses of the k,ℓ-th dummy oscillators can be evaluated, according to Eq. (3.21), in explicit form as:

$$\begin{aligned}&\mathbf{G}_{k\ell}(\omega,t)=\\&=\left|\varepsilon_5(\omega)\right|^2 G_0(\omega)\left\{\exp\left(-\beta_5^*(\omega)t\right)\left[\mathbf{B}_k^*(\omega)+t\,\mathbf{I}_2\right]-\boldsymbol{\Theta}_k(t)\mathbf{B}_k^*(\omega)\right\}\\&\times\mathbf{B}_k^*(\omega)\times\mathbf{v}\,\mathbf{v}^T\,\mathbf{B}_\ell^T(\omega)\left\{\exp\left(-\beta_5(\omega)t\right)\left[\mathbf{B}_\ell^T(\omega)+t\,\mathbf{I}_2\right]-\mathbf{B}_\ell^T(\omega)\boldsymbol{\Theta}_\ell^T(t)\right\};\end{aligned}\tag{A.25}$$

where $G_0(\omega)$ is the embedded one-sided *PSD* function of the stationary counterpart process. Substituting Eq.(A.25) into Eq. (3.21) the pre-envelope covariance matrix between the state variable responses of the k,ℓ-th dummy oscillators is obtained.

A.2. Sigma-oscillatory process model

In the Conte and Peng (1996) model the fully non-stationary process is a particular sigma-oscillatory process composed by the summation of *N* uniformly modulated random processes $X_q(t)$. The modulating function of each component sub-process, $X_q(t)$, is defined as $a_q(t)=\varepsilon_q\,(t-t_q)^{r_q}\,e^{-\alpha_q(t-t_p)}\,\mathbb{U}(t-t_q)$. Then this function starts at time $t=t_q$ where the initial condition of the *j*-th quiescent modal oscillator, $\mathbf{Y}_j(\omega,t_q)=\mathbf{0}$, are imposed. It follows that the particular solution vector of the *j*-th differential equation (4.6), forced by the function $f(\omega,t)=\exp\left[\mathrm{i}\omega\left(t-t_q\right)\right]a_q(t)$, can be evaluated in closed form by a translation of the time axis with respect to Eq.(A.1) and it is given by:

$$\mathbf{Y}_{\mathrm{p},j}^{(q)}(\omega,t) = -\varepsilon_q \exp\left[-\beta_q(\omega)(t-t_q)\right] \times\left[\sum_{s=0}^{r_q}\frac{r_q!}{s!}(t-t_q)^s\,\mathbf{B}_{j,q}^{r_q-s+1}(\omega)\right]\mathbf{v}\,\mathbb{U}(t-t_q); \tag{A.26}$$

with

$$\beta_q(\omega) = \alpha_q(\omega) - \mathrm{i}\omega;$$
$$\mathbf{B}_{j,q}(\omega) = \left[\mathbf{D}_j + \beta_q(\omega)\mathbf{I}_2\right]^{-1} = \tag{A.27}$$
$$= \chi_j(\omega)\begin{bmatrix}\beta_q(\omega) - 2\xi_j\omega_j & -1\\ \omega_j^2 & \beta_q(\omega)\end{bmatrix}.$$

Indeed, in this case the particular solution pertaining to initial conditions prescribed at time instant $t = t_q$ can be obtained straightforwardly from Eq.(A.1) assuming as time parameter t - t_q. It follows that in this case the general solution can be written as (Borino and Muscolino 1986, Muscolino 1996):

$$\mathbf{Y}_j^{(q)}(\omega,t) = \left[\mathbf{Y}_{\mathrm{p},j}^{(q)}(\omega,t) - \mathbf{\Theta}_j(t-t_q)\,\mathbf{Y}_{\mathrm{p},j}^{(q)}(\omega,t_q)\right]\mathbb{U}(t-t_q). \tag{A.28}$$

Since the N zero-mean uniformly modulated Gaussian sub-processes $X_q(t)$ are assumed independent, the one-sided *EPSD* function matrix, $\mathbf{G}_{k\ell}(\omega,t)$, between the state variable responses of the k,ℓ-th dummy oscillators, can be evaluated, according to Eq. (3.21), in explicit form as:

$$\mathbf{G}_{k\ell}(\omega,t) = \sum_{q=1}^{N}\left[G_q(\omega)\,\mathbf{Y}_k^{(q)*}(\omega,t)\,\mathbf{Y}_\ell^{(q)T}(\omega,t)\,\mathbb{U}(t-t_q)\right]\mathbb{U}(t). \tag{A.29}$$

Finally, by substituting Eq.(A.29) into Eq. (3.21) the pre-envelope covariance matrix between the state variable responses of the k,ℓ-th dummy oscillators is obtained.

A.3 Adaptive chirplet decomposition

When the adaptive chirplet decomposition of the forcing input is used, the modal *TFR* vector function corresponding to the *k*-th chirplet $\mathbf{Y}_j^{(k)}(\omega,t)\ (k=0,2,\ldots,K)\ \ (j=r,s)$ can be obtained as the solution of the following first order differential equation:

$$\dot{\mathbf{Y}}_j^{(k)}(\omega,t)=\mathbf{D}_j\,\mathbf{Y}_j^{(k)}(\omega,t)+\mathbf{v}\,AS_k(\omega,t)\,\mathbb{U}(t);\quad \mathbf{Y}_j^{(k)}(\omega,0)=\mathbf{0} \qquad \text{(A.30)}$$

where $\mathbb{U}(t)$ is the *unit step function* defined in Eq. (2.15), $\mathbf{D}_j$ and $\mathbf{v}$ have been defined in Eq.(4.8) and $AS(\omega,t)$ is the adaptive spectrogram:

$$AS(t,\omega)\cong\sum_{k=0}^{K}2A_k^2\exp\left\{-\alpha_k\left(t-t_k\right)^2-\left[\omega-\omega_k-\beta_k\left(t-t_k\right)\right]^2/\alpha_k\right\}. \qquad \text{(A.31)}$$

If the particular solution of equation (A.30), $\mathbf{Y}_{\mathrm{p},j}^{(k)}(\omega,t)$, can be determined in explicit form, the *modal TFR vector function*, solution of Eq.(A.30), can be written as (Borino and Muscolino 1986, Muscolino 1996):

$$\mathbf{Y}_j^{(k)}(\omega,t)= \\ =\left[\mathbf{Y}_{\mathrm{p},j}^{(k)}(\omega,t)+\mathbf{\Theta}_j(t-t_k)\left(\mathbf{Y}_j^{(k)}(\omega,t_k)-\mathbf{Y}_{\mathrm{p},j}^{(k)}(\omega,t_k)\right)\right]\mathbb{U}(t-t_k). \tag{A.32}$$

Furthermore, the contribution of the last term in the right member of Eq.(A.32) decreases in the time because of the transition matrix satisfies the condition (4.10).

The analytical expression of the particular solution vector $\mathbf{Y}_{\mathrm{p},j}^{(k)}(\omega,t)$, which appears in Eq.(A.32), can be easily obtained in closed form when the forcing term is represented by the *k*-th element of the adaptive spectrogram obtained in Eq.(2.31).

By very simple algebra the particular solution vector $\mathbf{Y}_{\mathrm{p},j}^{(k)}(\omega,t)$ can be written as

$$\mathbf{Y}_{\mathrm{p},j}^{(k)}(\omega,t)=\varepsilon_{j,k}(\omega)\exp\left[-\varphi_j^*(t-t_k)\right]\mathbf{B}_{j,k}(\omega,\mathrm{t})\mathbf{w}_{j,k}(\omega,\mathrm{t}) \tag{A.33}$$

with

$$\varepsilon_{j,k}(\omega)=\frac{\psi_k(\omega)\sqrt{\pi}}{4\mathrm{i}\,\bar{\omega}_j\sqrt{\tau_k}}$$

$$\mathbf{B}_{j,k}(\omega)=$$

$$=\begin{bmatrix} \exp\left[\frac{\left(\varphi_j^*+\gamma_k(\omega)\right)^2}{4\tau_k}\right] & \exp\left[\frac{\left(\varphi_j+\gamma_k(\omega)\right)^2}{4\tau_k}+2\mathrm{i}\bar{\omega}_j\left(t-t_k\right)\right] \\ \varphi_j^*\exp\left[\frac{\left(\varphi_j^*+\gamma_k(\omega)\right)^2}{4\tau_k}\right] & \varphi_j\exp\left[\frac{\left(\varphi_j+\gamma_k(\omega)\right)^2}{4\tau_k}+2\mathrm{i}\bar{\omega}_j\left(t-t_k\right)\right] \end{bmatrix};$$

$$\mathbf{w}_{j,k}=\begin{bmatrix} Erf\left(\frac{2\tau_k+\varphi_j^*+\gamma_k(\omega)}{2\sqrt{\tau_k}}\right)-Erf\left(\frac{2\tau_k\left(t-t_k\right)+\varphi_j^*+\gamma_k(\omega)}{2\sqrt{\tau_k}}\right) \\ -Erf\left(\frac{2\tau_k+\varphi_j+\gamma_k(\omega)}{2\sqrt{\tau_k}}\right)+Erf\left(\frac{2\tau_k\left(t-t_k\right)+\varphi_j+\gamma_k(\omega)}{2\sqrt{\tau_k}}\right) \end{bmatrix}$$

$$\left(j=r,s\right)$$

(A.34)

where $Erf(\bullet)$ is the Error Function defined as:

$$Erf(x)=\frac{2}{\pi}\int_0^x\exp\left(-\tau^2\right)\mathrm{d}\tau, \tag{A.35}$$

$\bar{\omega}_j=\omega_j\sqrt{1-\xi_j^2}$ $(j=r,s)$ is the damped circular frequency of the j-th dummy oscillator, φ_j and φ_j^* are the eigenvalues of the matrix $\mathbf{D}_j$, with the positions

$$\psi_k(\omega) = 2A_k^2 \exp\left[-\frac{(\omega-\omega_k)^2}{\alpha_k}\right]$$
$$\gamma_k(\omega) = -2\frac{\beta_k}{\alpha_k}(\omega-\omega_k) - i\omega \tag{A.36}$$
$$\tau_k = \alpha_k + \frac{\beta_k^2}{\alpha_k}.$$

Substituting the vector $\mathbf{Y}_{\mathrm{p},j}^{(k)}(\omega,t)$ into Eq.(A.32), the solution vector, $\mathbf{Y}_j^{(k)}(\omega,t)$, of the *j*-th oscillator in state variable, can be evaluated in closed-form solution as:

$$\begin{aligned}\mathbf{Y}_j^{(k)}(\omega,t) = \varepsilon_{j,k}(\omega)\Big\{&\exp\left[-\varphi_j^*(t-t_k)\right]\mathbf{B}_{j,k}(\omega,\mathrm{t}) \\ &-\boldsymbol{\Theta}_j(t-t_q)\mathbf{B}_{j,k}(\omega,\mathrm{t})\Big\}\mathbf{w}_{j,k}(\omega,\mathrm{t})\,\mathbb{U}(t-t_q);\end{aligned} \tag{A.37}$$

where the condition $\mathbf{Y}_j^{(k)}(\omega,t_q) = \mathbf{0}$ has been satisfied. It has to be emphasized that this very remarkable result is obtained because of the state variable formulation has been adopted.

The one-sided *EPSD* function matrix, $\mathbf{G}_{rs}(\omega,t)$, between the state variable responses of the r,s-th dummy oscillators, can be evaluated in explicit form as:

$$\mathbf{G}_{r,s}(\omega,t) = G_0(\omega)\sum_{k=0}^{K}\Big[\ \mathbf{Y}_r^{(k)*}(\omega,t)\,\mathbf{Y}_s^{(k)T}(\omega,t)\,\mathbb{U}(t-t_k)\Big]. \tag{A.38}$$

Finally, by substituting Eq.(A.38) into Eq.(3.20) the pre-envelope covariance matrix between the state variable responses of the r,s-th dummy oscillators is obtained.

References

Abdel-Ghaffar A.M. and Rubin L.I. "Suspension bridge response to multiple support excitations", *Journal of Engineering Mechanics (ASCE)*, (1982), **108**(2), 419-435.

Alderucci T. and Muscolino G. "Fully nonstationary analysis of linear structural systems subjected to multicorrelated stochastic excitations", *ASCE-ASME Journal of Risk and Uncertainty in Engineering Systems. Part A: Civil Engineering*, (2015), **2**, 4015007-1, 4015007-14.

Amin M. and Ang A.H.S. "Non-stationary stochastic model of earthquake motion", *Journal of Engineering Mechanics (ASCE)*, (1968), **94**, 559-583.

Barbato M. and Conte J.P. "Spectral characteristics of non-stationary random processes: Theory and applications to linear structural models", *Probabilistic Engineering Mechanics*, (2008), **23,** 416-426.

Barbato M and Conte J.P. "Time-variant reliability analysis of linear elastic systems subjected to fully-nonstationary stochastic excitations." *Journal of Engineering Mechanics (ASCE)*, (2015),

04014173, **141**(6), DOI: http://dx.doi.org/10.1061/(ASCE)EM.1943-7889.0000895

Barbato M. and Vasta M. "Closed-form solutions for the time-variant spectral characteristics of non-stationary random processes", *Probabilistic Engineering Mechanics*, (2010), **25**, 9-17.

Battaglia F. "Some extensions in the evolutionary spectral analysis of stochastic process", *Bollettino della Unione Matematica Italiana*, (1979), **16**(B), 1154-1166.

Bommer J.J. and Acevedo A.B. "The use of real earthquake accelerograms as input to dynamic analysis", *Journal of Earthquake Engineering*, (2004), **8**, 43-91.

Borino G. and Muscolino G. "Mode-superposition methods in dynamic analysis of classically and non-classically damped linear systems", *Earthquake Engineering and Structural Dynamics*, (1986), **14**, 705-717.

Borino G., Di Paola M and Muscolino G. "Non-stationary spectral moments of base excited MDOF systems", *Earthquake Engineering and Structural Dynamics*, (1988), **16,** 745-756.

Cacciola P. "A stochastic approach for generating spectrum-compatible fully nonstationary earthquakes", *Computers and Structures*, (2010), **88**, 889-901.

Cacciola P., Colajanni P. and Muscolino G. "Combination of modal responses consistent with seismic input representation", *Journal of Structural Engineering (ASCE)*, (2004), **130**, 47-55.

Cacciola P., D'Amico L. and Zentner I. "New insights in the analysis of the structural response to response spectrum-compatible accelerograms", *Engineering Structures*, (2014), **78**, 3-16.

Cacciola P. and Deodatis G. "A method for generating fully non-stationary and spectrum compatible ground motion vector processes", *Soil Dynamics and Earthquake Engineering*, (2011), **31**, 351-360.

Cacciola P. and Muscolino G. "Reanalysis techniques in stochastic analysis of linear structures under stationary multi-correlated input", *Probabilistic Engineering Mechanics*, (2011), **26**, 92-100

Cacciola P. and Zentner I. "Generation of response spectrum-compatible artificial earthquake accelerograms with random joint time frequency distributions", *Probabilistic Engineering Mechanics*, (2012), **28**, 52-8.

Caddemi S., Colajanni P., Duca I. and Muscolino G. "Non-geometric spectral moments for frequency varying filtered input processes", *Probabilistic Engineering Mechanics*, (2004), **19**, 21-31.

Caddemi S. and Muscolino G. "Pre-envelope covariance differential equations for white and non-white input processes", *Meccanica*, (1998), **33,** 1-10.

Caughey T. K. and O'Kelly M.E.J. "Classical normal modes in damper linear dynamic systems", *Journal of Applied Mechanics (ASME)*, (1965), **32**, 583-588.

Cecini D. and Palmeri A. "Spectrum-compatible accelerograms with harmonic wavelet", *Computers and Structures*, (2015), **147,** 26-35.

Chopra A.K. *Dynamics of structures–Theory and applications to earthquake engineering*, (1995), Prentice Hall, Upper Saddle River, N.J, USA.

Claret A.M. and Venancio Filho F. "A modal superposition pseudo-force method for dynamic analysis of structural systems with non-proportional damping", *Earthquake Engineering and Structural Dynamics*, (1991), **20**, 303-315.

Clough R.W. and Penzien J. *Dynamics of structures*, (1975), Mc Graw-Hill, New York.

Conte J.P. and Peng B.-F. "An explicit closed-form solution for linear systems subjected to nonstationary random excitation", *Probabilistic Engineering Mechanics*, (1996), **11**, 37-50.

Conte J.P. and Peng B.-F. "Fully nonstationary analytical earthquake ground-motion model", *Journal of Engineering Mechanics (ASCE)*, (1997), **123**, 15-24.

Corotis R.B. and Marshall A. "Oscillator response to modulated random excitation", *Journal of Engineering Mechanics (ASCE)*, (1977), **103**(4), 501-513.

Corotis R.B., Vanmarcke E.H. and Cornell C.A. "First passage of non-stationary random processes", *Journal of Engineering Mechanics (ASCE)*, (1972), **98**(2), 401-414.

Cramer H. and Leadbetter M.R. *Stationary and related stochastic processes*, (1967), John Wiley and Sons, Inc., New York, N.Y.

D'Aveni A. and Muscolino G. "Response of non-classically damped structures in the modal subspace", *Earthquake Engineering and Structural Dynamics*, (1995), **24**, 1267-1281.

Deodatis G. "Non-stationary stochastic vector processes: seismic ground motion application", *Probabilistic Engineering Mechanics*, (1996b), **11**, 149-168.

Deodatis G. "Simulation of ergodic multivariate stochastic processes", *Journal of Engineering Mechanics (ASCE)*, (1996a), **122**, 778-787.

Der Kiureghian A. "A coherency model for spatially varying ground motions", *Earthquake Engineering and Structural Dynamics*, (1996), **25**(1), 99-111.

Di Paola M. "Transient spectral moments of linear systems", *SM Archives*, (1985), **10**, 225-243.

Di Paola M. and Muscolino G. "Analytic evaluation of spectral moments", *Journal of Sound and Vibration*, (1988), **124**, 479-488.

Di Paola M. and Petrucci G. "Spectral moments and pre-envelope covariances of nonseparable processes", *Journal of Applied Mechanics (ASME)*, (1990), **57,** 218-224.

Di Paola M. and Zingales M. "Digital simulation of multivariate earthquake ground motion", *Earthquake Engineering and Structural Dynamics*, (2000), **29**, 1011-1027.

Eurocode 8 (2003). European Committee for Standardization: design of structures for earthquake resistance – part 1: general rules, seismic actions and rules for buildings, Brussels, Belgium.

Falsone G. and Settineri D. "A method for the random analysis of linear systems subjected to non-stationary multi-correlated loads", *Probabilistic Engineering Mechanics*, (2011), **26**, 447-453.

Fan F.G. and Ahmadi G. "Nonstationary Kanai-Tajimi models for El Cento 1940 and Mexico City 1985 earthquakes", *Probabilistic Engineering Mechanics*, (1990), **5**, 171-181.

Giaralis A. and Spanos P.D. "Wavelet-based response spectrum compatible synthesis of accelerograms—Eurocode application (EC8)", *Soil Dynamics and Earthquake Engineering*, (2009), **29**, 219-235.

Harichandran R.S. and Vanmarcke E.H. "Stochastic variation of earthquake ground motion in space and time", *Journal of Engineering Mechanics (ASCE)*, (1986), **112**(2), 154-174.

He J. "An efficient numerical method for estimating reliabilities of linear structures under fully nonstationary earthquake", *Structural Safety*, (2010), **32**, 200-208.

Heredia-Zavoni E. and Vanmarcke E. "Seismic random vibration analysis of multi-support structural systems", *Journal of Engineering Mechanics (ASCE)*, (1994), **120**(5), 1107-1128.

Housner G.W. and Jennings P.C. "Generation of artificial earthquakes", *Journal of Engineering Mechanics (ASCE)*, (1964), **90**, 113-150.

Hsu T.-I. and Bernard M.C. "A random process for earthquake simulation", *Earthquake Engineering and Structural Dynamics*, (1978), **6**, 347-362.

Iervolino I., Galasso C. and Cosenza E. "REXEL: computer aided record selection for code-based seismic structural analysis", *Bulletin of Earthquake Engineering*, (2010), **8**, 339-362.

Iwan W.D. and Hou Z.K. "Explicit solutions for the response of simple systems subjected to non-stationary random excitation", *Structural Safety*, (1989), **6,** 77-86.

Iyengar R.N. and Iyengar K.T. "Nonstationary random process for earthquake acceleration", *Bulletin of the Seismological Society of America*, (1969), **59**, 1163-88.

Jangid R.S. "Response of SDOF system to non-stationary earthquake excitation", *Earthquake Engineering and Structural Dynamics*, (2004), **33**, 1417-1428.

Jennings P.C., Housner G.W. and Tsai C. "Simulated earthquake motions for design purpose", *Proceeding 4th International Conference on Earthquake Engineering (Eds. Cakmak A. S. and Herrera I.)*, (1969), Santiago, **A-1**, 145-160.

Kanai K. "Semi-empirical formula for the seismic characteristics of the ground", *Bulletin Earthquake Research Institute*, (1957), University of Tokyo, **35,** 309-325.

Katsanos E.I., Sextos A.G. and Manolis G.D. "Selection of earthquake ground motion records: a state-of-the-art review from a structural engineering perspective", *Soil Dynamics and Earthquake Engineering*, (2010), **30**, 157-169.

Kaul M.J. "Stochastic characterization of earthquakes through their response spectrum", *Earthquake Engineering and Structural Dynamics*, (1978), **6,** 497-509.

Lam N., Wilson J. and Hutchinson G. "Generation of synthetic earthquake accelerograms using seismological modelling: a review", *Journal of Earthquake Engineering*, (2000), **4**, 321-354.

Langley R.S. "A first passage approximation for normal stationary random process", *Journal of Sound and Vibration*, (1988), **122**, 261-275.

Langley R.S. "Structural response to non-stationary non-white stochastic ground motion", *Earthquake Engineering and Structural Dynamics*, (1986a), **14**, 909-924.

Langley R.S. "On various definitions of the envelope of a random process", *Journal of Sound and Vibration*, (1986b), **105**, 503-512.

Li J. and Chen J.B. *Stochastic Dynamics of Structures*, (2009), John Wiley & Sons, Singapore.

Lin Y.K. *Probabilistic Theory of Structural Dynamics*, (1976), Huntington: Krieger Publisher.

Loh C.-H. and Ku B.-D. "An efficient analysis of structural response for multiple-support seismic excitations", *Engineering Structures*, (1995), **17**(1), 15-26.

Luco J.E., Wong H.L. "Response of a foundation to a spatially random ground motion", *Earthquake Engineering and Structural Dynamics*, (1986), **14**(6), 891-908.

Lupoi A., Franchin P., Pinto P.E. and Monti G. "Seismic design of bridges accounting for spatial variability of ground motion", *Earthquake Engineering and Structural Dynamics*, (2005), **34**(4-5), 327-348.

Lutes L.D. and Sarkani S. *Stochastic Analysis of Structural and Mechanical Vibrations*, (1997), Upper Saddle River: Prentice-Hall.

Mallat S.G. *A wavelet tour of signal processing: the sparse way*, (2009), 3rd ed. Academic Press.

Mallat S.G. and Zhang Z, "Matching pursuits with time-frequency dictionary", *IEEE Trans Signal Process*, (1993), **41**(12), 3397-3415.

Mann S. and Haykin S. "The chirplet transform: physical considerations", *IEEE Trans Signal Process*, (1995), **43**(11), 2745-2761.

Melchers R.E. *Structural reliability analysis and prediction*, (1999), John Wiley & Sons, Chichester, UK.

Michaelov G., Sarkani S. and Lutes L.D. "Spectral characteristics of nonstationary random processes - A critical review", *Structural Safety*, (1999a), **21**, 223-244.

Michaelov G., Sarkani S. and Lutes L.D. "Spectral characteristics of nonstationary random processes - response of a simple oscillator", *Structural Safety*, (1999b), **21**, 245-267.

Mukherjee S. and Gupta V.K. "Wavelet-based generation of spectrum-compatible time-histories", *Soil Dynamics and Earthquake Engineering* (2002), **22**, 799-804.

Muscolino G. "Nonstationary envelope in random vibration theory", *Journal of Engineering Mechanics (ASCE)*, (1988), **114**, 1396-1413.

Muscolino G. "Nonstationary pre-envelope covariances of nonclassically damped systems", *Journal of Sound and Vibration*, (1991), **149**, 107-123.

Muscolino G. "Dynamically modified linear structures: deterministic and stochastic response", *Journal of Engineering Mechanics (ASCE)* (1996), **122**, 1044-1051.

Muscolino G. and Alderucci T. "Closed-form solutions for the evolutionary frequency response function of linear systems subjected to separable or non-separable non-stationary stochastic excitations", *Probablistic Engineering Mechanics*, (2015), **40**(1), 75-89.

Muscolino G. and Cacciola P. "On the integral and differential evaluation of non-geometric spectral moments", *EURODYN 2011-Proceedings of the 8th International Conference on Structural Dynamics (Eds. De Roeck G., Degrande G., Lombaert G. and Muller G.)*, (2011), 2805-2812.

Muscolino G. and Palmeri A. "Maximum response statistics of MDOF linear structures excited by non-stationary random processes", *Computer Methods in Applied Mechanics and Engineering*, (2005), **194**, 1711-1737.

Newland D.E. "Harmonic and musical wavelets", *Proceedings of the Royal Society A, London*, (1994), **A 444**, 605-620.

Newland D.E. "Ridge and phase identification in the frequency analysis of transient signals by harmonic wavelets", *Journal of Vibration and Acoustic (ASME)*, (1999), **121**, 149-155.

Peng B.-F. and Conte J.P. "Closed-form solutions for the response of linear systems to fully nonstationary earthquake excitation", *Journal of Engineering Mechanics (ASCE)*, (1998), **124**, 684-694.

Perotti F. "Structural response to non-stationary multiple-support random excitation", *Earthquake Engineering and Structural Dynamics*, (1990), **19**(4), 513-527.

Pfaffinger D.D. "Calculation of power spectra from response spectra", *Journal of Engineering Mechanics (ASCE)*, (1983), **109**, 357-372.

Politis N.P., Giaralis A and Spanos P.D. "Joint time-frequency representation of simulated earthquake accelerograms via the adaptive chirplet transform", *CSM-5, Proceedings of the 5th International Conference on Computational Stochastic Mechanics (Eds. Deodatis G.and Spanos P.D.)*, (2006), Rhodes – Greece.

Pradlwarter H.J. and Schuëller G.I. "Uncertain linear structural systems in dynamics: Efficient stochastic reliability assessment", *Computers and Structures*, (2010), **88,** 74-86.

Preumont A. “The generation of spectrum compatible accelerograms for the design of nuclear power plants”, *Earthquake Engineering and Structural Dynamics*, (1984), **12**,481-497.

Preumont A. “The generation of nonseparable artificial earthquake accelerograms for the design of nuclear power plants”, *Nuclear Engineering and Design*, (1985), **88**, 59-67.

Priestley M.B. “Evolutionary spectra and non-stationary processes”, *Journal of the Royal Statistical Society. Series B (Methodological)*, (1965), **27**, 204-237.

Priestley M.B. “Power spectral analysis of non-stationary random processes”, *Journal of Sound and Vibration*, (1967), **6**, 86-97.

Priestley M. *Spectral analysis and time series*, (1999), Academic Press, London.

Qian S. and Chen D. “Signal representation via adaptive normalized Gaussian functions”, *Signal Process*, (1995), **36**(1),1-11.

Rezaeian S. and Der Kiureghian A. “Simulation of synthetic ground motions for specified earthquake and site characteristics”, *Earthquake Engineering and Structural Dynamics*, (2010), **39**, 1155-1180.

Rice S.O. “Mathematical analysis of random noise—Part III”, *The Bell System Technical Journal*, (1945), **24,** 46-108.

Saragoni G.R. and Hart C. “Simulation of artificial earthquakes”, *Earthquake Engineering and Structural Dynamics*, (1973), **2**, 249-267.

Saxena V., Deodatis G. and Shinozuka M. "Effect of spatial variation of earthquake ground motion on the nonlinear dynamic response of highway bridges", *WCEE-Proceedings of the 8th World Conference on Earthquake Engineering*, Auckland, New Zealand (2000), Paper 2227.

Senthilnathan A. and Lutes L.D "Nonstationary maximum response statistics for linear structures", *Journal of Engineering Mechanics (ASCE)*, (1991), **117**, 294-311.

Shinozuka M. "Simulation of Multivariate and Multidimensional Random Processes", *The Journal of Acoustical Society of America*, (1971), **49**, 357-367.

Shinozuka M. and Deodatis G. "Stochastic process models for earthquake ground motion", *Journal of Probabilistic Engineering Mechanics*, (1988), **3**(3), 114-123.

Shinozuka M. and Jan C.-M. "Digital simulation of random processes and its application", *Journal of Sound and Vibrations*, (1972), **25**, 111-128.

Shinozuka M., Sato Y. "Simulation of nonstationary random process", *Journal of Engineering Mechanics (ASCE)*, (1967), **93**, 11-40.

Spanos P. and Solomos G.P. "Markov approximation to transient vibration", *Journal of Engineering Mechanics (ASCE)*, (1983), **109**, 1134-1150.

Spanos P.D. and Failla G. "Evolutionary spectra estimation using wavelets", *Journal of Engineering Mechanics (ASCE)*, (2004), **130**, 952-960.

Spanos P.D., Giaralis A. and Politisc N.P. "Time–frequency representation of earthquake accelerograms and inelastic structural response records using the adaptive chirplet decomposition and empirical mode decomposition", *Soil Dynamics and Earthquake Engineering*, (2007), **27**, 675-689.

Spanos P.D., Tezcan J. and Tratskas P. "Stochastic processes evolutionary spectrum estimation via harmonic wavelets", *Computer Methods in Applied Mechanics and Engineering*, (2005), **194**, 1367-1383.

Suàrez L.E., Montejo L.A. "Generation of artificial earthquakes via the wavelet transform", *International Journal of Solids and Structures*, (2005), **42**, 5905-5919.

Suzuki Y. and Minai R. "Stochastic prediction of maximum earthquake response of hysteretic structures", *WCEE-Proceedings of the 7th World Conference on Earthquake Engineering*, Instanbul, Turkey, (1980), **6**, 697-704.

Suzuki Y. and Minai R. "Seismic reliability analysis of hysteretic structures based on stochastic differential calculus", *ICOSSAR 85- Proceedings of the 4th International Conference on Structural Safety and Reliability*, Kobe, Japan (1985), **2**, 177-186.

Tajimi H. "A statistical method of determining the maximum response of a building structure during an earthquake", *Proceeding 2nd International Conference on Earthquake Engineering*, Tokyo & Kyoto, Japan, (1960) **2**, 781-797.

Tubino F., Carassale L. and Solari G. "Seismic response of multi-supported structures by proper orthogonal decomposition",

Earthquake Engineering and Structural Dynamics, (2003), **32**(11), 1639-1654.

Vanmarcke E.H. "Properties of spectral moments with applications to random vibrations", *Journal of Engineering Mechanics (ASCE)*, (1972), **98**, 425-446.

Vanmarcke EH "On the distribution of the first-passage time for normal stationary random processes", *Journal of Applied Mechanics (ASME)*, (1975), **42**, 215-220.

Vanmarcke E.H. and Gasparini D.A. "Simulated earthquake ground motions", *Proceedings of the 4th International Conference on Smirt*, K1/9 (1977) San Francisco.

Vanmarke E., Heredia-Zavoni E. and Fenton G.A. "Conditional simulation of spatially correlated earthquake ground motion", *Journal of Engineering Mechanics (ASCE)*, (1993), **119**(11), 2333-2352.

Wang J., Fan L., Qian S. and Zhou J. "Simulations of non-stationary frequency content and its importance to seismic assessment of structures", *Earthquake Engineering and Structural Dynamics*, (2005), **31**, 993-1005.

Wirsching P.H., Paez T.L. and Ortiz K. *Random vibrations. Theory and Practice*, (1995), John Wiley and Sons, Inc., New York, N.Y.

Yang J.-N. "Non-Stationary envelope process and first excursion probability", *Journal of Structural Mechanics*, (1972), **1**, 231-248.

Yeh C.H. and Wen Y.K. “Modelling of nonstationary ground motion and analysis of inelastic structural response”, *Structural Safety*, (1990), **8**, 281-298.

Yin Q., Qian S. and Feng A. “A Fast Refinement for Adaptive Gaussian Chirplet Decomposition”, *IEEE Trans Signal Process*, (2002), **50**(6), 1298-1306.

Zanardo G., Hao H. and Modena C. “Seismic response of multi-span simply supported bridges to a spatially varying earthquake ground motion”, *Earthquake Engineering and Structural Dynamics*, (2002), **31**(6), 1325-1345.

Zerva A. “Effect of spatial variability and propagation of seismic ground motions on the response of multiply supported structures” *Probabilistic Engineering Mechanics*, (1991), **6**(3), 212-221.

Zerva A. “On the spatial vibration of seismic ground motions and its effects on lifelines”, *Engineering Structures*, (1994), **16**(7), 534-546.

Zhang Y.H., Li Q.S., Lin J.H. and Williams F.W. “Random vibration analysis of long-span structures subjected to spatially varying ground motions”, *Soil Dynamics and Earthquake Engineering*, (2009), **29**(4), 620-629.